THE UNIVERSITY OF MICHIGAN
COLLEGE OF LITERATURE, SCIENCE, AND THE ARTS
Computer and Communication Sciences Department

A COMPUTER SIMULATION OF IMPULSE CONDUCTION IN CARDIAC MUSCLE

John L. Foy, Jr.

December 1974

Technical Report No. 166

with assistance from:

National Science Foundation
Grant No. DCR71-01997
Washington, D.C.

and

Department of Health, Education, and Welfare
National Institutes of Health
Grant No. GM-12236
Bethesda, Maryland

Engn
UMR
1511

ACKNOWLEDGEMENTS

The author would like to express his appreciation to Professor Henry H. Swain, the Chairman of the doctoral committee, whose stimulating teaching first attracted the author to this area of research. Dr. Swain undertook personal tutoring of the author in cardiac anatomy and physiology, including many direct demonstrations on dog and rabbit preparations. He devoted generous amounts of his time and interest to this project, and was especially helpful during the final stages of writing and composition. Without Dr. Swain, there would have been no dissertation.

The author would also like to thank the other members of the doctoral committee: Professor Larry K. Flanigan, for many hours of fruitful discussion of the model and simulation techniques, and for his careful, critical reading of early drafts of the dissertation; and Professors John H. Holland and Benedict R. Lucchesi, for reviewing the manuscript and for their many helpful comments and suggestions, especially concerning ways in which the model might be extended.

The author is indebted to Professors Arthur W. Burks and John H. Holland, Directors of the Logic of Computers Group in the Department of Computer and Communication Sciences, for excellent research facilities and generous financial support during the course of this work. Several other members of the Logic of Computers Group contributed significantly: Daniel R. Frantz and Ronald F. Brender developed the specialized computing software used to great advantage

in this research, and Richard A. Laing directed the author's attention to the important series of Russian papers on the modelling of cardiac phenomena. William D. Tajibnapis, Morton D. Hoffman, and Monna Whipp provided valuable technical and secretarial assistance. Dr. Guy Curtis, of the Department of Pharmacology, provided many helpful ideas and useful experimental data.

Finally, the author is especially grateful to Dr. Hideaki Fukushima and Mr. Leon Mills for their swift and careful work in producing the figures that accompany this dissertation, and to Ms. Marilyn Miller, an expert typist, for her invaluable assistance under the pressure of a tight deadline.

The research reported here was supported in part by grants from the National Science Foundation and the National Institutes of Health to the Logic of Computers Group of the University of Michigan Computer and Communication Sciences Department.

TABLE OF CONTENTS

LIST OF TABLES

LIST OF FIGURES

Chapter I

INTRODUCTION

There are two modes of impulse conduction in cardiac muscle, one continuous and one discontinuous. The discontinuous mode is far more common, occurring whenever the heart is driven by its own normal pacemaker in the sino-atrial node, and also when the heart is following the rhythm of ectopic pacemakers in the Purkinje system or is being driven by an artificial electronic pacemaker (at least when the heart rate is in the low or intermediate ranges). In the discontinuous mode of activity, each wave of electrophysiologic activity begins at a discrete point in space and time, travels throughout the cardiac tissue, and ends. Between one wave and the next, there is an interval of time, during which there is no impulse conduction occurring at any point in the tissue.

The continuous mode of impulse conduction is seen during the abnormal rhythms of flutter and fibrillation, and when the heart is being driven at high rates by an artificial pacemaker. During the continuous mode, the discreteness of individual waves is lost. At all times there is conducted impulse activity somewhere in the tissue, and often it is impossible to identify a beginning or an ending to a particular wave of activity.

Flutter and fibrillation in cardiac muscle[1] are associated with continuous conduction of cardiac impulses, but there is not agreement

[1] The term "fibrillation" is used also to designate a state of activity in skeletal muscle, but there is no reason to believe that this is related in any fundamental way to the abnormal rhythm in heart muscle which happens to bear the same name.

as to whether the rhythms are the cause or the effect of the continuous mode of conduction. Two principal theories have been advanced to explain flutter and fibrillation. The first holds that the arrhythmias are caused by the rapid emission of impulses from an ectopic focus or pacemaker--that is, a cell or small group of cells becomes spontaneously active at a high frequency, thereby escaping from the domination of the normal pacemaker and causing the myocardium to be activated in an abnormal sequence. The rate of the putative pacemaker is sufficiently high that the tissue cannot respond to every impulse in an orderly fashion. Hence, successive waves are conducted erratically, producing the characteristic rapid, irregular trace on the electrocardiogram. Variants of this theory suggest that multiple ectopic foci are active simultaneously, either forming spontaneously or developing in response to rapid excitation from a previous focus.

According to the second major theory, fibrillation and flutter are produced when a wave of activity, diverted into irregular paths by conduction blocks, reenters areas of tissue that it had excited previously, thereby forming a closed circuit over which activity can be conducted continuously. According to variations on this theory, there may be one or more than one reentry path, and the circuit(s) may be shifting and irregular or (in the case of flutter) fixed and confined, possibly associated with the perimeter of an anatomic obstacle such as the opening of a great vein.

The numerous experimental attempts to resolve these differing views of the nature of flutter and fibrillation have been hampered by the difficulty of evaluating impulse conduction during the continuous mode. Discontinuous-mode conduction has been studied successfully in

humans and animals, in intact hearts and in isolated cardiac tissues, by means of conventional electrocardiograms, by surface electrograms, and by microelectrode recordings. From these studies has come a convincing description of the origin and propagation of low-rate cardiac impulses. However, during flutter and even more so during fibrillation, the patterns of activity are sufficiently irregular and erratic that it has not been possible to identify individual cellular events and relate them to the behavior of the tissue as a whole.

There have been many descriptions of the appearance of cardiac muscle during flutter and fibrillation, with emphasis upon the rapidity of the process, its irregularity, its lack of synchrony and the abruptness with which the rhythm can revert to the normal discontinuous mode of activity. Likewise, there have been developed a number of procedures for producing flutter and fibrillation experimentally, including: local ischemia, such as results from ligation of a coronary artery; a single, strong electric shock during the so-called "vulnerable period"; a series of rapid electric stimuli; mechanical irritation or injury to the myocardium, such as by jabbing with a needle; the local application of a chemical irritant, such as aconitine[2]; the infusion of a hypertonic solution of sodium chloride; and a number of other procedures. However, these observations and recipes do not explain why the rhythms begin, persist, and terminate as they do. (On the other hand, the great variety in the procedures which can initiate flutter

[2] Aconitine does not itself induce flutter and fibrillation, but causes the tissue to respond with repeated depolarizations the next time that it is excited by other means, and these rapid responses may lead to fibrillation.

and fibrillation suggests that the continuous mode of behavior is a very natural state of activity for these tissues).

Anatomically, the mammalian heart is a four-chambered organ, but electrically it consists of just two compartments, which have been called the bi-atrial and bi-ventricular chambers (Schamroth, 1971). There is no electrical boundary between the two atria, nor between the two ventricles; each pair of chambers forms a syncytium and normally is activated as a single unit. On the other hand, the bi-atrial chamber is essentially insulated from the bi-ventricular chamber, except for the specialized conducting fibers of the atrio-ventricular (A-V) node, which provides a slow-conducting pathway between the atrial and ventricular fibers.

Flutter and fibrillation can exist in atrial muscle and they can exist in ventricular muscle, but these arrhythmias are not transmitted across the A-V node (i.e. atrial fibrillation does not lead to ventricular fibrillation, nor vice versa). Although the consequences of the atrial arrhythmias are very different from those of their ventricular counterparts, many investigators believe (in the absence of strong evidence one way or the other) that the underlying mechanisms for these arrhythmias in the atria and the ventricles are probably the same.

Flutter appears as a slower, more coordinated rhythm than fibrillation, though both flutter and fibrillation meet the criteria for continuous impulse conduction. It has been known for nearly a century that stimulation of the vagus nerve can convert atrial flutter to atrial fibrillation, and that upon termination of the nerve stimulation, the rhythm usually reverts from fibrillation to flutter. Not un-

reasonably, this has led many workers to view flutter and fibrillation as two states in the same continuum, with the same underlying mechanism, and differing from one another only in some basic property (such as refractory period) of the cardiac tissue.

This often-made assumption that the shortening of the atrial refractory period (such as is caused by vagus nerve stimulation) would induce a regular continuous rhythm (flutter) to become an irregular one (fibrillation) is one example of the kind of hypothesis which can be tested by mathematical modelling. In fact, it is only in a modelling situation that such a question can be answered, because in animal experiments or human investigations, there is no maneuver which can be relied upon to change only a single parameter value. (For example, vagus nerve stimulation shortens the duration of the atrial muscle refractory period, but it alters many other properties as well, such as the homogeneity of the atrial muscle.)

A mathematical model of the myocardium can be endowed with well-defined structure and properties, its behavior under various conditions can be determined through simulation, and all of the variables can be controlled or measured, as appropriate. Thus, it is possible to determine some (though not necessarily all) of the behavior that is logically consistent with the assumed properties of the excitable medium, and to determine how the behavior is affected when those properties (parameters of the model) are altered. This has been the approach taken in the present study.

The ectopic focus theory is not treated in this study because too many of the essential questions would have to be settled in

advance, by arbitrary assumption, in order to define the model. That is, surely it would be possible to build one or more ectopic foci into the model of excitable tissue and thereby generate rapid, irregular rhythms, but the possibility for further, revealing experiments seems limited. Proper modelling of the ectopic focus will require, first, an adequate theory of the formation of ectopic foci, and would probably involve a direct representation of membrane phenomena and ion fluxes, a level of detail quite removed from the scale of the present model.

The present study explored the conditions under which reentry of excitation can be established in a network of excitable cells which do not have the property of automaticity. In particular, we have:

1. simulated on a computer the behavior of a network which is composed of cells that have been endowed with somewhat idealized representations of the known properties of atrial muscle cells;

2. demonstrated that this network conducts impulses in patterns which are to be expected from the conduction properties of atrial muscle; and, in fact, the simulation has produced several of the more complex conduction phenomena which have been described for atrial muscle but which were not specifically built into this model;

3. shown that patterns of electrical stimulation, known to induce flutter or fibrillation in atrial muscle, produce in this network a self-perpetuating state of activity which continues on after the stimulation has ceased;

4. varied systematically the parameter values of the individual cells and have observed the effects of these changes upon the ease with which continuous-mode activity can be induced, upon the duration for which it persists, and on the manner in which it terminates:

5. tested the ability of cellular parameter changes to convert a regular, single-wave (flutter-like) pattern of continuous activity into an irregular, multiple-wavelet (fibrillation-like) pattern; and

6. in a few instances, returned to the experimental laboratory, in the knowledge of the computer simulation results, and have found in atrial muscle certain patterns of behavior which previously were unknown and unsuspected.

The remainder of this dissertation is organized as follows: Chapter II is a brief review of some of the principal studies that have been concerned with the mechanism of fibrillation and flutter, particularly in the atria, and with emphasis on models that have been proposed for the fibrillatory process; Chapter III contains a description of the model used in the present study, a discussion of its physiological basis, an analysis of its properties in some simple cases, and a note on its implementation in computer programs for simulation; Chapter IV presents the results of simulation experiments concerned with properties of the model "tissue" itself--the relation between the timing and strength of external stimuli, the propagation of premature beats, and some effects produced by non-propagated stimuli; Chapter V describes the results of simulation experiments concerned with the the initiation and persistence of self-sustaining activity in the model and with the effects of variation in model parameters; and Chapter VI contains a summary and discussion of the simulation results. The reader who wishes a quick look at the results related to fibrillation should read the first part of Chapter III and then proceed to Chapter V; however, confidence in the model is greatly supported by the many

ways in which it reproduces known experimental behavior of cardiac muscle, as detailed in Chapter IV.

Chapter II

HISTORY

Fibrillation was probably observed as early as 1842 by Ericksen, who described how the forceful contractions of a dog's ventricles degenerated into "tremulous motion" after the coronary arteries were ligated. Ericksen did not remark further upon the phenomenon, but in 1850 Hoffa and Ludwig gave an unmistakable account of the condition sometimes produced by strong electric shocks to the dog ventricles:

> . . . it is never possible to induce a sustained contraction by means of electric shock. On the contrary, the following phenomenon appears: if a very strong electric current strikes a rather excitable heart, a localized tetanus arises around the electrode, observable as a small, weak bulge, particularly prominent in fish and frog hearts. Outside of this continuously contracted spot, the heart falls into an extraordinarily rapid, completely irregular motion of very low intensity. The irregularity of this motion derives from the fact that the individual anatomical elements lose connection with each other and cease contracting synchronously; whereby a chaotic relation of rhythm and intensity arises. . . .[1]

The first systematic investigation into the nature and mechanism of fibrillation was reported by J.A. McWilliam in 1887. Although his experiments (on "dog, cat, rabbit, rat, mouse, hedgehog, and fowl") dealt mostly with the ventricles, his principal discoveries and deductions underly the classical theories of both ventricular and atrial fibrillation.

Observing that rapid electrical stimulation of an isolated ventricle could induce a fibrillation which spread throughout the entire

[1] Hoffa, M., and Ludwig, C., Einige neue Versuche uber Herzbewegung. Z. rat. Med., 9, 107, 1850, pp. 128-129.

preparation, while the same preparation exhibited apparently normal contractions when stimulated at a more moderate rate, McWilliam concluded that

> The state of arhythmic fibrillar contraction is essentially due to certain changes occurring within the ventricles themselves. It is not due to the passage of any abnormal nerve impulses to the ventricles from other parts, or to the interruption of any impulses normally transmitted to the ventricles and necessary for their normal coordinated action. The condition is not due to injury or irritation of the nerves that pass over the ventricles from the base of the heart.[2]

McWilliam was probably the first to use the term "flutter" in describing the result of electrical stimulation of the atria: a rapid, regular rhythm developed, whose persistence appeared related to the strength of the initiating stimulus. He reported that flutter was abolished by stimulation of the vagus nerve, but in retrospect it seems more likely that vagal stimulation caused the conversion of a "coarse" fibrillation to a finer, less discernible fibrillation (Lewis, 1925).

As to the detailed mechanism of fibrillation in either atrium or ventricle, McWilliam could only guess; yet his speculation concerning ventricular fibrillation sounds remarkably like current hypotheses of reentry and continuous conduction:

> The peristaltic contraction travelling along such a structure as that of the ventricular wall must reach adjacent muscle bundles at different points of time, and since these bundles are connected with one another by anastomosing branches the contraction would naturally be propagated from one contracting fibre to another over which the contraction wave had already passed.[3]

[2] MacWilliam, J.A.: Fibrillar contraction of the heart. J. Physiol. 8:296, 1887, p. 297.

[3] Ibid., p. 308.

A.G. Mayer's experiments on scyphomedusae provided the earliest biological model for what later came to be known as the circus movement hypothesis for fibrillation and atrial flutter (Mayer, 1908; Rytand, 1966). By removing the center and periphery from the disk-shaped jellyfish Cassiopea xamachana, he obtained a ring of muscular tissue which could be excited by electrical, mechanical, or chemical stimuli. Once initiated, waves of activity would travel around the ring in both directions from the point of stimulation, meeting on the opposite side. According to Mayer's interpretation, cancellation of two such waves was incomplete, with the result that the stronger wave would remain circulating about the ring, in one direction, indefinitely (Mayer, 1908). Later work by Mayer and by others has pointed toward the site of stimulation, rather than the antipodal region, as the location of the asymmetry of conduction which produces a unidirectional wave (Mayer, 1917; Kinosita, 1941; Wiener and Rosenbleuth, 1946). (The presumed difficulty of initiating unidirectional waves in cardiac muscle has been cited as an objection to circus movement theories, but as the present study demonstrates, a "circus rhythm" need not originate with such waves.)

By making incisions in the scyphomedusa ring as shown in figure 2.1, Mayer caused the length of the conducting pathway to be essentially doubled. Instead of increasing conduction time by the expected factor of 2, the wave took only 1.72 times as long to complete a circuit. He concluded that the propagation rate had increased accordingly, due to the fuller recovery of the tissue between each activation. In recording this dependence of conduction velocity on the tissue's state of excitability, Mayer was the first to notice a relation important in

Figure 2.1. Doubling the Conduction Path in a Tissue Ring by Incision.

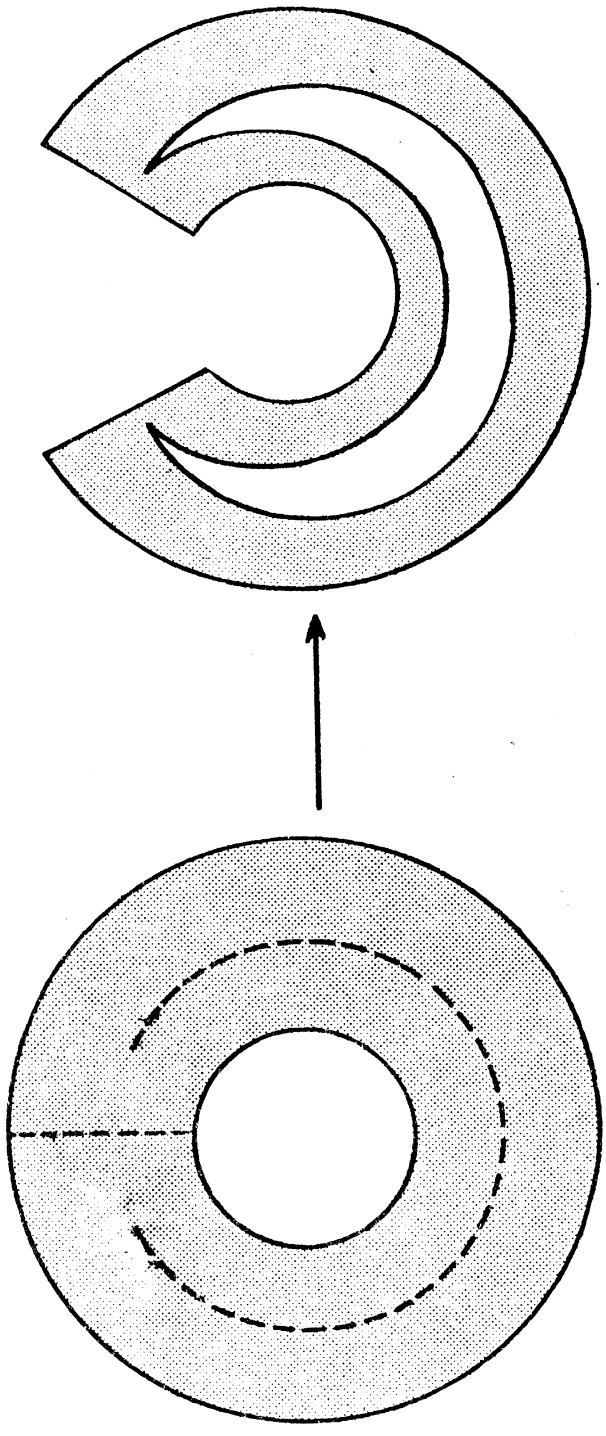

Figure 2.1

subsequent theories of cardiac arrhythmias, although he himself paid little attention to problems of cardiac physiology per se.

In experiments on frog hearts, G.R. Mines (1913) discovered several important properties of cardiac tissue. First, he noted the effect of heart rate on the cardiac electrogram, showing that the duration of the ventricular complex decreased as the heart rate increased. Second, he noticed that the rate of rise of the ventricular spike also decreased as the stimulation rate was increased, from which he concluded that the velocity of propagation was slowed at higher heart rates. Third, he found that increasing the heart rate shortened the duration of the ventricular refractory period. In the absence of accurately-timed stimulation, a direct measurement of the duration of the absolute refractory period was impossible. But Mines devised a simple experiment to obtain the information indirectly:

> If the absolute refractory phase of the ventricular muscle is directly related to the duration of the electric disturbance in the muscle, the ventricle should be able to take a higher rate of rhythm if this rate is approached gradually than if approached abruptly.[4]

Mines stimulated a frog ventricle at a low rate, so that it followed every stimulus. Increasing the rate, he reached a point at which the ventricle could not follow every beat, but responded only to alternate stimuli. He noted this rate, then reduced the stimulation frequency to a level at which the ventricle once again followed every stimulus. Then he increased the frequency slowly to a point just below the rate at which the 2:1 block had appeared previously. With the ventricle thus

[4] Mines, G.R.: On dynamic equilibrium in the heart. J. Physiol. 46:349, 1913, p. 363.

beating rapidly but regularly, he interrupted the stimulator for several cycles; upon restoring the connection, he found that the ventricle responded only to every alternate stimulus.

According to Mines,

> The explanation is simple enough. After the pause, the next response of the ventricle has a longer electric response and a longer absolute refractory period: the second stimulus of the new series therefore falls within the refractory phase and produces no response. The third stimulus finds the muscle excitable, the fourth inexcitable, and so on. But when the same rate of stimulation was approached by a gradual acceleration, each stimulus fell just outside the refractory period of the response due to the last, and thus while the rhythm was accelerated the duration of the refractory period, like that of the electric response of the ventricle, became shorter and shorter.[5]

Mines made a number of observations concerning the effects of rate and rhythm on the mechanical response of the heart muscle. In one series of particular interest to the understanding of arrhythmias, he considered the phenomenon of alternation, in which evenly-spaced stimuli elicit alternately large and small contractions. Mines concurred with an explanation offered earlier by Gaskell (1882), viz., that during each alternation, part of the muscle was refractory while another (unequal) part was excitable, so that each beat was really a partial systole.

Using a strip of tortoise atrium, Mines demonstrated that stimuli applied at the center could stimulate the left and right halves (A and B) alternately, provided a single, properly-timed, extra stimulus was applied either to A or to B. A second extrasystole, properly placed,

[5] Ibid., pp. 363-364.

could cause the preparation to revert to the condition in which both sides followed the driving stimuli synchronously. The important principle thus demonstrated was the establishment and persistence of a purely dynamic block in an otherwise reasonably homogeneous tissue. Mines appreciated the significance of what he had shown:

> The experiment provides a coarse model of extreme alternation in which the alternating portions of muscle are separated visibly. Its real interest lies in the fact that at any time, if the rather rapid rhythmic series of stimuli is interrupted, a stimulus applied to the region A or to B causes response all over the muscle. Their apparent independence during the course of alternation is essentially due to a special condition of the muscle which characterizes its dynamic equilibrium at a rather high level of activity.[6]

While investigating the phenomenon of reciprocating rhythm (also known as "echo beats"), Mines made incisions in the atrial and ventricular walls of a tortoise heart so as to form a ring of conducting tissue, in which he then easily established a circulating wave of excitation. In view of his previous experiments, which showed that at increased rates of stimulation the wave of activity shortened and its velocity of propagation decreased, Mines proposed that circulating waves of activity were the basis for fibrillation. He believed that closed circuits existed in the myocardium, and that these could form the path(s) over which circus movements would take place.

From Mines' description, it seems that he had in mind rather fixed circuits; moreover, his hypothesis assumed the existence of some (unspecified) initiating event which could start a wave going in only one direction around such a circuit. In view of the present study,

[6] Ibid., pp. 369-370.

these two properties appear unduly restrictive; yet they have formed the basis of many objections to the circus movement hypothesis. Nonetheless, Mines was probably the first to propose reentry of excitation and continuous conduction as the mechanism of cardiac fibrillation.

Additional evidence that fibrillation entails processes that involve the entire bulk of the myocardium was provided by W.E. Garrey's experiments on dog and turtle hearts (1914, 1924). Garrey showed that, in dog, small pieces of muscle separated from a fibrillating atrium by excision or clamping would cease fibrillating even though they retained normal excitability. Excising the section of tissue at which the fibrillation had been initiated (by electric shock), however, had no effect on the persistence of fibrillation in the remainder of the muscle. Larger sections cut from a fibrillating ventricle would continue fibrillating for a time roughly proportional to their mass; when such trimmings reduced the size of the main muscle mass below some critical value, it too stopped fibrillating. (It should be noted that Garrey's reports were almost wholly descriptive, containing neither details of the experimental procedures nor quantitative presentations of results. Interpretation of his findings is, therefore, somewhat speculative.)

Garrey found that fibrillation could not be transmitted from one muscle mass to another across a narrow connecting isthmus, and that, in general, fibrillation seemed impossible in narrow muscle strips. He also noticed that activity could propagate indefinitely around rings of tissue cut from turtle ventricles, but that the activity did not necessarily involve the whole cross-section of the muscle on every circuit; from this he concluded that dynamic conduction block and

multi-path propagation were likely mechanisms for fibrillatory activity. He suggested that in the ventricles, in particular, fibrillation was due to direct activation of the myocardium resulting in slow, irregular conduction along the muscle fibers, in contrast with the normal rapid activation of the myocardium by means of the specialized conducting system. Modern descriptions of this mechanism emphasize the difference between aberrant, slow, longitudinal conduction in the ventricle and the normal, rapid conduction in the transverse direction (endocardium to epicardium) mediated by the Purkinje system (Schamroth, 1971).

The careful, detailed studies of Sir Thomas Lewis (1925) formed the basis for the widespread acceptance of the circus movement theory as the mechanism of atrial (and ventricular) flutter and fibrillation. Lewis used electric shocks to initiate arrhythmias experimentally in dogs, and was cognizant of the difference between the arrhythmias that appeared during stimulation and those that persisted after the stimulator had been turned off; only the latter, he believed, were truly comparable to the conditions seen clinically. (This is an important distinction, which has been missed by some of Lewis' critics.)

By measuring the arrival times of flutter waves at various points on the atrial surface, relative to a standard EKG deflection, Lewis found that the wave of activity seemed to travel in a circular path around the orifices of the great veins in the right atrium. He called this the "mother wave", and referred to its offshoots--which were not separate waves, but merely the propagation of activity from the main loop--as "centrifugal" waves. The leading edge of the mother wave was considered to be advancing always in the incompletely-recovered wake

of its own trailing edge, which explained why the conduction velocity of a flutter wave was always lower than normal; this also explained the increased flutter rate on vagal stimulation, since the shortened refractory period (a known effect of stimulating the vagus) would allow the circus wave to follow a tighter, faster loop.

Lewis demonstrated the slow and erratic conduction of premature beats by means of an experiment in which a linear array of recording electrodes was arranged along a radius line drawn outward from the stimulating electrode: under conditions of rapid stimulation, the recording electrodes were not always activated in linear sequence, as they would have been with orderly propagation. Fibrillation, then, was said to involve the same basic circus movement, but with a shorter excitable gap (distance between the wave rear and the pursuing wave front) which caused the advancing wave to interlace with its own wake, resulting in a more sinuous conduction path and the characteristic irregularity of fibrillation. In support of this thesis, Lewis argued that the irregularity of electrocardiographic waves recorded during fibrillation was more apparent than real, often appearing transiently in only one lead while quite regular oscillations were visible simultaneously in the other leads.

The presence of an anatomical obstacle, and the initiation of a unidirectional wave around it by rapid stimulation when the muscle was approaching a state of half-rhythm (in which the fortuitously asymmetrical distribution of refractory islets allowed better conduction in one direction than in the other), were prominent features of Lewis' theory of circus movements in the atria. Since ventricular fibrillation was a similar phenomenon with respect to electrocardiographic and visual

appearance, methods of initiation, and persistence beyond the initiating stimulus, he believed that it also was due to a circus movement. As to what might constitute the central obstacle for a ventricular mother wave, however, Lewis was vague, saying only that his records were compatible with a single circus wave but that the actual case might not be that simple. Interestingly, Lewis seems to have been uncertain about the reasonableness of the concept of a circus wave without an anatomical obstacle:

> Theoretically, it is conceivable that a circus movement could exist, once started, in a flat sheet of muscle in the absence of a central aperture . . . but it is difficult to see how a simple circus movement could be started in such a sheet, or how it could continue regularly and without interruption or change.[7]

The present study provides a demonstration of exactly these properties, in a flat sheet of simulated muscle.

R.S. Lillie (1929a, 1929b) produced a chemical model of propagated activation waves in soft iron wire immersed in concentrated nitric acid. Touching the end of the wire with zinc initiated a transient oxidation reaction that propagated down the wire; there was a "refractory period", after which a second wave could be set off. Inserting the end of the wire into a glass capillary produced a spontaneously active focus from which waves were emitted repeatedly; when the ends of the wire were joined, forming a ring, a unidirectional wave could be initiated, establishing a self-perpetuating circus movement. An electrical "action potential" could be recorded with each passage of the oxidation wave.

[7] Lewis, T.: The Mechanism and Graphic Registration of the Heart Beat, 3rd ed. Shaw & Sons Ltd., London, 1925, p. 325.

Lillie suggested that rhythmic activity in cardiac muscle might involve similar oxidation phenomena at cell membranes.

In 1946, Wiener and Rosenblueth attempted to describe atrial flutter and fibrillation mathematically, considering them to be special cases of the general problem of describing the activity patterns which can arise in interconnected networks of excitable elements. (As another such particular network they mentioned the cerebral cortex, in which "reverberations" due to self-sustaining, localized circuits of impulses were believed to be associated with episodes of epileptic seizure.)

The mathematical treatment began with the following postulates, which specify the properties of the excitable medium, viz., the myocardium:

1. Waves of activity spread with constant velocity in all directions.

2. The activity is of constant amplitude and exceeds the thresholds of all neighboring regions which are not absolutely refractory.

3. Any small region can be in one of three states: active, refractory, or resting.

Transitions among the three activity states are governed by these rules:

1. If an active region is adjacent to a resting region, the resting region becomes activated.

2. A region remains in the active state for only an instant.

3. Immediately after becoming activated, a region becomes refrac-

tory for a fixed period of time, after which it returns to the resting state.

Constant conduction velocity and constant duration of refractory period imply that each active wave front is followed by a refractory "tail" of fixed size, which is also the minimum possible interval (in both space and time) by which two successive wave fronts may be separated. Wiener and Rosenblueth called this distance the "wave length", a recognizedly uncommon usage of the term.

The postulates and transition rules contain, implicitly or explicitly, a number of simplifying assumptions, of which the most important are that

a. the conduction velocity of a wave of activity is the same in all parts of the tissue, uniform in all directions, and independent of the past history of activity in the tissue;

b. the absolute refractory period has the same duration in all parts of the tissue, and is independent of other conditions or past history;

c. there is no relative refractory period;

d. the wave front has negligible thickness;

e. there is no variation in the tissue's response to stimulation;

f. the safety factor of conduction is "very large".

One effect of these assumptions is to reduce the differences between atrial and ventricular muscle to a matter of dimension: the atrium may be approximated by a plane, whereas the idealized ventricle must be represented as a solid, probably a nonuniform one.

Using informal, graphical arguments, Wiener and Rosenblueth applied the model described above to planar and solid bodies of various shapes with different-sized obstacles (unresponsive regions) located within them. The aim was to determine those configurations which would allow stable patterns of self-sustaining activity waves, under the supposition that atrial flutter might be explained as the result of waves circulating about the orifices of the venae cavae. Several likely cases were shown to be capable of supporting such activity; for example, they showed how a wave might be made to circulate indefinitely around an obstacle whose perimeter was greater than the wave length, irrespective of the presence of a second obstacle. A number of results were presented in the form of theorems, e.g., "A single stimulus applied to a single point or region can never result in flutter."[8]

Because the establishment of appropriate initial conditions is essential to the initiation of circulating waves such as described above, objections to the circus wave hypothesis can reasonably be raised on the grounds that the requisite initial state is highly improbable. Wiener and Rosenblueth therefore devoted some attention to ways of initiating circus waves. Careful examination of their method, though, shows that they needed to stretch the postulates of the model in order to deal with the central problem: how to initiate an asymmetric wave in a homogeneous medium.

With a planar or solid ring of tissue, the object is to establish a wave that circulates in only one direction; any simple stimulus will

[8] Wiener, N., and Rosenblueth, A.: The mathematical formulation of the problem of conduction of impulses in a network of connected excitable elements, specifically in cardiac muscle. Arch. Inst. Cardiol. Mex. 16:205, 1946, p. 231.

produce wave fronts travelling in both directions which will mutually cancel at a point antipodal to their origin. For a sheet or solid figure the problem is to establish a wave front containing a gap, i.e. one that does not propagate in all directions. A one-way wave in a ring leads to indefinitely self-sustained activity if the ring is large enough; a partial wave in a plane or solid may, upon encountering a suitably sized obstacle, circulate around it indefinitely. The two situations are really the same, and are set up with the same technique: a single stimulus closely followed by a second one applied a short distance away. It is argued that if the second stimulus is applied just as the edge of the refractory tail following the first wave passes by, then the second stimulus will be only partially effective and will propagate away from the refractory region but not into it, thereby creating the desired asymmetry. However, wave fronts in the Wiener-Rosenblueth model are defined as having no thickness, and therefore cannot overlap a resting-refractory boundary. Moreover, even if one could, the boundary will travel as fast as the new wave, so the latter should simply follow the retreating refractory tail. It seems that the establishment of asymmetric waves requires some notion of partial refractoriness and/or partial failure of conduction, neither of which is allowed by the postulates. The lack of a straightforward means of initiating, as opposed to maintaining, self-sustaining activity is a weakness this model shares with others.

Having established a reasonable theoretical basis for viewing flutter as the continuous circulation of one or more waves of activity about an anatomic obstacle, Wiener and Rosenblueth turned to the

question of fibrillation. They seemed to consider fibrillation a fairly distinct phenomenon from flutter:

> It is quite clear that, as opposed to flutter, fibrillation has not an anatomical but a histological basis. In other words, it is clear that the only uniformity from heart to heart in fibrillation is statistical and that the problem can only be approached, therefore, on a statistical basis.[9]

In a complex and lengthy development of statistical mechanics, they attempted to formulate mathematically a description of fibrillation in terms of the basic model described earlier. The result was a set of complicated formulae to which solutions were unavailable; solving these equations was, in Wiener's words, "a question for further and difficult mathematical work."[10]

Wiener and Rosenblueth concluded finally that atrial fibrillation was the result of a circus wave moving randomly about an obstacle. They admitted, though, that the existence of ectopic foci was a possible alternative explanation.

Although perhaps not definitive from an experimental standpoint, the descriptions of flutter and fibrillation given by Wiener and Rosenblueth capture the principal distinctions noted by other users of these terms:

> Flutter consists of a wave or waves of activity in a conducting system with a regular cyclic recurrence of paths, and therefore with a well-defined regular wave front and period.[11]

[9] Ibid., p. 235.

[10] Ibid., p. 251.

[11] Ibid., p. 254.

In flutter, activity is continous, while in normal rhythm beats are separated by periods of complete rest (diastole).

> Fibrillation consists of a continuous activity over randomly varying paths in a network of connected conducting elements.[12]

The main difference from flutter is thus the randomness of the paths, and concomitant lack of well-defined periods.

Two years later, Selfridge (1948) corrected and extended some of Wiener and Rosenblueth's results. Most important for the theory of arrhythmias was his demonstration that a circus movement (a "perpetual flutter") could be established in a homogeneous, planar sheet of muscle that was free of obstacles. Although the method shown for initiating such a flutter wave may appear somewhat unphysiological, this constituted the first rigorous demonstration that a self-sustaining reentry phenomenon was possible without the aid of an anatomical obstacle. Selfridge argued that such a wave, which had a rotating spiral pattern, would be unstable and would be halted by just an infinitesimal increase in the duration of the refractory period. Actually, such waves can be quite stable, if conduction velocity varies with excitability, as the present study shows for the case where the "muscle sheet" is made up of discrete elements; variations in the duration of the refractory period merely shift the locus around which the spiral turns, as long as the total area of the sheet remains adequate.

The first major challenge to Lewis' circus movement theory came in a series of papers by Scherf and his colleagues (Scherf and Terranova,

[12] Ibid., pp. 254-255.

et al., 1953), where experimental flutter and fibrillation were induced by the topical application of aconitine to dog atria. Criticizing Lewis' experiments, they rejected the circus movement theory and argued instead that atrial flutter and fibrillation were due to the rapid emission of impulses from one or more ectopic foci. Aconitine application caused very rapid atrial tachycardia, with rates consistent with those usually associated with flutter; upon stimulation of the vagus, the atrial beats became even more rapid and irregular, just as in fibrillation. The evidence that these arrhythmias were due to impulses from a single focus is convincing: (1) after cooling the site of aconitine application, or separating it from the rest of the atrial muscle by means of a clamp, the arrhythmia stopped; the transition between flutter and fibrillation was a gradual change of rate produced by cooling or warming the aconitine focus; at slow flutter rates, the electrocardiogram showed long isoelectric sections between beats, seemingly incompatible with the idea of continuous conduction; and so on.

Scherf offered a number of cogent criticisms of the mother wave hypothesis, e.g., that Lewis did not examine the entire pathway of the putative circus wave, and that interruption of the supposed pathway by means of a ligature did not stop (aconitine-induced) flutter. But the central question, which Scherf seems to have settled by assumption, is whether the aconitine preparation really constitutes an adequate model of clinical flutter and fibrillation. There is no doubt that aconitine induces a focus of very rapid, sometimes irregular activity. But it is much less clear that the production of arrhythmias by the deliberate establishment of a focus constitutes proof that similar arrhythmias occurring naturally or after electrical stimulation are also due to

focal activity. Indeed, the very differences on which these disputes were based suggest that two or more distinct mechanisms may be involved.

Lewis' experiments concerned primarily arrhythmias which persisted after the initiating electric current had been shut off, while topical aconitine seems to act as a continuing irritant. Scherf held that the arrhythmias induced by aconitine were unifocal, whereas those induced electrically were multifocal; that is, that the electrical stimulus established a focus of rapid activity, whose emanations then triggered other foci, presumably in the sinoatrial and atrioventricular nodes. However, he was not able to explain why the activity from an aconitine focus should not also excite secondary centers.

Using the same aconitine preparation, Prinzmetal et al. (1952) made high-speed motion pictures of fluttering and fibrillating atria in an attempt to determine the patterns of activation. They saw no evidence of circus contractions. Nevertheless, these experiments are subject to the same criticism as those described above, namely, the possible artificial nature of aconitine-induced arrhythmias. Moreover, the relation between the muscle's electrical activity and contractions visible at its surface is not sufficiently clear to warrant definite conclusions about the former based solely on observation of the latter (Dawes, 1952; Tenney and Wedd, 1954).

Finally, the mechanism by which ectopic foci might be initiated and maintained over long periods of time has not been explicitly determined, although various possibilities have been suggested (e.g., Scherf and Schott, 1953). Brown and Acheson (1952) have shown that topical aconitine can produce "electrical" flutter, that is, an arrhythmia which

persists even when the aconitized site is clamped off and in which various parts of the atrium show activity at rapid but differing rates. This lends strong support to the view that a combination of mechanisms may be active, whereby any focal stimulation may, if rapid enough, initiate a self-sustaining activity based on some form of reentry and continuous conduction (e.g., Hecht, et al., 1953). Excellent reviews of these arguments have been published by Katz and Pick (1960) and by Rytand (1966).

The first computer simulation of fibrillatory processes was probably performed in 1962, by Farley--who was modelling not the heart, but nerve nets. He established networks of model neurons whose thresholds were normally distributed; when such nets were "densely connected", i.e. with many local and few distant synapses, stimulation sometimes resulted in self-sustained activity:

> There are many different 'modes' of self-excited oscillation possible. A particularly pervasive and striking one consists of one or more continuously rotating spirals.[13]

Farley noticed that the firing patterns of his model neurons sometimes became periodic, or nearly so. Unfortunately, he did not pursue further experiments related to cardiac arrhythmias.

Swain and Yanagita (1963) constructed an electronic model of circus conduction, consisting of five units connected circularly in series. Each unit contained resistance-capacitance timing networks, relays, and indicator lamps arranged so that, on receipt of an electric signal, it would undergo transition into an absolute and then a relative "refrac-

[13] Farley, B.G.: Some results of computer simulation of neuron-like nets. Fed. Proc. 21:92, 1962, p. 93.

tory period" before returning to the quiescent state. A signal arriving during the absolute refractory period was ignored; one arriving during the the relative refractory period was passed on delayed; one during the quiescent phase was passed on immediately. Using this model, Swain and Yanagita illustrated how a series of premature stimuli could engender conduction delay at every stage of propagation, so that by summation of delay a circus movement could be established in a small system without excessively slowed conduction at any point. Their further suggestion, that the dependence of conduction delay on prematurity should exert a stabilizing effect on circus waves in cardiac tissue, has been supported by the present study.

The computer simulation technique was first applied to cardiac arrhythmias by Moe, et al. (1964). Atrial muscle was modelled as a planar array of units arranged in a hexagonal pattern, so that each unit (except those at the edges) had six neighbors. The units were allowed five states of excitability: quiescent, absolutely refractory, and three stages of relative refractoriness. A unit was excitable whenever not absolutely refractory; when excited, it "fired" after a delay of one to four time-steps, depending on its state when excited. A firing unit transmitted excitation of constant amplitude to all of its neighbors, exciting any which were not absolutely refractory. The duration of the absolute refractory period depended on the duration of the immediately preceding cycle of the unit in question, according to an empirically-based square root law:

$$\text{ARP duration} = k \cdot (\text{cycle length})^{1/2}$$

where the constant k for each unit was drawn from a pseudo-random sequence, values ranging from $\sqrt{10}$ to $\sqrt{20}$. This random variation in refractory period duration was the only source of variation between the units, for they were identical in all other respects. Each time-step represented five milliseconds. Each stage of relative refractoriness lasted two time-steps, for a total relative refractory period equivalent to 30 milliseconds.

Although this model embodies many simplifying assumptions, its implementation on the computing equipment available at the time--an IBM 650--and the sophistication of the experiments performed constituted a true tour de force on the part of Moe and his associates. They were able to demonstrate the development of dynamic conduction blocks, in which rapid external stimulation leads to progressively increasing disorder on successive waves of activity; eventually, isolated conduction failures occur, permitting a reentry that can become self-sustaining. They showed that inhomogeneity among the units is necessary for the initiation of reentrant activity, but not for its maintenance. Finally, they found that moderate changes in the refractory period duration had little effect on the arrhythmia, while substantial (50%) increases in k led to a merging of reentrant waves, followed by arrest.

During simulated fibrillation, the firing frequency differed at different units of the networks. A crude "electrogram", generated from instantaneous counts of the numbers of units in various stages of activity, resembled real electrograms recorded during fibrillation. Trimming off the peripheral layers of the network, or making "cuts" in its interior, caused the activity to become more regular but did not terminate it. Altogether, the model resembled in many respects the

behavior seen in atrial muscle subject to rapid electrical stimulation.

An extensive series of papers has appeared recently in the Russian literature concerning mathematical models of cardiac muscle related to theories of fibrillation. Much of the theoretical research seems to have been stimulated by Wiener and Rosenblueth's 1946 paper on the conduction of impulses in excitable media. Most of the papers are concerned with reentry phenomena and varieties of circus movements (Krinskii, 1966, 1970, 1971; Balakhovskii, 1965; Kholopov, 1968), though a few discuss "echoes" in single fibers (Krinskii and Kholopov, 1967; Kholopov, 1968). Of particular interest are the papers of Krinskii on reentrant theories of fibrillation (1966, 1970, 1971); Krinskii et al. (1967) on the critical mass for fibrillation; Krinskii and Kholopov (1967) on problems of modelling with discrete vs. continuous media; Krinskii et al. (1971) on the mechanism of anti-arrhythmic drugs; Balakhovskii (1965) and Kholopov (1968) on fibrillation theory; Abakumov et al. (1970) on errors in the Wiener and Rosenblueth paper; Berkinblit et al. (1965a, 1965b) on the electrical properties of syncytial structures; Arshavskii et al. (1964) on the conduction failure in premature beats; Arshavskii et al. (1965) on the steady-state behavior of pulses in a ring of excitable tissue; and Gel'fand and Cetlin (1960) and Gel'fand and Kazdan (1961) on the supporting mathematics.

There are several papers on the simulation of cardiac arrhythmias (Lukashevich, 1964, 1964; Chebotarev, 1968), but these are generally unsatisfying due to inadequacies in the description of the models, in the establishment of a physiological basis for the assumptions of the models, and in the presentation of the results of simulation.

A complete review of these Russian papers would be quite valuable, since they contain many interesting ideas and are not cited often in the Western literature; that task, however, is beyond the scope of this work.

Chapter III

THE MODEL

I. General Features

The model of atrial tissue used in this study is essentially that devised by Flanigan and Swain (1968; Flanigan, 1965), who investigated the effects of tissue geometry on conduction in the atrioventricular node. It consists of a planar array of units called cells, each of which represents a small region of muscle tissue.[1] Alternate rows in the array are offset by one-half cell, thereby creating a uniform hexagonal neighborhood structure in which each cell (except at the edge of the array) has six equidistant neighbors. The cells constitute a network, in that each is "connected" to its neighbors, to which it can send and from which it can receive stimulation.

The cells are "excitable", and have an activity cycle characterized by five principal states[2] which occur in the following sequence: Quiescent, or resting; Stimulated, in which a cell has received superthreshold stimulation but has not yet responded to it; Firing, in which a cell responds to stimulation by providing excitation to its neighbors; the Absolute Refractory Period (ARP), in which a cell is completely

[1] A model cell, so called because the model network is formally equivalent to a cellular automaton, is not to be confused with a cardiac muscle cell. Each model cell represents an aggregation of thousands of muscle cells.

[2] Strictly speaking, only the quiescent state is really a single state; the others are composed of chains of substates, whose transitions mark the passage of time.

insensitive to stimulation; and the Relative Refractory Period (RRP), in which a cell can be excited only by a supernormal stimulus.

Passage of a cell from one state to another is governed by a common rule or transition function, which is applied to all the cells simultaneously; a single application of the transition function constitutes, by definition, one time-step of the simulation. Repeated application of the transition function generates a state history of the model over a simulated interval of time, which is referred to as the behavior of the model. The correspondence between simulated time and real time is determined by the parameter values used to define the cell states and transition function. In the present model, a simulation time-step is roughly equivalent to one millisecond of real time.

A cell is potentially excitable whenever it is in either the quiescent or the relatively refractory states. During these periods a cell may receive excitation from its neighboring cells and/or an "external" stimulator. The excitation from these sources is summed (spatial summation) and compared with a threshold; whenever the sum exceeds the threshold, the cell "fires". The threshold is high early in the relative refractory period, declining linearly during the RRP to a lower value. At the end of the RRP the cell enters the quiescent state, in which the threshold remains constant.

When firing, a cell first enters the stimulated state for a variable period of time, which represents conduction delay. The simulated state's duration is longer, i.e. the conduction delay is greater, whenever the cell is incompletely recovered from a previous firing or when the stimulus is just barely adequate. Upon entering the firing state, the cell produces a local response, which will be

included in the summation of excitation to each neighboring cell. The local response decays linearly over the duration of the firing state; the fact that it persists across several time-steps allows adjacent firing cells to contribute to the excitation of a neighbor even when they are not in exact synchronization--a kind of temporal summation. At the end of the firing period the local response becomes zero, and the cell enters the absolute refractory period. Even though the local response is expressed only during the firing period, its decay is computed as though it began at the moment the cell was stimulated; thus, a greater conduction delay (longer duration of the stimulated state) reduces both the magnitude and the duration of the local response.

The duration of a cell's absolute refractory period depends on the rate at which it is firing. The interval between successive excitations of a cell is called the cycle length[3]; the duration of the ARP is proportional to the square root of the immediately preceding cycle length (Moe, et al., 1964; Bazett, 1918). The constant of proportionality varies from cell to cell, being assigned at the beginning of an experiment from a pseudo-random sequence. In almost all of the experiments reported here, this random component in the determination of the ARP duration was the only source of variation in the array of cells, which were otherwise identical.

At the end of the ARP the cell enters the relative refractory period, which is of fixed duration and during which the threshold of excitation decays toward its resting value. At the end of the RRP the cell is said to be in the quiescent state; it remains there, with the

[3] Also called activation interval, when necessary, to distinguish it from the cycle length of the external stimulator (q.v.).

threshold constant, until it next receives superthreshold stimulation.

The major activity states of the model cells correspond approximately to various phases of the cardiac cell action potential, and the recovery of excitability represented by the threshold function in the model is associated with restoration of resting potential in the real tissue. Nevertheless, the cell membrane potential is not explicitly represented anywhere in the model: the cells' functional characteristics are being simulated, not their detailed physical states.

Initially, all cells of the network are quiescent. Since the quiescent state is a stable one, there being no automaticity in the model, activity can be initiated only from an external source. The simulation therefore includes a representation of a stimulating electrode, whose position may be specified by the experimenter and whose strength may be varied. Cells "under" the stimulator simply include its output (when it is "on") in the summation of stimulation from their neighbors; if the total stimulus exceeds their thresholds, they fire. In early versions of the simulation the external stimulator had a fixed effective radius and affected all cells within that radius equally, but later the effective radius was made variable and the stimulus strength was made to fall off with distance according to an inverse-square law.

The maximum size of the model network was determined by the computing system used for a particular experiment (see below). For most experiments, the array contained 25 rows and 25 columns, although in some cases arrays up to 51 by 51 were used. With hexagonal packing, these could most logically be arranged to form either a near-square or a parallelogram. But in either case, it is advantageous to cut off the

corners of the figure in order to reduce the computing requirements without significantly affecting the behavior of the system (Moe, et al., 1964); the result is a hexagon-shaped network (figure 3.1). The addition of a sixth, "unresponsive" state to the cells' state space afforded a convenient means of altering the shape of the network: unresponsive cells could be used to form slits, holes, etc. By making the entire outer layer(s) of cells unresponsive, the size of the network could be effectively reduced.

Stimulation applied to cardiac muscle during the relative refractory period is often termed premature. Such stimulation, when superthreshold, commonly results in a response which is delayed in time and/or reduced in amplitude as compared with a normal action potential. The resulting delayed conduction of premature beats is a functionally important characteristic of cardiac tissue. Premature excitation of the model cells also results in impaired conduction, and is the major mechanism by which various "arrhythmias" can be produced in the simulated tissue.

II. The Neighborhood

The simplifying assumptions which were adopted in the construction of this model are probably nowhere more evident than in the definition of the model's geometry, i.e. the neighborhood structure of the cellular automaton. First, in modelling a section of atrial muscle large enough to demonstrate the conduction phenomena we wished to study, the simulation of individual cardiac fibers is ruled out simply by pragmatic consideration of computing capacity. Hence, each model cell is said to represent an aggregation of muscle fibers comprising a small region of atrial myo-

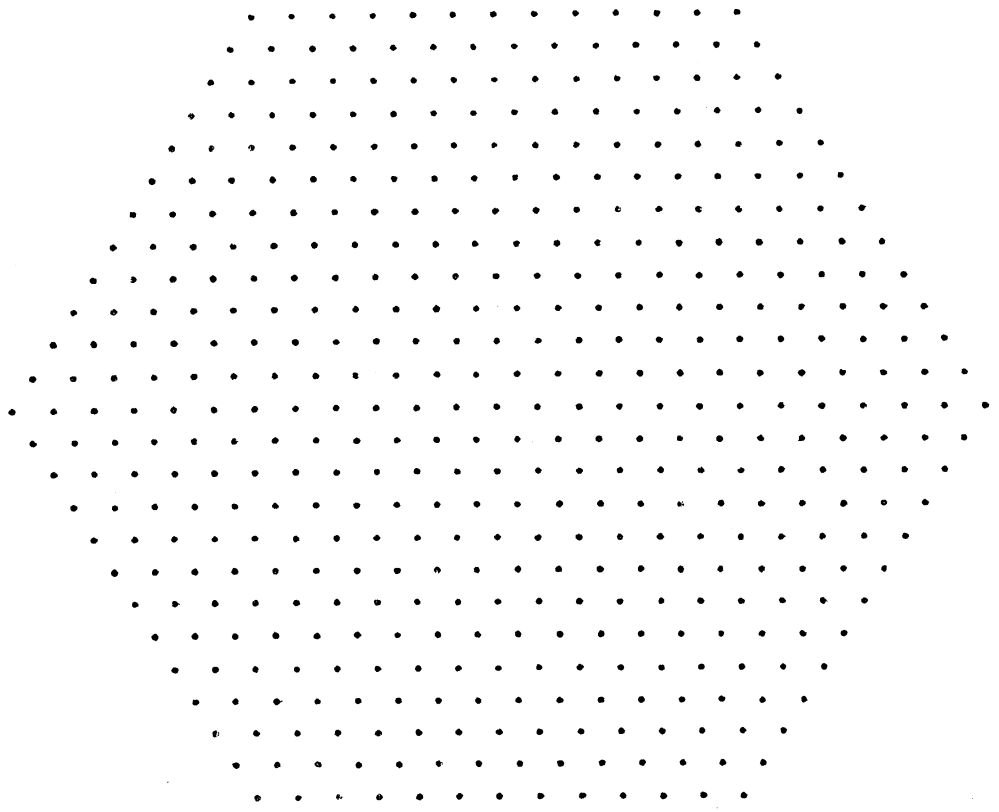

Figure 3.1. A 469-cell Hexagonal Array (25 rows, 25 columns).

cardium, and it is assumed that, with respect to excitability, the cardiac cells of such a region behave approximately as a single entity. (See the discussion of "scale", below.)

Second, since except for their auricles the atria are relatively thin-walled chambers, the muscle is modelled as a two-dimensional structure. That is, the aggregation which forms a model cell includes the entire thickness of the myocardium. Conduction time for an activity wave to penetrate the muscle, and variations in wave velocity with depth or muscle thickness, are assumed to be negligible.

Third, the muscle is assumed to be isotropic, that is, without any preferred direction(s) of conduction. This property was approximated by arranging the simulated cells in a hexagonal array, so that each cell has six equidistant neighbors. Such an array is obviously not isotropic, there being six "preferred directions of conduction", symmetrically disposed; but it is an improvement over a rectangular space, and is probably the best that can be done short of a random-placement scheme, which would entail substantially greater complexity.

III. The Transition Function

The events in a typical cell's firing cycle are shown on figure 3.2, which is drawn to scale for a cycle length of 200. The time axis is integer-valued and labelled in milliseconds, although, strictly speaking, its units are simulation time-steps. The magnitudes of thresholds and local responses are both reckoned in the same (arbitrary) real-valued units, which are marked on the ordinate.

In recognition of the distinction between a model and its realization in any particular computer program, this section describes the

transition function informally, using more or less conventional mathematical notation.[4] In the following description[5], the five states of a cell's activity cycle will be abbreviated to their initial letters: Q (quiescent), S (stimulated), F (firing), A (absolutely refractory), R (relatively refractory). Simulated time is indicated by the integer-valued variable t, which may take on values 0, 1, 2, ... Particular moments in simulated time will be indicated by subscripts on t; for example, the time-step on which a given cell undergoes a transition from the stimulated to the firing state would be represented as t_{SF}. In the simulation program, whenever the cell is in state S, F, A, or R, the variable TCS contains the time at which the next change of state will occur. Thus, during a firing cycle, this variable successively represents t_{SF}, t_{FA}, t_{AR}, and t_{RQ}.

Duration of the various states is denoted by τ, appropriately subscripted; the duration of a given cell's absolute refractory period, for example, is designated τ_A.

1. Threshold

In states R and Q, a cell is excitable and has a threshold of excitation, θ. In the quiescent state, the threshold remains constant at its minimum value,

$$\theta(t) = \theta_{min}$$

where $\theta(t)$ is the threshold at time t.

When a cell enters the relatively refractory period its threshold has a higher value, θ_{max}; during the RRP the threshold declines linearly with

[4] See table 3.1 for a list of variable names. Not all of the variables in the following equations appear explicitly in the simulation program.

[5] In the interest of clarity, the physiological basis for this model is presented separately; see section V of this chapter.

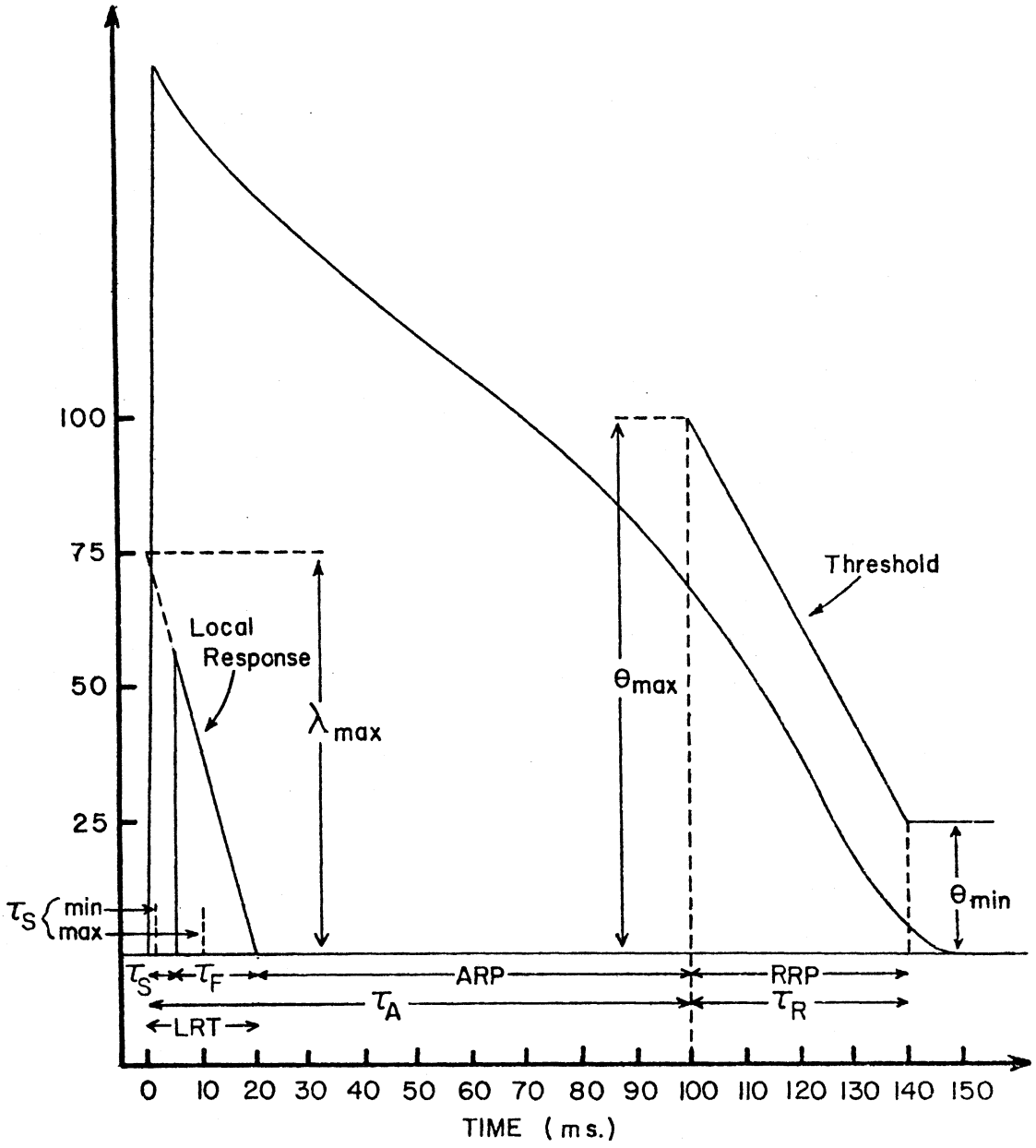

Figure 3.2. Model "Action-Potential".

The simulation variables are shown in relation to the events of a typical cycle. Drawn to scale at a cycle length of 200 time-steps.

Table 3.1. The Principal Global Parameters and Local Variables of the Simulation Programs

Global Parameters	Parameter Name
Maximum strength of local response (λ_{max})	LRMAX
Maximum value of threshold (θ_{max})	THMAX
Minimum value of threshold (θ_{min})	THMIN
Mean value of k_i ($\bar{k}$)	KMEAN
Range (±) of variation in k_i from $\bar{k}$ (k_σ)	KSIGMA
Duration of relative refractory period (τ_R)	RRP
Duration of local response period ($\tau_S + \tau_F$)	LRT
Conduction delay factors (F_1,F_2,F_3)	F1, F2, F3
Strength of external stimulator (Ψ)	EXTSTIM
Location of external stimulator (X_0,Y_0)	X0, Y0
Maximum value of repolarization-phase stimulus	REPOLMAX
Random number generator seed	ISEED

Local ("Cell") Variables	Variable Name
Current state number	STATE
ARP constant	K
Wave number	WVNO
Last firing time (time cell most recently entered S state)	LFT
Time to change state (time-step on which next state change is due)	TCS
ARP duration in current firing cycle	ARPD
Conduction interval (see "statistics")	CI

time to the resting value, θ_{min}:

$$\theta(t) = \theta_{min} + (\theta_{max} - \theta_{min}) \frac{t_{RQ} - t}{\tau_R}$$

or, in terms of computer program variables,

```
TH = THMIN + (THMAX - THMIN)*(TCS - T)/RRP
```

2. Summation of Stimulation

Let $\theta_i(t)$ be the threshold of the i^{th} cell at time t, N_i the index set of neighbors of the i^{th} cell, $\lambda_j(t)$ the local response of the j^{th} cell at time t, and $\psi_i(t)$ the input to the i^{th} cell from the external stimulator at time t. (The computation of these quantities will be discussed below.) Then $\Lambda_i(t)$, the total stimulation to the i^{th} cell at time t, is defined as

$$\Lambda_i(t) = \psi_i(t) + \sum_{j \epsilon N_i} \lambda_j(t)$$

Whenever $\Lambda(t)$ equals or exceeds $\theta(t)$ for a given cell, that cell "fires" by entering the S state. When $\Lambda(t)$ is less than $\theta(t)$, the cell's state is not affected.

In states other than Q and R, a cell is unexcitable; θ is undefined, and the computation of Λ is not performed.

3. Conduction Delay

The stimulated state is a latent period preceding the firing state, representing conduction delay. The greater the duration of this state, the longer is the interval between stimulus and response at the cell in question, and hence the greater is the delay in the propagation of the

activity wave "through" that cell. In this model, the major determinant of conduction delay is the cell's own state of excitability at the time it is stimulated: a fully excitable (i.e. quiescent) cell delays much less than a cell which is poorly excitable (i.e. in early RRP). A minor component of the conduction delay is determined by the strength of the stimulus the cell receives, relative to its threshold: a just-barely-adequate stimulus increases the delay, while a strong stimulus affects it negligibly.

The duration of the S state, then, is computed by the formula

$$\tau_S = F_1 \frac{\theta(t)}{\theta_{min}} + F_2 \frac{\theta(t)}{\Lambda(t)} + F_3$$

where t is the time at which the cell is stimulated, and F_1, F_2, and F_3 are constants specified by the experimenter for each run.

In the first term, the ratio of present threshold to resting threshold is a measure of the cell's excitability, being 1 when the cell is quiescent and greater than one (up to a maximum of $\theta_{max}/\theta_{min}$) when it is relatively refractory. It provides a direct measure of the "earliness" of a premature stimulus, owing to the linear slope of the threshold-recovery curve. In the usual case, with F_1 set to 2.0 and θ_{max} equal to four times θ_{min}, the first term's contribution to conduction delay ranged from 2 to 8 time-steps.

The ratio of present threshold to stimulus strength, in the second term, is at most 1, else the cell is simply not excited. As the stimulus strength increases, the ratio grows smaller and smaller. In most experiments F_2 was equal to 2.0, so the delay contribution from the second term varied from 2 time-steps to essentially zero.

The constant term, F_3, was included for convenience in performing certain experiments, such as making the conduction delay independent of dynamic factors. Its normal value was zero.

During the S state, a cell has no effect on its neighbors, and is unaffected by them.

4. Local Responses

During the firing state a cell is a source of stimulation to its neighbors, corresponding to cardiac tissue in the early phases of the activity cycle. This stimulating force, known as the local response, is measured in the same arbitrary units as threshold and follows the time-course shown in figure 3.2. In the model, variation in the local response is achieved through a complementary relationship between the S and F states. That is, the magnitude of the local response is determined by a curve which has the value λ_{max} at the beginning of the S state and decays linearly to zero at the end of the F state. The total duration of the S and F states, that is, $\tau_S + \tau_F$, is constant. But the local response is only expressed during the F state; the greater the duration of the S state, the smaller the magnitude of the local response when it occurs, and the shorter the time remaining in the F state over which it acts. (See figure 3.3.)

For any cell in the F state, then, the magnitude of its local response is given by the formula

$$\lambda = (t - t_{FA}) \frac{\lambda_{max}}{(\tau_S + \tau_F)}$$

or, in terms of computer program variables,

LR = (T - TCS) * LRMAX / LRT

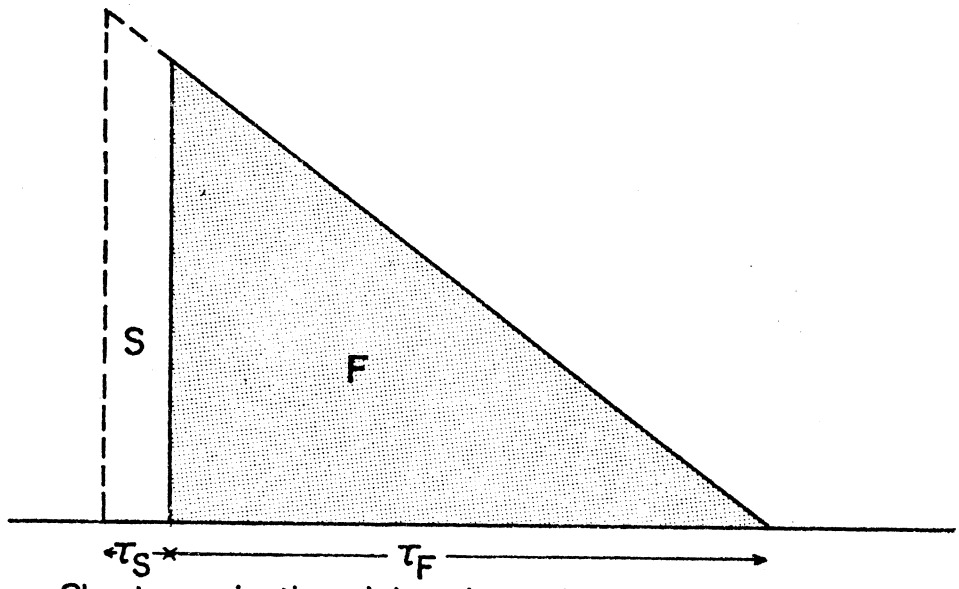

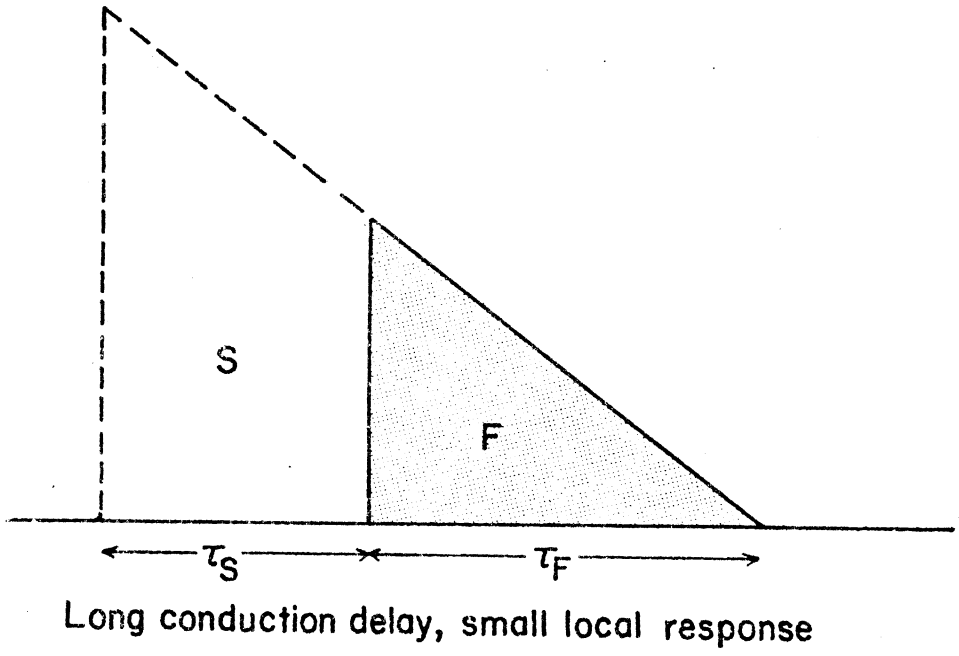

Figure 3.3. Complementary Relation Between Stimulated and Firing States of the Model Cell.

In general, the local response will vary from cell to cell in both magnitude and duration, even though all are following a common time course, because of variation in the duration of the S state. The total stimulation to a cell is computed by summing the local responses of all its neighbors which are in the F state, plus input from the external stimulator, if any; the result is compared with the cell's present threshold. This computation is repeated on every time-step, so that a firing cell contributes to the stimulation of its neighbors over the entire duration of its F state.

A firing cell stimulates all of its neighbors equally.

5. The Absolute Refractory Period

The duration of the absolute refractory period for a given cell depends on the rate at which that cell has been firing.[6] Specifically, the ARP duration is proportional to the square root of the immediately preceding "cycle length":

$$\tau_A = k_i\sqrt{C_i}$$

where C_i is the interval between the current and the immediately preceding firings of the i^{th} cell, and

k_i is a constant which is unique to the i^{th} cell.

Whenever a cell is stimulated (i.e. at t_S: the time it enters the S state), the time interval since its previous stimulation is computed;

[6] See section V of this chapter.

the square root of that interval, multiplied by the cell's k, yields the duration of the ARP for that firing cycle. For the purpose of this computation, the simulation program records each cell's t_S as its "last firing time":

```
ARPD = K * SQRT(T - LFT); LFT = T;
```

where all variables except T are local to the cell in question, and the computations are performed as part of the process of putting a cell into the S state.

The coefficients k are independent, identically distributed random variables. When the model network is initialized, a k value for each cell is drawn from a uniformly distributed pseudo-random sequence with mean $\bar{k}$ and range $2k_\sigma$. Once assigned, the k's amount to constant parameters of the model which are not modified by execution of the simulation (although, like all such parameters, they may be changed by the experimenter during the course of simulation--either explicitly, by specifying new k values for specific cells, or implicitly, by changing $\bar{k}$, k_σ, or the seed of the random number generator.)

These randomly assigned k's constitute the only source of built-in variation in the model network, for in all other respects the cells are initially identical to each other. The differences in k, however, induce differences in refractory period durations, which in the presence of premature stimuli, result in a variety of activity patterns. But if the k's are made to be all the same ($k_\sigma = 0$), or if no stimuli are applied prematurely, then the patterns of activity in the network will always be perfectly symmetrical.[7]

[7] This applies to the "leading edges" of activity waves. Whenever $k_\sigma > 0$, there will be some irregularity in the trailing edges (i.e. the A-R boundary) of activity waves.

As defined above, the cycle length is the interval between two successive stimulations of a cell. That is (using a prime to denote the value of a variable on the previous firing cycle),

$$\text{cycle length} = t_S - t_S'$$

But the cycle length could equally well be defined in terms of the interval between successive firings of a cell, i.e.

$$\text{cycle length} = t_F - t_F'$$

These two quantities will differ whenever τ_S differs from τ_S'. Several conduction-time experiments were run in which cycle length was computed both ways, for purposes of comparison. The results indicate that the difference is not significant when, as here, the maximum differences in τ_S are small relative to the duration of the relative refractory period.

The square root law relating refractory period duration to the cycle length has been chosen rather arbitrarily, principally for consistency with previous simulations of this sort (Moe, et al., 1964; Flanigan, 1965)--there being no compelling arguments in favor of some other function. However, the following exponential relationship has been proposed by Hoffman and Cranefield (1960):

$$\tau_A = A_\infty(1 - e^{-\alpha C})$$

where A_∞ is the ARP duration at "infinitely long" cycle lengths,

C is the cycle length of the given cell, and

α is a decay constant.

This formula has the advantage that refractory period duration does not become arbitrarily large with increasing cycle length, but rather tends toward a limiting value, just as it does in animal experiments. More-

over, the exponential relation seems somewhat more "natural" for a physical process.

The exponential function was incorporated into the simulation programs on an optional basis, in anticipation of using it in place of the square root law. (By proper choice of A_∞ and α, the former can be made to approximate the latter over the range of interest.) However, for the sake of comparability, all of the experiments reported here were performed using the square root relationship.

The computation of the ARP duration is the only part of the transition function that depends explicitly on the cell's history prior to the beginning of the current firing cycle. The only memory retained by a quiescent cell is the time-step on which it was most recently stimulated.

6. The Relative Refractory Period

In this model the relative refractory period is characterized by an elevated threshold of excitation, which declines linearly toward its resting value. The properties of the cells during this period have already been discussed.

The duration of the RRP is a global constant, that is, its value is the same in all cells. Its value is established when the model is initialized, and ordinarily remains unchanged thereafter (see table 3.2 and figure 3.2.) However, the RRP duration may be modified by the experimenter during the course of the simulation, as has been done in several of the series reported here.[8]

[8] If the RRP duration is to be changed at arbitrary times, care must be taken to avoid compromising the validity of the computations. Each of the three simulation programs handles this problem somewhat differently.

7. The External Stimulator

The simulated external stimulator is the ultimate source of all activity in the model network, since there is no provision for activity to arise within the cells spontaneously.

Distance

The external stimulator is said to be located "over" the cell whose coordinates are (x_0,y_0), where x_0 and y_0 are parameters under the control of the experimenter. Around the cell at (x_0,y_0) are six other cells, distributed in a hexagonal pattern; around these are twelve more cells, forming a larger hexagon, and so on in a series of concentric hexagons in which the n^{th} hexagon contains 6n cells. The concentric hexagons centered on (x_0,y_0) are called ranks. A cell's distance from the external stimulator is defined by the rank in which it lies, i.e. a cell in rank n is said to be at distance n from the external stimulator. Thus, the six cells surrounding the one at (x_0,y_0) are at distance 1, the twelve around them are at distance 2, and so on. For convenience, the cell at (x_0,y_0) is also said to be at distance 1.

Distance bias

External stimulation is applied to the model network according to an inverse-square law. Letting $\psi_i(t)$ denote the strength of the external stimulation received by the i^{th} cell at time t, we have

$$\psi_i(t) = \Psi/d_i^2 \quad \text{if the stimulator is on at time t}$$

$$= 0 \quad \text{if the stimulator is off at time t}$$

where Ψ is the strength of the external stimulator and

d_i is the distance of the i^{th} cell from it.

Table 3.2. Standard Network Parameter Values Used in Simulation Experiments

All values apply to Program B unless otherwise noted.

Network "N":

Network size (NROWS, NCOLS)	= 25 x 25
$\bar{k}$ (KMEAN)	= 7.0
k_σ (KSIGMA)	= 1.5
τ_R (RRP)	= 40
θ_{max} (THMAX)	= 100
θ_{min} (THMIN)	= 25
λ_{max} (LRMAX)	= 75
$\tau_S + \tau_F$ (LRT)	= 20
Ψ (EXTSTIM)	= 200
Stimulator radius (STIMRAD)	= 1
F_1 (F1)	= 2
F_2 (F2)	= 2
F_3 (F3)	= 0

Variations:

N_1: Stimulator radius (STIMRAD)	= 12
N_2: Ψ (EXTSTIM)	= 750
N_3: $\bar{k}$ (KMEAN)	= 6.0

The following networks used the distance-based stimulator:

N_4: $\bar{k}$ (KMEAN)	= 6.0
N_5: Ψ (EXTSTIM)	= 750 (Program A)
N_6: Network size (NROWS, NCOLS)	= 25 x 25 (Program C)
N_7: Network size (NROWS, NCOLS)	= 51 x 51 (Program C)

The quantity $\psi_i(t)$ is simply added to the stimulation the i^{th} cell receives from its neighbors at time t (assuming the cell is in state Q or R); the total is compared with the cell's threshold to determine whether the cell should fire. If the cell is not in state Q or R, it ignores external stimulation. In the simulation programs, Ψ is represented by the variable "EXTSTIM". In early versions of the programs, external stimulation was limited to the cells at distance 1, and (x_0,y_0) was fixed at the center of the network. These cases are termed "fixed-radius" or "radius-1" stimulation in the discussion of results, while the cases which used the inverse-square law are called "distance-biased" or "radius-n" stimulation.

Stimulation patterns

Provision is made in the simulation programs for applying external stimulation automatically in either of two regimens: 1) every m time-steps for a total of n stimuli, n and m set by the experimenter; 2) at preselected time-steps t_1, t_2, . . . , t_n. In addition, the experimenter can switch on the stimulator at any time-step during the course of simulation. Regardless of how it was turned on, the external stimulator is always turned off automatically after a single time-step has elapsed--i.e. the stimulator's "pulse duration" is one time-step.

IV. Scale

The primitive element in this model of cardiac tissue is the model cell, the fundamental unit of the cellular automaton, the element to which the transition function applies. The transition function itself, and its parameters, have been chosen such that the activity

cycle of a model cell approximates that of a real cardiac cell (as seen by a microelectrode) when the time-step of the simulation is taken to represent about one millisecond of real time. But it is clear that if we wish to simulate conduction phenomena which in the heart occur over an area (presumably) several centimeters square, then each model cell must actually represent an aggregation of many cardiac cells. Otherwise, the number of model cells required would be so large as to be unmanageable with the available computing capacity. Therefore, it is an assumption of this model that small regions of atrial tissue, containing perhaps thousands of muscle cells, may be considered to behave approximately as a single unit with respect to excitability and refractoriness.[9]

Identifying the time-step of the simulation with a given quantity of real time--in this case, one millisecond--not only fixes the time scale of the simulation, but also fixes the distance (or spatial dimension) scale, for any given transition function. The reason is that the transition function determines the propagation velocity of activity waves in the simulation; if the latter is to be a faithful representation of real tissue, then the "distance" (number of cells) traversed by the simulated wave in n time-steps must be equivalent to the dis-

[9] This assumption is not solely imposed by practical necessity; in fact, some kind of aggregation is made appropriate just by the sort of experiments we wish to perform with this model, since they are directed toward the macroscopic behavior of the whole network rather than toward the behavior of microscopically small regions. Moreover, the grain of this model is reasonably in accord with the level of knowledge about how cardiac cells interact with each other: a model truly at the level of individual cells would probably be quite different, involving direct representations of membrane potentials and ionic fluxes and, no doubt, significant additional assumptions.

tance an actual activity wave travels in n milliseconds, assuming normal excitability in both cases.

By definition, there is a minimum delay of one time-step in propagating state-change information from a cell to its neighbor in a cellular automaton. The transition function of this model imposes additional delay, namely the duration of the stimulated state, τ_S. In most of the experiments reported here, the minimum value of τ_S was 2. Thus, in the model, the maximum velocity of activity waves is one cell every three time-steps. Since an excitation wave in fully-responsive atrial muscle travels at about one millimeter per millisecond, each cell of the simulation must represent a region of tissue roughly 3 mm. in diameter.[10] Such an area would contain on the order of 10^6 cardiac muscle cells.

V. Bases for the Present Model

Historical Basis

Computer simulation was first applied to the study of atrial fibrillation by Moe, et al. (1964). Several elements of their model are also present in this one: a fixed number of discrete units arranged

[10] Let d = distance, t = times; subscripts R and M denote real and model quantities, respectively. Then d_M/d_R is the ratio of model to real distance, and t_M/t_R the ratio of model to real time. We have

$$\frac{d_M}{d_R} = \frac{d_M/t_M}{d_R/t_R} \cdot \frac{t_M}{t_R}$$

$$\text{or model/real distance} = \frac{\text{1 cell / 3 time-steps}}{\text{1 mm./ms.}} \cdot \frac{\text{1 time-step}}{\text{1 ms.}}$$

$$= 1/3 \text{ cell/mm.} = 3 \text{ mm./cell}$$

in a planar array, one layer thick; a hexagonal neighborhood structure (i.e. 60° coordinate system); a state space including quiescent, absolutely refractory, and relatively refractory states; calculation of the ARP duration from the length of the preceding cycle according to a square root law, where the coefficient varied randomly from unit to unit and constituted the only source of variation among the units; and provision for conduction delay (latency between stimulus and response) depending on a unit's state of refractoriness at the time it receives a stimulus.

Taking advantage of faster computers, Flanigan and Swain (1968; Flanigan, 1965) developed a model of cardiac tissue that incorporated a number of extensions and refinements of the Moe model. Although they used it to study conduction in the atrio-ventricular node, Flanigan and Swain's model is quite suitable as a representation of atrial tissue if certain of its parameters are adjusted appropriately. The principal features it introduced were: a threshold of excitation, that was elevated in proportion to a unit's degree of relative refractoriness; spatial summation of stimuli from neighboring units (which is almost a corollary of the threshold concept); temporal summation of stimuli from units whose firing times were not identical, with a concomitant firing state during which the local response latency and amplitude depend on a unit's state of refractoriness and the strength with which it was stimulated.

The Flanigan-Swain model used a smaller step size than the Moe model (one millisecond instead of five), which facilitated a finer subdivision of some of the units' properties, such as degrees of relative refractoriness (forty versus three). In the Moe model, which

had a minimum conduction delay of one time-step (five milliseconds) per unit and which assumed a maximum atrial conduction velocity of 0.8 meters per second, each unit represented about 4 mm. of tissue. In the atrial version of the Flanigan-Swain model, the units (called "cells") have a minimum conduction delay of three time-steps, or three milliseconds; assuming a maximum atrial conduction velocity in the range 0.8 to 1.0 meters per second (Hoffman and Cranefield, 1960; Curtis, 1971), each cell corresponds to a section of tissue 2.4 to 3.0 mm. in diameter. The maximum conduction delay per unit in the Moe model was 20 milliseconds, twice that of the Flanigan-Swain model.

The present study has required no essential changes in the Flanigan-Swain model, although the simulation programs have been rewritten incorporating several additional features important for some of the experiments reported here. Among these are the variable network size, the movable external stimulator with distance-biased strength, the cathode-ray-tube display of the simulated tissue, and the collection of statistics during simulation. For one experiment (p. 238), a repolarization-phase excitation mechanism was added to the model and incorporated into one of the simulation programs.

The elements of the Moe and the Flanigan-Swain model are in accord with the known properties of mammalian cardiac muscle tissue, or are reasonable assumptions about those characteristics whose nature has not yet been very well determined. The aim in designing models such as these is not to produce an exact replica of the system in question, but rather to abstract what seem to be its essential features in order to study their interactions, and their contributions to the system's behavior, under controlled conditions. Many simplifications are thus

made quite deliberately, in the hope of obtaining a model whose behavior sufficiently resembles the real system's to be interesting, but whose structure remains relatively simple and controllable. Such models permit the investigator to conduct experiments using the terms in which he understands the system and to which his data apply.

Physiological Basis

Atrial muscle, for the most part, is quite thin, especially with respect to the speed with which it conducts activity. It is not a homogeneous mass, but specialized fibers are not prominent (outside the sinoatrial and atrioventricular nodes) and their significance is unclear; for experimental purposes, it is often considered relatively homogeneous, histologically. A planar array of unit thickness thus constitutes a reasonable representation of an excised section of atrium. (It would not be as adequate a model for ventricle, which has substantial thickness, well-defined layers, and prominent conducting fibers.) Anatomic obstacles are represented in the model simply by putting cells in a special permanently unresponsive state; they have been omitted from most of these experiments because we are interested in determining the behavior that is possible in the absence of specific obstacles.

A hexagonal neighborhood is used because it is the best simple approximation to a continuous sheet, in which all the cells are symmetrically disposed with respect to each other.

The cells' quiescent, absolutely refractory, and relatively refractory activity states correspond directly to well-known portions of the activity cycle of cardiac muscle cells, while the stimulated and firing states represent properties of cell-to-cell conduction that

are known but not well quantified. Except where the scale is directly relevant, such as in the calculation of the conduction delay, most of the properties of the model cells are patterned closely after properties of single muscle cells as revealed in microelectrode studies, on the assumption that the fibers in a small region are likely to be relatively synchronous with each other much of the time. A model cell thus averages or typifies the behavior of the muscle cells in the region it represents.

The square root law relating ARP duration to the length of the preceding cycle is a classical relationship (Bazett, 1918), although purely empirical. Hoffman and Cranefield (1960) have argued convincingly that an exponential law is preferable on both empirical and theoretical grounds, but, as pointed out earlier in this chapter, the two laws need not differ substantially over the range of interest here. For the sake of comparability, all the experiments reported here used the square root relationship.

Vagal stimulation always shortens the refractory period of atrial muscle, but to a marked degree at some sites, very little at others (Alessi, et al., 1958). Since the vagi are tonically active, one may expect ARP durations to be distributed quite unevenly throughout the atrium. This effect is simulated by distributing the ARP coefficients k of the model cells randomly about a specified mean value (using a uniform distribution, for lack of better information). Data[11] from

[11] For consistency, numerical quantities are all taken from experiments on canine hearts, although important relationships may also be supported by reference to experiments on rabbits and other mammals. (Hence this model represents, more or less, a simulated dog heart.) For convenience, durations are stated in milliseconds; the transformation to time-steps is implied where a model is involved.

Brooks, et al. (1955) suggests that a mean k value of 6 or 7 is probably correct, although in the Moe model a mean k of about 8.5 was normally used. (The Moe model also used larger networks, and as the present study shows, larger nets readily accommodate larger k values.) The fact that conduction velocity, in the present model, is not depressed until the stimulator cycle length is shortened to 140 ms. or so may suggest that the total refractory duration is somewhat short.

The duration of the relative refractory period has been shown to remain fairly constant, independent of variation in cycle length, in both ventricle (Brooks, et al., 1955) and atrium (Curtis, 1971). In the Moe model, RRP duration was set at 30 ms.; Brooks, et al. (1955) indicate values ranging from 25 ms. up to 70 or 80 ms. Most of the experiments in this study used an RRP duration (τ_R) of 40 ms.

Since membrane potentials are not directly represented in this model, the recovery of excitability during RRP is measured simply by a declining threshold, which is expressed in arbitrary units. A linear threshold decay function is used, for simplicity; Flanigan (1965) has reported that a quadratic relationship, though possibly more accurate, is not noticeably different in effect.

The threshold's maximum value is four times its resting level. This approximation receives some support from strength-interval data (Brooks, et al., 1955) if one assumes, as this study indeed suggests, that the moderately-sloped portion of a strength-interval curve is largely a measure of the increasing thresholds of "individual cells", and that the sharp changes in slope are due to the emergence of other mechanisms. The threshold's resting level is set arbitrarily, the only requirement being that it be consistent with the equally arbitrary

magnitude of the model cells' local response, λ. Here, the best test of reasonableness seems to be the safety factor of conduction, that is, the ratio of stimulus strength to threshold. Hoffman and Cranefield (1960) have estimated the safety factor for normal propagated action potentials to be in the range 4.5 to 6.5; the measured safety factor for a wave propagating normally in the model tissue is about 4.9.

The term "local response" has been used in the literature to mean both a non-regenerative response to subthreshold stimulation, and a regenerative depolarization which does not propagate. Our use of the term is similar to the latter, except that we call every response to stimulation a "local response", regardless of whether it propagates. The maximum value of the model cells' local response, λ_{max}, is set arbitrarily for consistency with the threshold, as described above. Both the time period ($\tau_S + \tau_F$) over which the local response decays to zero, and the linearity of that decay, are estimates, since it is known neither how long a depolarized region acts as a stimulator to adjacent regions nor the manner in which that stimulation fades.

Polarity of stimulation is not represented in this model; for both external and internal (cell-to-cell) stimulation, the stimulus strength is simply an unsigned quantity.

Brooks, et al. (1955) have shown that the latency of a response increases progressively as the stimulus is moved earlier into the relative refractory period, but that the latency is reduced by increasing the stimulus strength. Moreover, they have demonstrated that the relationship between response latency and stimulus prematurity is a roughly linear one. These dependencies are explicitly represented in the expression by which conduction delay in the model (the analog of

response latency) is calculated. The delay factors F_1 and F_2 are set to give reasonable numerical values to the conduction delay, and to ensure that prematurity is the primary determining factor in delay, with stimulus strength of secondary importance.

In the model, increasing conduction delay also implies a reduced magnitude of the local response, which is intended to represent the reduced magnitude and rate of rise (and thus net stimulating effectiveness) of action potentials evoked by premature stimuli. This factor also reduces the speed with which a premature stimulus is propagated to a distant point. These mechanisms have been summarized succinctly by Hoffman and Cranefield (1960, p. 250):

> . . . First, the time required for the local response to rise to an effective level varies with both the strength of the stimulus and the level of membrane potential during phase 3. Second, the rate of rise and amplitude of the resulting action potential vary and thus influence the rate at which activity spreads in the immediate vicinity of the stimulating electrode.

No doubt there is some random variation, in both time and space, in essentially all of the cells' properties described above. Randomness in the model is limited to ARP durations, not only for the sake of simplicity, but also because such variation is prominent in atrial tissue, and because the presence of premature stimulation induces random variation in other important variables, such as threshold and local response.

Automaticity has been omitted from this model not because it would be difficult to include (in fact, the repolarization-phase stimulation mechanism is a form of automaticity), but because we explicitly wish to see what sort of behavior can arise independently of automaticity.

VI. Analysis of Simple Cases

Even small networks of these model cells are sufficiently complex that analysis of their interactions becomes quite tedious; hence, we simulate. However, certain cases are simple enough to permit straightforward analysis and yet still provide some insight into the behavior of the cells. We shall consider the response of a single cell to premature excitation, and the passage of a premature stimulus along a row of cells. The situation is depicted graphically in figure 3.4, which shows how the variables defined below relate to the activity cycle of a typical cell.

To determine how the local response of cell 1 depends on the prematurity of the excitation to cell 1, define

C_i = prematurity of test stimulus at cell i

= 0 if the stimulus is not premature, i.e., arrives when cell i is quiescent; increases linearly, reaching τ_R when the test stimulus is as early as possible.

D_i = delay between stimulus and response at cell i, i.e., the value of τ_S following the test stimulus.

From the transition function, λ_i depends on D_i:

$$\lambda_i = \lambda_{max} - \frac{\lambda_{max}}{\tau_S + \tau_F} D_i \qquad (1)$$

D_i, in turn, depends on θ_i:

$$D_i = \theta_i \left(\frac{F_1}{\theta_{min}} + \frac{F_2}{\Lambda_i} \right) \qquad (2)$$

$$D_i \approx \theta_i \left(\frac{F_1}{\theta_{min}} \right) \qquad \text{when } \Lambda_i >> \theta_i \quad \text{(strong stimulus)} \qquad (2a)$$

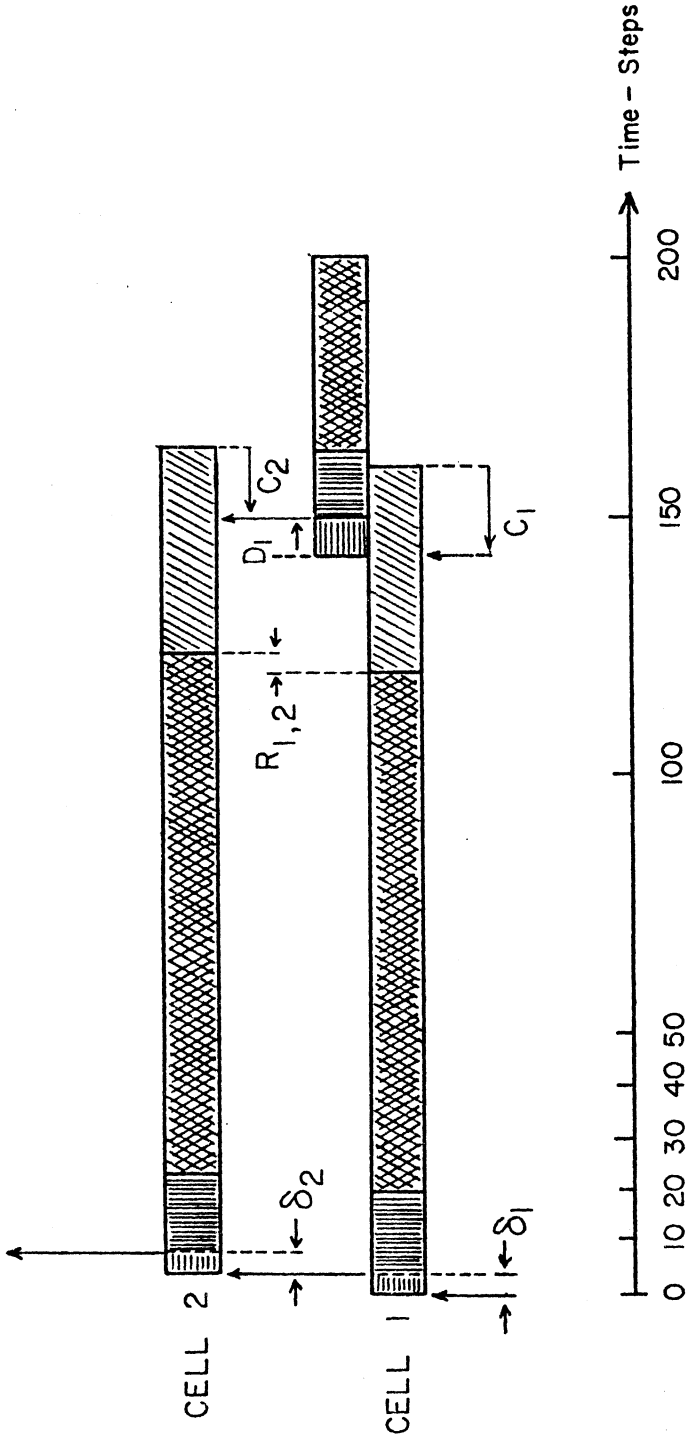

Figure 3.4. Cell-to-Cell Conduction. Typical Relations Between Events in the Activity Cycles of Adjacent Cells.

Variables defined in the figure are discussed in the text.

$$D_i \approx 0.15\, C_i + 4, \quad \Lambda_i \approx \theta_i \qquad (4 \le D_i \le 10) \tag{10a}$$

$$D_i \approx 0.15\, C_i + 2, \quad \Lambda_i >> \theta_i \qquad (2 \le D_i \le 8) \tag{10b}$$

$$\lambda_i \approx 60 - \frac{9}{16} C_i, \quad \Lambda_i \approx \theta_i \tag{11a}$$

$$\lambda_i \approx 67.5 - \frac{9}{16} C_i, \quad \Lambda_i >> \theta_i \tag{11b}$$

These relationships are graphed in figure 3.5.

To determine how conduction between cell 1 and cell 2 depends on the prematurity of the stimulus at cell 1, we must consider cell 2's threshold. Define $R_{1,2}$ as the relative difference in the time origins of the RRP's of the two cells:

$R_{1,2}$ = (time cell 2 enters RRP) - (time cell 1 enters RRP)

Then $C_2 = R_{1,2} + C_1 - D_1$ (see figure 3.4) (12)

Substituting (7a) into (12) yields C_2 in terms of C_1 as the "initial condition", $R_{1,2}$:

$$C_2 = R_{1,2} - F_1 - F_2 + (1 - \frac{S_\theta F_1}{\theta_{min}}) C_1, \quad \Lambda_i \approx \theta_i \tag{13}$$

At the usual values of the parameters,

$$C_2 = R_{1,2} - 4 + 0.85\, C_1, \quad \Lambda_1 \approx \theta_1 \tag{13a}$$

$$C_2 = R_{1,2} - 2 + 0.85\, C_1, \quad \Lambda_1 >> \theta_1 \tag{13b}$$

Hence, by substitution of (13) into (6), we have a relation between θ_2 and C_1:

$$\theta_2 = \theta_{min} + S_\theta [R_{1,2} - F_1 - F_2 + (1 + \frac{S_\theta F_1}{\theta_{min}}) C_1] \tag{14}$$

With the usual parameters, this becomes

$$\theta_2 = 17.5 + 1.59\, C_1 + 1.875\, R_{1,2}, \quad \Lambda_1 \approx \theta_1 \tag{14a}$$

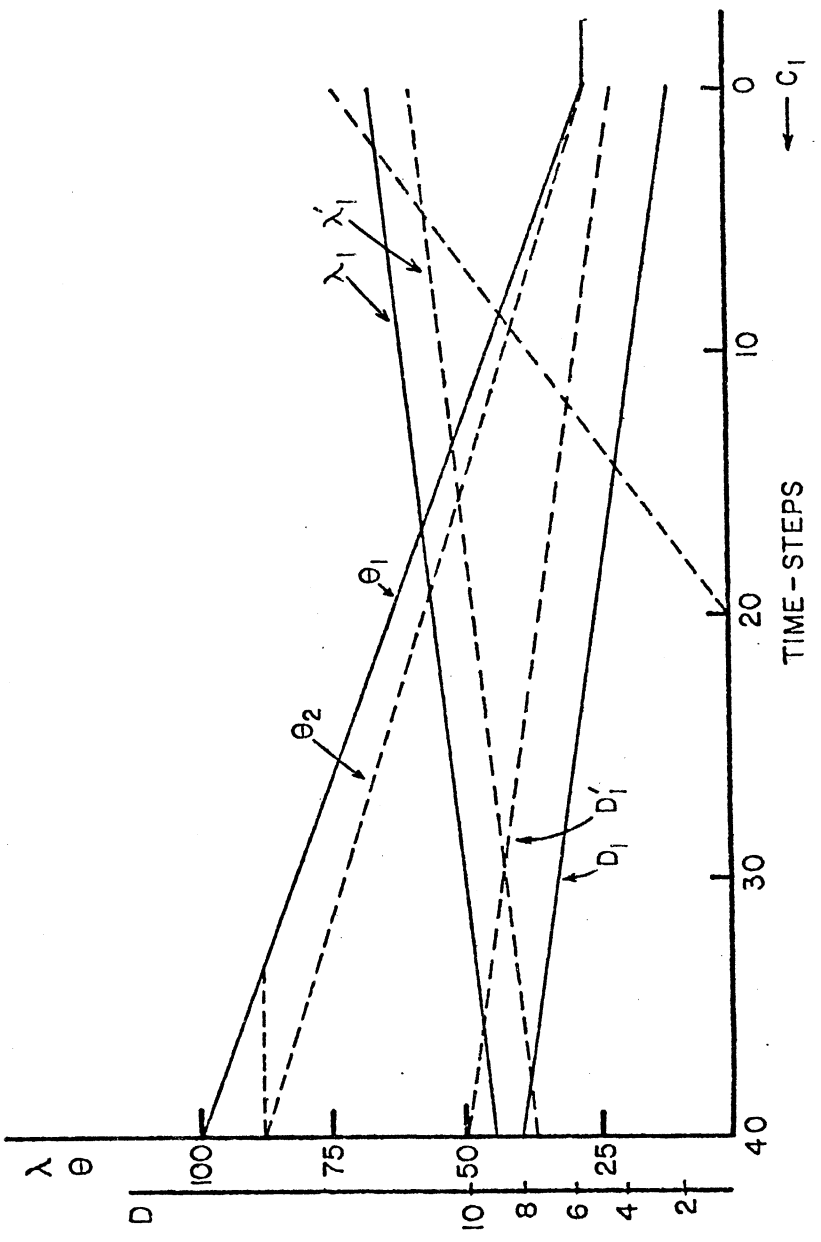

Figure 3.5. Relationship Between the Prematurity of a Stimulus and Cell Threshold, Local Response, and Conduction Delay.

$$D_i \approx \theta_i \left(\frac{F_1}{\theta_{min}} \right) + F_2 \qquad \text{when } \Lambda_i \approx \theta_i \quad \text{(weak stimulus)} \tag{2b}$$

Finally, θ_i depends on C_i:

$$\theta_i = \theta_{min} + \frac{\theta_{max} - \theta_{min}}{\tau_R} C_i \tag{3}$$

For convenience, we define S_λ and S_θ as the slopes (with respect to time) of the local response and threshold, respectively:

$$S_\lambda = \frac{\lambda_{max}}{\tau_S + \tau_F} \tag{4}$$

$$S_\theta = \frac{\theta_{max} - \theta_{min}}{\tau_R} \tag{5}$$

Substituting back,

$$\theta_i = \theta_{min} + S_\theta C_i \tag{6}$$

$$D_i = (\theta_{min} + S_\theta C_i) \left(\frac{F_1}{\theta_{min}} + \frac{F_2}{\Lambda_i} \right) \tag{7}$$

$$D_i \approx (\theta_{min} + S_\theta C_i) \frac{F_1}{\theta_{min}} + F_2, \qquad \Lambda_i \approx \theta_i \tag{7a}$$

$$D_i \approx (\theta_{min} + S_\theta C_i) \frac{F_1}{min}, \qquad \Lambda_i >> \theta_i \tag{7b}$$

$$\lambda_1 = \lambda_{max} - S_\lambda D_i \tag{8}$$

$$\lambda_i \approx \lambda_{max} - S_\lambda (F_1 + F_2 + \frac{F_1 S_\theta}{\theta_{min}} C_i), \qquad \Lambda_i \approx \theta_i \tag{8a}$$

$$\lambda_i \approx \lambda_{max} = S_\lambda (F_1 + \frac{F_1 S_\theta}{\theta_{min}} C_i), \qquad \Lambda_i >> \theta_i \tag{8b}$$

At the usual values of the simulation parameters,

$$\theta_i = 25 + 1.875\ C_i$$

$$\theta_2 = 21.25 + 1.59\ C_1 + 1.875\ R_{1,2}, \quad \Lambda_1 >> \theta_1 \tag{14b}$$

With expressions for both λ_1 and θ_2 in terms of C_1, we can determine the maximum value of C_1 consistent with conduction, that is, the earliest premature stimulus at cell 1 that will still be propagated to cell 2. At the critical point where conduction just fails, $\lambda_1 = \theta_2$; call this point C_1^*.

For example, assume that cell 1 and cell 2 have identical ARP durations and that a just-adequate stimulus is being used. Then $R_{1,2} = 4$, and from (11)

$$\lambda_1 = 60 - 0.562\ C_1 \tag{15a}$$

From (14),

$$\theta_2 = 17.5 + 1.59\ C_1 + 7.5 \tag{15b}$$

Equating (15a) and (15b) and solving for C_1, we find

$$C_1^* = (42.5 - 1.875\ R_{1,2})/2.15 = 35/2.15 \tag{16}$$
$$= 16.3$$

Thus, in this case, stimulating cell 1 more than 16 time steps prematurely will cause conduction to fail. Conversely, if conduction is observed to fail at a particular value of C_1, equations (11) and (14) can be used to solve for $R_{1,2}$, the initial phase difference between the two cells.

From equation (13), we see that if we assume marginal conduction,[12] then premature stimulation at the i'th cell depends on prematurity

[12] That is, $\Lambda_{i-1} \approx \theta_{i-1}$. Actually, Λ_{i-1} depends on C_{i-2} and Λ_{i-2} in a complicated way, hence so does the a_i term in (17). We use the approximation in the interest of simplicity, since the contribution of Λ_{i-1} to variation in a_i is limited.

at the i-1'st cell by an equation of the form

$$C_1 = a_i + \alpha C_{i-1} \tag{17}$$

where

$$a_i = R_{i-1,i} - F_1 - F_2, \quad i > 1$$

$$\alpha = 1 - \frac{S_\theta F_1}{\theta_{min}}$$

$$C_0 = 0$$

$C_1 \equiv a_1 \equiv$ prematurity of the test stimulus

i.e.,

$$C_1 = a_1$$

$$C_2 = a_2 + \alpha a_1$$

$$C_3 = a_3 + \alpha(a_2 + \alpha a_1) = a_3 + \alpha a_2 + \alpha^2 a_1$$

$$C_4 = a_4 + \alpha a_3 + \alpha^2 a_2 + \alpha^3 a_1$$

$$\vdots$$

With the usual parameter values, $\alpha = 0.85$.

If all the cells have the same ARP constant and if they are synchronized by a normal drive stimulus preceding the test stimulus, then

$$a_i = 0, \quad i > 1$$

In that case, the prematurity of the stimulus to the i'th cell bears a simple relationship to the prematurity of the test stimulus:

$$C_i = \alpha^{i-1} a_1 \tag{18}$$

where a_1 is the prematurity of the test stimulus.

In any case, the effect of the prematurity of the test stimulus dies out exponentially with distance from the stimulating electrode.

Since, with the usual parameters, $\alpha^4 \approx 0.52$, the prematurity should be reduced to about half its original value after conduction through four model cells. As inspection of the conduction-time graphs

in Chapter IV shows, the simple exponential relationship is often distorted by multiple-cell interactions.

VII. Organization of the Simulation Programs

In the course of this study, three separate simulation programs were employed, all of which used the same basic algorithms. The first, designated Program A and written in the Fortran language, was a modified version of the atrioventricular node simulator used by Flanigan and Swain (1968; Flanigan, 1965). It was implemented on a large scale, general purpose time-sharing system.[13] This program was primarily used to verify the appropriateness of the model for studying self-sustaining rhythms and to test various techniques for conducting simulation experiments. It was used for a number of the early experiments, but suffered from awkward graphic facilities and was relatively expensive to run. Consequently, Program B was implemented on a small computing system[14] which was dedicated to simulation projects and which included a specially-developed language for the simulation of cellular automata (Brender, 1970; Frantz and Brender, 1971). Most of the experiments reported here were performed using this system, whose chief advantages were its graphical display capability and its negligible marginal cost of computation. However, its limited processing speed and storage capacity restricted the size of the model network to the 469-cell (25 x 25) case.

[13] The Michigan Terminal System.

[14] Logic of Computers Group, University of Michigan.

Program C, written in the PL/1 language, was implemented on the same time-sharing system as program A. Its principal virtue was that it established the simulation space dynamically, thus permitting the network size to be varied arbitrarily. The cost of calculating the state transitions[15] became the limiting factor, rather than the availability of storage or the need for reprogramming. It was primarily used for experiments on large (1951-cell) networks.

The functions performed by the simulation program can be grouped into several major categories which are present to a greater or lesser extent in all three programs. They are mentioned here for completeness' sake, though only the discussion of statistics collection is directly relevant to the interpretation of the results of this study.

1. Compute the state-transition function for all the cells in the network.

Procedure: iterate over the space, examining each cell. If its "time for change of state" (recorded therein) has arrived, change the cell's state indicator to the proper new value, and compute and record a new "time for change of state" in that cell. If, at the end of this process, a cell is in state Q or R[16], sum the stimulation provided by its neighbors[17] and the external stimulator (if any), and compare this with the cell's threshold. If stimulus exceeds threshold, then place

[15] Excessive computational overhead was avoided by coding the state transition routine in assembly language.

[16] Recall Q = quiescent, R = relative refractory, S = stimulated, F = firing, A = absolute refractory.

[17] Care must be taken to determine whether or not the neighboring cells have been updated yet and handle them accordingly.

the cell in the S state, compute the conduction delay and, hence, the time at which the cell should enter the F state (this is recorded as the cell's new "time for change of state"); compute the cycle length (elapsed time since previous firing of this cell) and, from this, the duration of the upcoming absolute refractory period. A complete iteration over all cells constitutes one time-step of the simulation.[18] Between each scan of the network a list of "event times" is consulted to determine whether some additional function(s) should be performed. Some functions, e.g., the printing of statistics, reschedule themselves regularly; others, such as stopping the simulation, are scheduled by the experimenter.

2. Display and modify parameters of the simulation--either interactively, or according to a prearranged sequence.

3. Print a log, in order to have an automatic record of each experiment. It is particularly important to record initial parameter values and subsequent changes therein.

4. Display the state of the network, i.e. selected elements of each cell's state vector. It is helpful to have several mappings of cell state to graphic representation.

5. (Re-)Initialize--to minimize the cost of performing series of experiments. This function and item (2) have certain procedures in common.

6. Save and restore the state of the simulation.

7. Collect and display statistics as the simulation proceeds.

[18] It is not necessary to scan the network on every time-step, but only on those at which some cell undergoes a transition that can affect a neighbor (e.g., firing) or be affected by a neighbor (e.g., leaving the absolute refractory period). Since such times can be calculated easily, the programs do this; as a result, there are sometimes "jumps" in simulated time.

VIII. Statistics

In a sense, it is the patterns of activity which arise in the model network that constitute the real "output" of this simulation. Such things as regular and irregular wave fronts, fast and slow conduction, and reentries, are often more readily perceived on a graphic display than quantified numerically. However, in an attempt to produce some more objective measures of the network state and, if possible, to correlate the behavior of the network with the activity of the individual cells, some additional computations were incorporated into the various simulation programs.[19] The information generated primarily concerns wave numbers, conduction intervals, counts of the number of cells in various states, and means and variances of cell variables.

1. Wave Numbers

One element of the state vector of each cell is an integer variable known as the wave number. Its initial value is zero. There is also a wave number associated with the external stimulator; it starts at zero, and is incremented by one every time the stimulator is turned on. When a cell is fired by the external stimulator, its wave number is set equal to the stimulator's. When a cell is fired by excitation from its neighbors, its wave number is set equal to the maximum of its neighbors' wave numbers. The result of this is that waves "entering" the net from the external stimulator are numbered sequentially, and the wave number propagates along with the wave itself. Displaying the network wave numbers aids in sorting out the sequence of

[19] Not all of the statistics are generated by each program.

activation when conduction becomes irregular, and also makes it clear where conduction failure has occurred. Moreover, the wave numbers make it convenient to determine exactly where reentries occur: if a cell is stimulated by neighbors whose wave numbers are no greater than its own, then it is being reexcited by the same wave which fired it previously (or possibly by an even earlier one). Such "reentry cells" are flagged,[20] so that a map of the network's reentry sites can be printed, if desired; also, the reentry wave is assigned a unique number so that its statistics can be kept separate from those of externally-stimulated waves present at the same time.[21]

2. Conduction Intervals

Whenever the external stimulator is turned on, a new wave number is assigned and the time of this event is recorded as the time of the wave's origin. Each time a cell fires, the difference between its firing time and the time of origin of the wave which excited it is computed and stored as the "conduction interval" for that cell. These data can be printed whenever desired, to facilitate the study of the conduction of activity waves.

3. Counts

Running counts are kept of the number of cells in the stimulated, firing, and absolutely refractory states. Printed periodically, these serve as the chief monitor of activity in the network; plotted against

[20] In Program C only; Programs B and A are more primitive in this respect.

[21] Several reentry waves may arise with the same wave number, due to multiple reentry sites on a given wave. But the "next generation" of reentry waves will be numbered differently, as will any stimulated waves.

time, they constitute a crude "electrogram" of the simulated tissue.

4. Means and Variances

When a cell is being fired, several quantities must be calculated to determine its detailed behavior. Of these, means and variances are accumulated for the following:

(a) activation interval (also called cycle length or inter-stimulus interval[22]), the elapsed time since the cell was previously fired;

(b) delay on firing, the duration of the stimulated state, τ_S;

(c) safety factor of conduction, the ratio of the total stimulus received by the cell to its threshold of excitation;

(d) ARP duration, τ_A.

Program B records items (a) - (c). These are collected on a global basis, that is, over the entire network. At regular intervals the current totals are printed out and the accumulators reset to zero. Program C records items (a) - (d), and, in addition, counts the number of "stimulation failures", that is, the number of cases in which an excitable cell (state Q or R) received some stimulation from its neighbor(s), but not enough to exceed its threshold. The "safety factor" in these cases, i.e. the ratio of stimulation to threshold, is accumulated in the same manner as item (c). In program C, these statistics are collected separately for each activity wave (using the wave numbering scheme described above), rather than globally; thus it is

[22] When we wish to distinguish between the cycle length (i.e. period) of the external stimulator and the cycle length of the cells, we use the term "activation interval" or "inter-stimulus interval" for the latter.

Chapter IV

RESULTS I: EXCITATION AND CONDUCTION

The response of individual units to stimulation is clearly defined and relatively simple, as described in Chapter III. The question is: Do networks of such cells also exhibit simple, predictable, easily described behavior when subjected to external stimulation? To find the answer, the model network was subjected to various patterns of stimulation, as detailed below. Its responses to these stimuli confirm the suspicion that behavior of the aggregate is often a different matter entirely from simply the sum of the responses of its components, because of the complex interactions which can arise as the components lose synchrony with each other.

I. The Strength-Interval Relationship

A. Fixed-Radius Stimulation

A common functional measurement of cardiac tissue, made in the course of pharmacological and electrophysiological studies, is the strength-interval curve. This is essentially a graph of the time course of recovery of excitability of a segment of cardiac tissue either *in vivo* or *in vitro*, and serves as a base line against which to gauge the effects of experimental variables. Accordingly, it seemed appropriate to determine the strength-interval characteristics of the model tissue.

Procedure

Network N of table 3.2 was initialized with cycle length 200. One stimulus of strength 25 was applied at time 200, and the state was

saved in file 1 at time 260. Then the sequence [restore file 1, apply test stimulus] was repeated for test stimulus timings in the range 325 to 305 in steps of 5, and below 305 in steps of 1. At each timing of P_1 the same sequence was repeated while the stimulus strength was incremented from a low value until a propagated response occurred. In algorithmic notation, the procedure was

```
    INITIALIZE NETWORK N, BASIC CYCLE LENGTH 200;
    AT TIME 200 APPLY STIMULUS OF STRENGTH 25;
    AT TIME 260 SAVE IN FILE 1;
A:  DO P1 = 325 TO 305 BY -5, 304 TO 300 BY -1;
       DO SS = 25 TO 2000; (increment varied by experimenter)
       RESTORE FILE 1;
       AT TIME P1 APPLY STIMULUS OF STRENGTH SS;
       IF (propagated response) THEN DO NEXT A;
       END;
    END;
```

Thus, the network was driven at a basic cycle length of 200, which it followed easily. Increasingly stronger test stimuli were applied at specified times (relative to the immediately preceding drive stimulus) until a propagated response was observed, with enough time allowed between test stimuli for the network to recover fully. Figure 4.1 shows a strength-interval curve obtained by this procedure.

Results

When a test pulse of strength equal to the cells' resting threshold was placed later than about 150 time-steps after the preceding drive, it elicited a uniform, symmetric response, since the stimulated cells

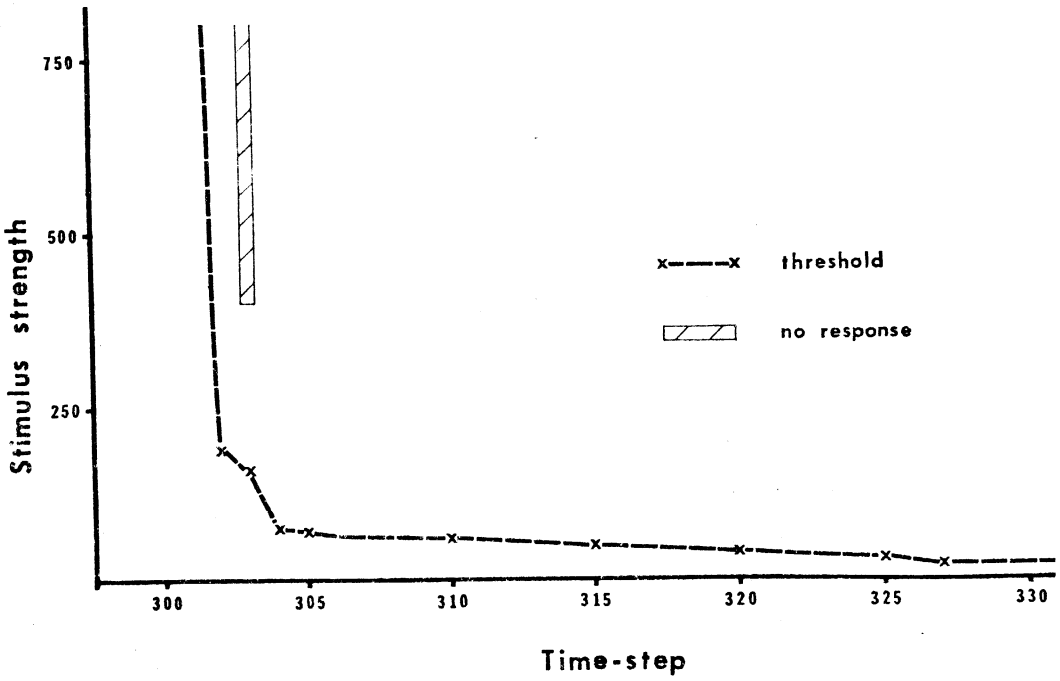

Figure 4.1. Strength-Interval Relation with Fixed Radius Stimulation (Radius = 1).

were in the fully recovered state. As the test pulse was advanced toward the preceding drive stimulus, the cells directly "under" the stimulator began failing to respond, one by one, owing to their differing ARP durations. Finally a time was reached at which the resting-threshold stimulus failed to elicit any response; this point, at which the earliest-recovering (shortest ARP) cell under the stimulator was not quite fully recovered, marked the beginning of the relative refractory period for the network as a whole.

As the test pulse was moved still earlier, the threshold rose linearly at the same slope at which an individual cell's threshold changes; the test stimulus was measuring the recovery characteristic of only one cell, namely the earliest-recovering one in the set of cells subject to the full strength of the external stimulator. The linear rise in threshold was maintained over an interval of about 23 time-steps, or more than half of the individual cell's relative refractory period. In Chapter III, some formulas were developed which predict the behavior of this model in very simple cases. Applying equation (16) to this case, which involves a single cell being stimulated and in turn stimulating one or more of its neighbors, we have $C_1^* = 23$. That is, conduction between rank 1 and rank 2 fails when the test stimulus is more than about 23 time-steps premature. Solving for $R_{1,2}$, we find that the second cell (which is in rank 2) must be recovering about 4 time-steps earlier than the earliest cell in rank 1, whereas it should recover about four time-steps later than the rank 1 cell if all refractory periods were of the same duration. This difference in recovery time, however, is consistent with the difference in k-values between the earliest-recovering cell in rank 1 and its

most excitable neighbor in rank 2. Hence we can ascribe this linear part of the strength-interval curve simply to the threshold-recovery characteristics of a single cell.

A different situation arises in the experiment shown in figure 4.3 (which is described below). Here, the distribution of k-values is such that the earliest-recovering cell in rank 1 has the same refractory period duration as its most excitable neighbor in rank 2. Hence, according to equation (16) of Chapter III, conduction should fail when the test stimulus is more than 16 time-steps premature; yet the strength-interval curve is linear for more than 25 time-steps.

The explanation is that conduction does indeed fail at time 304 (which is 16 time-steps into the RRP of the earliest-recovering cell, whose RRP ends at time 320); but a very slight increase in stimulus strength causes the next most excitable cell to be stimulated also. Since these two excited cells are in close proximity to each other, their local responses add and thereby propagate the activity wave where the single cell, firing alone, could not. In effect, the network threshold graph shifts from the threshold-decay curve of the most excitable cell to the parallel, but slightly higher, threshold-decay curve of the next most excitable cell. In figure 4.3, the shift is simply too small to be noticed, so the graph appears linear over the whole range.

As the test pulse is advanced into very early RRP, spatial and temporal summation become important in conduction of the activity beyond the cells stimulated externally. Conduction delays (influenced by stimulus strength) and the distribution of k-values (ARP durations) interact in such a way that only a substantially stronger stimulus,

which imposes additional synchrony on the cells' responses, generates enough summation that the wave "escapes" to the second rank of cells. Once there, conduction delay is sufficient to permit further propagation through better-recovered regions. Thus the threshold rises abruptly to six or eight times its resting value; then stimulation fails completely, no matter how strong the stimulus. (Actually, what fails is conduction. The external stimulus fires a number of cells, but they are unable to excite enough of their neighbors for propagation to occur.)

No-Response

After the threshold-recovery curve had been delineated as described above, another simulation run was made to determine the response of the model to suprathreshold stimuli during RRP. A steady-state network at cycle length 200 was established; then the timing of P_1 was stepped in one-millisecond increments while, for each increment, stimuli of strength ranging from 200 to 2000 were applied. In algorithmic notation,

```
    INITIALIZE NETWORK N, BASIC CYCLE LENGTH 200;
    AT TIME 200 APPLY STIMULUS OF STRENGTH 25;
    AT TIME 260 SAVE IN FILE 1;
A:  DO P1 = 300 TO 320 BY 1;
B:      DO SS = 200 TO 1000 BY 100, 1200 TO 2000 BY 200;
        RESTORE FILE 1;
        AT TIME P1 APPLY STIMULUS OF STRENGTH SS;
        [observe response]
        END B;
    END A;
```

The result of this experiment (figure 4.1) is noteworthy at only one point, namely time-step 303, where stimuli of strength 400 or greater failed to elicit any propagated response. On this time-step six of the seven central cells were in their relative refractory periods and hence capable of excitation by the external stimulator. A strong stimulus caused these cells' firing delays, which are influenced by the stimulus strength, to be slightly reduced; the cells fired too soon for their neighbors (whose thresholds are quite elevated) to become excited, and so conduction failed. This no-response phenomenon occurred only on time-step 303, as shown by the line in figure 4.1. At all other time-steps, suprathreshold stimuli elicited one and only one propagated response.

B. Distance-Biased Stimulation

It was evident from the foregoing that conduction in the immediate vicinity of the external stimulator is an important factor in the strength-interval relationship. Yet the external stimulus was applied only to the seven central cells of the network, a recognizedly unrealistic situation, especially when the stimulus strength was varied over a wide range. Consequently, a second strength-interval determination was made on the same network, following the same procedure as outlined above but using the distance-biased stimulator described in Chapter III (network N_1), in which the stimulus strength varies inversely with the square of the cell's distance from the stimulator. The result is shown in figure 4.2

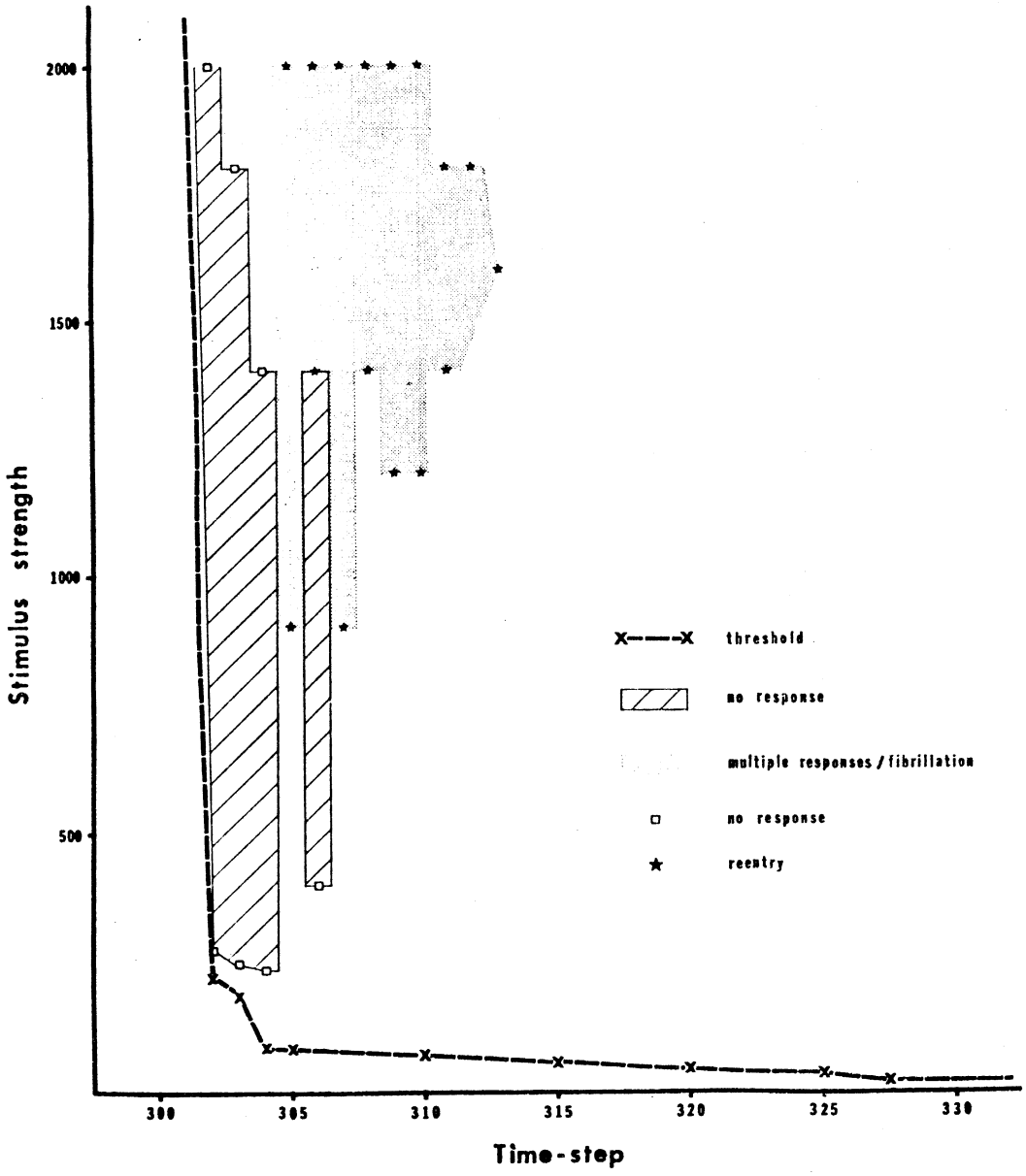

Figure 4.2. Strength-Interval Relation with Distance-Biased Stimulation.

No-Response

As expected, the threshold-recovery curve was identical to that in figure 4.1, for when the stimulus is just suprathreshold only the cells at distance 1 from the stimulator--that is, the seven central cells--are effectively excited. However, the no-response phenomenon, where a stimulus of a certain strength elicits a conducted response while a stronger stimulus at the same time fails to produce a conducted response, occurred much more readily. There was a threshold associated with the no-response phenomenon, so that stimuli whose strength was above the response threshold and below the no-response threshold produced conducted responses, whereas stimuli below the response threshold or above the no-response threshold elicited no propagated activity. The no-response region, as shown in figure 4.2, was seen only in quite early RRP. As the respone threshold rises, the distance between it and the no-response threshold decreases, leaving a relatively small range of stimulus strengths over which conducted beats can be initiated. One may think of the effective refractory period as the point where the response and no-response thresholds come together, closing off propagated excitation.

Multiple-Response

If strong stimuli are applied slightly later than the earliest time in RRP at which a conducted beat is possible, then instead of no-response, the stimulus may cause a reentry pattern to develop, leading to multiple responses. The regions in which these various phenomena occur are mapped on the strength-interval diagram in figure 4.2. It is apparent that a clear separation of "no-response" from

"multiple-response" regions is not possible: one response, no response, or multiple responses may be produced with only slight variation in stimulus strength and timing. "Multiple responses" may range from a single extra beat to a seemingly persistent pattern lasting thousands of time-steps.

The mechanism by which these aberrations arise is essentially that hypothesized by Brooks, et al. (1955, p. 149 ff.). The site where external stimuli are applied is surrounded by an irregular margin of partially recovered tissue. In order to produce a conducted response, a stimulus must be strong enough to excite some of these cells, whose thresholds are all elevated to varying degrees. But this initial excitation must be delayed enough in its propagation for a path of more recovered cells to open up in front of it, or else the excitation will not be conducted much beyond the region of the external stimulator. This is what happens when the stimulus is too strong: a larger area is excited, pushing the leading edge of the activity wave closer to the retreating border of the absolute refractory period from the previous wave. These cells on the wave front, having relatively high thresholds at the time they become excited, experience nearly the maximum delay before firing; but their response is thereby reduced in magnitude, and their neighbors' thresholds are still quite high, so conduction fails. Consequently the stronger stimulus produces a larger local response, but no conducted response.

Reentries arise, when the timing is right, because of the irregular pattern of excitability in the region around the stimulator. A strong stimulus may produce a large local excitation, some of whose edges may lie in more excitable regions than others. If conduction

then fails completely at most places along the wave front (as with the no-response situation described above) but proceeds, delayed, at a few spots, then after a short time there will be a patch of absolutely refractory cells in the area around the stimulator with a few regions of activity at its borders, all surrounded by increasingly excitable cells. The small activity regions grow and propagate in all directions, except that the excitation wave must skirt the area where the stimulus was originally applied, as that section is absolutely refractory. If that refractory region is large enough, then portions of it may be beginning to recover their excitability by the time the activity wave(s) reach them; then reentry occurs, and continuous conduction may ensue.

Because the no-response/multiple-response phenomena appear to be so dependent on the local distribution of excitability in the region near the stimulator, another strength-interval graph was made using procedures identical to those above but with the k-values assigned from a different sequence of random numbers. The result is shown in figure 4.3. The rise in threshold at early RRP was much less abrupt, and the no-response/multiple-response phenomena appeared in different places on the diagram. The no-response region was quite large, and its threshold in early RRP was quite close to the threshold of excitation, leaving a very small range of effective stimulus strengths. The multiple-response region lay somewhat later and at rather lower stimulus strengths than in figure 4.2; it was also much smaller. However, multiple responses occurred frequently at isolated spots fairly late in RRP.

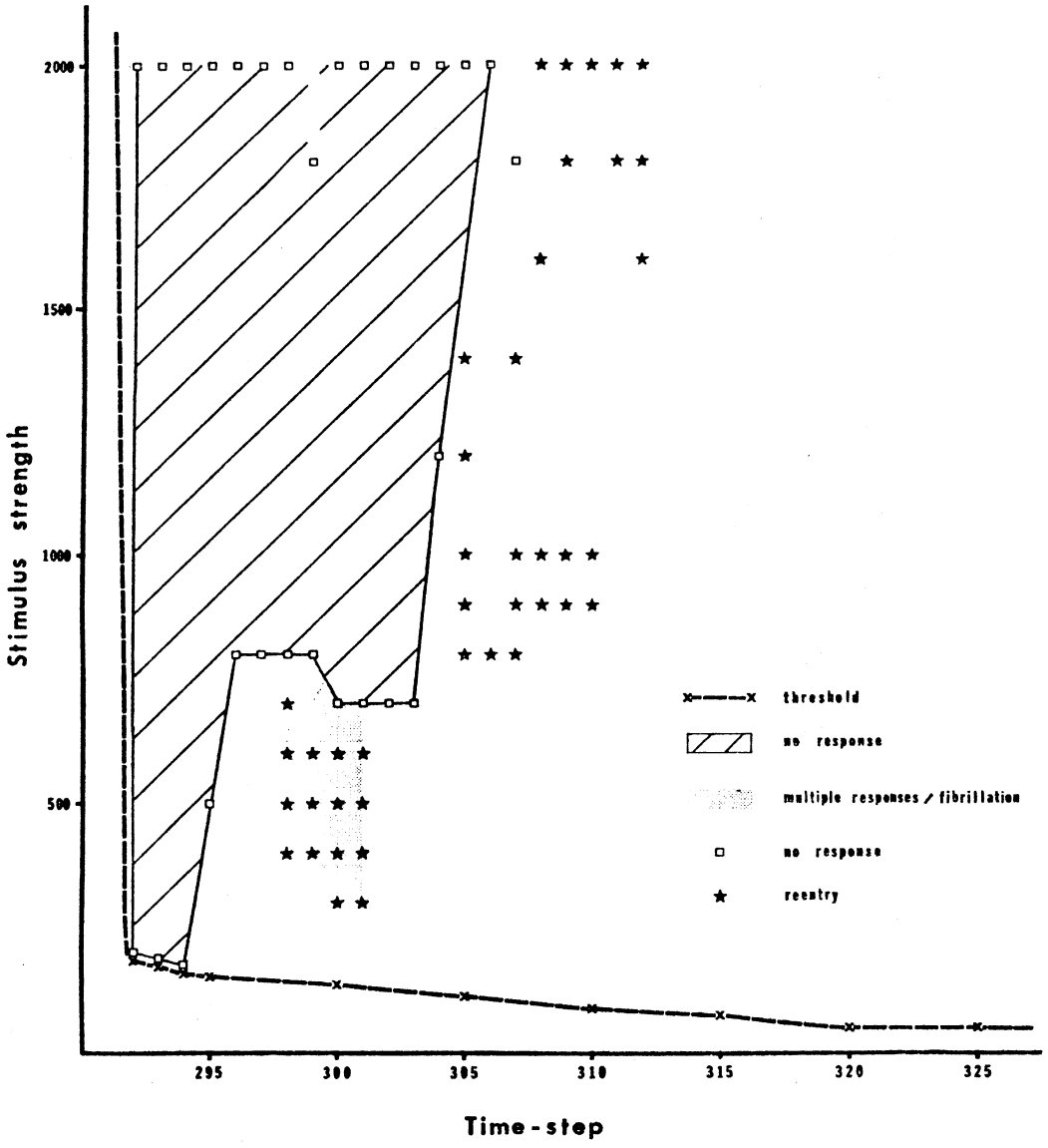

Figure 4.3. Strength-Interval Relation with an Alternate k-Distribution.

Some indication of the reasons for these differences between figures 4.2 and 4.3 can be obtained from figure 4.4, where the k-values for each case are shown for cells near the stimulator. In the first case (a) the sample mean values of k are fairly close to each other and to the mean of the distribution, 7.0. But in the second case (b) the average k-value of cells at radius 1 from the stimulator is only 6.4, which is rather low; and at radius 2 the mean is 6.6, still somewhat low. Only at radius 3 is the cells' mean near, in fact slightly above, the mean of the distribution. The low k-values near the stimulator mean that the cells there will be more easily excited, all other things being equal, and will show less conduction delay. Hence it will be easier to "bump into" the refractory border as stimulus strength is increased in early RRP, and one would expect the no-response phenomenon to appear more readily.

A typical strength-interval curve obtained from a dog's atrium is shown in figure 4.5. Comparing this graph with figures 4.2 and 4.3, perhaps the most significant difference is that the simulated cells show no response at all in very early RRP, while the real tissue continues to respond if the stimuli are strong enough. That is, the simulated cells simply cut off at a certain degree of prematurity, and remain unexcitable regardless of the strength of the stimulus.

There are a number of possible explanations, of course, for the real tissues response to very strong stimuli in early RRP, but most would seem to involve some change in local properties of the tissue wrought by the strong current, such as drastic changes in ionic concentrations or alterations in the characteristics of the cell membrane. Another possibility, which does not require any change in the local

8.4 5.8 7.1 8.2 7.9

5.9 6.7 6.2 8.4 5.9 7.4

8.3 7.5 7.3 7.1 6.8 6.9 6.4

7.7 6.8 7.8 6.9 6.5 7.8 6.9 6.3

7.3 8.1 6.4 6.4 6.8 7.8 7.2 7.8 6.3

7.5 7.2 7.3 6.2 6.5 8.3 6.2 5.9

6.9 6.9 5.5 7.9 5.8 5.8 7.0

7.9 6.5 7.7 7.6 6.2 6.2

5.9 6.1 7.8 7.8 7.5

(a) Network corresponding to figure 4.2

5.8 5.7 7.4 7.2 8.3

5.8 8.0 8.4 7.1 8.2 7.5

8.4 6.5 6.0 5.7 6.2 5.8 6.7

8.4 5.7 8.4 7.1 6.2 8.3 6.6 6.8

5.6 6.9 5.8 6.5 6.0 5.7 5.8 7.8 7.4

5.5 7.6 7.8 5.7 7.1 5.7 7.6 5.9

5.8 7.9 6.1 7.6 5.7 5.9 6.8

7.2 8.2 6.6 7.3 5.7 6.3

8.3 6.7 6.2 5.8 7.0

(b) Network corresponding to figure 4.3

Figure 4.4. ARP Coefficients (k values) in the Region of the Stimulator (center of the network).

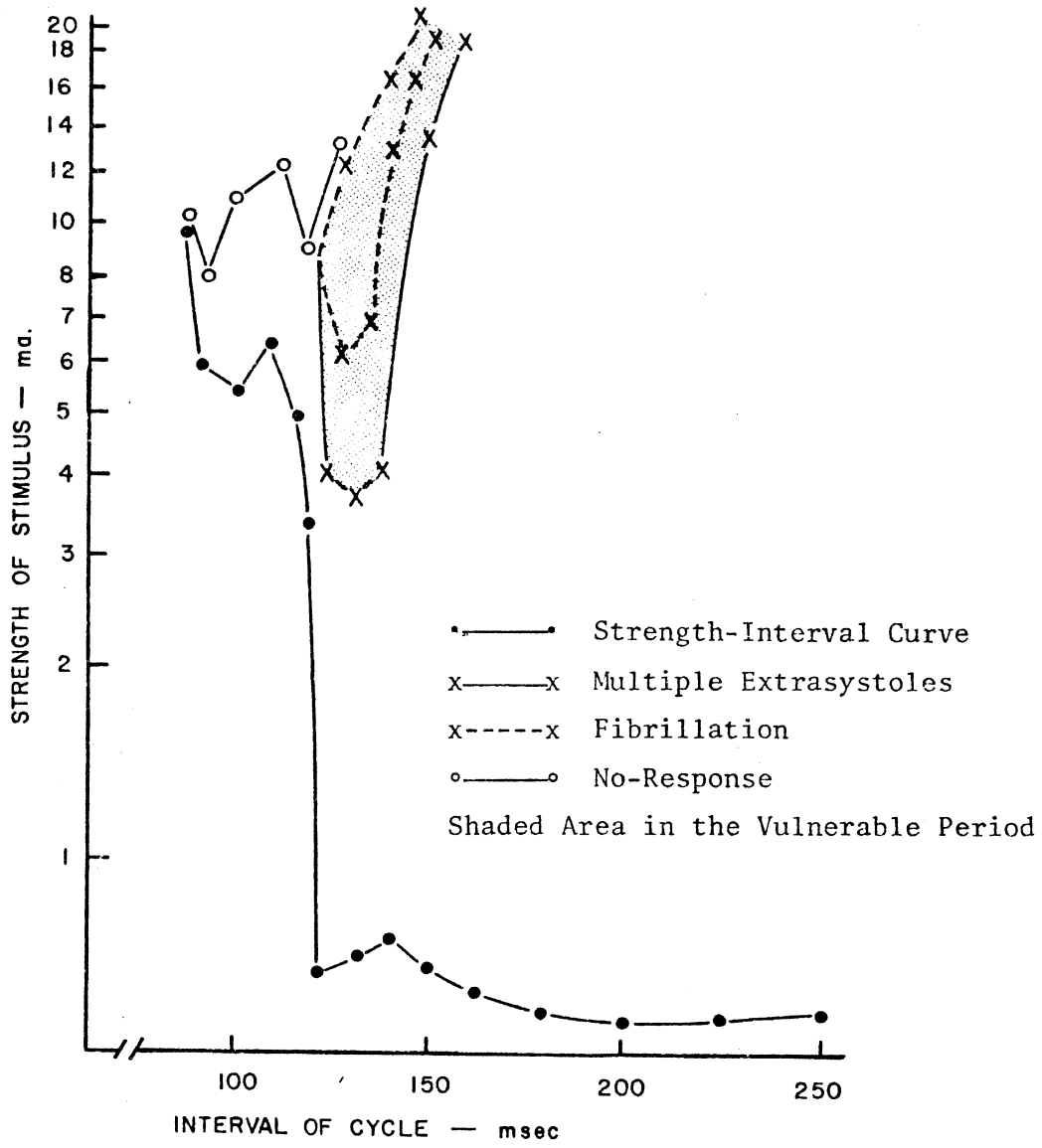

Figure 4.5. Typical Strength-Interval Relation in Dog Atrium. (Redrawn from Brooks, et al., 1955, p. 139.)

properties, was suggested by observation of the simulated tissue and by description of the procedures used to obtain strength-interval curves in an animal laboratory [Brooks et al., 1955]: namely, some spatial separation of the test electrode from the driving electrode.

Reflection on the behavior of the model led to the idea that responses elicited by very strong stimuli might be due to the existence of areas a short distance from the test electrode that would be excitable when the region right around the stimulator was incapable of a conducted response. This condition might be produced by a drive beat originating at a slightly different place than the test stimulus; when it was discovered that such was indeed the situation in some animal experiments, a similar experiment was arranged with the simulation. The procedure was exactly as described above (figures 4.2 and 4.3), except that the drive stimulus was applied at coordinates (-3,0), while the test stimulus was applied at the usual place, (0,0). The resulting strength-interval graph is shown in figure 4.6.

The threshold curve is similar to the prior cases, except that very strong stimuli at early RRP produce conducted responses where none occurred previously. The no-response region is greatly reduced in size, and appears only at relatively low stimulus strengths. The multiple-response region is larger, and occurs earlier in the relative refractory period. Neither effect is unexpected, for with a more-recovered region located further from the site of the test electrode, it will be more difficult to stimulate enough of the total excitable region that conduction would fail completely; yet it should be less difficult to produce an asymmetric activity pattern that would be prone to reentry.

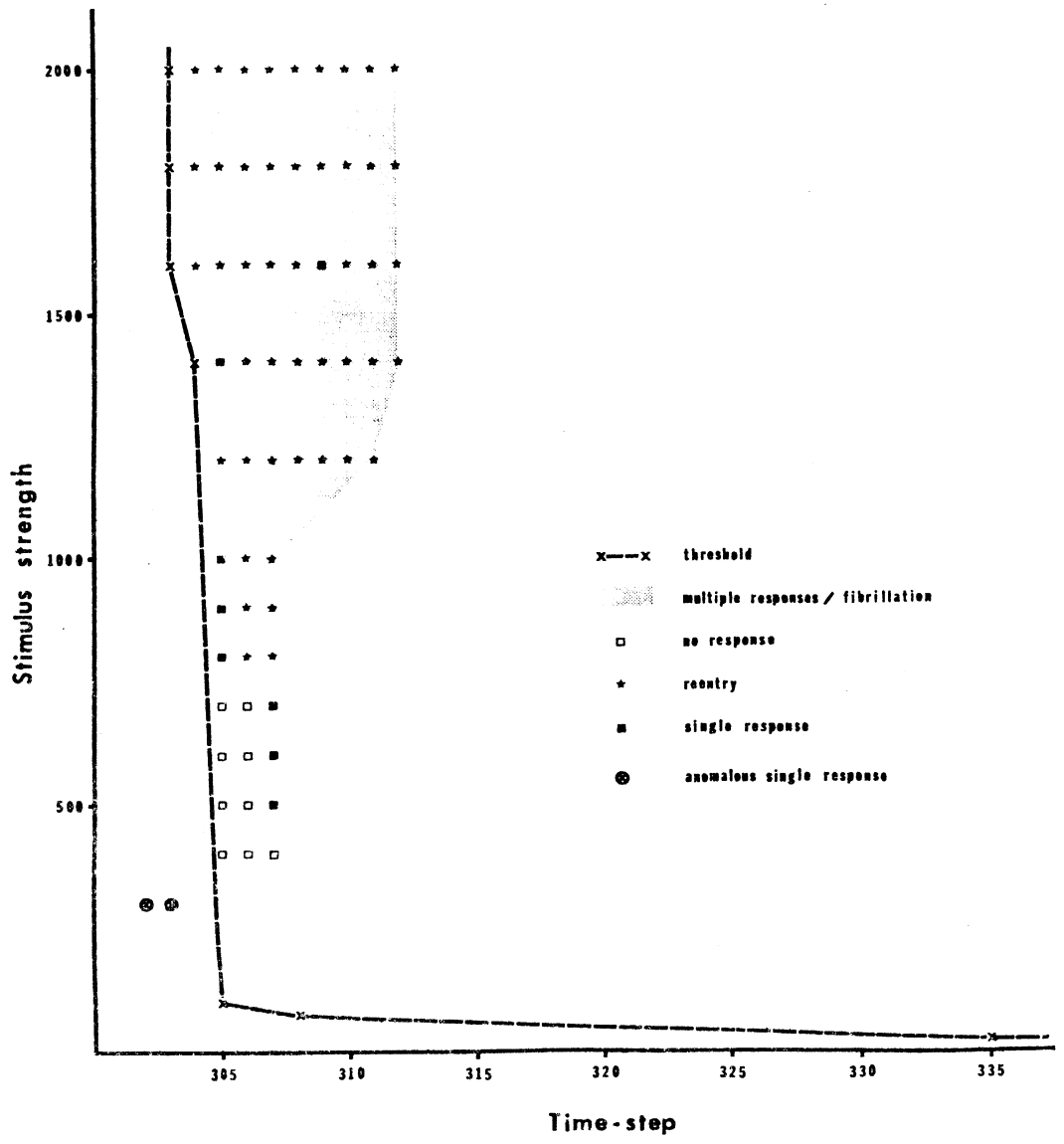

Figure 4.6. Strength-Interval Relation with Driving and Testing Stimuli Applied at Different Sites.

It should be observed that the strength-interval determination affords a clear illustration of the distinction between properties of individual components of a cellular system and the properties of the aggregate. Considering only individual elements, in this case the units which represent small tissue regions, the strength-interval characteristic is immediately apparent; in fact, it is built into the model directly, as the linear slope of threshold during RRP. It is perhaps not obvious that the strength-interval, or equivalently, the threshold-recovery, curve for aggregates of units should be any different. Yet the curve departs considerably from linearity in early RRP, because where the aggregate is concerned the response of interest is a propagated wave, not simply the firing of single units.

It might also be noted that in no case did the minimum effective stimulus cause a multiple response; the same observation was made by Brooks, et al. (1955, p. 69):

> . . . it was possible to avoid fibrillation even when testing during the vulnerable period of the cardiac cycle because no period was ever found during which the minimum effective stimulus produced fibrillation in a normal heart.

II. Conduction of Premature Beats

In laboratory animals, atrial fibrillation is commonly induced by premature stimuli. One shock is rarely sufficient, but two or more shocks placed in early diastole frequently elicit a series of propagated responses which often then passes into the disordered rhythm of fibrillation.

The mechanism by which fibrillation arises under these conditions is not known, but the principal theories are two: that the premature

beats somehow initiate repetitive firing at one or more ectopic foci; or that the premature wave fails to propagate in certain regions of the tissue which other parts of the same wave later find excitable, producing continuous conduction via circus movement or reentry. The former mechanism involves automaticity, which is not present at all in this model. The latter mechanism supposes that very premature beats suffer impaired conduction of a sort that allows reentry to occur; it therefore seems appropriate to investigate the conduction of premature beats in the model, particularly as influenced by their number and degree of prematurity.

"Premature stimuli", as the term is used here, refers to near-threshold shocks applied to the experimental preparation before it has completely recovered from the previous beat; the threshold of stimulation is elevated from its resting value, and/or the resulting beat is conducted at reduced velocity. (Such premature stimuli are much weaker than the strong shocks which sometimes elicit arrhythmias when applied during the so-called vulnerable period, as described in the previous section.)

Certain advantages accrue to studying premature conduction in a computer model. The discrete time scale allows precise measurement of conduction times and inter-stimulus intervals (although, by the same token, timing differences less than one time-step will be obscured). It is relatively easy to measure the conduction of a wave along any desired path; in fact, the passage of a wave can be made to leave a permanent record of the state of every cell, so that the choice of a measurement path may be made after the fact. Since situations can be exactly reproduced, it is possible to run various cases under identical

conditions. And it is possible to perform experiments on such idealized "preparations" as the completely homogeneous network described below.

If reentry and continuous conduction are significant factors in the maintenance of atrial fibrillation, they certainly must involve something analogous to premature conduction; hence better knowledge of premature conduction ought to aid our understanding of the fibrillatory state. It would also be desirable, if possible, to establish a criterion by which beats which result in arrhythmias might be distinguished, on the basis of their conduction, from those that do not.

In order to gain some understanding, then, of the way premature stimuli are conducted in the model, the following series of experiments were performed.

A. Conduction of a Single Premature Beat

Procedure

Network N of table 3.2 was initialized with basic cycle 250. Stimuli were applied at the basic rate until the network appeared to have reached a relatively stable state, at which time it was saved in a file. Then the sequence [restore state from file, apply test stimulus] was repeated while the test stimulus was moved progressively earlier, starting in very late RRP and ending when the ERP was reached. For each cell in the network, the arrival times of the activity waves were recorded. That is, the time at which each cell was excited, by both the normal drive and the premature waves, was stored in a file, so that the course of each wave could be reconstructed later. In algorithmic notation, the procedure was:

```
    INITIALIZE NETWORK N, BASIC CYCLE 250
    AT TIME 280 SAVE IN FILE 1;
A:  DO P1 = (values selected by experimenter);
    RESTORE FILE 1;
    AT TIME P1 APPLY STIMULUS;
    AT TIME P1 + 250 WRITE CONDUCTION-INTERVALS;
    END A;
```

Several radial paths extending outward from the site of stimulation are shown in figure 4.7 and numbered for reference in the discussion below. Graphs of arrival time vs. distance along a path are plotted with the independent variable on the ordinate so that the slope of the curve has dimensions of velocity.

This procedure was repeated using basic drive cycle lengths of 200, 150, and 100. Conduction-time graphs for representative cases are shown in figures 4.8 and 4.9.

Results

1. Delay Near the Stimulator

Figure 4.8(b) shows a typical case. Stimuli placed late in the relative refractory period caused beats which were conducted at essentially normal velocity. As the stimulus was moved progressively earlier, the premature wave began to be conducted more slowly. The slowing was most pronounced in the vicinity of the stimulator; this delay allowed the "recovery wave" to outrun the premature activity wave (see figure 4.18), so that further from the stimulator the wave encountered cells which had had additional time to recover, and conduction velocity increased. The more premature a beat, the more slowly

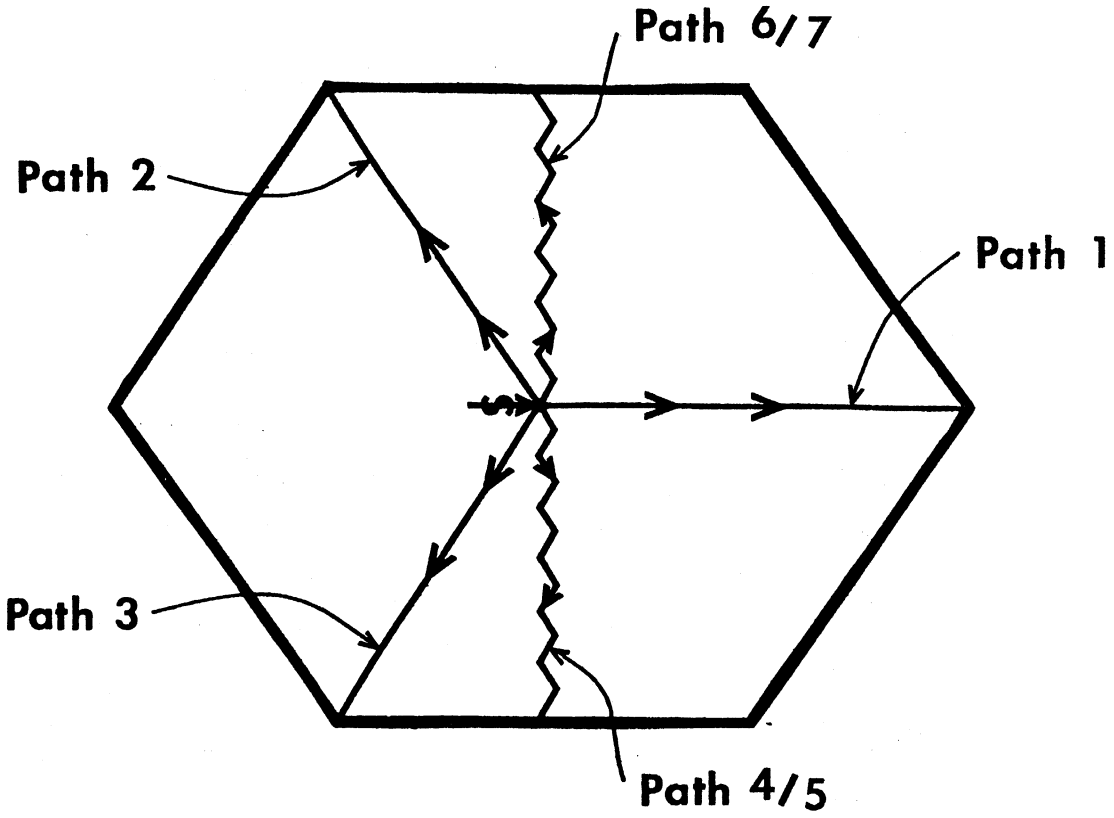

Figure 4.7. Paths Along Which Impulse Conduction was Measured.

it was conducted near the stimulator and the longer the distance over which its velocity was depressed. Even very premature waves, however, finally reached a point, distant from the stimulator, at which sufficient delay had been accumulated that the tissue in front of the wave was well-recovered and the wave attained normal conduction velocity.

2. Focal Block

Figure 4.8(a) shows another conduction-time graph from the same experiment as figure 4.8(b). The only difference between the two graphs is the path along which the waves' progress was measured: path 3 in figure 4.8(b), path 1 in figure 4.8(a). Yet figure 4.8(a), while similar to figure 4.8(b) for moderately premature waves, is radically different for beats initiated at time 120 or less. The latter show very large conduction delays near the stimulator--much larger than a single cell can sustain--followed by very high apparent conduction velocities, with some cells near the stimulator actually being excited later than cells more distant.

The explanation is to be found in the random distribution of k-values. The cells along path 1 happened to have relatively high k's near the stimulator, while the k's along path 3 were, in general, lower. Therefore, at very short cycle lengths, conduction block occurred on path 1 but not on path 3. Cells along path 1 were not activated by a wave spreading radially from the center, but rather by waves that originally began on other paths, including path 3. This activity skirted the block and eventually crossed path 1 from the side, thereby exciting some distal cells earlier than more proximal ones (the latter, part of the original block, having recovered excitability

Figure 4.8. Premature Conduction, Basic Cycle 250 Time-Steps.

(a) Conduction Measured Along Path 1.

(b) Conduction of the Same Beat Measured Along Path 3.

(c) Inter-Response Interval as a Function of Inter-Stimulus Interval.

Figure 4.9. As Above, but with a Basic Cycle of 150 Time-Steps.

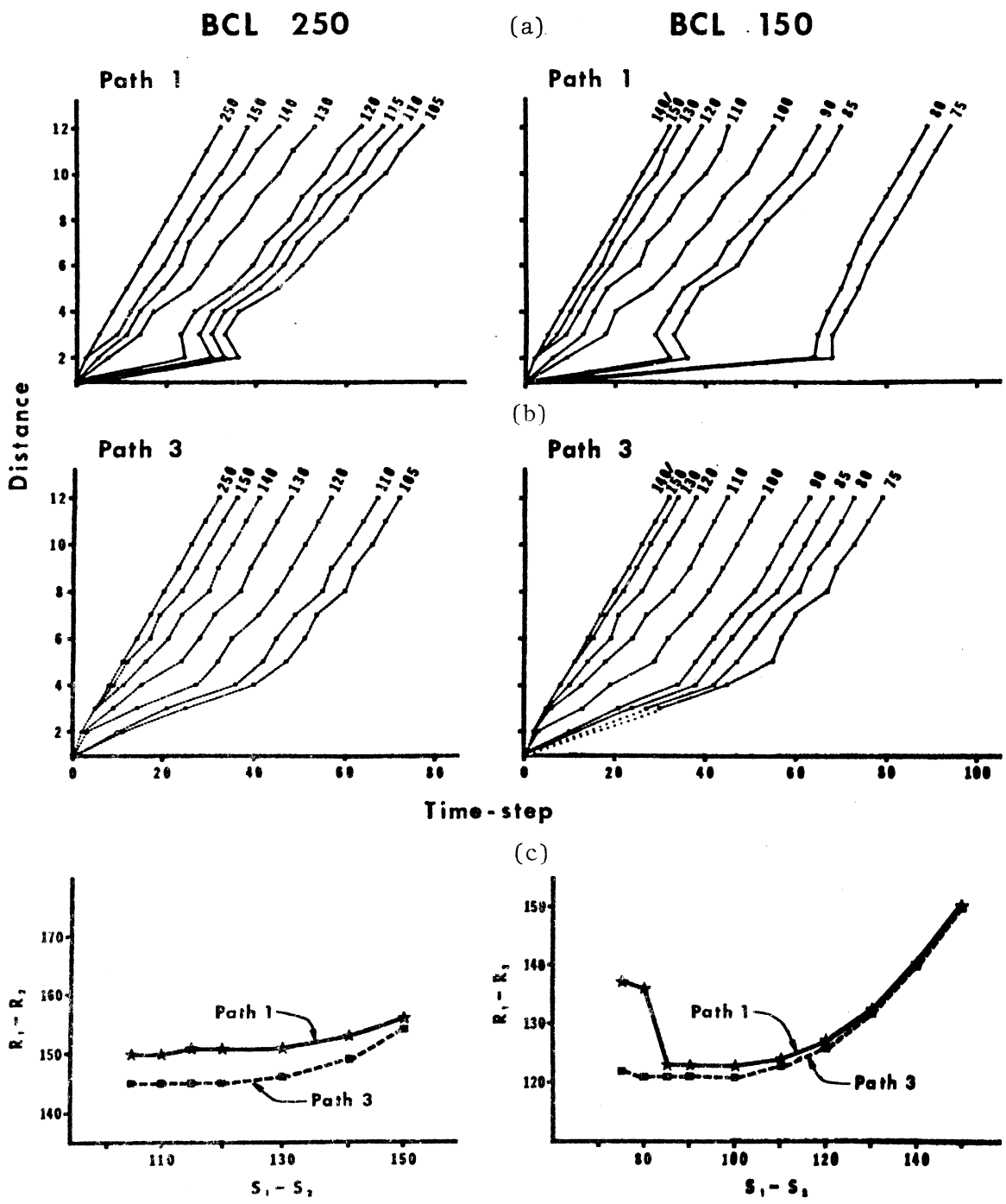

Figure 4.8

Figure 4.9

by the time the skirting wave arrived). The fact that the activity wave crossed path 1 at an angle accounts for the (nearly) simultaneous activation of many cells along the path; the high apparent conduction velocity is really a "phase velocity".

Comparison of figures 4.8(a) and 4.9(b) shows that the overall conduction times to the edge of the network (d=12) were nearly independent of path--certainly the difference in final arrival time between path 1 and path 3 was slight, compared to the radical difference in conduction patterns closer to the site of stimulation. The sudden appearance of a conduction block on path 1 when the premature stimulus was advanced from time 130 to time 120 (relative to the preceding drive) had almost no effect on the ultimate propagation times. Yet, as will be seen later, such blocks can lead to reentry and self-sustaining activity quite suggestive of fibrillation and other arrhythmias.[1]

3. Effect of Rapid Drive

To test the effect of increased basic drive rates on premature conduction, the experiment described above was repeated with the cycle length of the driving stimulus reduced to 200, 150, and 100 time-steps. Figure 4.9 is representative of the results.

The ERP was, of course, shortened at higher drive rates, because of the reduced duration of the absolute refractory period. Consequently

[1] If a similar situation obtains in cardiac muscle, one must wonder whether gross conduction-time measurements can be very revealing with regard to the genesis of arrhythmias. Indeed, recent studies indicate that the initiation of arrhythmias in experimental atrial preparations is not associated with consistent changes in conduction time to various widely-spaced recording sites on the atrial surface (Curtis, 1971).

conduction block, if it occurred, happened with earlier stimuli. The range of premature stimuli over which conduction block occurred also varied, erratically, with the rate of basic drive.

The faster basic drive rates did not appear to cause premature block to occur on paths where it did not occur previously; but the delay due to such blocks was sometimes greater, owing to the depressed conduction of the skirting wave. This caused the total path propagation time to become significantly longer than on a path where no conduction block occurred, with the result that a noticeable difference in arrival time was observed at a distal recording "electrode". Thus, increasing the rate of basic drive revealed the presence of a conduction block which was in fact present even at a slower rate, but which was undetectable by a gross conduction-time measurement.

When the driving rate was relatively high, the drive beats themselves were conducted at reduced velocity, since they amounted to a continuous train of premature stimuli. Such a situation occurred when the basic cycle length was reduced to 100, where the drive beats propagated at a rate of 0.2 cells per time-step (compared with 0.33 cells per time-step at slower driving rates). The conduction velocity of premature beats was depressed still further, at least near the stimulator; further away their velocity increased to match, but not exceed, that of the driving beat. It would appear, then, that a premature wave tends to be delayed in its early stages of propagation just long enough for cells more distant from the stimulation site to reach their average recovery state, but that this average recovery state is different from full recovery in the case of high basic drive rates.

4. Response Latency

Several of the properties of premature conduction discussed above can be seen quite clearly in figures 4.8(c) and 4.9(c), which show response latency as a function of prematurity at each of the basic driving rates tested. The driving stimulus is denoted S_1, and the premature stimulus S_2. The respective responses are denoted R_1 and R_2; these were measured at the edge of the network (distance 12 from the stimulator). Plotting the $R_1 - R_2$ interval yields a straight line of slope 1, when the $S_1 - S_2$ interval is large. That is, any change in the interval between stimuli is reflected as an identical change in the interval between responses. As the $S_1 - S_2$ interval shortens, however, the $R_1 - R_2$ interval does not decrease by quite the same amount, due to the increased $S_2 - R_2$ interval resulting from depressed conduction of the S_2 wave. This appears on the graph as a departure from the 45° line. When conduction delay just compensates for prematurity, the latency curve becomes flat. At very short $S_1 - S_2$ intervals the conduction of the S_2 wave may be so depressed that the $S_2 - R_2$ interval becomes excessive, appearing as an actual upturn of the latency curve. Similar conduction patterns in cardiac muscle have been observed by Moe, et al. (1956).

As figures 4.8(c) and 4.9(c) show, these phenomena are path-dependent: All paths show a flattening of the $R_1 - R_2$ curve as S_2 becomes more premature, but noticeable upturn occurs only on paths where a conduction block occurred. (Significantly, at some $S_1 - S_2$ intervals, the block may be quite pronounced and yet have no effect on the latency curve.) These curves are not affected greatly by changes in the basic

drive rate, except at quite fast driving rates where only the flat part of the curve is present.

B. Conduction in Homogeneous Networks

Because of the variation from path to path seen in the previous experiments, an additional series was performed in which the network of simulated cells was made completely homogeneous by setting the parameter k_σ to zero during initialization, so that each cell was given the same k. This made all cells identical, but, as noted below, did not have the effect of making all conduction paths identical. Nevertheless, when all cells are the same, it is much easier to discern the timing relationships between them and to determine the interactions of delay, threshold, local response, and so forth in some detail.

Procedure

These experiments were performed in essentially the same manner as those described in section A (above) with the obvious extensions being made in cases where more than one premature beat was required.

Results

1. Conduction of a Single Beat

Figure 4.10 shows single premature stimuli at various coupling intervals, under different rates of basic drive. These curves are quite similar to those discussed previously (figures 4.8, 4.9), except that they are much smoother because of the uniformity of the conduction path. It is evident that most of the delay, especially on early beats, occurred quite close to the stimulator, and that it varied in a compensatory way with prematurity so that activity reached distant points

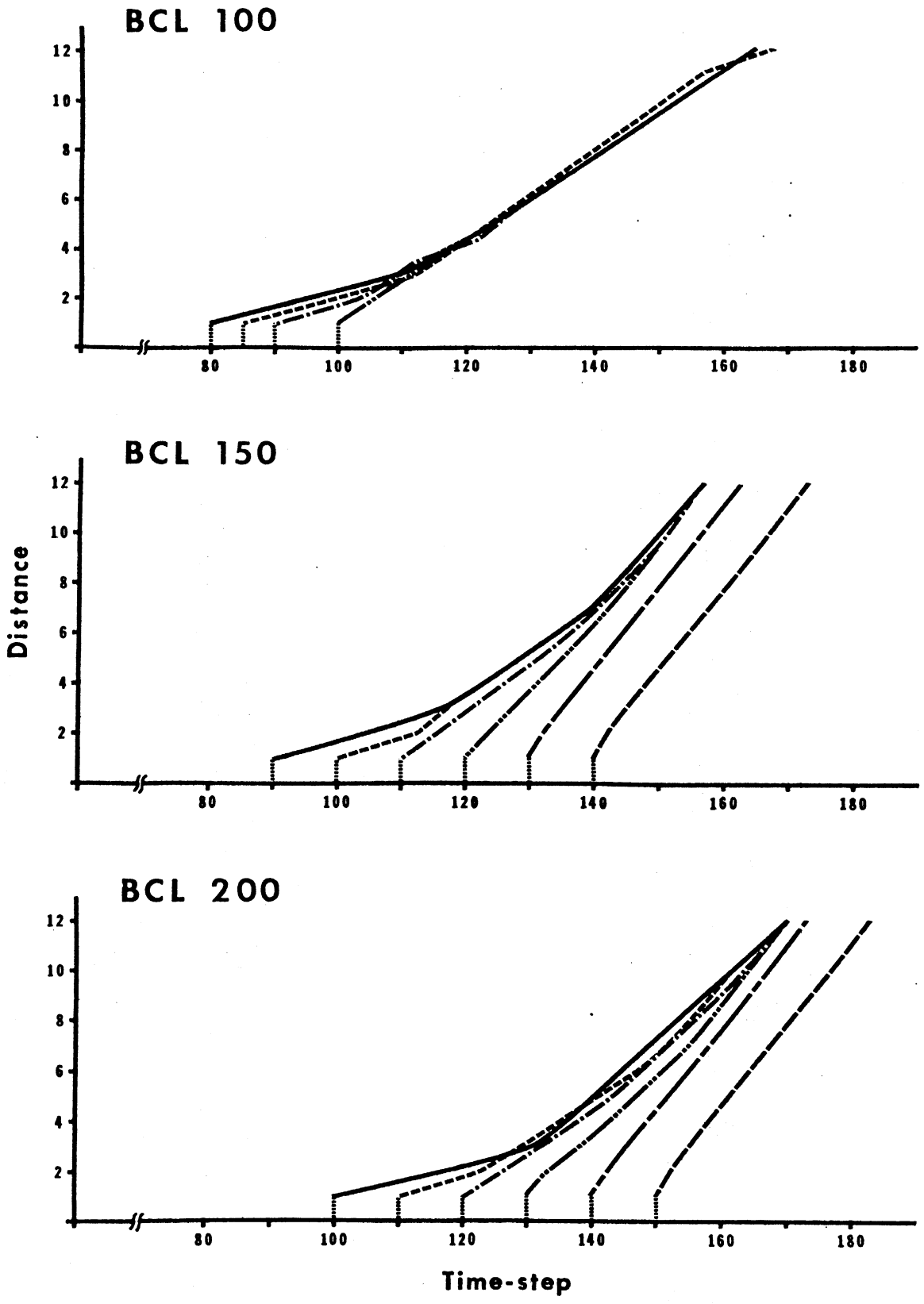

Figure 4.10. Conduction of Premature Beats in a Homogeneous Network.

at a fixed time even when the S_1 - S_2 interval was varied over a range of some 30 time-steps. Regardless of the prematurity of the stimulus, the resulting wave eventually propagated at normal velocity, unless the basic drive rate was quite high, in which case all waves propagated at subnormal velocity.

2. Accumulation of Delay

Figure 4.11 shows the conduction of four successive premature beats under different rates of basic drive. Each premature stimulus was applied just outside the ERP of the previous wave, i.e. these were the earliest-possible premature beats. The accumulation of delay over successive waves was quite evident in the prolongation of the early slowed-conduction phase: the breakpoints (at which velocity increases toward its normal value) moved further and further from the stimulator on successive beats. (In fact, the second, third, and fourth premature waves reached the edge of the network before they achieved full speed.)

3. Delay at a Distance

A case of delay at a distance, due to a rapidly-conducted wave running into the refractory tail of the preceding wave, is evident in figure 4.12, where the first two premature beats, P_1 and P_2, were elicited as early as possible while the timing of the third premature beat, P_3, was varied. Early P_3's were similar to cases seen previously; that is, they were conducted quite slowly initially and tended to merge into a single curve over a range of inter-stimulus intervals. However, when P_3 was applied later, the region near the stimulator was relatively well recovered, so the wave moved rapidly. Soon it caught up with the

Figure 4.11. Conduction of Multiple Premature Beats in a Homogeneous Network.

(The curve showing P_2 at a basic cycle length of 100 is approximately correct; the exact data were lost due to a computer malfunction.)

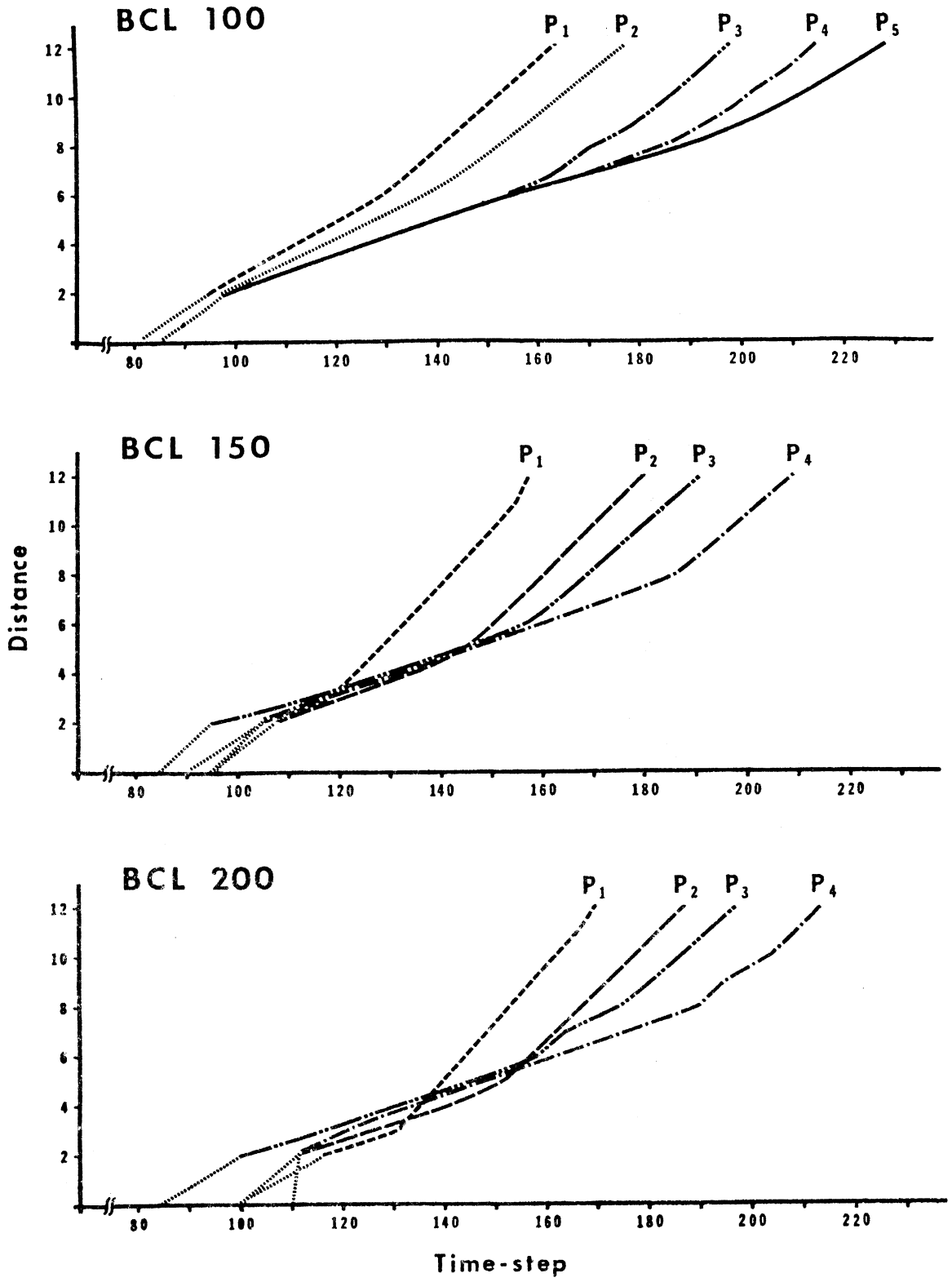
BCL 100
P1
P2
P3
P4
P5
BCL 150
P1
P2
P3
P4
BCL 200
P1
P2
P3
P4
Distance
Time-step
2
4
6
8
10
12
80
100
120
140
160
180
200
220

Figure 4.11

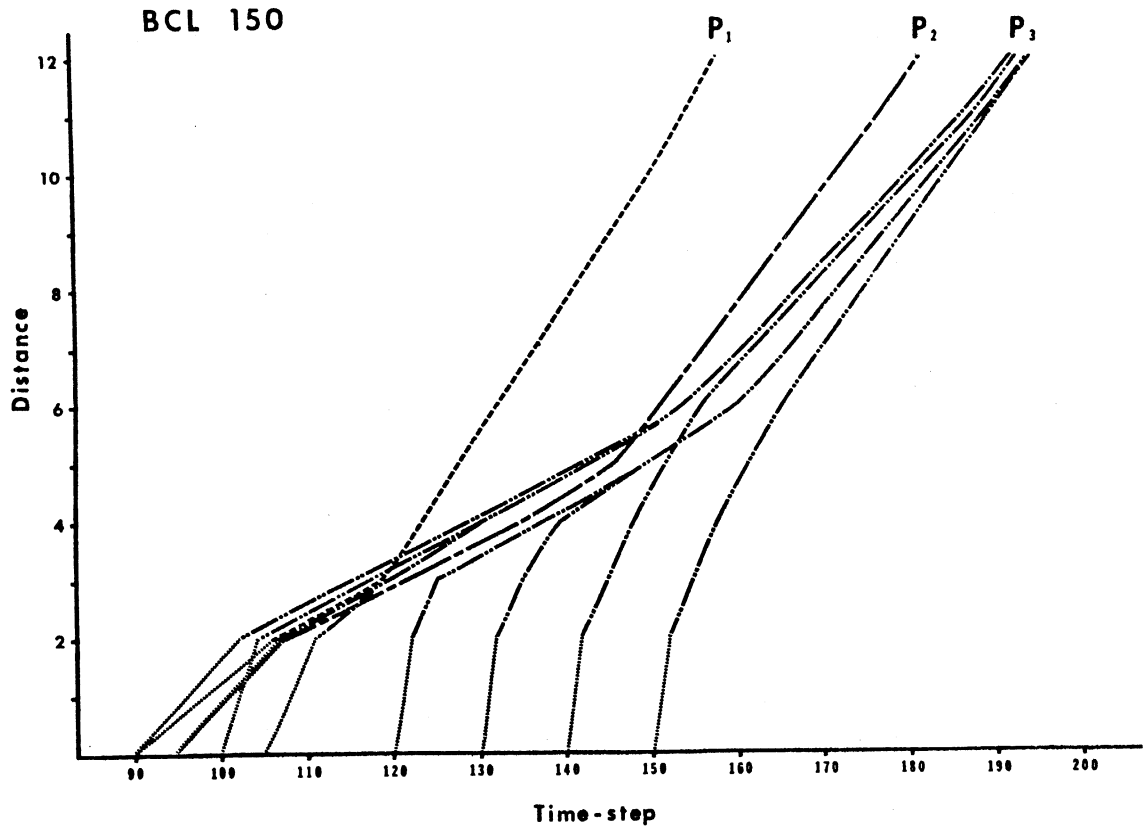

Figure 4.12. Delay at a Distance: Conduction of a Third Premature Beat in a Homogeneous Network.

partially refractory trailing edge of the P_2 wave, whereupon it slowed suddenly to a velocity even less than that of P_2. The later P_3 is applied, the more distant is the point at which this "collision" occurs.

4. Effect of the Hexagonal Neighborhood

When the network is homogeneous, conduction is always symmetric about six axes radiating outward from the site of stimulation. Nevertheless, conduction is not the same in all directions, for certain path differences are inherent in the hexagonal neighborhood structure, viz., that some cells in rank n have only one neighbor in rank n-1 while other cells in rank n have two neighbors in the lower rank. For example, compare paths 1 and 4, as defined in figure 4.7 (see also figure 3.1). When an activity wave is progressing outward in a symmetrical fashion, rank by rank, each cell along path 1 receives stimulation from only one cell in the next lower rank, while cells along path 4 each have as neighbor two cells in the next lower rank. (Path 4 thus represents a slightly preferred direction of conduction.) There is no difference when the wave is progressing through well-recovered regions, because then stimulation from even a single cell is more than adequate. But when the area is in early RRP and the conduction velocity is depressed, the magnitude of the local responses is depressed as well; and for very premature waves it may sometimes be impossible for a single cell to fire another. Then conduction can be sustained along one path by summation while it fails along another; the activity wave advances slowly along a zig-zag path, and the net propagation velocity is very low. These path differences are accentuated over successive premature beats, particularly when the latter are all very early, because then the thresholds are high, safety factors of conduction are low, and temporal and spatial

summation become important in the maintenance of conduction (see figure 4.17). If enough early beats are evoked, the difference in propagation velocities along two adjacent paths, e.g., path 3 and path 4, may cause conduction failure on one but not on the other, so that an excitable path opens up through the (fragmented) wave front, and re-entry occurs.[2] Such a situation is shown in figure 4.13.

This sort of reentry through "cracks in the neighborhood" is certainly an artifact of the model and does not, presumably, correspond very directly to any property of cardiac muscle. However, it provides a dramatic demonstration of the way in which premature beats, whose conduction is fairly marginal, can greatly magnify the effects of minor variations in the conducting properties of the excitable medium.[3] By analogy, cardiac tissue might be expected to conduct increasingly premature beats with increasing irregularity.

C. Conduction of a Second Premature Beat in Non-Homogeneous Networks

Single premature beats always show some conduction delay, and sometimes encounter focal conduction blocks. When two or more premature

[2] Interestingly, it is in the preferred directions of conduction that conduction failure occurs, as the wave runs abruptly into absolutely refractory cells. Activity along the other paths is delayed more near the stimulator, giving the cells further away more time to recover.

[3] Many of the interesting effects observed in the experiments reported here are due to the non-uniform conducting properties of the model, but the reader should be aware that such differences are predominantly due to variations in k from cell to cell, not to the neighborhood structure, as is evidenced by the fact that reentry can occur after only two premature beats in the presence of k-variation but requires five premature beats in its absence.

stimuli are applied in succession, these effects are usually enhanced. Such conditions of marginal conduction can lead to various interesting phenomena, such as the unexpectedly long effective refractory period (ERP) which follows a very premature beat (see figure 4.15). They can also lead to reentry, particularly when the premature stimuli are closely spaced. Reentries may or may not result in self-sustaining activity, but they always complicate the measurement of premature conduction because the concept of an activity wave with a definite origin becomes muddied when such a wave activates some cells more than once. The situation is still more uncertain when reentries occur at more than one locus and/or time. In the computer simulation these effects can be minimized by proper selection of the path along which to make conduction measurements.[4]

Procedure

Network N_1 of table 3.2 was initialized with initial cycle 200. The conduction-time characteristics for single premature beats at various time intervals were determined as described in the preceding section. Then the same series was re-run under identical conditions except that, for each placement of the first premature beat, a second premature beat was elicited over a range of inter-stimulus intervals. That is, after applying the first premature stimulus P_1, the state of the network was saved in file 2; then the sequence [restore file 2, apply P_2] was repeated for various intervals of the second premature stimulus P_2. Then the whole step was repeated at a different timing of P_1.

[4] Obtaining adequate conduction-time data in spite of interference from reentires, and without adding undue complications to the computer program, required judicious operation of the simulation system, for which purpose the graphic display facility was quite useful.

Figure 4.13. The Development of Reentry in a Homogeneous Network

Computer-printed state of the network at time-steps 819 and 859. Network N_1 of table 3.2 was initialized at cycle length 150; stimuli were applied at time-steps 150, 300, 390, 485, 570, 655, and 745 (i.e. 5 premature stimuli, as early as possible).

Legend: $ = stimulated
* = firing
- = absolutely refractory
· = relatively refractory
blank = quiescent

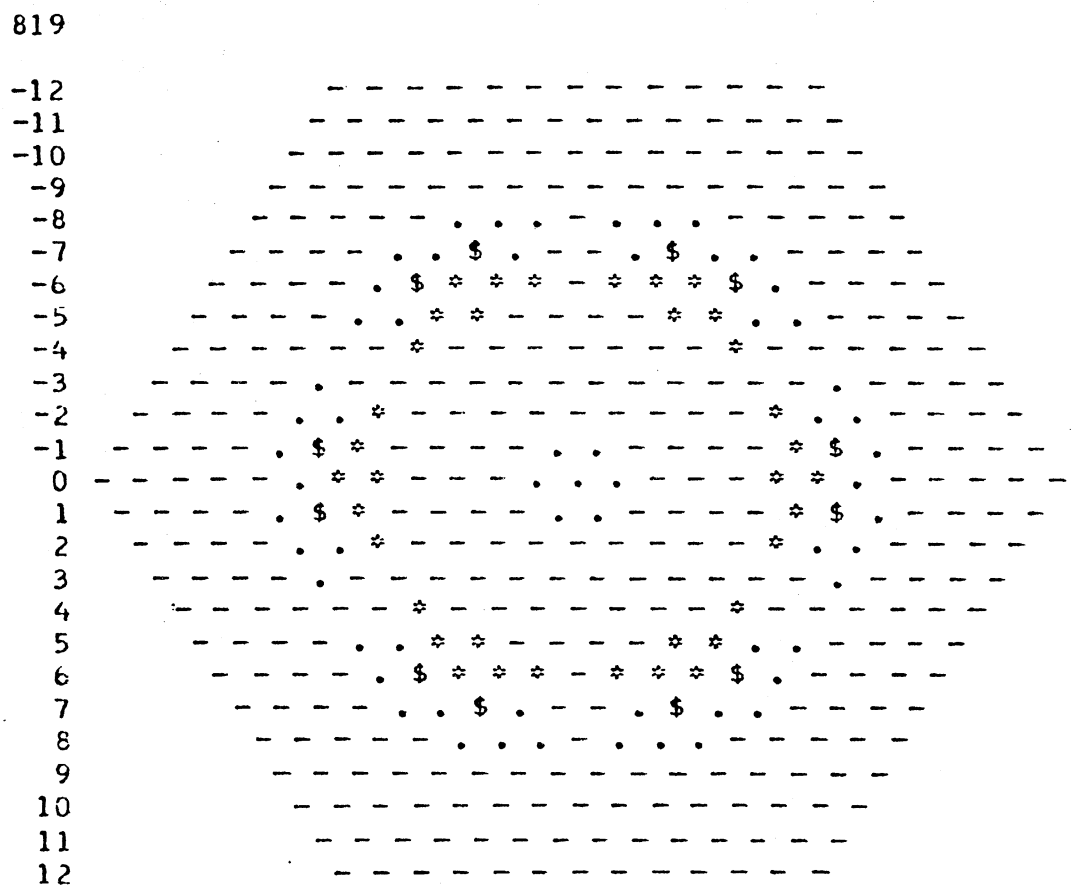
819
-12
-11
-10
-9
-8
-7
-6
-5
-4
-3
-2
-1
0
1
2
3
4
5
6
7
8
9
10
11
12

Figure 4.13

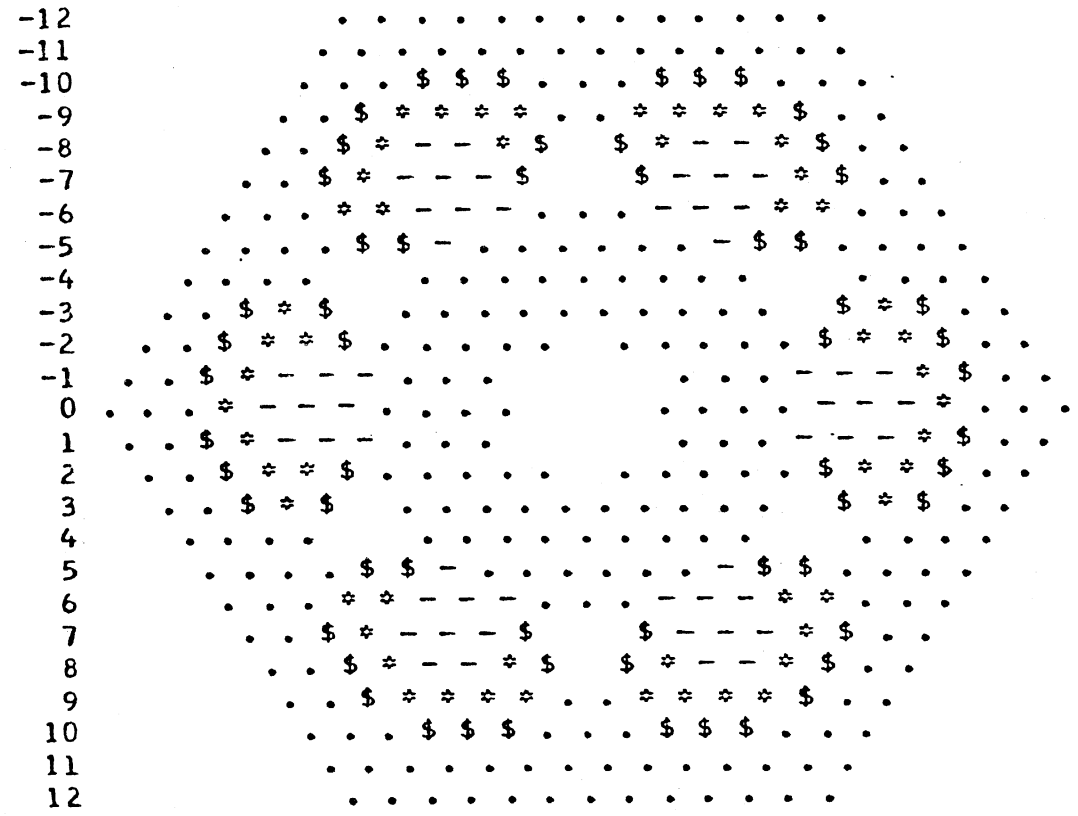
859
-12
-11
-10
-9
-8
-7
-6
-5
-4
-3
-2
-1
0
1
2
3
4
5
6
7
8
9
10
11
12

In algorithmic notation,

```
INITIALIZE NETWORK N1, BASIC CYCLE 200;
AT TIME 260 SAVE IN FILE 1;
A:  DO P1 = 300, 305, 310, 315, 320, 330, 350;
    RESTORE FILE 1;
    AT TIME P1 APPLY STIMULUS;
    AT TIME P1 + 50 SAVE IN FILE 2;
B:      DO P2 = (values selected by experimenter);
        RESTORE FILE 2;
        AT TIME P2 APPLY STIMULUS;
        AT TIME (selected by experimenter) WRITE CONDUCTION-INTERVALS;
        END B;
    END A;
```

Representative results are shown in figures 4.14(a) through 4.14(d). Path 1 was chosen for display because it was least affected by conduction block, yet shows the principal features of P_2's propagation.

Results

1. Accumulation of Delay

When a second premature beat, P_2, was initiated soon after the first premature beat, P_1, P_2 was always conducted more slowly than P_1, regardless of how premature P_1 was. As was usually the case with P_1, most of the conduction delay on P_2 occurred near the stimulator; however, incontrast to P_1, the conduction velocity of early P_2 beats remained subnormal over the entire path. If a conduction block was present in the path of a P_2 wave, then the apparent propagation delay may have been exceptionally long because of the greatly reduced velocity of the wave which skirted the block (see figure 4.14(a)).

Figure 4.14. The Conduction of P_2 After Various Placements of P_1.

Network N_1, Driving Stimulus

at Time-Step 200

(a) P_1 at time-step 300 (the earliest possible), scan P_2.

(b) P_1 at time-step 305, scan P_2.

(c) P_1 at time-step 310, scan P_2.

(d) P_1 at time-step 350, scan P_2.

In each graph, the conduction curve of P_1 has been translated to the origin for comparison with the curves of P_2.

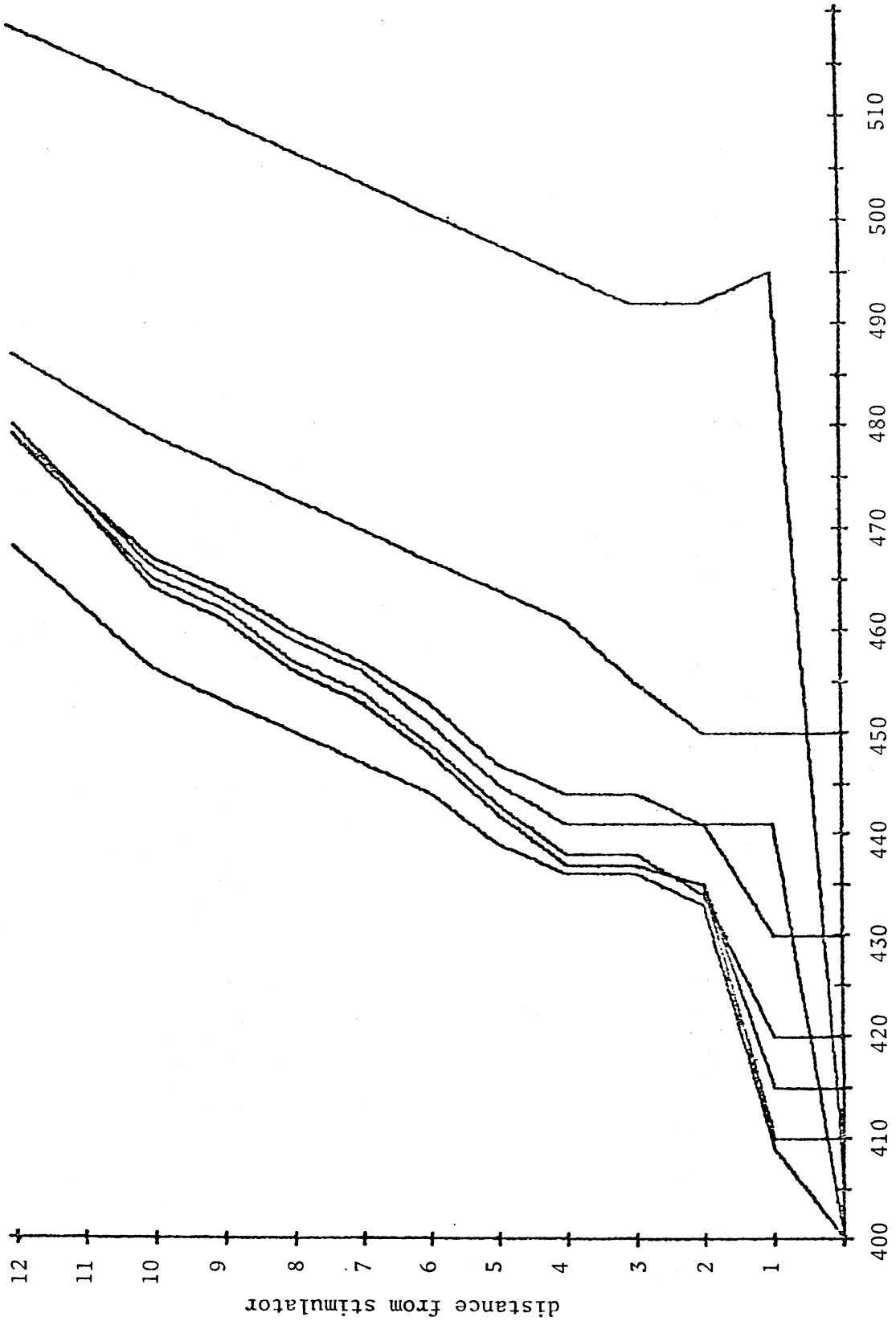
distance from stimulator
12
11
10
9
8
7
6
5
4
3
2
1
400
410
420
430
440
450
460
470
480
490
500
510
Time-step

Figure 4.14(a)

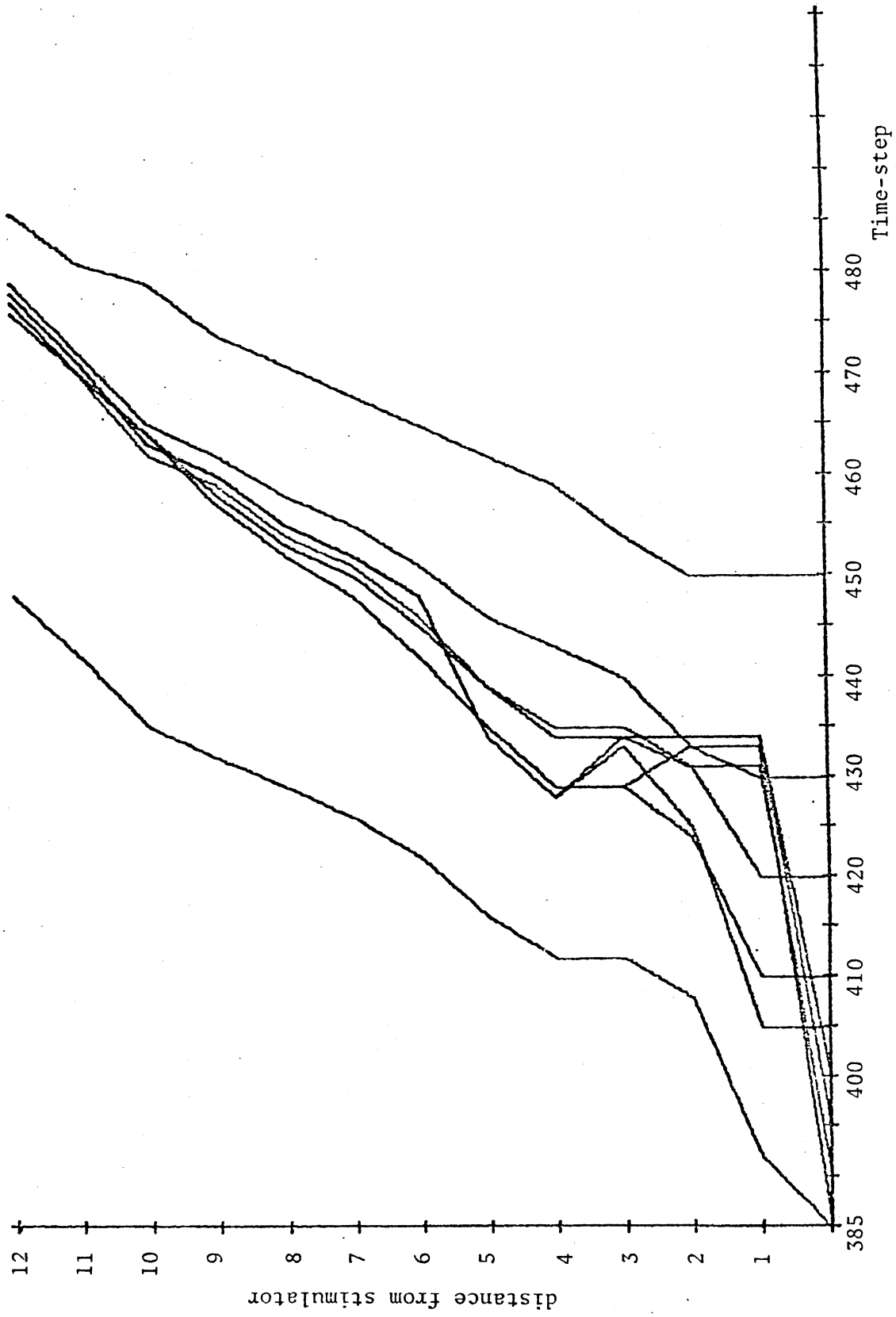
distance from stimulator
12
11
10
9
8
7
6
5
4
3
2
1
385
400
410
420
430
440
450
460
470
480
Time-step

Figure 4.14(b)

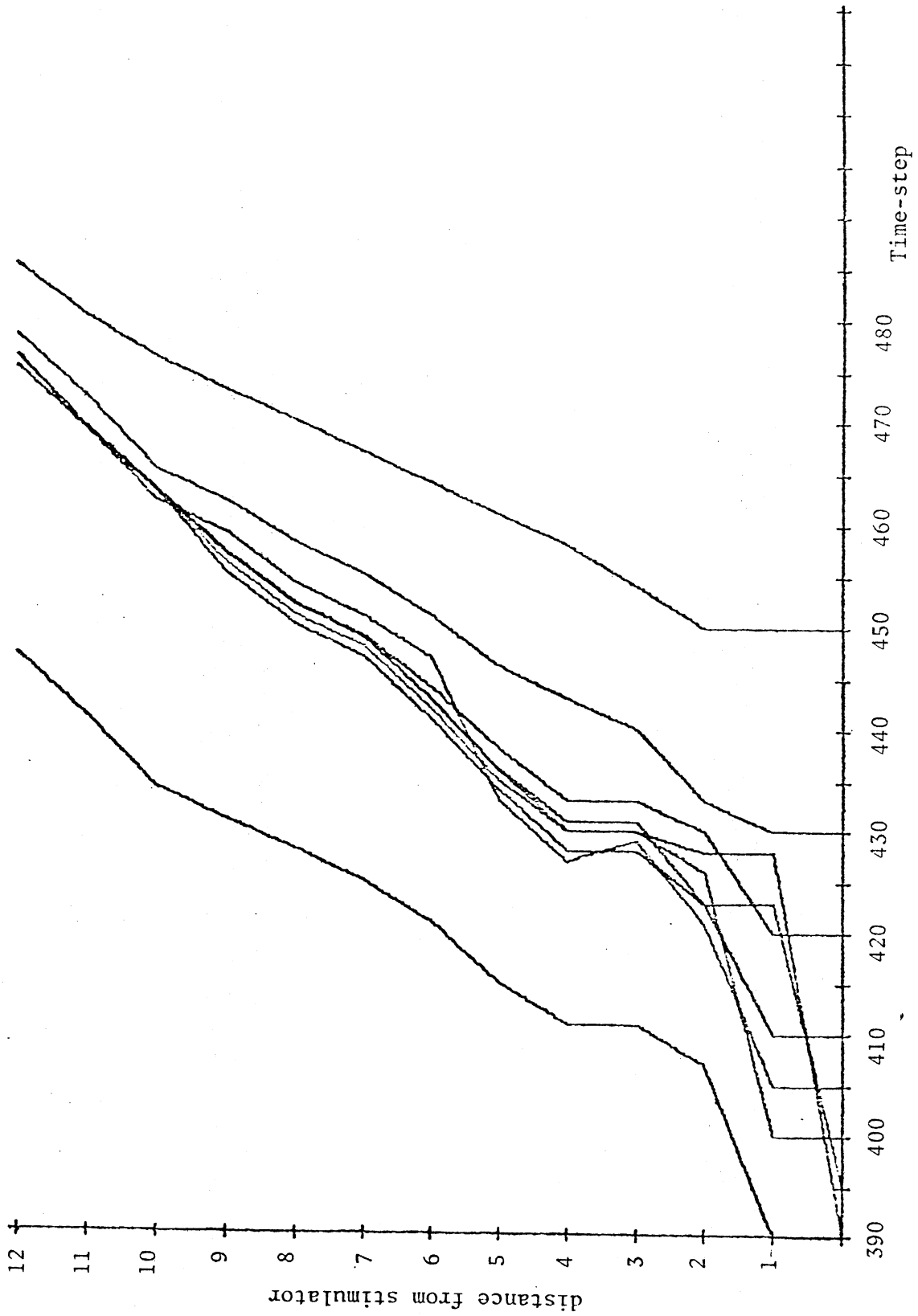
distance from stimulator
12
11
10
9
8
7
6
5
4
3
2
1
390
400
410
420
430
440
450
460
470
480
Time-step

Figure 4.14(c)

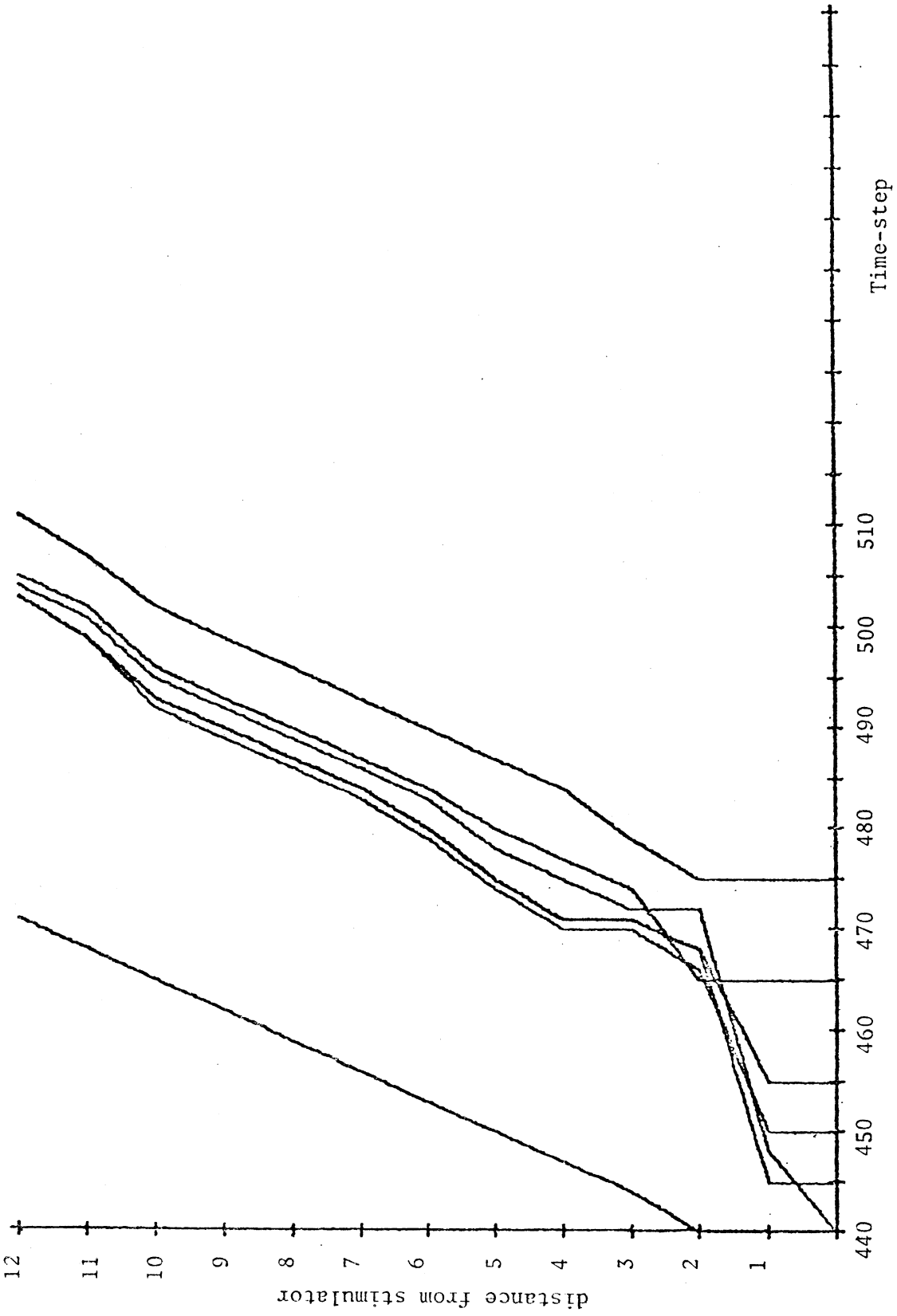
distance from stimulator
12
11
10
9
8
7
6
5
4
3
2
1
440
450
460
470
480
490
500
510
Time-step

Figure 4.14(d)

The same compensatory delay mechanism observed with P_1 also operated on P_2 beats: There was a range of inter-stimulus intervals over which final propagation time along a given path remained constant. This range was greater when P_1 was early, becoming smaller as P_1 was placed later and later (figure 4.14); however, its maximum occurred not at the earliest P_1, which was at time 100 (figure 4.14(a)), but rather when P_1 was placed slightly later at time 105 (figure 4.14(b)).

As the P_1 - P_2 interval was increased, the conduction velocity of P_2 rose. The improvement came first in the vicinity of the stimulator, where conduction had been slowest; in fact, conduction sometimes improved so quickly that, in the region near the stimulator, P_2 was conducted more rapidly than P_1, with P_2's conduction velocity then falling off as the wave moved away from the stimulator, finally becoming slower than P_1. (This phenomenon is accentuated by the rate-related foreshortening of the refractory period of P_1 near the stimulator, as discussed on page 137.) The P_2 wave, in such cases, actually caught up with the refractory tail of the preceding (slowed) P_1 wave, whereupon P_2 slowed also. Lengthening the P_1 - P_2 interval still further caused the conduction velocity of P_2 to improve along the entire path, finally reaching normal speed (which may, of course, be greater than that of the preceding P_1 wave).

2. Conduction Failure

In general, conduction anomalies--"kinks" in the conduction-time graph, mainly due to the erratic path taken by the advancing wave--were greater on P_2 than on P_1. As with delay (above), the most pronounced aberrations of P_2 conduction were associated with P_1 slightly later than

the earliest (at time 305), as a comparison of figures 4.14(a) and 4.14(b) will show. The graph of P_2 conduction does, of course, depend on the path chosen for measurement; but it is the case that when P_1 was initiated at time 305, there was no simple path along which P_2 was conducted in a relatively uniform way. Partial conduction failures seem, then, to be widespread on early P_2's, not confined to certain paths as with early P_1's.

III. Non-Propagated Responses to Stimulation

Conduction failure as seen in conduction-time graphs takes the form of some sort of focal block, usually of a quite transitory nature, which is responsible for abnormally large conduction delays. Another form of conduction failure occurs when a premature stimulus elicits a local response which is not conducted at all; that is, the premature stimulus (usually, but not necessarily, from an external stimulator) excites some poorly-recovered cells whose own responses are not strong enough to excite their equally-poorly-recovered neighbors in sufficient numbers to propagate the activity. Such non-propagated responses are believed to be responsible for two phenomena seen in cardiac tissue: (1) the ability of a very premature stimulus, which itself produces no observable response, to interfere with a slightly later stimulus which ordinarily would have produced a response, and (2) the abnormally prolonged effective refractory period following a very premature stimulus.

A. Unexpected Prolongation of ERP

It has long been supposed that, in general, the refractory period following a premature beat will be shortened, due to the reduced cycle length. This relationship has been directly programmed into the simulated cells (see Chapter III), but the distinction between properties of the elements of the model and properties of the aggregate must be observed. In particular, it is not apparent a priori just what the relation between refractory period and prematurity in the model will be when speaking of conducted beats rather than simply the "local response" of isolated units.

Accordingly, a series of experiments was performed in which the simulated tissue was driven at a moderate rate that was interrupted periodically by the interpolation of a premature stimulus. The refractory period following the premature beat was measured by applying a second premature stimulus shortly after the first and noting whether or not a conducted beat resulted. By varying the timing of P_2 relative to P_1 the effective refractory period of P_1 could be measured accurately. By varying the timing of P_1 relative to the preceding drive, the dependence of refractory period on degree of prematurity could be determined.

Procedure

Network N_1 of table 3.2 was initialized with initial cycle length 200. One stimulus of strength 200 was applied at time 200, and the state was saved in file 1 at time 290. The following sequence was then done repetitively: [restore state from file 1, apply P_1; if P_1 elicits a propagated response, determine the refractory period]. The refractory

period was determined by saving in file 2 the simulation state some time after the activity wave due to P_1 had developed, but before recovery from that wave had begun. Then the following sequence was iterated: [restore state from file 2, apply P_2, note result], with the time of application of P_2 initially quite short but increased on each iteration. The iteration was stopped when P_2 elicited a conducted beat.

In algorithmic notation, the procedure used was essentially

```
    INITIALIZE NETWORK N1, . . , BASIC CYCLE LENGTH 200;
    AT TIME 200 APPLY STIMULUS OF STRENGTH 200;
    AT TIME 290 SAVE IN FILE 1;
A:  DO P1 = 290 TO 304 BY 1, 305 TO 375 BY 5;
    RESTORE FILE 1;
    AT TIME P1 APPLY STIMULUS OF STRENGTH 200;
    IF (propagated response occurs)
B:    THEN DO;
      AT TIME 380 SAVE IN FILE 2;
      P2 = 380;
C:    RESTORE FILE 2;
      AT TIME P2 APPLY STIMULUS;
      IF (propagated response) THEN DO NEXT A;
      ELSE P2 = P2 + 1, GO TO C;
      END B;
    END A;
```

The above procedure was applied to four cases: the standard network N_1 of table 3.2 (where $k_\sigma = 1.5$), and that same network with k_σ reduced successively to 1.0, 0.5, and 0.

Results

The dependence of the refractory period of P_1 on its degree of prematurity is illustrated in figure 4.15(a), where for each time of application of P_1, plotted along the abscissa, the minimum value of P_2 at which a propagated response to P_2 occurred is plotted on the ordinate. The variation of k_σ corresponds to a variation in the amount of inhomogeneity in the network. The general form of all four curves is roughly the same: the refractory period duration drops smoothly as P_1 becomes more and more premature, until a minimum duration is reached; then occurs an upswing, whose sharpness depends on the amount of inhomogeneity present in the network. A more gradual upturn in the curve is associated with the more homogeneous networks, whereas the network with the greatest amount of inhomogeneity from cell to cell also shows the smallest minimum value of refractory period and the sharpest rise in refractory period at very premature cycle lengths.

The smooth decrease in refractory period with increased prematurity of the test stimulus is in accord with classical observations (Bazett, 1918; Moe, et al., 1964) and is a direct reflection of the incorporation of such a relation into the definition of the individual cells of the model. The sudden upturn in R.P. duration following very premature test stimuli is entirely unanticipated, and seemingly at variance with observations on real cardiac tissue.[5]

Detailed analysis of the behavior of the inhomogeneous networks (those for which $k_\sigma > 0$) is very complicated and tedious; those cases

[5] However, recent careful studies of rabbit atrium have shown that the refractory period following a premature stimulus is, indeed, lengthened when the test stimulus is very premature, as shown in figure 4.15(b) (unpublished results of Dr. H. Fukushima). The similarity to the results of computer simulation (figure 4.15(a)) is apparent.

are best "analyzed" by observing the results of simulation. A homogeneous network ($k_\sigma = 0$), though, because of its symmetry, is amenable to a degree of analysis sufficient to explain the principal features of the curve shown in figure 4.15. Since the discussion of this case will, of necessity, involve detailed properties of the model cells, the reader should remember that the aim here is to understand why the model behaves as it does, and not to imply that directly analogous statements would necessarily be true of cardiac tissue.

For P_1 later than time 325, the ERP curve follows the $k\sqrt{C}$ relation of refractory period to cycle length: increasingly premature stimuli mean a progressively shorter cycle and, hence, a shorter refractory period. This property is, of course, directly programmed into the model. The question is, why does this relation fail as P_1 becomes still more premature?

Figure 4.16 shows the arrival time of the stimulus wave P_1 at each of the cells along a radial path from the point at which the stimulator was located. For P_1 placed after time 340, the conduction velocity of the premature wave is the same as that of the normal drive stimulus, that is, the P_1 wave is not really premature, since it travels entirely through fully-recovered tissue. As P_1 is moved earlier, it begins to encounter incompletely recovered cells at the site of stimulation, and so the initial conduction velocity decreases. The delay due to this reduced conduction velocity allows the regions in front of the advancing P_1 wave front additional time to recover, so that the premature wave encounters cells that are increasingly more excitable as it moves outward. These more fully recovered cells suffer less delay between receipt of stimulus and response, so the wave's

Figure 4.15. The Dependence of Refractory Period on the Degree of Prematurity.

(a) in the Simulation
(b) in Rabbit Atrium

Figure 4.15

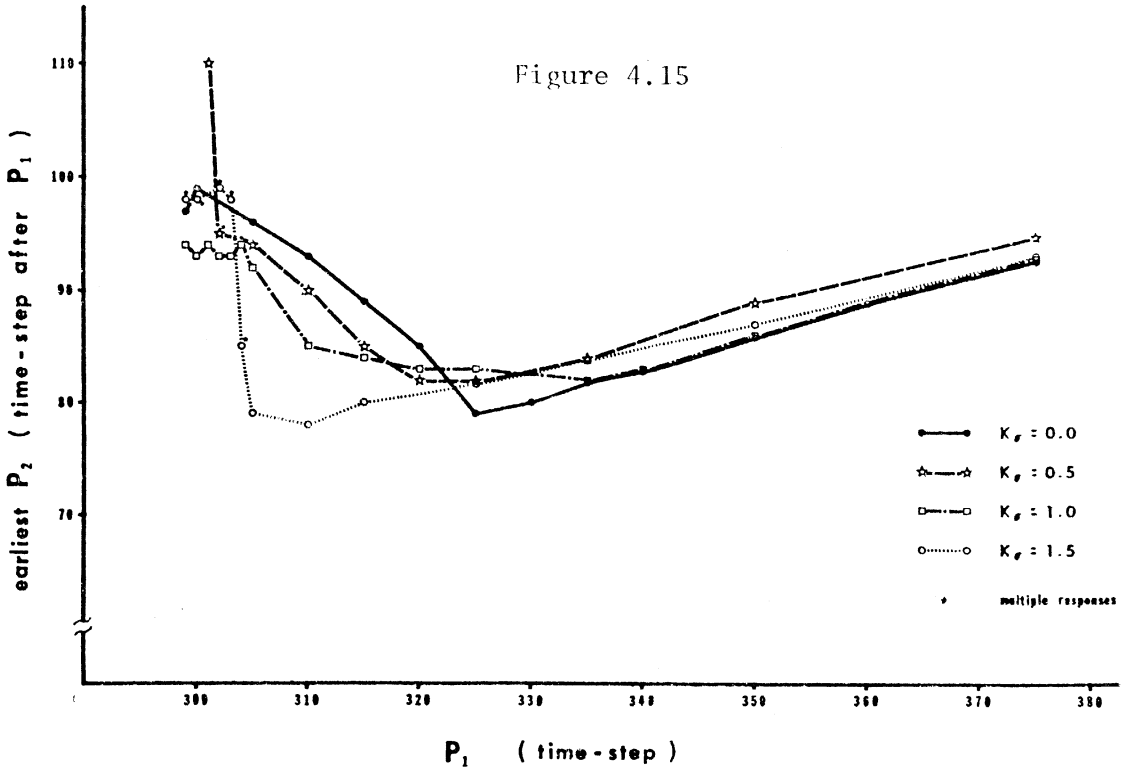
earliest P_2 (time-step after P_1)
110
100
90
80
70
300
310
320
330
340
350
360
370
380
P_1 (time-step)
K_σ = 0.0
K_σ = 0.5
K_σ = 1.0
K_σ = 1.5
multiple responses

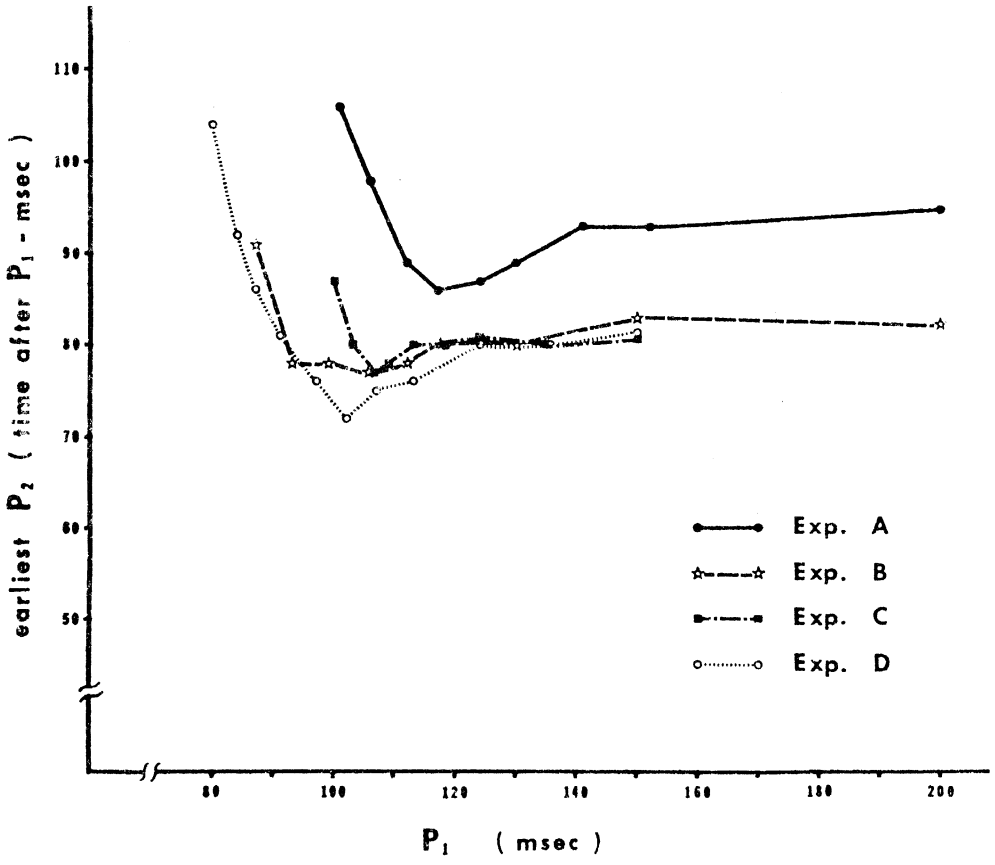
earliest P_2 (time after P_1 - msec)
110
100
90
80
70
60
50
80
100
120
140
160
180
200
P_1 (msec)
Exp. A
Exp. B
Exp. C
Exp. D

Figure 4.16. Conduction of a Single Premature Beat in a Homogeneous Network.

Same network as in figures 4.14 and 4.15. The driving stimulus was applied at time-step 200; its conduction curve has been translated to the origin of this graph for comparison with the curves of P_1.

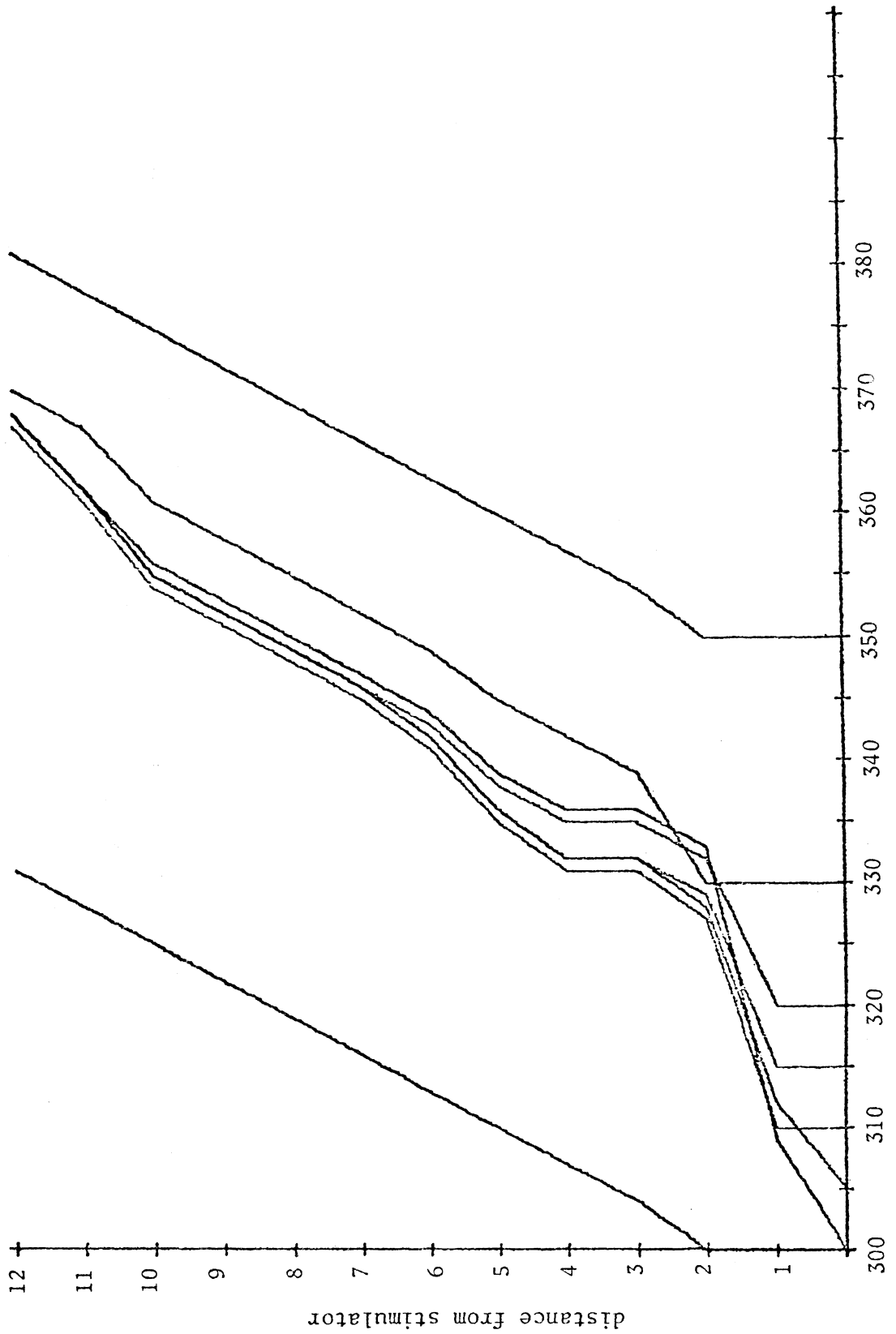
distance from stimulator
12
11
10
9
8
7
6
5
4
3
2
1
300
310
320
330
340
350
360
370
380
Time-step

Figure 4.16

conduction velocity rises. Eventually, as is apparent in figure 4.16, the premature wave becomes conducted at normal velocity.

If one thinks of a "wave of recovery" passing over the tissue behind a wave of depolarization, then the situation here can be viewed as a case of the slowed premature wave being outrun by the preceding recovery wave, which moves at the same speed as the driving wave. As figure 4.16 shows, the more premature a wave becomes, the more it is delayed, particularly during its early stages of propagation. The net result is that conduction delay largely compensates for prematurity, so that the conduction time graphs for all premature waves coalesce to a single curve at a point remote from the site of stimulation.

This compensatory delay effect, which means that the interval between P_1 and the preceding drive beat, as measured, say, 10 units from the site of stimulation, cannot be reduced below some fixed minimum regardless of how early P_1 is applied, explains the phenomenon of increased ERP at short P_1 cycle lengths.

Essentially, P_2 is constrained by two factors: the time course of recovery of excitability following P_1, and the maximum delay per cell that can be achieved without failing to sustain propagation. In the example shown here, moving P_1 earlier than approximately time 325 does not cause the resulting wave to reach portions of the tissue distant from the stimulator any sooner (in fact, it may reach some places later) than it would have otherwise; thus P_2 cannot be applied any earlier in spite of the earlier application of P_1, given the assumption that P_2 was already as early as possible and was sustaining the maximum possible conduction delay.

A second effect which occurs as P_1 is placed earlier and earlier can be seen in figure 4.16: reduction in effective radius of the external stimulator, due to the distance bias. For P_1 earlier than about time 325, units at radius 2 from (X_0,Y_0) (the coordinates of the external stimulator), which receive a stimulus of strength $\Psi/4$, are insufficiently recovered to be excited, whereas those units at radius 1, in the same recovery state as the units at radius 2 (because the drive stimulus fired both sets at the same time), are excited by virtue of the stronger stimulus they receive, Ψ. The concomitant increased conduction delay between rank 1 and rank 2 accounts for the conpensatory phenomenon described above. It will be noted that the breakpoint in the ERP vs P_1 curve comes just at the value of P_1 where the partial failure of external stimulation is encountered.

The extra delay induced by the diminished radius of the stimulator more than offsets the time increment gained by moving P_1 from 325 to 320 (figure 4.16), so that the activity wave actually arrives at the cells in rank 2 later when P_1 is applied earlier.

A third mechanism comes into play when P_1 is moved still earlier, in this case from time 320 to time 315, which allows conduction delays to become even larger than the apparent maximum allowed by the equations of the model, i.e. 10 time-steps per cell.[6] What happens is that the conduction paths indicated by the graphs no longer represent the actual paths followed by the advancing activity waves when the latter are very premature, even though the network is homogeneous.

[6] If we call this minimum sustainable conduction velocity the "critical conduction velocity", then it represents the absolute maximum delay that a wave can accumulate under the terms of the model as it spreads from cell to cell.

The conduction times shown in the graph of figure 4.16 were recorded along path 1 in the network, as defined in figure 4.17. As described previously, it is possible for the hexagonal neighborhood structure to affect the propagation of premature beats. This happens in the present case: when P_1 is applied at time 315, there is a conduction failure along path 1 but not along path 4 in passing from rank 1 to rank 2. Hence some cells in rank 2 receive excitation from other cells in the same rank, rather than exclusively from cells in rank 1. The effective path length is thereby lengthened, and may be lengthened still further as the same process occurs in the higher-numbered ranks. This temporal dissociation among the cells may increase on P_2, providing additional zig-zag routes for the activity wave to follow. In this case, paradoxically, breakup of the wave front actually enhances conduction by virtue of the extra delay it allows, whereas one might ordinarily expect the more integrated waves to be conducted better because of the added summation that takes place. Consequently, the P_2 wave can be initiated earlier than would have been possible had the dissociation not developed. This factor contributes to the reduced slope, and even downturn, of the ERP vs P_1 curve at very short cycles.

The solid lines in figure 4.17 show the P_1 and P_2 waves' progress along path 1 for the earliest possible beats; the conduction velocity is greatly slowed, particularly on P_2. (Compare with the "minimum" conduction velocity line also shown in figure 4.17, which indicates the maximum attainable conduction delay per cell. The conduction delay appears larger than this maximum because, as explained above, the path actually involves more than one cell.) The dashed lines in figure 4.17

show the same waves, along path 4. In both cases the P_2 wave propagates faster, initially, than the P_1. This seemingly contradictory behavior can be understood by recalling the dependence of absolute refractory period duration on the interval between stimuli (the "cycle length"). The large delay in the early conduction of P_1 means that the region near the stimulator sees a substantially shorter interstimulus interval than does the region further away; consequently the region near the stimulator recovers its excitability somewhat earlier, relative to the more distant region, than would be expected on the basis of conduction time alone. That is, the "recovery wave" from P_1, as shown in figure 4.18, has a time course that is similar to that of the P_1 activity wave but is foreshortened during the early phase. It might appear that this extra shortening of the early P_1 refractory period should allow P_2 to be placed earlier than shown in figure 4.18. In fact, P_2 can be placed earlier and still be effective, that is, excite the cells under the stimulator; but the activity will not be propagated. The shallow slope of the P_1 recovery curve implies a very slow rate of recovery with respect to distance from the simulator, which in turn requires very long delays in the early phases of P_2 if that wave is to find excitable cells always in its path. The required delay is simply too large for the cells to sustain. Therefore, a propagated wave can result only when P_2 is applied somewhat later. But by then the rank 1 cells are relatively well recovered, due to their foreshortened refractory period on P_1, and so the initial conduction velocity is larger than it was on P_1.

In summary, the duration of the effective refractory period following a single premature beat, in this idealized, homogeneous model,

Figure 4.17. Conduction of Early First and Second Premature Beats, Showing Path Differences.

Homogeneous network (network N_1 of table 3.2, with $k_\sigma = 0$; basic cycle length 200).

Figure 4.17

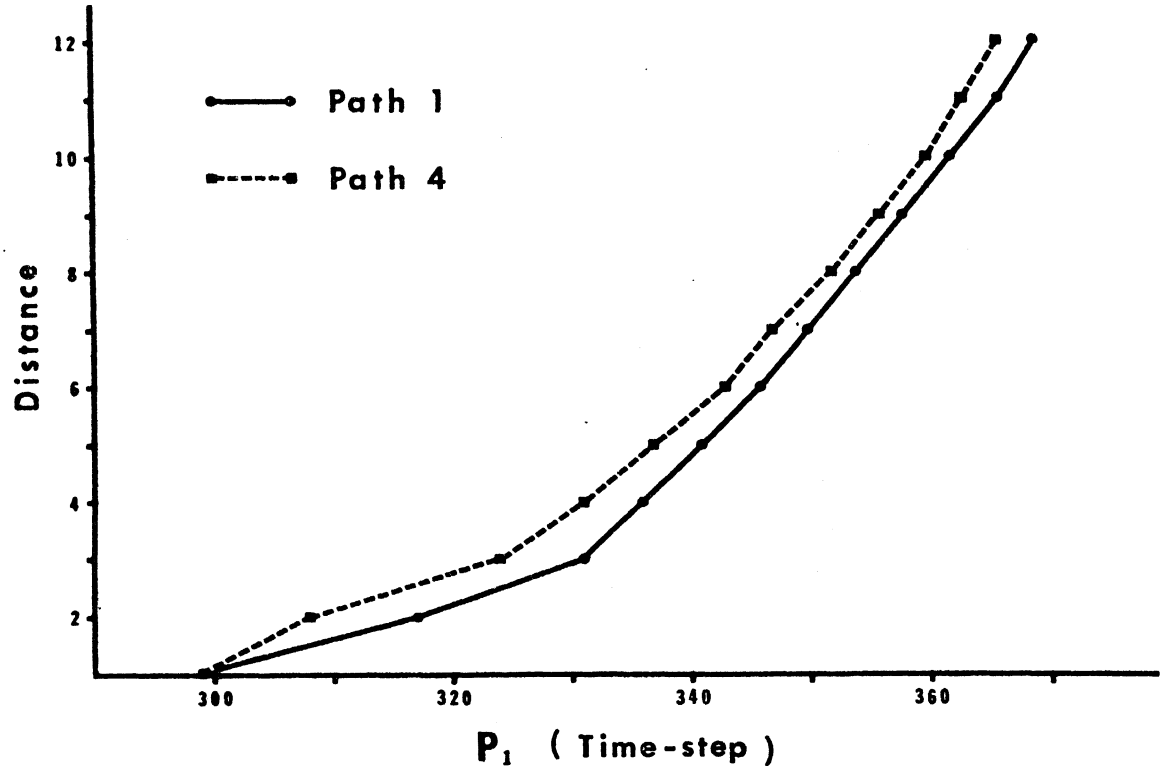
Path 1
Path 4
Distance
12
10
8
6
4
2
300
320
340
360
P1 (Time-step)

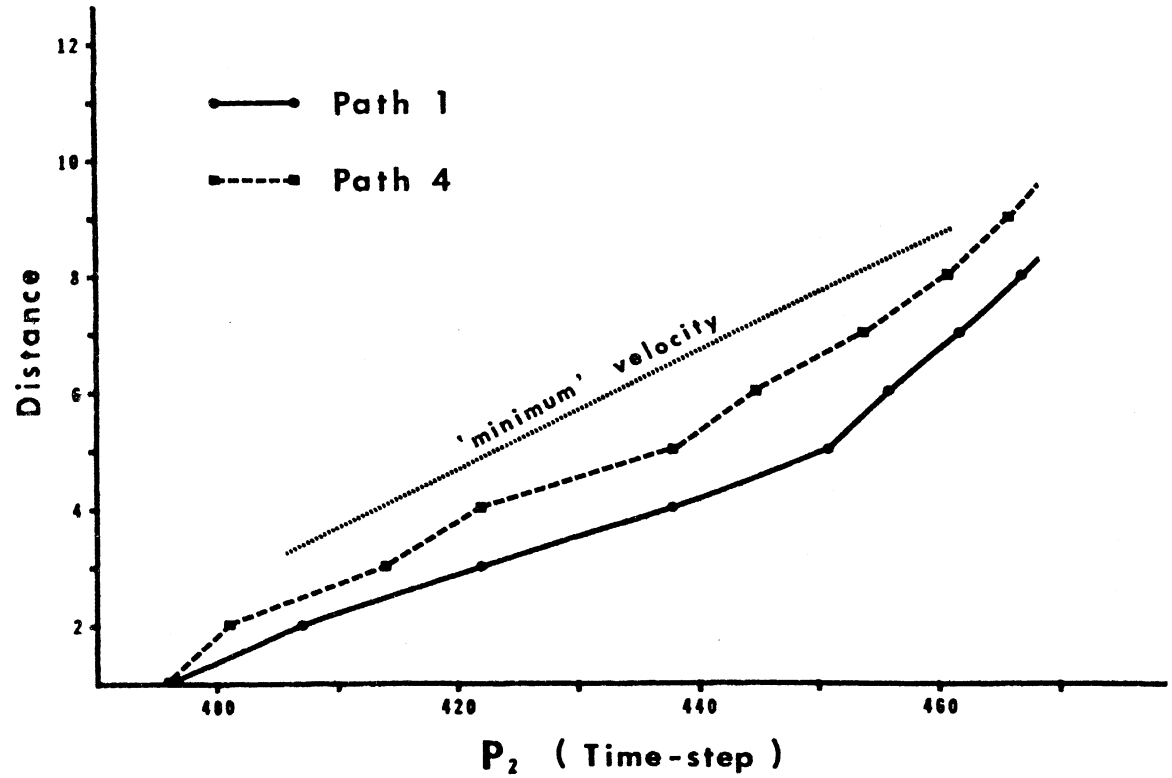
Path 1
Path 4
'minimum' velocity
Distance
12
10
8
6
4
2
400
420
440
460
P2 (Time-step)

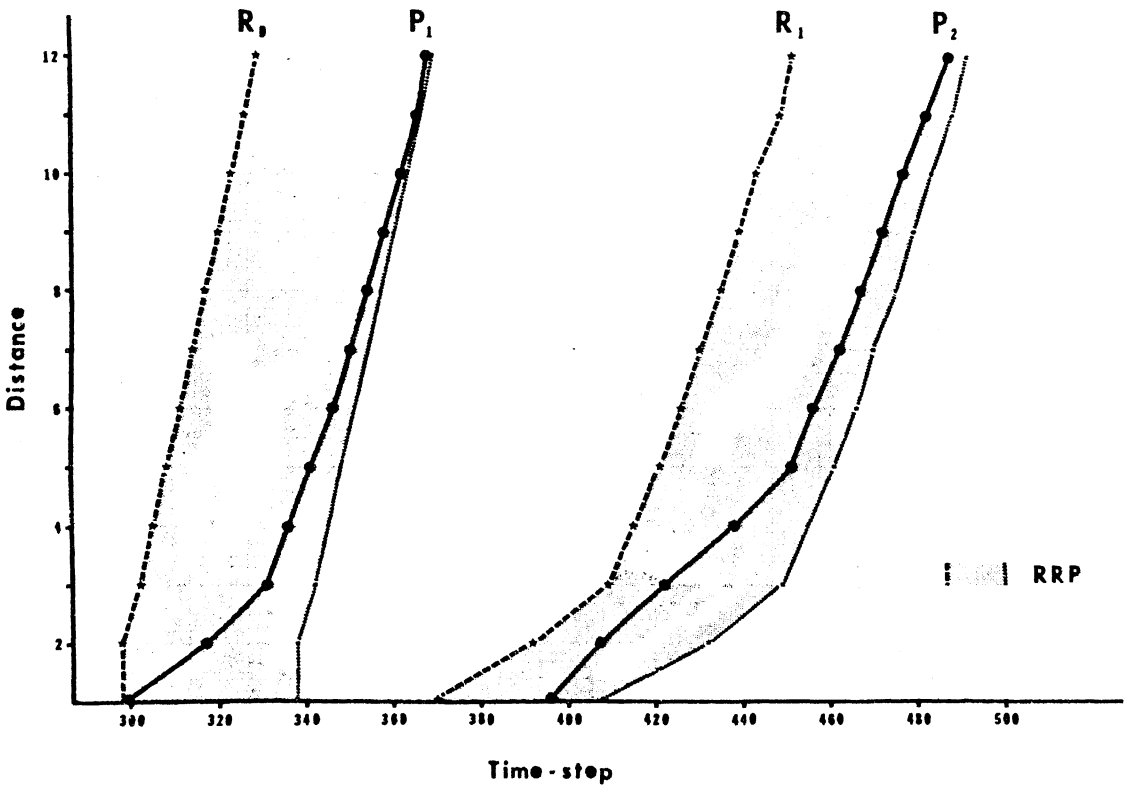

Figure 4.18. Conduction of Early First and Second Premature Beats Showing Relation to Recovery of Excitability (Homogeneous Network).

P_1, P_2 indicate conduction of activity on first and second premature beats;

R_D, R_1 indicate "conduction" of the recovery process (i.e. the ARP-RRP boundary) following the driving and first premature beats;

Shaded area indicates relative refractory period.

(Network N_1 of table 3.2, with $k_\sigma = 0$; basic cycle length 200.)

depends in a somewhat complicated way on the degree of prematurity of that beat. Denoting the first premature stimulus as P_1, we define its ERP as the earliest time at which a second premature stimulus, P_2, can produce a propagated response. The following factors, then, relate the ERP duration to the timing of P_1:

1. The dependence of the absolute refractory period duration on cycle length, causing the ERP to shorten, at first, as P_1 is made more premature;
2. the increase in conduction delay at more premature P_1 timings;
3. the partial failure of external stimulation, entailing additional conduction delay reflected in a sharp breakpoint in the ERP vs. P_1 curve;
4. the temporal dissociation of cells due to (mainly spatial) summation of stimuli, resulting in increased effective path lengths and permitting, thereby, the propagation of very premature P_1 and P_2 at velocities less than the "critical conduction velocity."

B. Interference

In animal experiments on the conduction of premature beats, it has been observed that certain very early stimuli, which do not themselves elicit a propagated response, nevertheless interfere with slightly later stimuli which ordinarily would have produced propagated responses (Lewis and Drury, 1926). That is, if a driving stimulus D applied to an experimental preparation at time t is followed by an effective refractory period of duration e, then a sufficiently strong premature stimulus P will ordinarily produce a conducted response if applied

later than time $\underline{t+e}$. But if an additional premature stimulus P' is applied slightly earlier than time $\underline{t+e}$, the conducted response to P may be abolished--in spite of the fact that (in keeping with the definition of "effective refractory period") no propagated response to P' is observed.

The time range over which the response to P is abolished depends on the timing of P'. Moving P' earlier decreases its effect; when P' falls within the absolute refractory period, it has no effect on P.

This phenomenon has been hypothesized to result from the existence of a local response to P' which is too weak to produce a propagated beat, but which pre-empts some of the excitable tissue that would have responded to P; thus the local response to P is rendered inadequate to generate a conducted beat. Since a local, non-propagated response is known to occur in the model, a series of simulation experiments was performed to see if the interference phenomenon also existed.

Procedure

Network N_1 of table 3.2 was initialized with cycle length 200. From previous experiments the duration of the effective refractory period at various timings of P_1 was known. (Had it not been known, it could have been determined by trial.) A drive stimulus was applied at time 200, followed by a single premature stimulus at time 325, which is fairly late in the RRP of P_1. With P_1 at time 325, the ERP duration was 82, i.e. the earliest time at which P_2 elicited a conducted response was time 407. The state of the network shortly after the application of P_1 was saved in file 1. Then the sequence [apply P_2 at time T_2, apply P_3 at time T_3] was repeated with T_2 equal to 406 and T_3 ranging from 407 upward in steps of 1 until a propagated response to P_3

occurred. This determined the range of interference for the given values of P_1 and P_2. The timing of P_2 was then advanced in steps of 2, and at each step the above procedure was repeated. The result is shown in figure 4.19(b).

In algorithmic notation,

```
    INITIALIZE NETWORK N1, CYCLE LENGTH 200;
    AT TIME 200 APPLY STIMULUS;
    AT TIME 325 APPLY STIMULUS;
    AT TIME 350 SAVE IN FILE 1;
A:  DO P2 = 406 TO 350 BY -2;
    RESTORE FILE 1;
    AT TIME P2 APPLY STIMULUS;
    AT TIME 407 APPLY STIMULUS;
    IF (propagated response) THEN STOP;
B:      DO P3 = 408 TO 450 BY 1;
        RESTORE FILE 1;
        AT TIME P2 APPLY STIMULUS;
        AT TIME P3 APPLY STIMULUS;
        IF (propagated response) THEN DO NEXT A;
        END B;
    END A;
```

The experiment was repeated with P_1 applied earlier in RRP, at time 310, to see if a more premature P_1 would leave the cells in such a state that P_2 would produce a larger local, non-propagated response and hence interfere more with P_3. This did happen, as shown in figure 4.19(c).

Figure 4.19. Interference From a Non-Propagated Stimulus--Computer Simulation.

Cross-hatched regions indicate the zone in which propagated response to premature stimulus P_3 was abolished by the presence of P_2, even though P_2 alone produced no propagated activity.

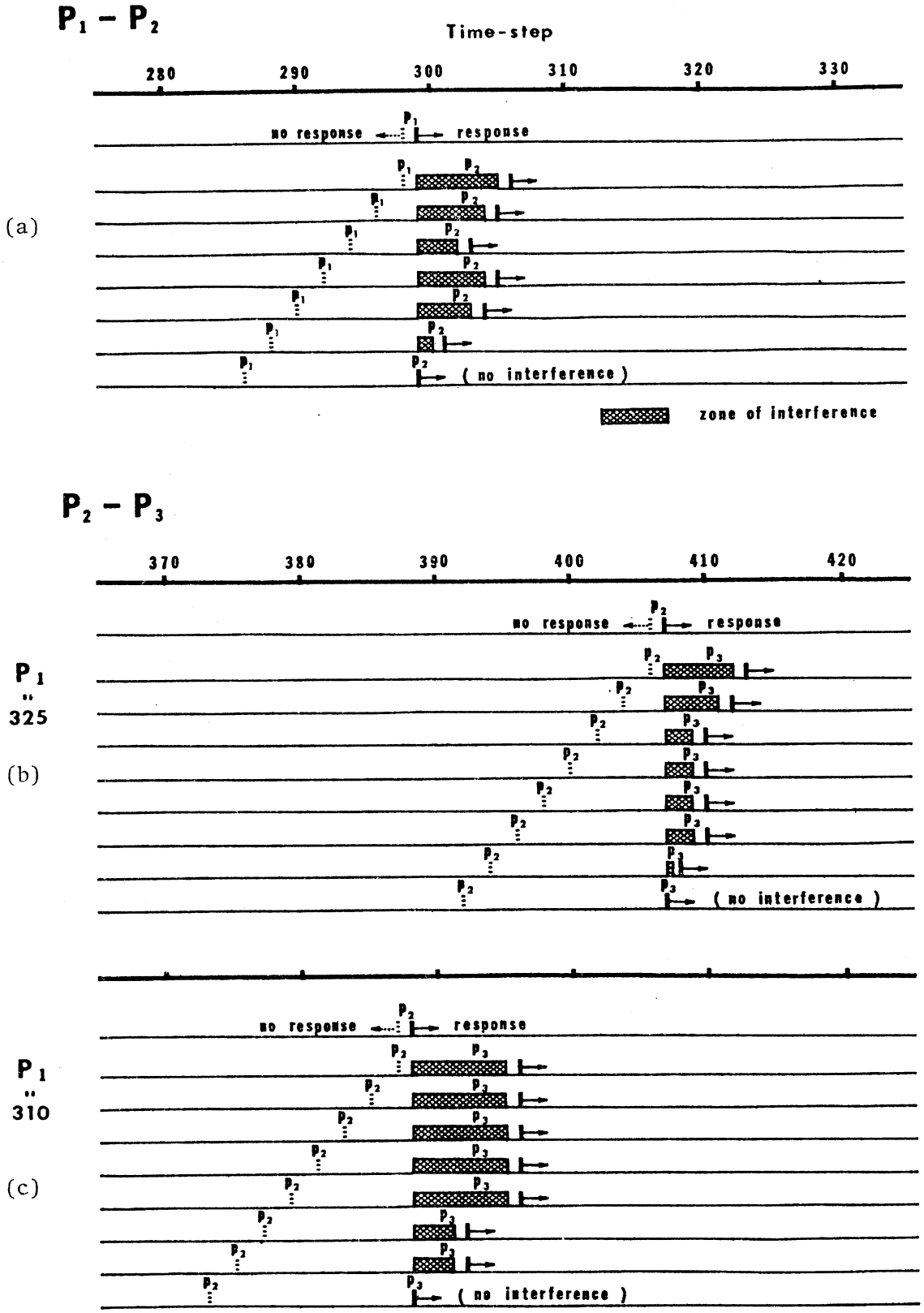
P1 – P2
Time-step
280
290
300
310
320
330
no response
response
(a)
(no interference)
zone of interference
P2 – P3
370
380
390
400
410
420
P1 = 325
(b)
(no interference)
P1 = 310
(c)
(no interference)

Figure 4.19

Finally, to test whether P_1 could interfere with P_2, an experiment analogous to the above was performed with P_1 applied just earlier than the end of the effective refractory period of the drive beat and P_2 applied just later. Results are shown in figure 4.19(a).

Results

In all three cases, a stimulus within the ERP of the preceding beat did indeed produce a local response which interfered with a second stimulus closely spaced. The interference was greatest when the non-conducted stimulus occurred as late as possible in the ERP, which is not surprising since at that timing it excited more cells than when placed earlier. As the non-conducted stimulus was advanced into the ERP its interfering effect diminished, although irregularly; finally it disappeared entirely. Referring to the time in the ERP during which the non-conducted stimulus produced an interfering effect as the "blocking zone", and to the time following the ERP in which conducted responses are prevented as the "zone of interference", we see that the size of the zone of interference is not directly related to the size of the blocking zone. The blocking zones associated with P_2 are evidently not much affected by the timing of P_1, as they are the same in both cases. The size of the zone of interference following P_2 is larger, however, when P_1 is more premature (compare figures 4.19(b) and 4.19(c).) When P_1 is the interfering stimulus, the blocking zone is smaller than with P_2, but the zone of interference is intermediate in size between those produced by P_2.

Similar experiments performed on rabbit atrium also reveal the interference phenomenon, as shown in figure 4.20 (unpublished results of Dr. H. Fukushima). The size of the zone of interference decreases

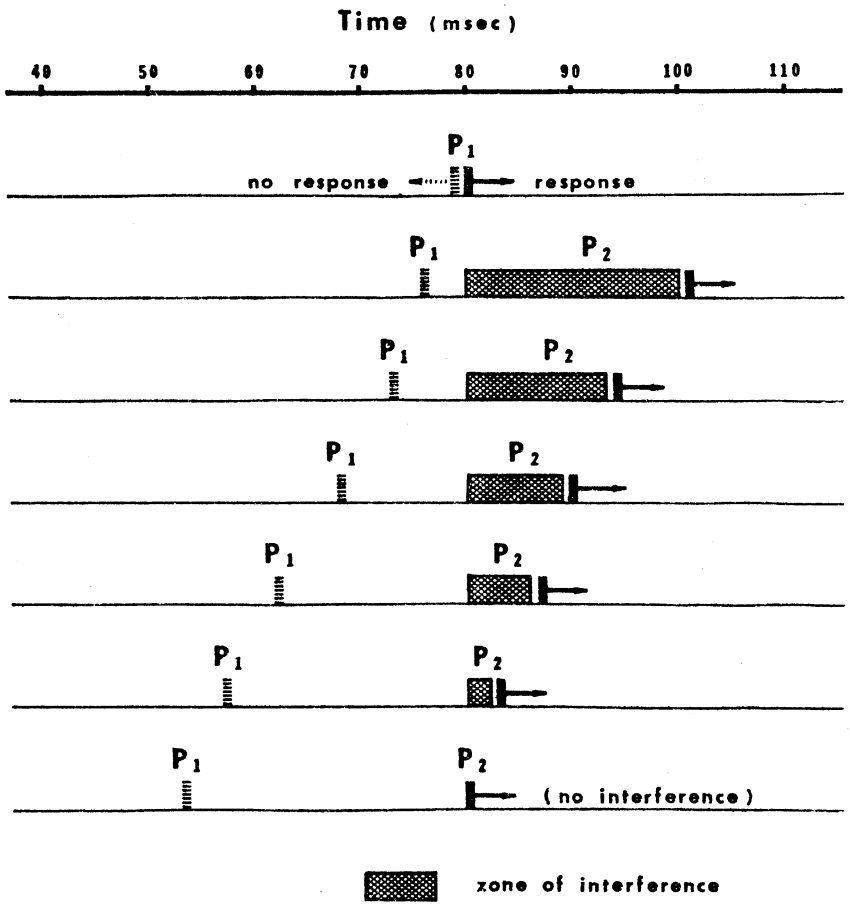

Figure 4.20. Interference From a Non-propagated Stimulus. Rabbit Atrium.

Cross-hatched regions indicate the zone in which propagated response to premature stimulus P_2 is abolished by the presence of P_1, even though P_1 alone produced no propagated activity.

as the blocking stimulus is placed earlier. Comparison of figure 4.20 with figure 4.19 shows that the behavior of the simulated cells is quite analogous to that of real tissue, so that it is not unreasonable to think in terms of comparable mechanisms in both cases.

IV. Reentry

As noted in the legend of figure 4.15, the second premature stimulus (P_2) sometimes was followed by more than one response. That is, P_2 generated a train of activity waves, each of which excited essentially the entire network. The number of extra beats varied with the circumstances: sometimes there was only a single extra response, at other times the train seemed to be of indefinite length.

These unstimulated waves ultimately derived from the network's inhomogeneity with respect to ARP duration and its consequent asymmetric response to premature stimulation. A premature wave might be conducted adequately in some parts of the network while encountering a local, temporary conduction block in another part where the refractory periods happened to be longer. This conduction failure would leave a gap in the wavefront. If the gap was large enough, activity from its edges could propagate back through it as the region of the original conduction block recovered its excitability. In this way an activity wave could reenter regions that had previously been excited by the same wave, causing an extra beat. Often, the reentrant process occurred again on the extra beat, leading to a self-sustaining series of waves.

The initiation and persistence of such reentry waves is the subject of the following chapter.

Chapter V

RESULTS II: REENTRANT ACTIVITY

The studies of premature beats have revealed a number of phenomena which arise from the aggregation of model cells even though they are not "programmed into" the individual cells directly. The strength-interval relation and the abnormal ERP prolongation are prominent examples; but the most significant phenomenon to appear is reentry, for reentrant waves, once initiated, can become completely self-sustaining. It is as though the excitable network has a second stable mode of action, in which one or more waves of excitation are conducted continuously, with activity always being present somewhere in the network. Yet the individual cells undergo significant change in neither their properties nor their behavior. Only the relations between them are altered, so that new patterns of a spatial and temporal nature emerge, while, on the average, the cells themselves remain very much the same.

I. General Observations from Simulation Experiments

The common feature of all reentry waves, however they originate, is a gap in the wavefront. The gap is usually caused by a region of tissue which, for one reason or another, is temporarily inexcitable as the leading edge of an activity wave approaches it. In order for a reentry to occur, this region must

1) form a conduction block, so that the wavefront breaks along each side of the region without penetrating it;

2) recover its excitability sufficiently that part of it, at least, can be stimulated by the activity wave before the latter's active region (that part which acts as an effective stimulus) has completely passed;

3) be large enough to constitute a conduction path through the entire wavefront, reaching the excitable region behind it.

Whether a region satisfies these requirements depends not only on its own size and conducting properties, but also on the duration of the refractory period in the tissue surrounding it and on the speed with which the original activity wave is conducted. Three representative lines of development are shown schematically in figure 5.1. Frame 1 depicts the common starting configuration. In frames 2 and 3, the block region is too small, or recovers too slowly, or the activity wave is too fast; the wavefront passes before the region recovers sufficient excitability to be stimulated. In frames 2' to 4', conduction through the block region is not sufficiently slowed, or the original activity wave is too fast, or the refractory period duration is too long in the tissue surrounding the block; a potential reentry wave develops, but cannot penetrate the refractory wake of the normal wave. In frames 2" to 4", conditions are such that a reentry occurs: tissue which was excited by the normal wave becomes re-excited by activity from that same wave.

A reentry occurring in this way can quite readily lead to repeated reentries, as shown in frames 5" to 7". The reentering wave has, of course, a gap in its wavefront from the beginning, because of the refractory wake it leaves behind as it proceeds to re-excite areas that are recovering from the activity wave's first passage. The expanding reentry wave sweeps slowly back along either side of the (now refrac-

Figure 5.1. Schematic Representation of the Development of Reentry at a Transitory Conduction Block.

From the common starting configuration depicted in frame 1, three representative lines of development are shown·

Frames 2 and 3 - the block region is not excited at all by the passing activity wave;
Frames 2' to 4' - the block region is excited by the passing wave, but reentry does not occur,
Frames 2" to 7" - the block region is excited by the passing wave, and a self-sustaining reentry develops. (See text.)

Legend:

Diagonally-hatched region:	transient conduction block
Dark stippled region:	wave of depolarization (active wave front and its absolutely refractory wake)
Light stippled region:	relatively refractory cells (frames 2" - 7")
Light gray region:	absolutely refractory cells of the externally-stimulated wave (to be distinguished from the ARP region of the reentrant wave, which is indicated by dark stippling).

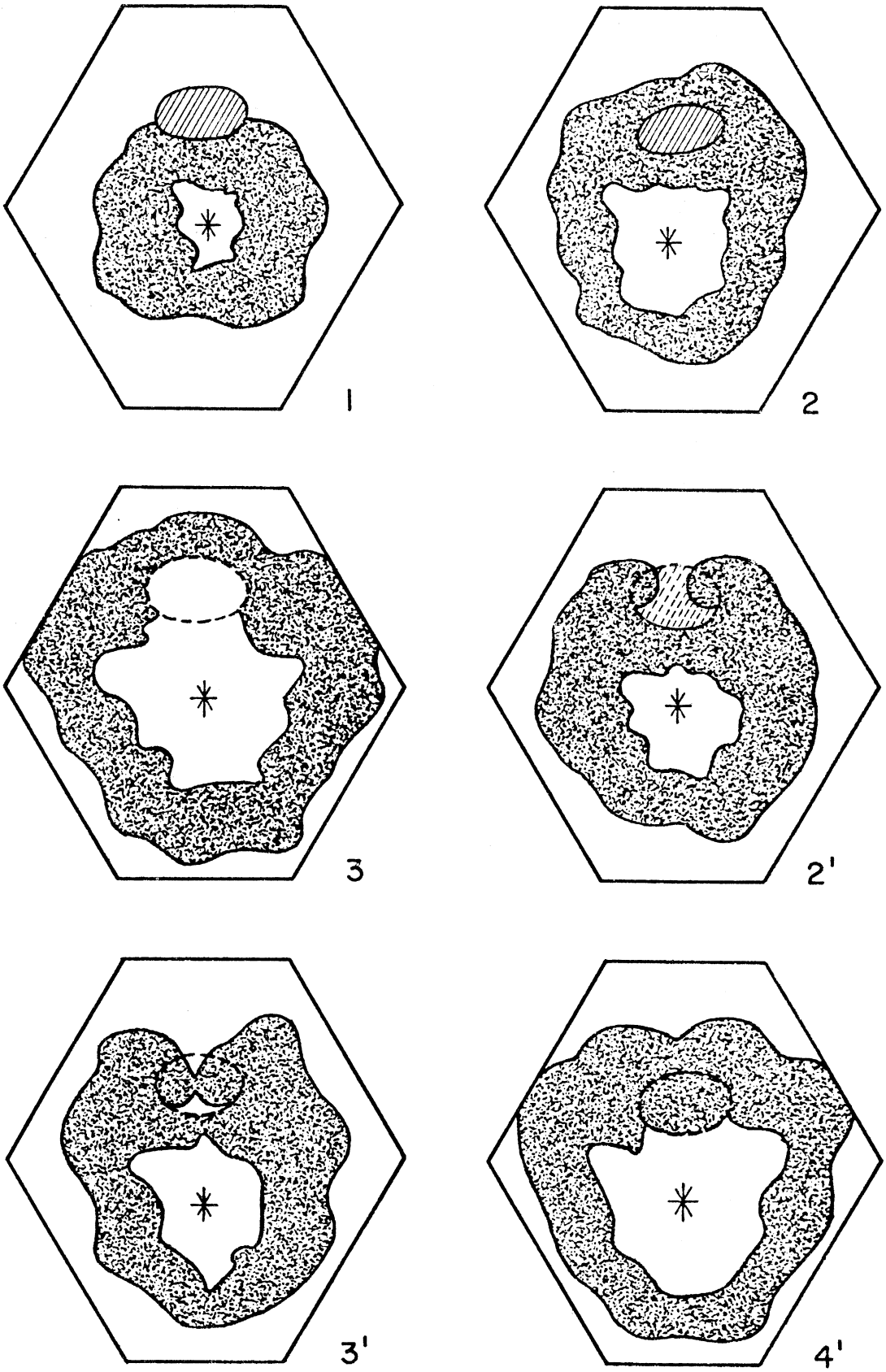

Figure 5.1

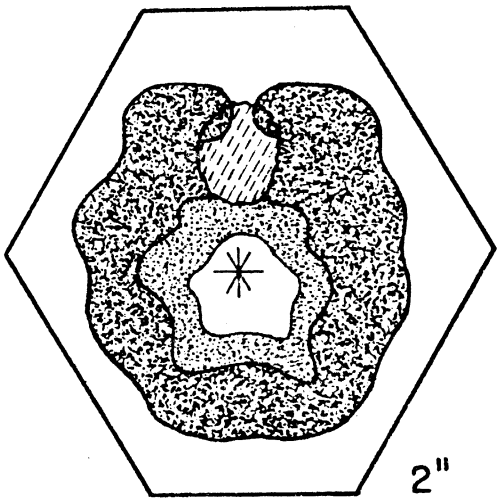
2"

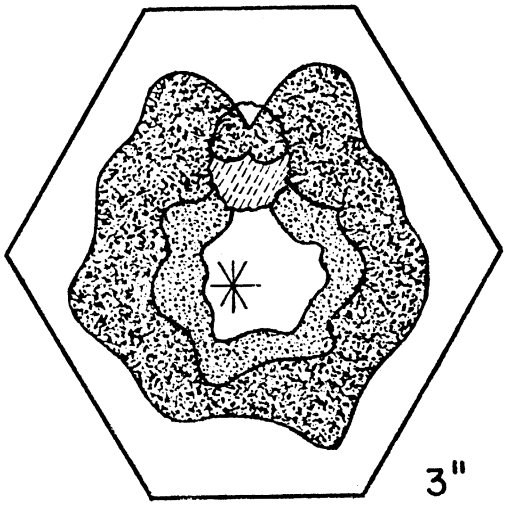
3"

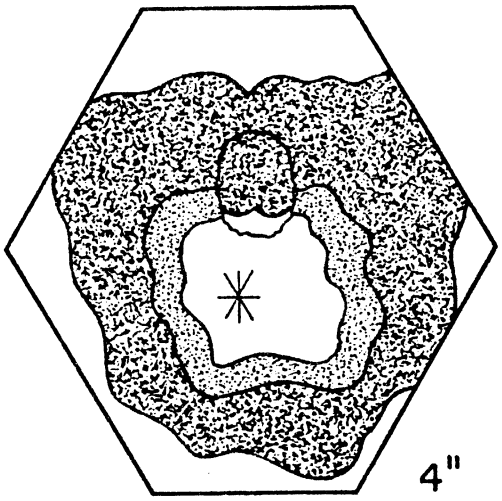
4"

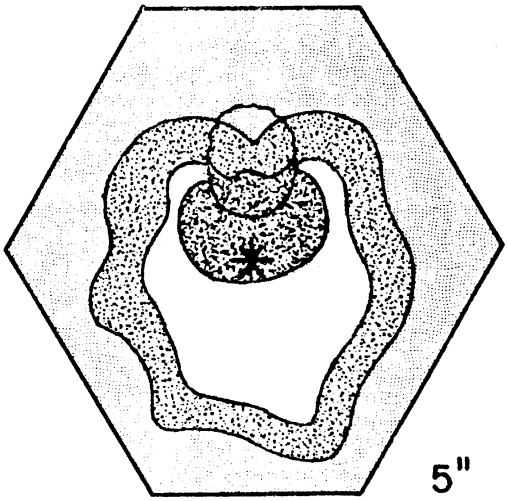
5"

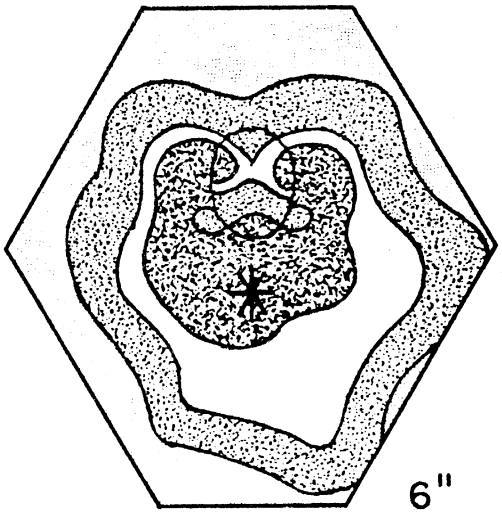
6"

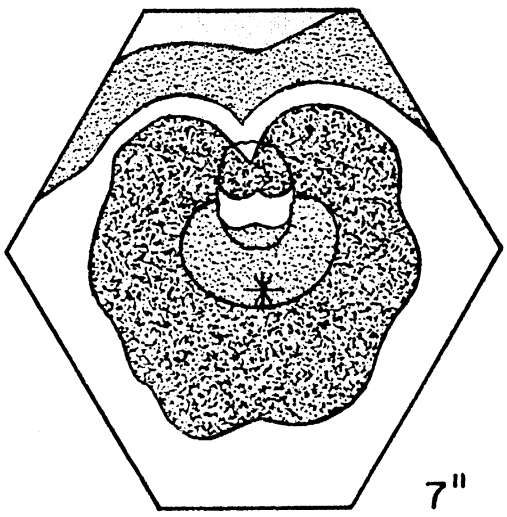
7"

tory) pathway through which it initially penetrated the previous wavefront, just as foam spills down the sides of a brimming stein. If this wave moves slowly enough--which is likely, since it rather closely follows the original stimulated wave--then the outermost end of the original block region will have recovered excitability by the time the reentry wave arrives. The configuration, shown in frame 7" of figure 5.1, resembles that shown in frame 4", which led to the first reentry. Hence we have a cyclic situation, which can persist indefinitely.

The basic form of a reentry wave is a rotating spiral (figure 5.7), although the spiral shape may be severely distorted by irregular conduction. There is always a focus, a region "around" which the reentry may be said to be occurring; but it is usually ill-defined, and often of shifting location.

The mechanism described above really generates two reentry waves: one from each side of the conduction block region. These form a double spiral, or, perhaps more accurately, a pair of spirals, whose foci are distinct yet fairly close together. In simulation experiments, it was unusual for both members of the pair to remain stable; usually one of the waves died out, either through conduction failure (often at the edge of the network) or through collision with the other wave. The resulting single spiral wave generally seemed more stable than the original pair; long-persisting reentries were usually composed of single waves, rather than pairs, even though a pair was more likely to be formed initially.

A single spiral wave is equivalent to the notorious "unidirectional wave," whose presumed difficulty of generation has been a chief classical argument against circus rhythm mechanisms. The conversion

of a symmetric situation into a non-symmetric one through failure of a self-sustaining spiral wave is not only possible, but even likely, and yet demands no change in the fundamental conducting properties of the medium.

This discussion of reentry has been framed in terms of a large activity wave with a relatively small gap in its wavefront. It is also possible to have reentry from what amounts to a small wave with a large gap, that is, an isolated patch of activity adjacent to a large refractory region. The former situation tends to result from rapid, fixed-rate stimulation, the latter from vulnerable-period stimulation; a sequence of early premature stimuli produces an intermediate case.

The evidence from simulation experiments indicates that the timing of activity waves, conduction blocks, and so forth is not as critical as one might suppose. Reentry is not a matter of unlikely coincidence; rather, it happens readily whenever the network is stressed sufficiently by external stimulation.

A. Initiation

Reentrant activity can be induced in the model by any of several procedures, all of which are analogous to known methods of initiating fibrillation in atrial tissue.

1) Stimulation at a Fixed Rate

A train of equally spaced stimuli applied to the model network at a slow rate will produce a series of symmetrically conducted activity waves (figure 5.2). Because of the random variation in the duration of the cells' absolute refractory periods, some areas of the network

Figure 5.2. A Symmetrically-conducted Wave of Activity in a Fully-recovered Network.

Legend: $ = stimulated
* = firing
- = absolutely refractory
. = relatively refractory
blank = quiescent

```
 90

-12
-11
-10
 -9
 -8
 -7
 -6
 -5
 -4
 -3                $ $ $ $
 -2              $ * * * $
 -1            $ * * * * * $
  0          $ * * * * * * * $
  1            $ * * * * * $
  2              $ * * * $
  3                $ $ $ $
  4
  5
  6
  7
  8
  9
 10
 11
 12
```

Figure 5.2

```
110

-12
-11
-10                  $ $ $ $ $ $ $ $ $ $ $
 -9                $ * * * * * * * * * * * $
 -8              $ * * * * * * * * * * * * * $
 -7            $ * * * * * * * * * * * * * * $
 -6          $ * * * * * * * * * * * * * * * $
 -5        $ * * * * * * * * * * * * * * * * * $
 -4      $ * * * * * * * * * * * * * * * * * * * $
 -3    $ * * * * * * * - - - - * * * * * * * $
 -2  $ * * * * * * * - - - - - * * * * * * * $
 -1 $ * * * * * * * - - - - - - * * * * * * * $
  0 $ * * * * * * * - - - - - - - * * * * * * * $
  1  $ * * * * * * * - - - - - - * * * * * * * $
  2    $ * * * * * * * - - - - - * * * * * * * $
  3      $ * * * * * * * - - - - * * * * * * * $
  4        $ * * * * * * * * * * * * * * * * * $
  5          $ * * * * * * * * * * * * * * * $
  6            $ * * * * * * * * * * * * * $
  7              $ * * * * * * * * * * * $
  8                $ * * * * * * * * * $
  9                  $ * * * * * * * $
 10                    $ $ $ $ $ $ $ $ $ $ $
 11
 12
```

will recover their excitability more rapidly than others. Thus, the activity wave's trailing edge--what one might call the "recovery wave" --will be irregularly shaped even when the leading edge is perfectly regular. This asymmetric recovery has no significant consequences when the stimulation rate is low.

If the rate of stimulation is increased, the network partially compensates through shorter refractory periods, since the ARP duration depends on cycle length. The compensation is not complete, however, so that if the stimulating rate is increased sufficiently, each stimulus will fall within the relative refractory period of the preceding wave. When this happens, the wavefronts become irregular, as the activity waves adapt, more or less, to the shape of the recovery waves, since conduction is slowed in proportion to refractoriness.

A poorly-recovered region will tend to become excited later than its more excitable neighbor, and may also "see" a somewhat longer cycle length; hence, the disparities in excitability will be accentuated on the next wave. Distortion of the wavefront thus tends to increase with successive stimuli. If the rate is not too fast, the network may accommodate and settle into a steady state in which each wave, though irregular, is conducted similarly to the previous one. But if the stimulation rate is simply too fast for some region(s) of the network to follow, then slowed conduction progressively becomes conduction failure. This temporary conduction block produces a gap in the wavefront--exactly the conditions for reentry described earlier (figure 5.3). The block region may not, at first, be large enough for a successful reentry; but it will tend to grow in size if the external stimulation is continued, making reentry progressively more likely on

succeeding waves.

There is a fairly sharp threshold (with respect to the frequency of stimulation), below which the network can accommodate stimuli without producing reentry, and above which multiple extra beats and even persistent activity appear. This effect is illustrated in table 5.1, which shows the response to varying numbers of stimuli applied at various rates[1] to network N of table 3.2. At cycle length 91, the network followed each stimulus; the activity waves were distorted, but stable --each was like the previous (after a while), and the distortion did not increase with time. At cycle length 90, some parts of the network were unable to follow every beat, and some relatively short-lived reentry waves developed. Over successive stimuli, though, the network accommodated to the rapid drive and on about the 20th wave settled into a stable, if distorted, pattern for each wave with no further reentries. A similar situation obtained at cycle length 89, where the activity pattern had still not stabilized after 34 waves, although there were fewer reentries. At cycle length 88, reentries occurred after the sixth and seventh stimuli, and after the eighth stimulus a persistent circus rhythm developed. Cycle lengths 90-88 thus represent the frequency threshold for this particular network. Swain and Valley (1970) have shown that a sharp frequency threshold for fibrillation is characteristic of ventricular muscle, and have termed the threshold the "critical fibrillation frequency."

2) Successive Premature Stimuli

A stimulus placed very early in the relative refractory period of

[1] Rate is specified in terms of cycle length, the interval between stimuli.

Figure 5.3. Activity Patterns Induced by Fixed-Rate Stimulation.

(Network N_1 of table 3.2; six stimuli at a cycle length of 84 time-steps.)

(a) 42 time-steps after P_1
(b) 48 time-steps after P_2
(c) 44 time-steps after P_3
(d) 40 time-steps after P_4
(e) 46 time-steps after P_5
(f) 106 time-steps after P_5 Reentry begins

Legend: $ = stimulated
* = firing
- = absolutely refractory
• = relatively refractory
blank = quiescent

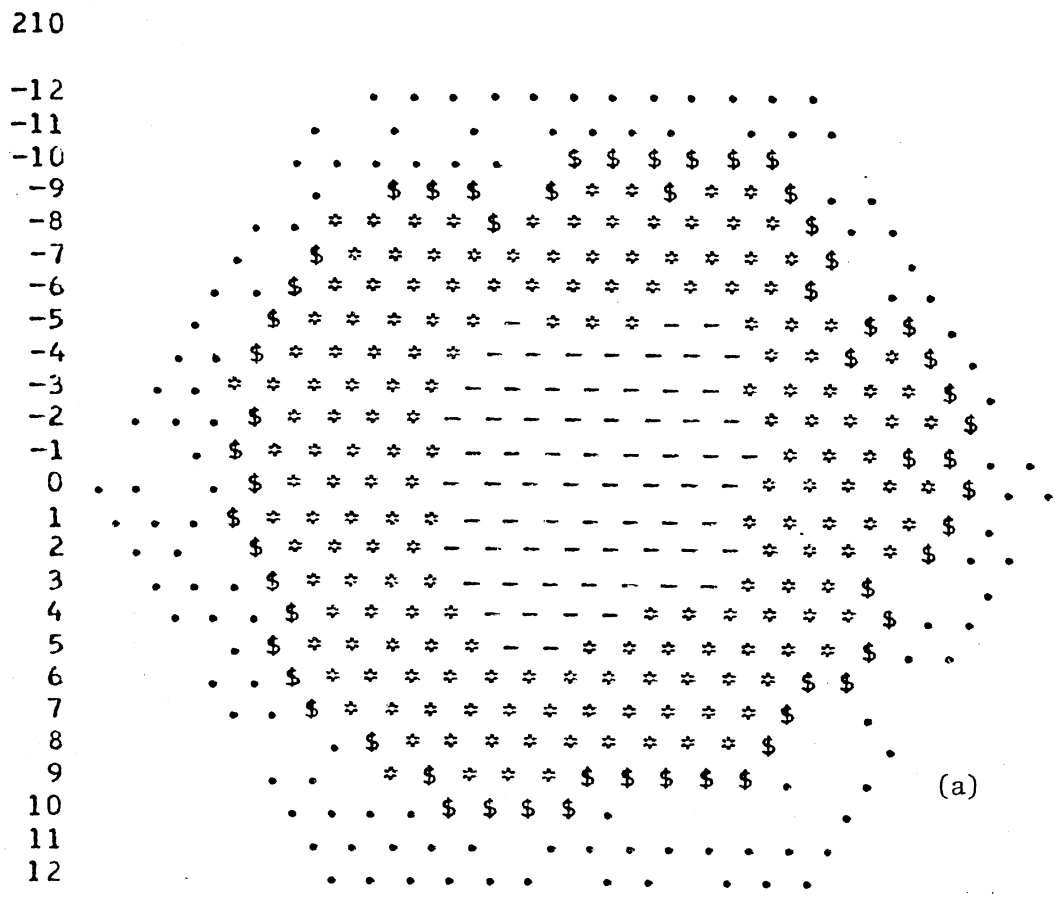
210
-12
-11
-10
-9
-8
-7
-6
-5
-4
-3
-2
-1
0
1
2
3
4
5
6
7
8
9
10
11
12
(a)

Figure 5.3

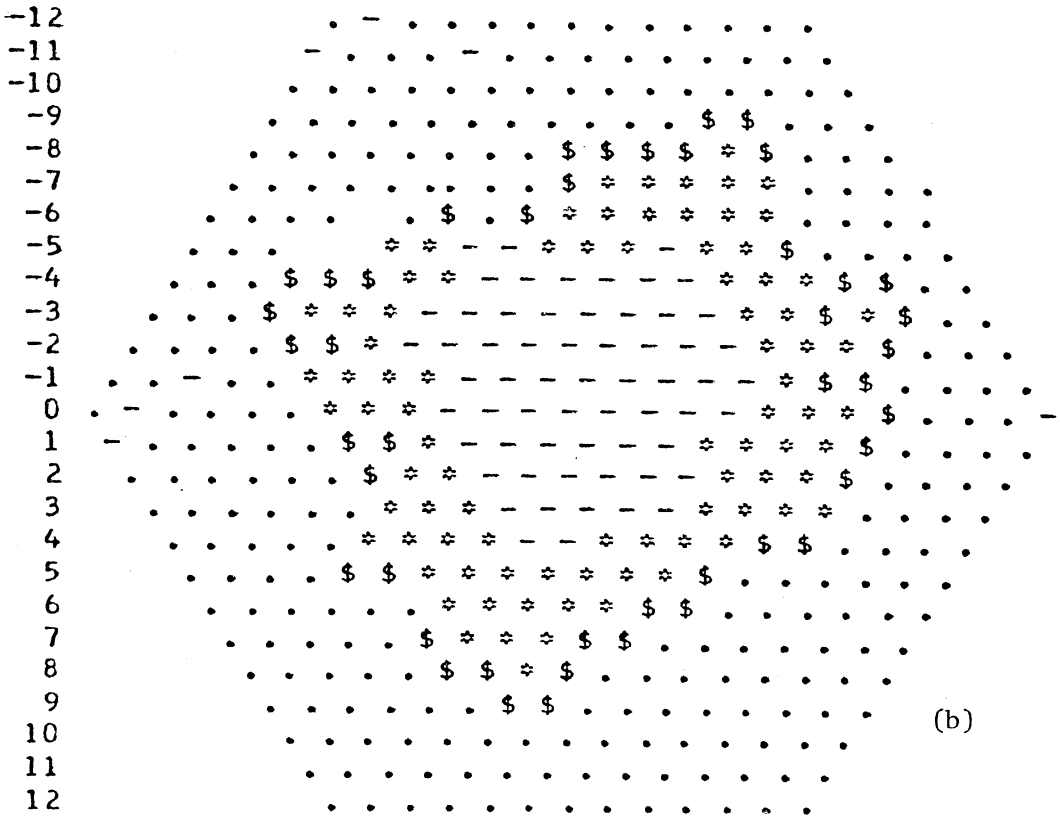
300
-12
-11
-10
-9
-8
-7
-6
-5
-4
-3
-2
-1
0
1
2
3
4
5
6
7
8
9
10
11
12
(b)

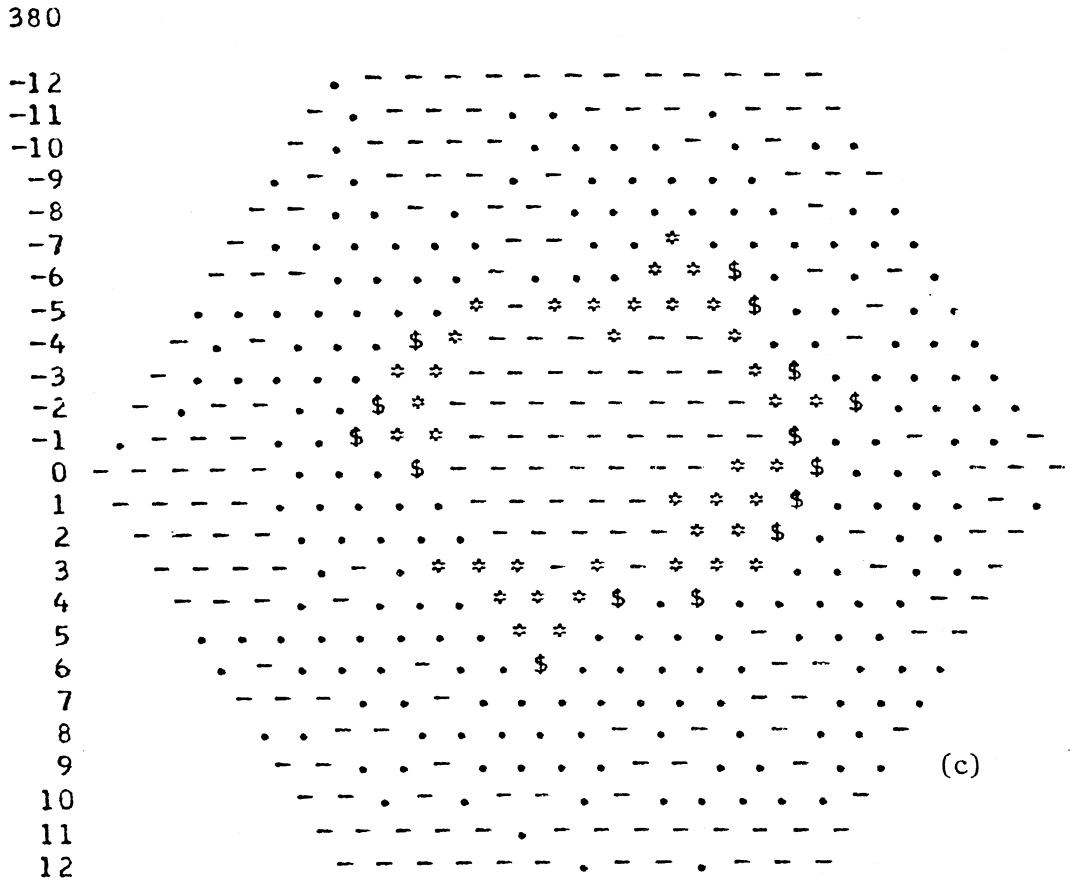
380
-12
-11
-10
-9
-8
-7
-6
-5
-4
-3
-2
-1
0
1
2
3
4
5
6
7
8
9
10
11
12
(c)

Figure 5.3

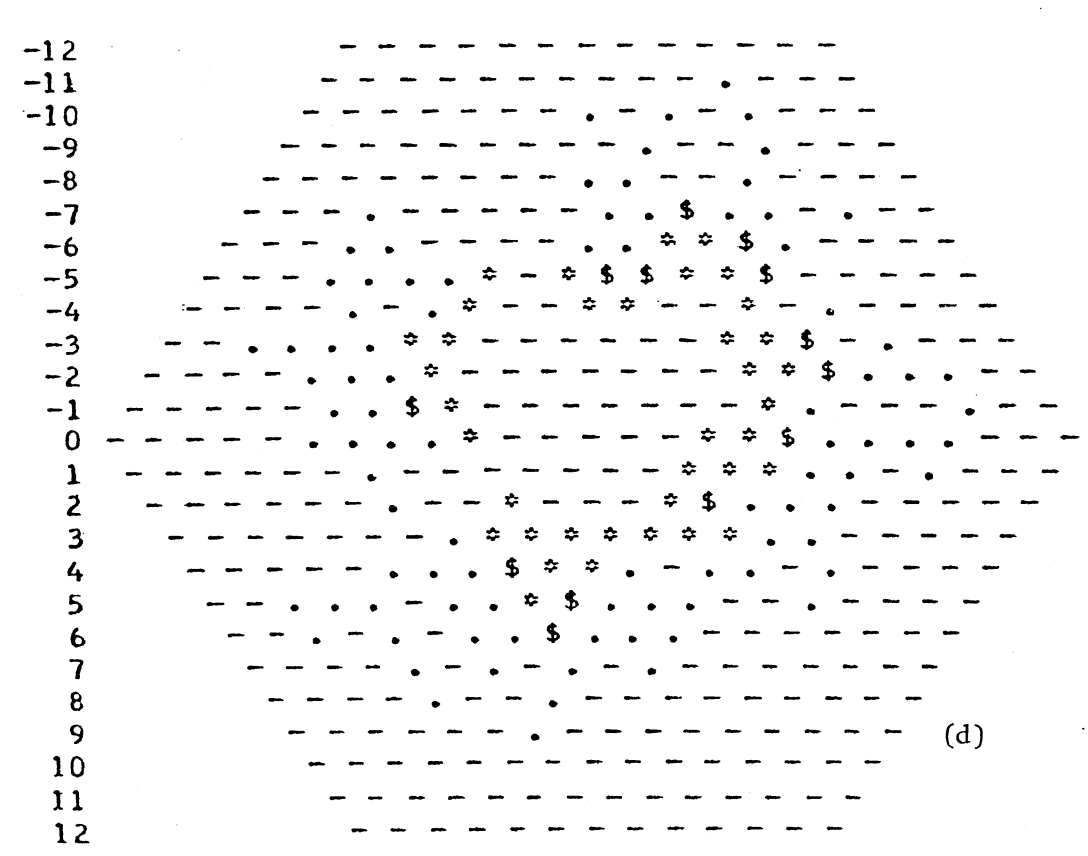
460
-12
-11
-10
-9
-8
-7
-6
-5
-4
-3
-2
-1
0
1
2
3
4
5
6
7
8
9
10
11
12
(d)

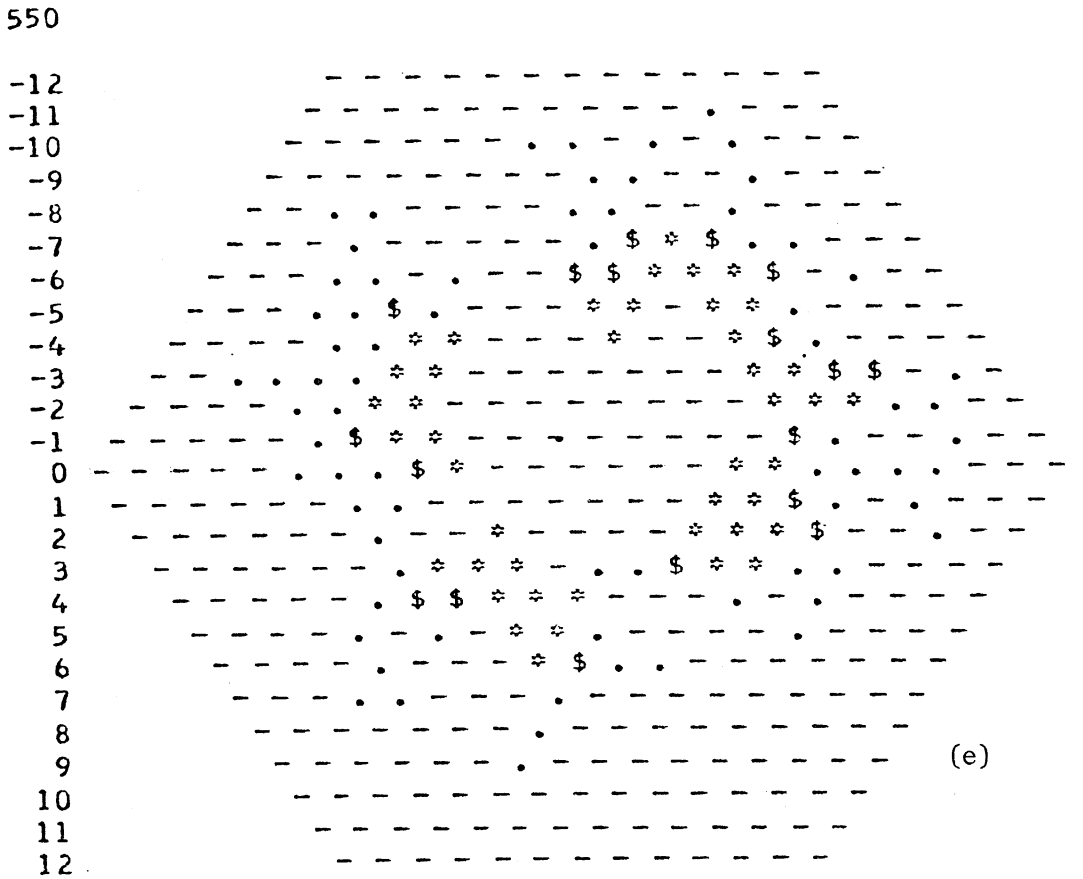
550
-12
-11
-10
-9
-8
-7
-6
-5
-4
-3
-2
-1
0
1
2
3
4
5
6
7
8
9
10
11
12
(e)

Figure 5.3

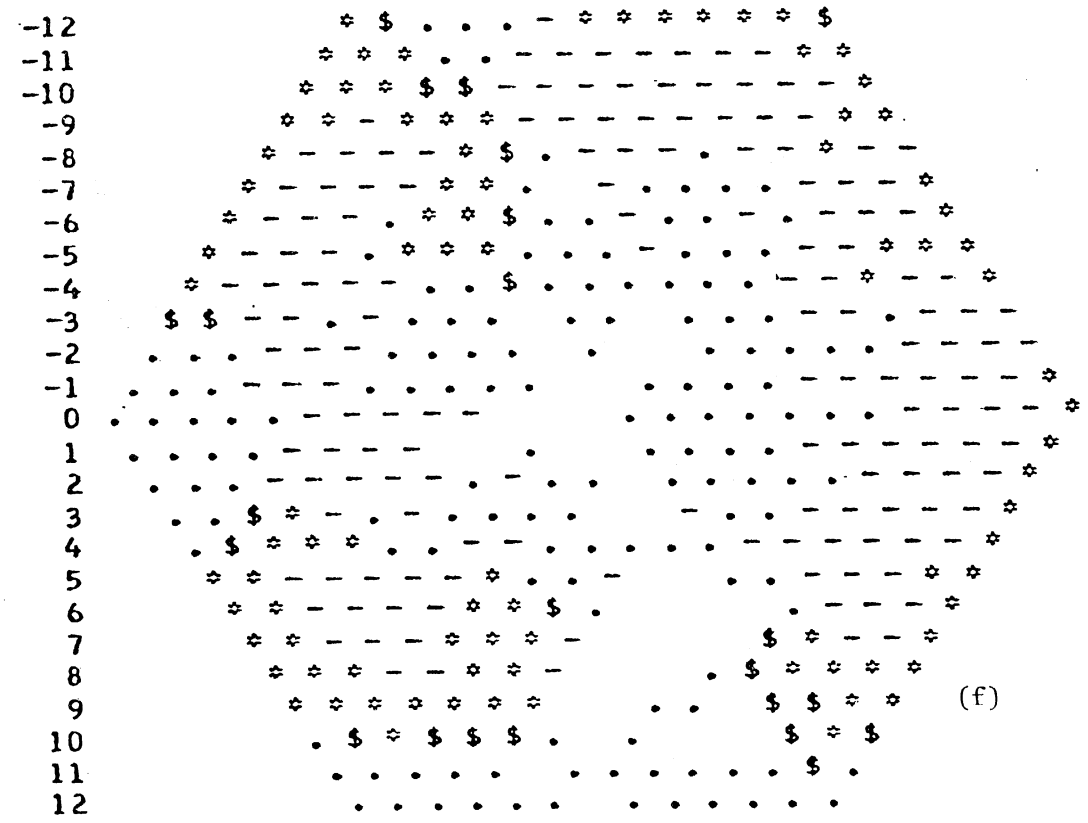
610
-12
-11
-10
-9
-8
-7
-6
-5
-4
-3
-2
-1
0
1
2
3
4
5
6
7
8
9
10
11
12
(f)

Table 5.1. Response of the Model Network to Fixed-Rate Stimulation (Radius-1 stimulator)

Stimulator Cycle Length	No. of Stimuli	No. of Extra Beats
95	1-14	0 (Stable after wave 13)
91	1-29	0 (Stable after wave 12)
90	1-7	0
	8	4
	9	2
	10	1
	11	1
	12-50	0
89	1-11	0
	12	1
	13-21	0
	22	1
	23-50	0
88	1-5	0
	6	1
	7	4
	8	∞ (becomes cyclic)

the preceding beat can elicit an activity wave whose conduction pattern is highly asymmetric (figure 5.4). The wavefront may develop gaps almost immediately, owing to the presence of quite refractory regions near the stimulator. In fact, the wave's early spread may depend on just a few marginally excitable cells, with conduction improving and a recognizable wavefront forming only as the previous wave's recovery process outruns the slowed premature wave. This delayed conduction allows time for surrounding cells to become more recovered, so that even an early premature wave may be fairly regular by the time it reaches the edges of the network.

The timing of the premature stimuli and the recovery state of the network seem to be fairly critical to the production of reentries. In simulation experiments, reentry almost never followed a single premature stimulus[2]; presumably, the preceding drive beat simply did not leave the network in a sufficiently asymmetric condition to produce an adequate conduction block on the premature wave. Moving the premature stimulus earlier only increased the delay with which it was initially conducted, thus allowing the potential conduction blocks more time to recover. The irregular conduction of a first premature wave (P_1), however, left the network in a sufficiently asymmetric state of excitability that a second premature beat (P_2) could result in a persistent reentrant wave. The specific outcome was dependent on the timing of P_1 and P_2.

[2] Reentry was observed to occur after a single premature stimulus in experiments where the refractory period had been shortened substantially ($\bar{k} = 5.0$) or where a lesser shortening of the refractory period ($\bar{k} = 6.0$) was coupled with an increase in inhomogeneity ($k_\sigma = 2.5$).

Figure 5.4. Activity Pattern Induced by Early Premature Stimulation.

(Network N_1 of table 3.2. Drive stimulus at time-step 200, P_1 at 305, P_2 at 400.)

(a) 15 time-steps after P_1. Early asymmetry
(b) 45 time-steps after P_1. Later asymmetry; the wavefront is unbroken
(c) 20 time-steps after P_2. Early asymmetry.
(d) 50 time-steps after P_2. Later asymmetry; a large gap has formed in the wavefront.
(e, f) 60, 70 time-steps after P_2. Further spread of the activity wave.
(g, h) 90, 100 time-steps after P_2. The formation of a distinct reentrant wave.

Legend: $ = stimulated
* = firing
\- = absolutely refractory
· = relatively refractory
blank = quiescent

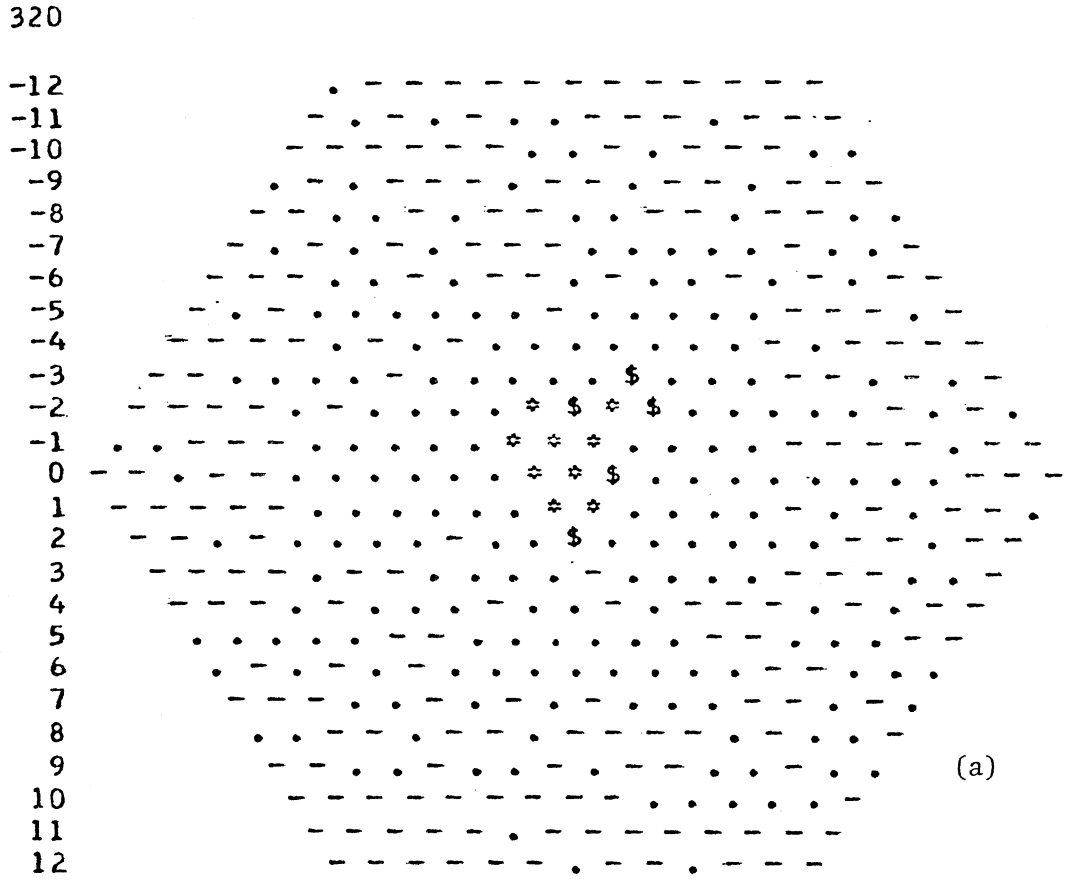
320
-12
-11
-10
-9
-8
-7
-6
-5
-4
-3
-2
-1
0
1
2
3
4
5
6
7
8
9
10
11
12
(a)

Figure 5.4

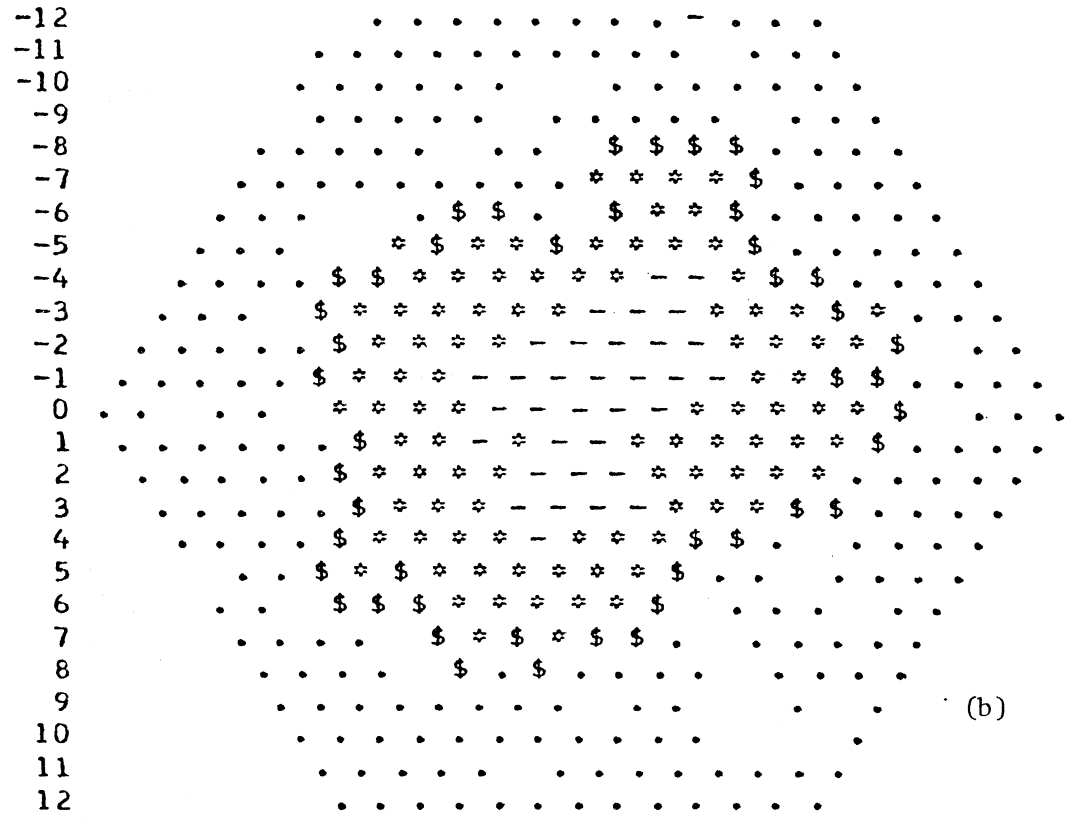
350
-12
-11
-10
-9
-8
-7
-6
-5
-4
-3
-2
-1
0
1
2
3
4
5
6
7
8
9
10
11
12
(b)

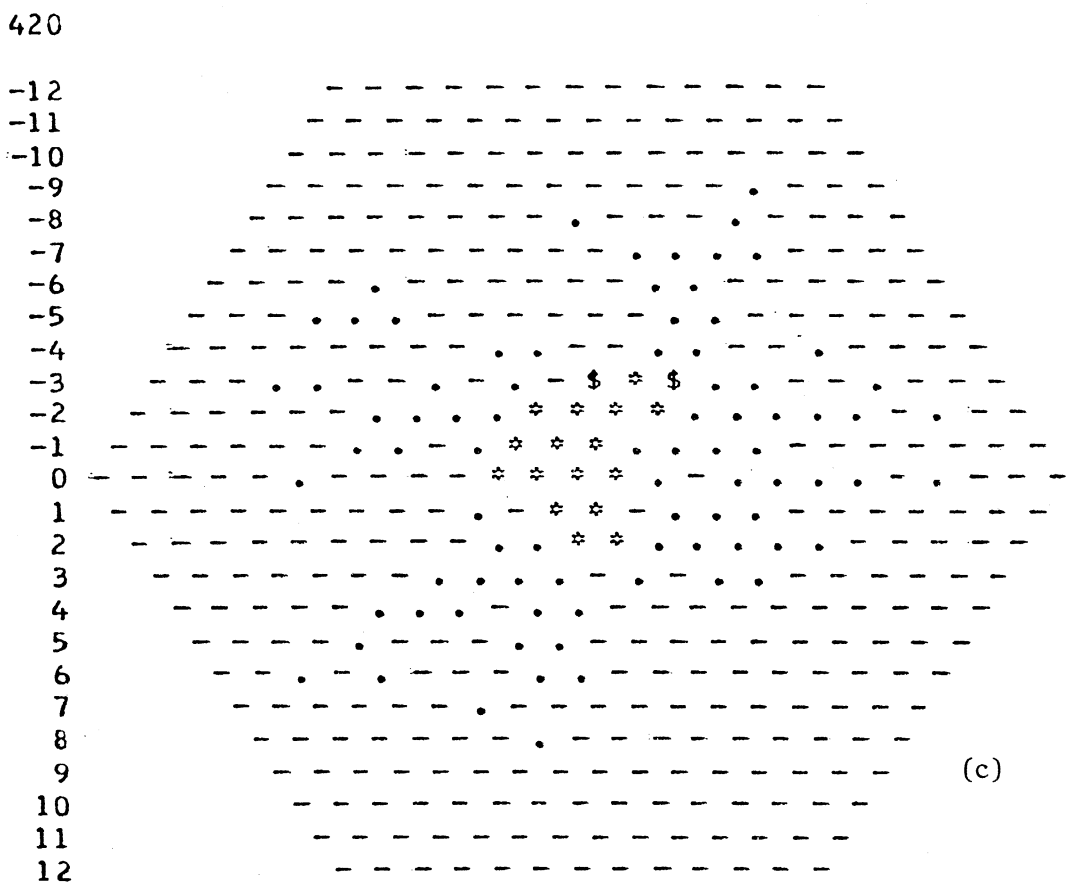
420
-12
-11
-10
-9
-8
-7
-6
-5
-4
-3
-2
-1
0
1
2
3
4
5
6
7
8
9
10
11
12
(c)

Figure 5.4

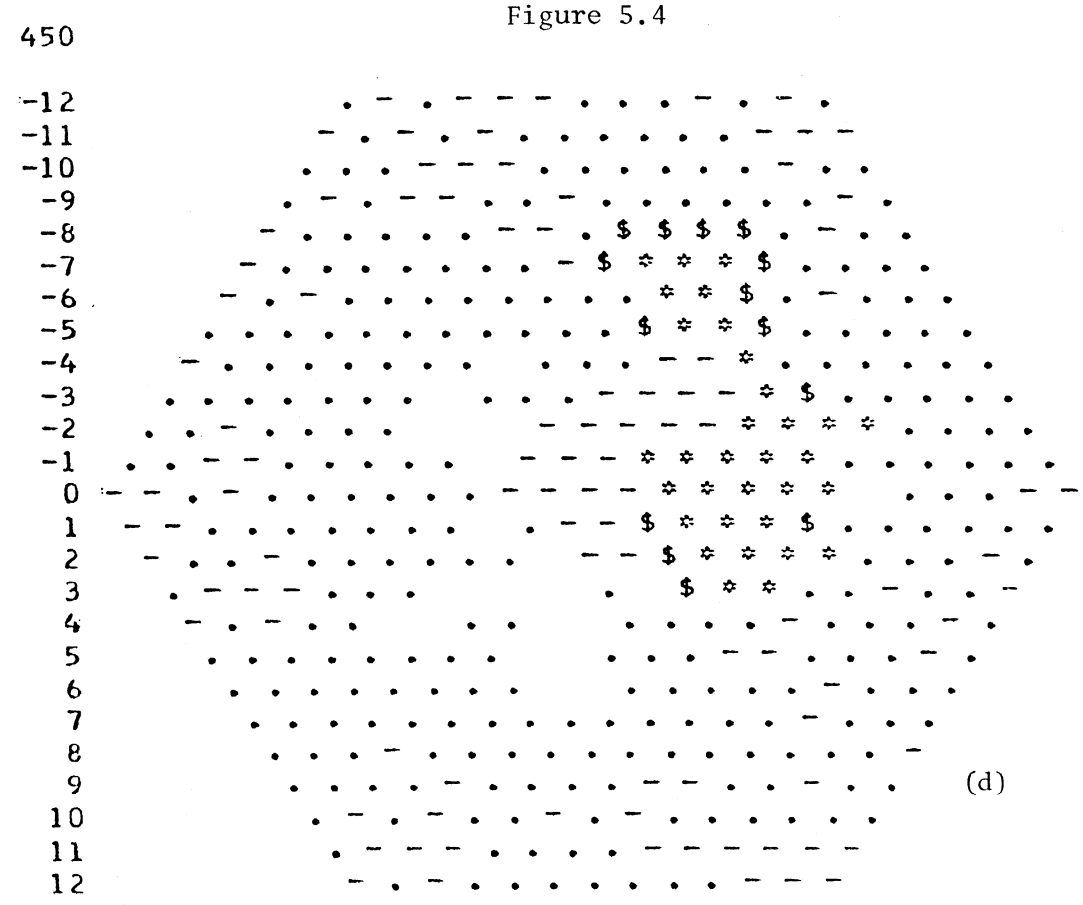
450
-12
-11
-10
-9
-8
-7
-6
-5
-4
-3
-2
-1
0
1
2
3
4
5
6
7
8
9
10
11
12
(d)

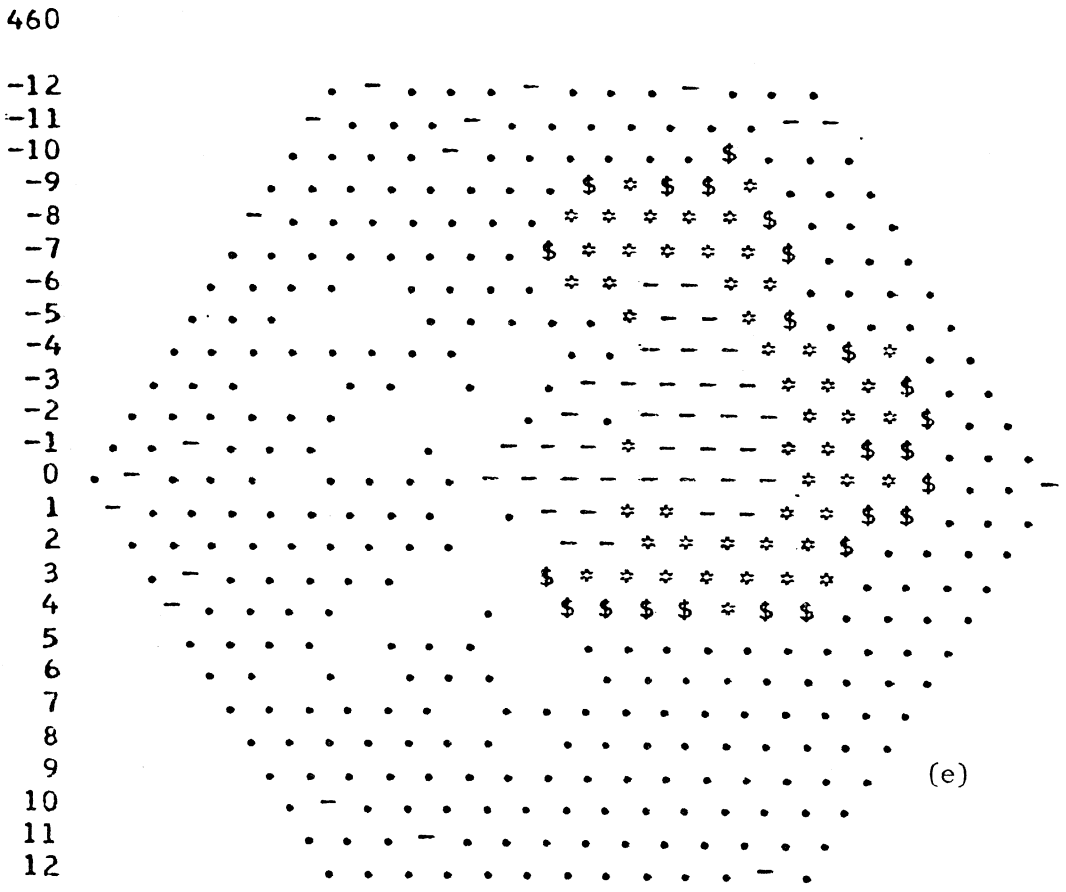
460
-12
-11
-10
-9
-8
-7
-6
-5
-4
-3
-2
-1
0
1
2
3
4
5
6
7
8
9
10
11
12
(e)

Figure 5.4

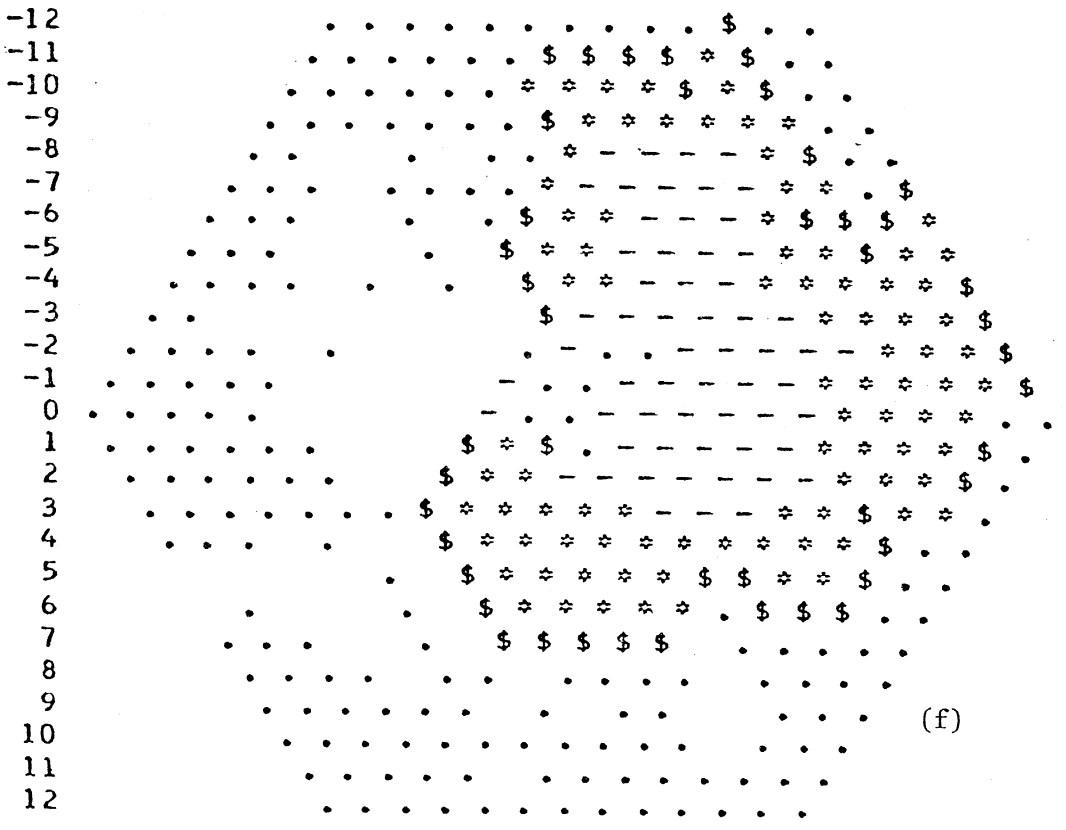
470
-12
-11
-10
-9
-8
-7
-6
-5
-4
-3
-2
-1
0
1
2
3
4
5
6
7
8
9
10
11
12
(f)

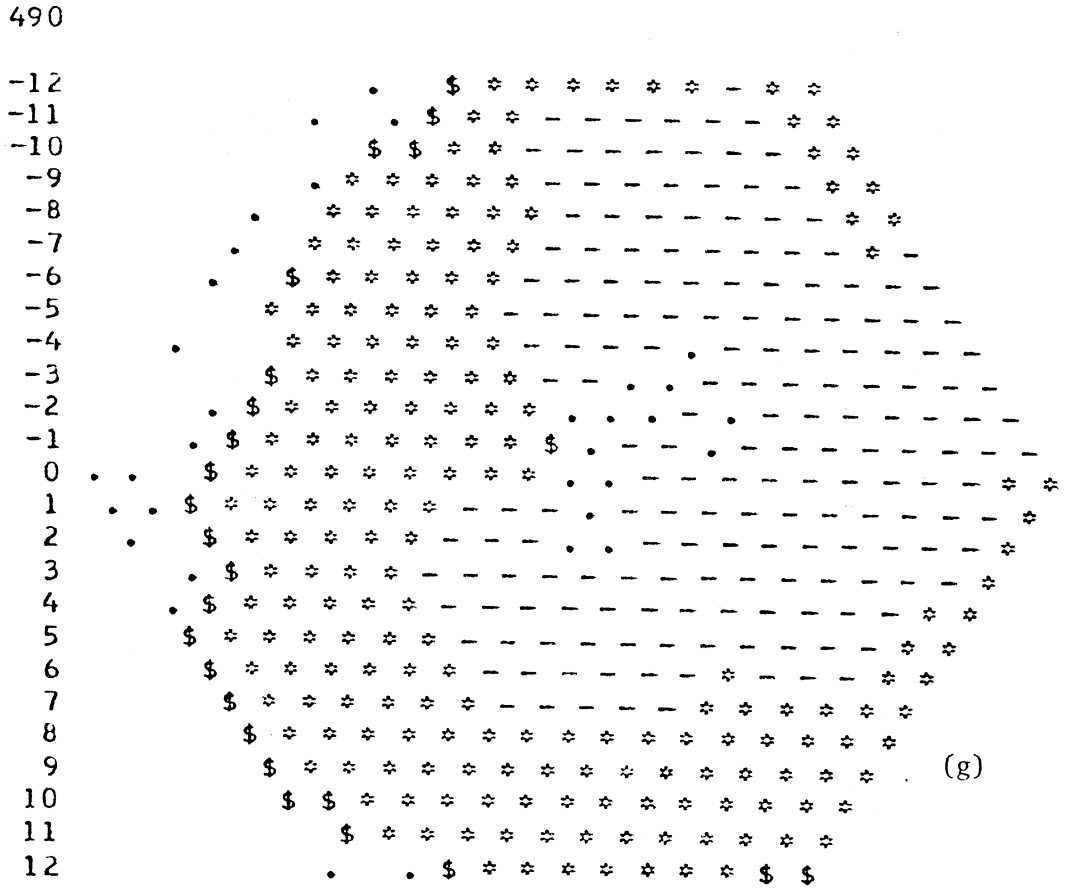
490
-12
-11
-10
-9
-8
-7
-6
-5
-4
-3
-2
-1
0
1
2
3
4
5
6
7
8
9
10
11
12
(g)

Figure 5.4

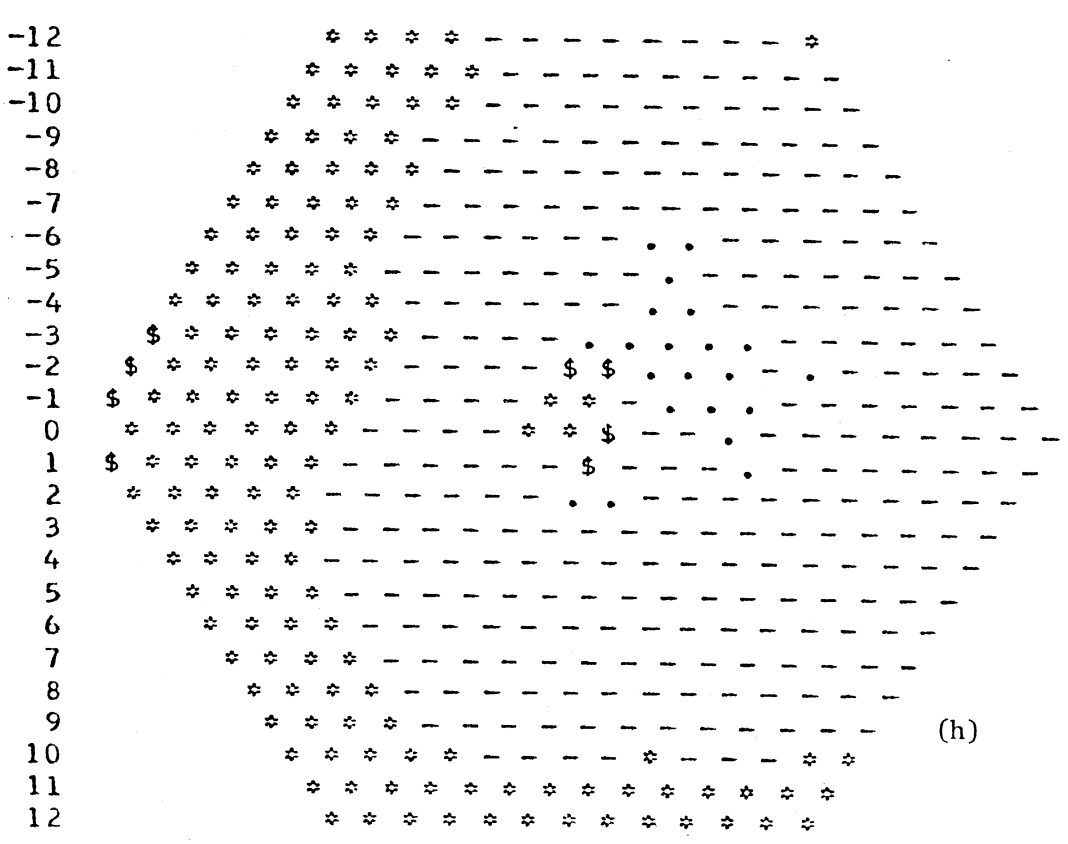
500
-12
-11
-10
-9
-8
-7
-6
-5
-4
-3
-2
-1
0
1
2
3
4
5
6
7
8
9
10
11
12
(h)

Figure 5.5 shows the response to P_2 for various timings of P_1 and P_2, using network N_1 of table 3.2 with a driving cycle length of 200 time-steps. The total range of P_1 values over which reentry developed was 17 time-steps; for P_2 the maximum range was 22 time-steps, but for any given P_1 timing the P_2 range was no greater than 14 and usually no more than 7 or 8. It is evident that the response varied considerably with only slight changes in the timing of P_1 and/or P_2, going from no-response to a single response to multiple responses, and vice versa, over intervals of only a few time-steps.

3) Vulnerable-period Stimulation

A single strong stimulus applied just outside the effective refractory period of the network will sometimes elicit a sufficiently asymmetric pattern of activity that a reentry occurs (figure 5.6). The mechanism has been described earlier in connection with the strength-interval relation; both the timing and the strength of the premature stimulus are fairly critical to the production of reentries.

The basic patterns of reentry waves are quite similar regardless of the method of initiation, and it is impossible to tell from the wave pattern, after the fact, which method was actually used.[3]

B. Termination

1) After a Single Reentry

If the reentry pathway was thin, or the reentering wave encountered

[3] The term "reentry" is used here to mean the re-excitation of more than a few cells, i.e. a clearly discernible extra wavelet (not necessarily propagated, however,), even though the re-excitation of just a single cell by a given activity wave is, strictly speaking, a reentry.

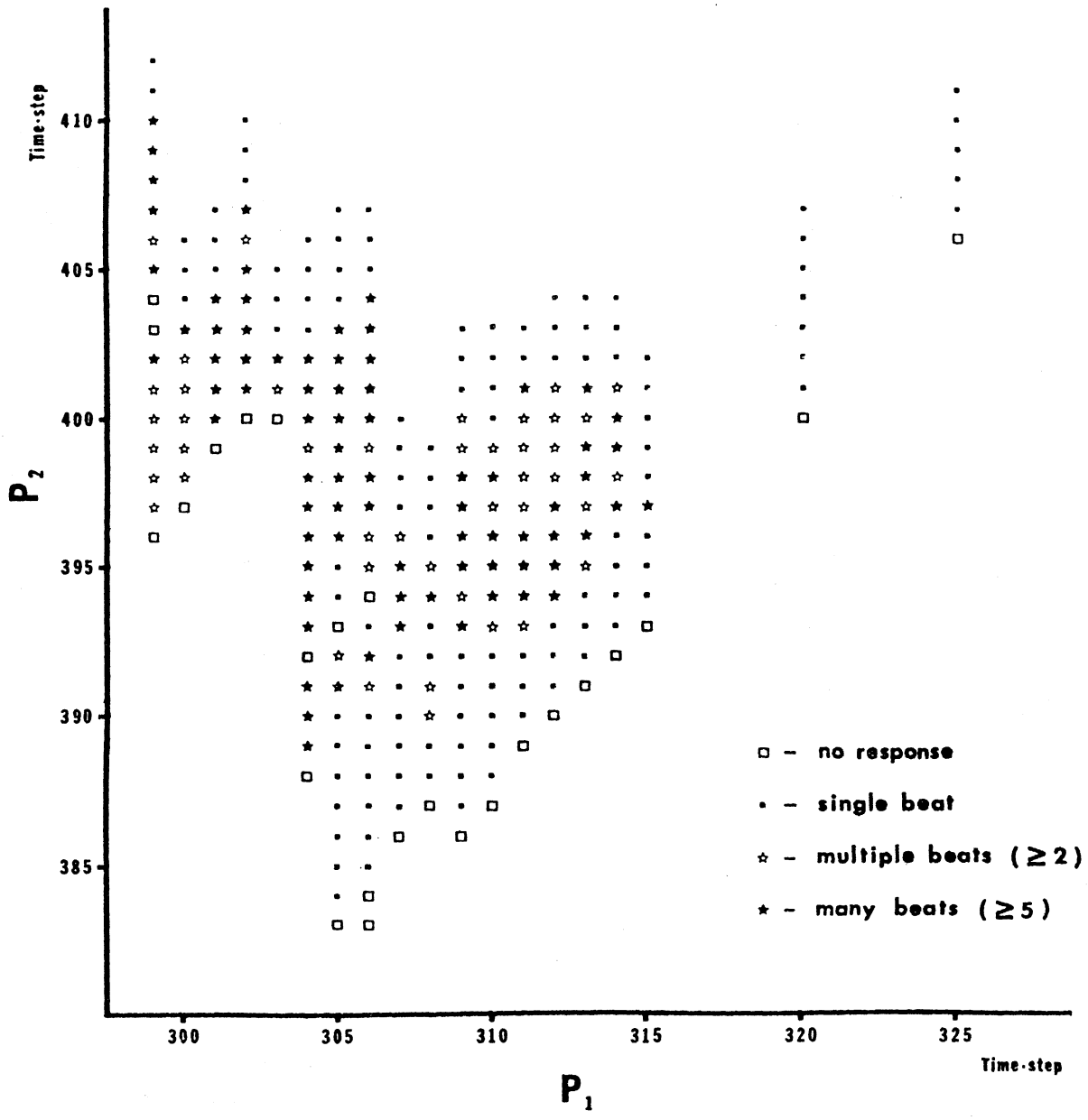

Figure 5.5. Response of the Network to P_2, as a Function of the Timing of P_1 and P_2.

Figure 5.6. Activity Patterns Induced by Vulnerable-period Stimulation.

(Network N_1 of table 3.2; drive stimulus at time-step 200, P_1 at 305, strength 1200.)

(a) 5 time-steps after P_1. The initial excitation produced by the strong stimulus.
(b) 25 time-steps after P_1. Early asymmetric propagation of activity.
(c) 55 time-steps after P_1. Later asymmetry.
(d) 75 time-steps after P_1. The beginning of reentry.

Legend: $ = stimulated
* = firing
- = absolutely refractory
· = relatively refractory
blank = quiescent

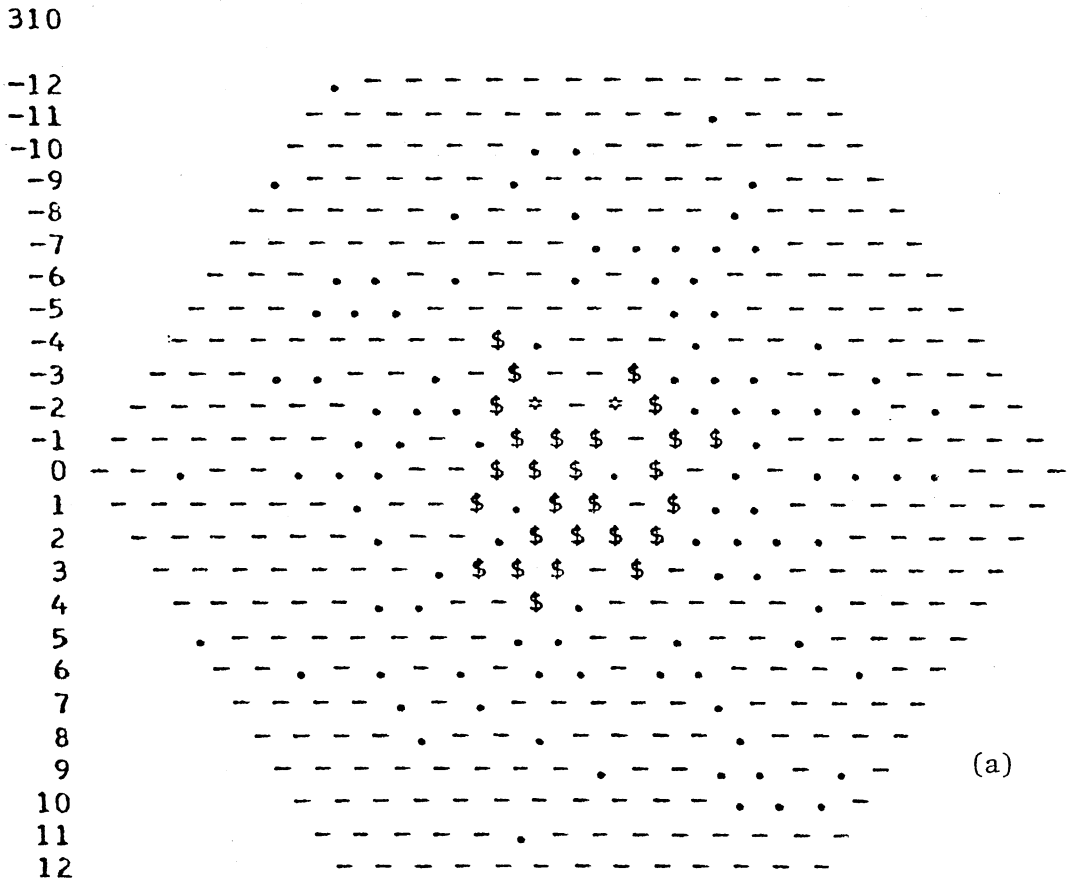
310
-12
-11
-10
-9
-8
-7
-6
-5
-4
-3
-2
-1
0
1
2
3
4
5
6
7
8
9
10
11
12

(a)

Figure 5.6

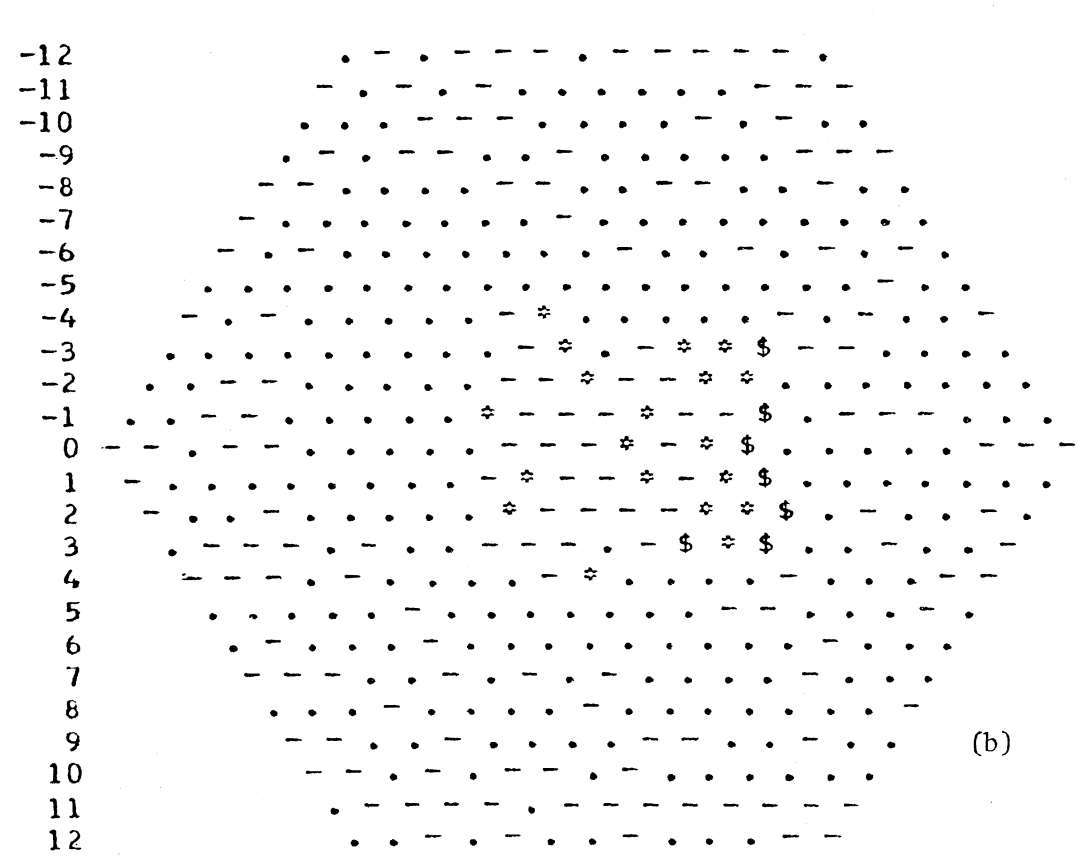
330
-12
-11
-10
-9
-8
-7
-6
-5
-4
-3
-2
-1
0
1
2
3
4
5
6
7
8
9
10
11
12

(b)

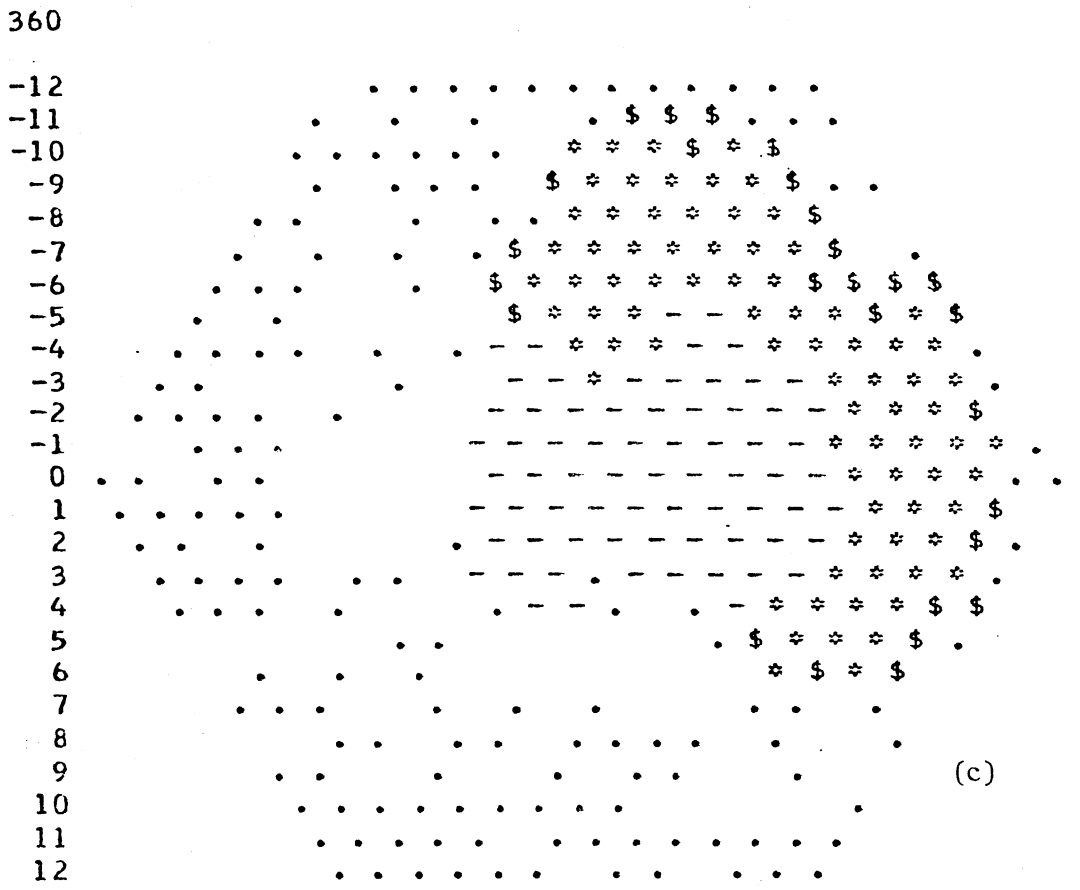
360
-12
-11
-10
-9
-8
-7
-6
-5
-4
-3
-2
-1
0
1
2
3
4
5
6
7
8
9
10
11
12
(c)

Figure 5.6

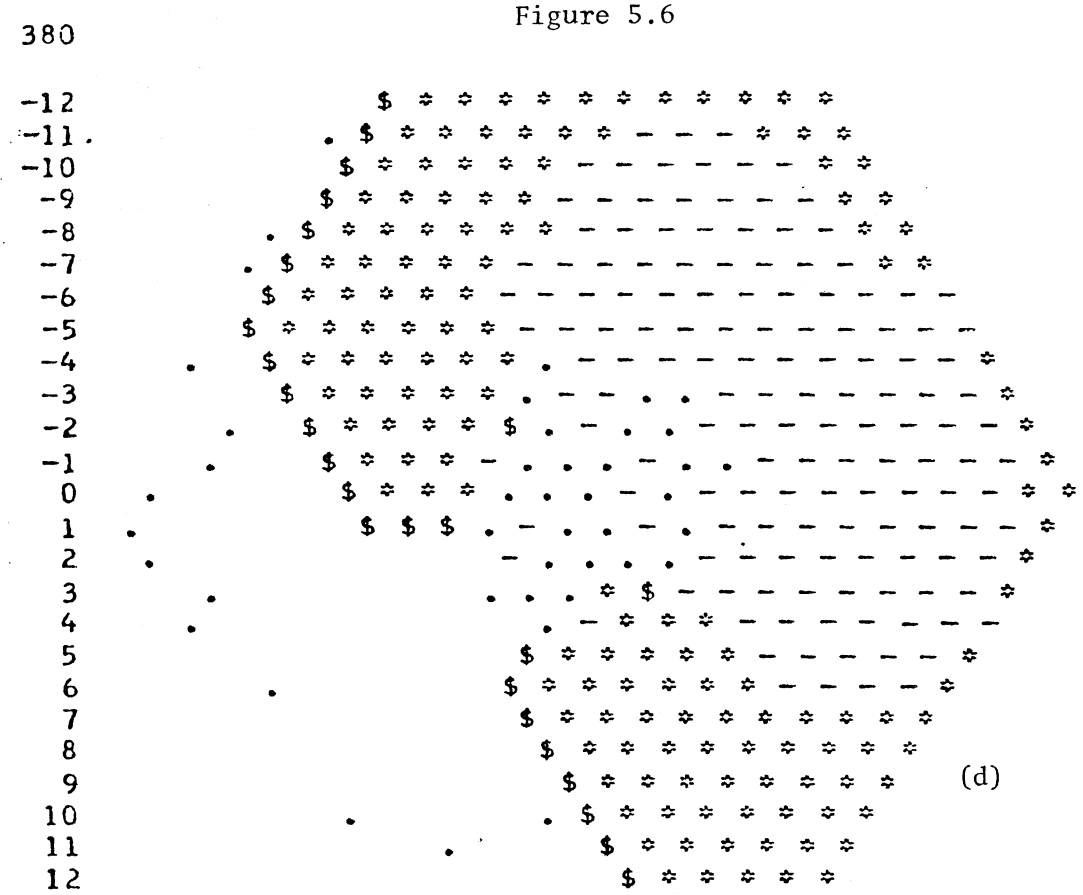
380
-12
-11
-10
-9
-8
-7
-6
-5
-4
-3
-2
-1
0
1
2
3
4
5
6
7
8
9
10
11
12
(d)

excessive delay, or both, then the expanding reentry wave may close over the path's distal[4] end without propagating a second reentry wave down it. Invariably, there will be at least the beginnings of a second reentry wave, for the distal end of the original reentry path becomes progressively more excitable as the reentry wave expands outward adjacent to it, thus making a "re-reentry" inevitable. In order for the second reentry to be propagated, however, its conduction must be delayed enough that the pathway can recover in front of it; this is facilitated by thicker, longer pathways. A thinner path has difficulty sustaining conduction reliably yet with substantial delay; but if the first reentry is delayed excessively, then too much of the reentry pathway will have recovered by the time the second reentry takes place, and the latter will run abruptly into quite refractory cells and conduction failure.

Sometimes, especially with fixed-rate stimulation, where the reentry gaps tend to develop further away from the stimulator, the reentry pathway will lie quite close to the edge of the network. In such cases, a small change in the propagation of the reentry wave can cause it to pass too close to the edge, whence conduction may fail for lack of summation and/or enough excitable cells.

2) After Multiple Reentries

As the preceding discussion implies, the first reentry wave contains the seeds of the second, the second the third, and so on. Each will flourish in its turn unless the conditions are particularly un-

[4] The outermost end, furthest from the external stimulator; presumably, the part of the pathway that the reentry wave excited first.

favorable. Successive reentry waves do not differ from the first in any fundamental aspect, although they may be completely different in detail. Hence, the mechanism of spontaneous termination after multiple reentries is much the same as after one. However, spontaneous termination is less likely after several reentries, by a simple process of natural selection: a wave which persists for several reentries probably arose in a fairly stable configuration or became more stable--by chance--over successive reentries. A wave whose early reentry patterns are precarious is, by the obvious probabilistic argument, unlikely to survive many cycles.

In other words, there does not seem to be any strong tendency for reentry patterns to become more stable simply by the passage of time, even though it is true that most (but not all) reentries that persist more than a few cycles will persist for many more. This fact is certainly demonstrated by the waves which suddenly terminate, spontaneously, after continuous self-sustained activity for thousands of time-steps.

Each reentry predisposes the next to follow the same path, but this is only a general tendency. Frequently the path shifts slightly --sometimes even radically--from one reentry to the next. When such shifts move the reentry pathway close to the border of the network, spontaneous termination becomes more probable even though the basic wave pattern may remain quite stable. Less commonly, two or more reentry waves may coexist peacefully for awhile in the same network and then, by chance shift in pattern, collide and annihilate each other.

C. Persistence

The basic pattern assumed by all reentrant waves is that of a rotating spiral (figure 5.7). In the simplest case there is only a single spiral, with one end intersecting the edge of the network and the other following a fairly small, roughly circular path somewhere in the interior (not necessarily near the center) of the net. Such waves often trace a similar path from one cycle to the next, not unlike the classical idea of a "mother wave" traversing a fixed circuit. The circuit in such cases may indeed by relatively fixed, but it is a purely dynamic thing; that is, there is nothing in the model corresponding to an anatomical basis for such paths. The distribution of k values, which is responsible for the conduction block which allowed the reentry to form, undoubtedly influences its subsequent course; but there is no obvious relation between the cells comprising the circuit and their values of k, no "path of low refractoriness."

The absence of structurally based reentry paths in the model is further demonstrated by the fact that some waves follow a varying course from cycle to cycle. Sometimes the spiral precesses, that is, its center (an admittedly ill-defined thing) moves around the network. Less commonly, the wave may be diverted by patches with long refractory periods, or "short-circuited" by cells that recover quickly. Infrequently, a reentrant wave may follow exactly the same path on each cycle; that is, the network becomes completely cyclic.[5] The cells in

[5] In principle, all model networks are periodic by virtue of the discrete nature of the computer, but their periods are extremely long. The surprising thing is that some, but not all, nets have periods as short as the activity cycle of a cell.

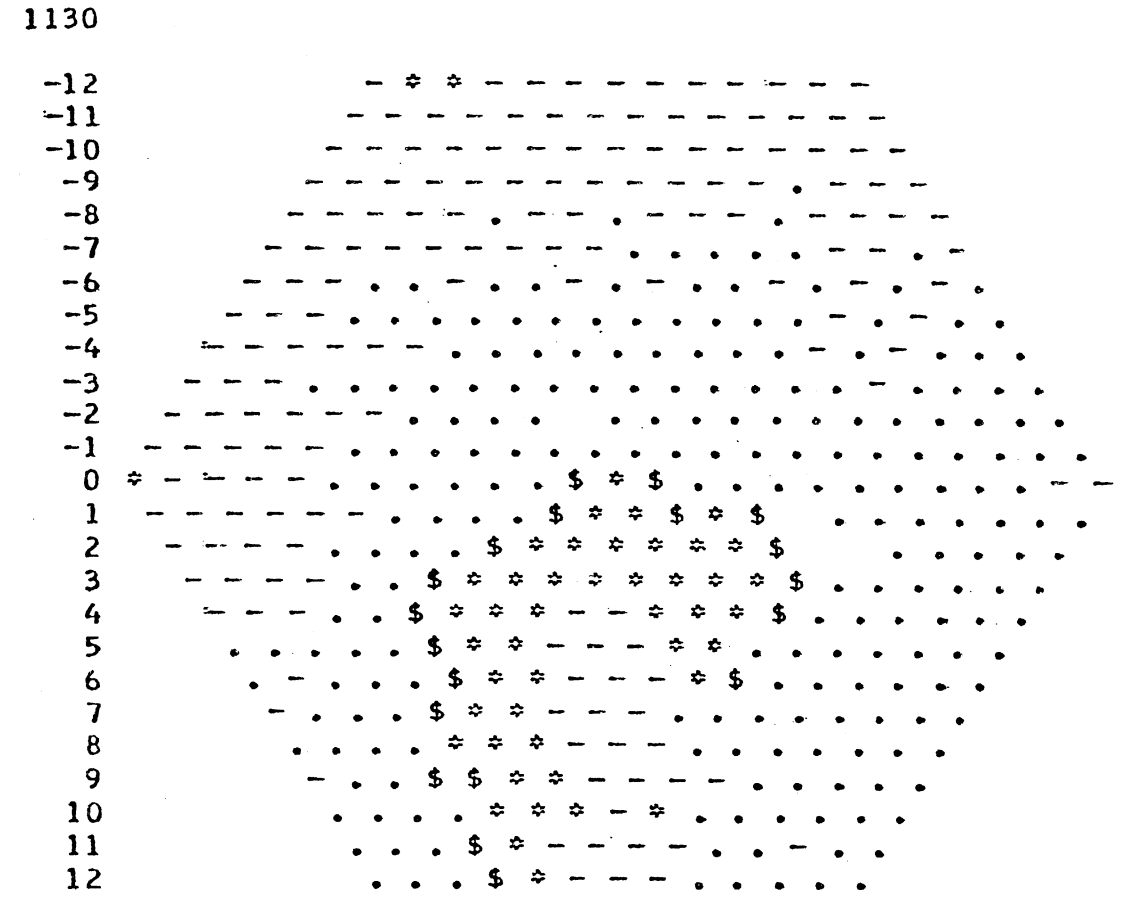

Figure 5.7. A Rotating Spiral Wave, the Commonest Pattern of Self-Sustaining Activity in the Model.

Legend: $ = stimulated
* = firing
- = absolutely refractory
. = relatively refractory
blank = quiescent

such nets are all perfectly synchronized and exactly periodic (but, of course, out of phase with each other to varying degrees). This is the ultimate case of a stable reentry, for once in such a state the network "locks in" and does not vary thereafter.

Although the single spiral is the most prevalent form, more complex patterns are not uncommon. As noted earlier, the basic reentry mechanism produces a double spiral. If the wave which gives rise to the original reentry contains more than one gap, then additional reentry pathways may develop, each producing an incipient pair of spirals. The 25 by 25 network of Program B is too small to support more than a few independent waves, so simultaneous reentries quickly lead to collisions that eliminate some of them. In the 51 by 51 network of Program C a larger number of separate waves can survive. In both cases, however, interactions among the several waves often divert them into irregular circuits, so the simple spiral patterns disappear.

Complex, multi-wave patterns are the exception rather than the rule, and they seldom develop spontaneously from simpler forms. Their usual origin is fixed-rate stimulation, where repeated stress from the external stimulator can elicit multiple conduction blocks. That is, externally stimulated waves are sometimes forced into ill-recovered areas where conduction then fails, while a wave propagating internally might have been slowed enough to find the same area more excitable. Once initiated, though, multiple waves may persist for quite a while, even in the smaller networks. But eventually, most multiple waves coalesce into a single spiral.

Fragmentation of an existing reentry wave can be caused by variation of certain parameters of the model which change the conducting properties of the cells, as discussed below. But in the normal network spontaneous fragmentation was almost never seen.

D. Statistical Measures of Stability

An attempt has been made to relate the stability of reentrant waves to the behavior of the individual cells, that is, to find some simple measure of the condition of the cells that would aid in predicting the persistence of a particular reentry pattern. No such measure has been found. Various statistics which were computed during simulation runs have been described in Chapter III; a representative sample of these for both fixed-rate and multiple premature stimulation is shown in table 5.2. Scrutiny of this table leads to the following generalizations about the statistical data:

1. Waves that reenter are not easily discriminated from those that do not; compare, for example,

   (a) P_1 305, P_2 410--more than 4 extra beats

   P_1 305, P_2 415--one extra beat

   P_1 305, P_2 420--no extra beats

   (b) Wave 7 at CL 88--no reentry

   Wave 7 at CL 86--more than 5 extra beats

   (c) Wave 4 at CL 88--no reentry

   Wave 4 at CL 86--no reentry

   Wave 4 at CL 84--4 extra beats

   In each case, waves which are quite similar statistically behave very differently with respect to reentry.

Table 5.2. Statistics of the Network's Response to Various Patterns of Stimulation.

μ = mean
σ = standard deviation

(a). Fixed-rate stimulation at cycle lengths of 88, 86, and 84. Unstimulated (reentry) waves are shown with "stimulus number" in parentheses. A single series of self-sustaining waves is indicated by a prime ('); where a second series was produced by backing up the simulation and inserting another external stimulus, the second series is indicated by a double prime (").

(b). Multiple-premature stimulation at drive cycle length 200, P_1 and P_2 timings as shown.

NSS = number of stimulation successes: the number of cells which were fired.

NSF = number of stimulation failures: the number of times a cell received subthreshold stimulation from its neighbors (may happen more than once per cell.)

λ = "wave length" of a reentrant wave: average activation interval divided by average delay per cell.

Stimulus Cycle Length	Stimulus No.	Stimulation Success (no.)	Stimulation Failure (no.)	Delay μ	Delay σ	Safety Factor μ	Safety Factor σ	Activation Interval μ	Activation Interval σ	Wave Length λ
88	1	1951	0	2.0	0.1	4.9	0.7	-	-	
	2	1951	105	2.9	1.2	2.7	1.3	105	3.7	
	3	1951	662	3.7	1.5	2.2	1.0	105	4.7	
	4	1951	1507	4.2	1.6	1.9	0.9	101	4.8	
	5	1951	2438	4.6	1.6	1.7	0.7	98	4.6	
	6	1951	3194	4.9	1.6	1.6	0.6	95	4.3	
	7	1948	4107	5.1	1.5	1.6	0.6	93	4.5	
	8	1949	4500	5.2	1.5	1.6	0.6	92	5.1	
	(9')	1942	2062	3.9	1.8	1.7	0.7	93	7.7	24
	<backup>									
	9	1949	5179	5.3	1.5	1.5	0.5	91	5.2	
	(10")	1943	3377	4.3	1.9	2.2	1.4	101	19.6	24
	(11")	1950	1653	3.3	1.7	2.8	1.5	113	19.0	34
	(12")	1944	1678	3.7	1.7	2.3	1.2	108	10.4	30
	(13")	1950	1887	4.1	1.7	2.0	0.9	104	7.1	26
	(14")	1944	2247	4.3	1.7	1.9	0.8	100	5.8	23
	(15")	1875	2688	4.7	1.6	1.7	0.6	97	5.6	21
	(16")	1947	3090	4.8	1.5	1.7	0.6	95	4.4	20
	(17")	1890	3091	4.8	1.6	1.7	0.6	94	4.0	20
	⋮									
86	1	1951	0	2.0	0.1	4.9	0.7	-	-	
	2	1951	111	2.9	1.2	2.7	1.2	104	4.4	
	3	1951	677	3.7	1.5	2.2	1.0	104	4.9	
	4	1951	1607	4.3	1.6	1.9	0.8	101	4.8	
	5	1951	2476	4.7	1.6	1.7	0.7	97	4.6	
	6	1951	3328	4.9	1.6	1.7	0.6	94	4.5	
	7	1948	4289	5.1	1.5	1.6	0.5	93	4.9	
	(8')	1950	4884	5.2	1.5	1.6	0.5	91	4.6	18
	(9')	1943	5266	5.1	1.6	1.6	0.6	92	7.9	18
	(10')	1932	3948	4.6	1.8	2.0	1.2	97	15.0	21
	(11')	1932	3467	4.6	1.7	1.8	0.8	97	9.7	21
	(12')	1928	3283	4.5	1.7	1.8	0.8	97	8.0	22
	⋮									

Table 5.2a. Statistics of the Network's Response to Various Patterns of Stimulation.

Table 5.2a cont.

		Stimulation Success (no.)	Stimulation Failure (no.)	Delay μ	Delay σ	Safety Factor μ	Safety Factor σ	Activation Interval μ	Activation Interval σ	Wave Length λ
84	1	1951	0	2.0	0.1	4.9	0.7	-	-	
	2	1951	111	2.9	1.2	2.7	1.3	103	3.7	
	3	1951	707	3.6	1.5	2.2	1.0	105	4.7	
	4	1951	1575	4.2	1.6	1.9	0.9	101	4.9	
	(5')	1949	2424	4.6	1.6	1.8	0.7	98	4.6	21
	(6')	1949	3273	4.8	1.6	1.7	0.6	96	4.3	20
	(7')	1950	3711	4.9	1.6	1.7	0.7	94	4.2	19
	(8')	1945	3836	4.9	1.6	1.6	0.6	93	4.0	19
	<backup>									
	5	1950	2520	4.6	1.6	1.8	0.7	98	4.6	
	(6")	1949	3460	4.8	1.6	1.7	0.6	95	4.6	20
	(7")	1946	4037	5.0	1.6	1.6	0.6	94	4.7	19
	(8")	1950	4373	5.0	1.6	1.6	0.6	93	5.7	19
	(9")	1940	4800	5.0	1.6	1.7	0.7	93	5.9	19
	(10")	1938	2832	4.3	1.8	2.2	1.2	99	14.1	23
	(11")	1944	1923	4.0	1.7	2.1	1.0	101	9.8	25
	(12")	1929	1676	3.9	1.6	2.2	1.1	103	8.7	26
	(13")	1794	2012	4.3	1.6	1.9	0.8	100	6.8	23
	(14")	1937	2751	4.7	1.6	1.7	0.6	97	5.5	21
	⋮									
	⋮									

Stimulus (timing)	NSS	NSF	Delay μ	Delay σ	Safety Factor μ	Safety Factor σ	Activation Interval μ	Activation Interval σ	Wave Length λ
Drive 200	1951	0	2.0	0.1	4.9	0.7	-	-	
P_1 305	1951	314	2.9	1.3	2.9	1.3	142	5.3	
P_2 410	1951	678	3.5	1.5	2.3	1.1	118	5.2	
-	1948	1248	4.0	1.6	2.0	1.0	107	4.6	27
-	1944	1652	4.2	1.6	1.9	0.8	102	5.2	24
-	1937	2137	4.4	1.6	1.8	0.8	99	5.0	22
-	1943	2635	4.7	1.6	1.7	0.7	97	4.6	21
P_2 415	1951	674	3.5	1.5	2.3	1.1	118	5.1	
-	1949	1250	4.0	1.6	2.0	0.9	107	4.5	27
P_2 420	1951	686	3.5	1.5	2.3	1.1	118	5.0	
P_1 310	1951	472	3.2	1.5	2.5	1.2	138	5.1	
P_2 400	1951	1023	3.7	1.6	2.1	1.0	116	5.4	
-	1951	1610	4.1	1.6	2.0	0.9	106	5.2	26
-	1949	2041	4.4	1.6	1.8	0.7	101	4.8	23
-	1946	2440	4.6	1.6	1.8	0.7	98	4.3	21
-	1948	2653	4.7	1.5	1.7	0.6	96	3.8	20
P_2 405	1951	1211	3.9	1.7	2.1	0.9	114	5.3	
P_2 410	1951	1207	4.0	1.7	2.1	0.9	114	5.3	
P_1 315	1951	423	3.2	1.5	2.6	1.2	138	4.7	
P_2 400	1951	776	3.6	1.6	2.3	1.0	117	4.9	
-	1949	974	3.8	1.6	2.1	1.0	108	4.5	28
-	1945	1272	4.0	1.6	2.0	0.9	104	4.7	26
-	1918	1677	4.3	1.6	1.9	0.8	101	4.2	23
P_2 405	1951	729	3.6	1.6	2.3	1.1	117	5.6	
P_2 410	1951	1094	3.9	1.6	2.1	1.0	115	5.1	
P_1 320	1951	379	3.2	1.5	2.6	1.3	138	4.5	
P_2 405	1951	978	3.8	1.6	2.1	1.0	115	4.7	

Table 5.2b. Statistics of the Network's Response to Various Patterns of Stimulation.

2. Reentrant waves which persist in self-sustained activity are not easily discriminated from those that do not; for example,
   (a) At cycle length 88, wave 8 results in only one reentry wave while wave 9 results in more than eight.
   (b) At cycle length 84, wave 4 produces four extra beats while wave 5 leads to more than nine.
3. A reentrant wave which terminates does not necessarily show any exceptional statistical properties; for example, compare
   (a) CL 88, wave 9' vs. 10" - 17"
   CL 84, wave 8' vs. 6" - 14"

For fixed-rate stimulation, the waves' statistics follow quite similar trends, at least up to the point of the first reentry. Moreover, the statistics from the multiple-premature stimulation patterns are reasonably similar both to each other and to the fixed-rate cases. This suggests that these statistics are determined more by the maximum rate at which changes can be propagated through the network (a property implied by the transition function) than by the pattern of stimulation. Yet the stimulating pattern has an important bearing on the initiation of reentrant activity. It is clear that gross measurements, averaged over all the cells, are inadequate predictors of reentry; for, in this model, at least, reentrant activity is a distinctly local phenomenon.

II. Effects of Factors Related to the Duration of the Absolute Refractory Period ($\bar{k}$, k_σ, Network Size)

The conduction velocity and the duration of the effective refractory period together determine the minimum path over which a reentrant wave can be conducted. The minimum path length influences the minimum

network size in which a reentry can be sustained, but the relationship is complicated by the fact that the path need not be regular and can, by folding, attain greater length in a fixed area.

The refractory period duration also determines the maximum rate at which an excitable network can follow external stimulation. Stimulation near this maximum rate causes a greater amount of disorder than stimulation at slower rates, and hence might be expected to be most effective in establishing reentries. The initiation of reentry also depends on the existence of focal blocks which, in turn, derive from the inhomogeneity of the medium. Consequently, a given stimulation pattern ought to be less effective in initiating reentrant waves when the amount of inhomogeneity is reduced.

In order to test the interactions among these factors in the initiation of reentry, a series of experiments was performed in which reentrant patterns were established by external stimulation at fixed rates, under different conditions of refractory period duration (varying $\overline{k}$), homogeneity (varying k_σ) and network size. The use of a standard stimulation pattern would facilitate comparisons among these cases, but unfortunately, no single pattern is uniformly effective across changes in parameters. Moreover, slight changes in the stimulus cycle length, even the addition or omission of a single stimulus in a train, can make the difference between eliciting a persistent reentry or just a single response. Using a single pattern of test stimuli might therefore be very misleading when attempting to gauge the effect of parameter variation on the initiation of reentrant waves.

Procedure

To mitigate the effects of sensitivity to the stimulation pattern, in many of the experiments each parameter combination of interest was "scanned" across a range of stimulator frequencies and train lengths. That is, stimulation was applied at several different frequencies, using various numbers of stimuli at each frequency, according to the following procedure. The stimulator frequency was set, two stimuli were applied, and the network was allowed to run until either it became quiescent or a fixed number of time-steps had elapsed. Then the simulation was "backed up" to the point at which the third stimulus would have been due, that stimulus was applied, and the network again allowed to run until the result was clear. Then it was backed up again and a fourth stimulus applied, and so on for the fifth through tenth stimuli. In this way the response of the network was measured for 2, 3, 4, ..., 10 stimuli, all applied at the same cycle length. Because the "backing up" was done by exactly restoring a previously saved state,[6] the successive stimuli were applied under identical conditions except for their relative positions in the train. The stimulator frequency was then reduced slightly and the sequence of 2, 3, ..., 10 stimuli again applied; all this was repeated across a range of stimulator frequencies. When such a run was finished, the result was the network response to varying numbers of stimuli at varying cycle lengths, thus, presum-

[6] When applying n stimuli, the network state at the time the n+1'st stimulus would have been applied was recorded in a secondary storage file, and further stimuli were suppressed; thus the response to n stimuli ensued. Then the network state was restored from the file, the n+1'st stimulus applied, the state saved again just prior to the n+2'nd stimulus, and the stimulator turned off; and so on.

mably swamping out any aberrations due to chance sensitivities to specific stimulation patterns.

In algorithmic notation, the procedure was:

```
A:  DO NETSIZE = 25 TO 15 BY -2;
B:     DO CL = C1 TO C2 BY -2;    (C1, C2 set by experimenter)
       INITIALIZE NETWORK N, BASIC CYCLE CL;
       (set parameters as desired)
       X = CL;
       AT TIME X APPLY STIMULUS;
       X = X + CL;
       AT TIME X APPLY STIMULUS;
C:        DO I = 3 TO 10;
          X = X + CL;
          AT TIME X APPLY STIMULUS;
          AT TIME(X + CL - 1) SAVE IN FILE 1;
          IF (ACTIVITY CEASES OR TIME > 10000)
             THEN RESTORE FILE 1, DO NEXT C;
          END C;
       END B;
    END A;
```

The results of such runs are displayed in bar graphs (figures 5.8 - 5.13). The abscissa is blocked off in groups, where each group represents a fixed stimulator cycle length; each group is subdivided by the successive elements of a train of stimuli at the given cycle length, starting usually with the fourth and ending with the tenth. The height of each bar represents the persistence of activity in the network when stimulated by the specified train-length/cycle-length combination.

In some experiments, the effect of parameter changes on persistence of reentrant activity was tested by varying the parameter in question after a persistent reentry wave had been established by using a stimulation pattern of known effectiveness. Since simulation experiments can be exactly repeated, it is possible to determine what the course of a particular reentrant pattern would have been had the parameter change not been made, or to determine the effect of making the same change at a different time, say, before the reentry has been established or after it had persisted a longer time. These experiments, which allow us to compare individual cases of initiation and persistence of reentrant activity, are complementary to the "scan" series, which allow us to draw more general conclusions about the effect of various factors on initiation and persistence.

A. Effect of Mean Value of k

Figure 5.8(a) shows the result of using the "scan" procedure to stimulate network N of table 3.2, in which the average value of k is 7.0. Reentrant waves were initiated by stimuli whose cycle lengths ranged from 80 to 90, but persistent activity was established only over the range 80-86. In each case it took at least four stimuli to establish a reentry.

Figure 5.8(b) shows the "scan" result for a network which was identical to that of figure 5.8(a), except that the k values for all the cells had been scaled down proportionately so that the mean value of k for the network was 6.0 (network N_3 of table 3.2). As expected, the effective stimulator cycle length was shortened: reentries were initiated over the range 64 to 74. Relatively persistent activity was established over the entire range; or, put another way, there was

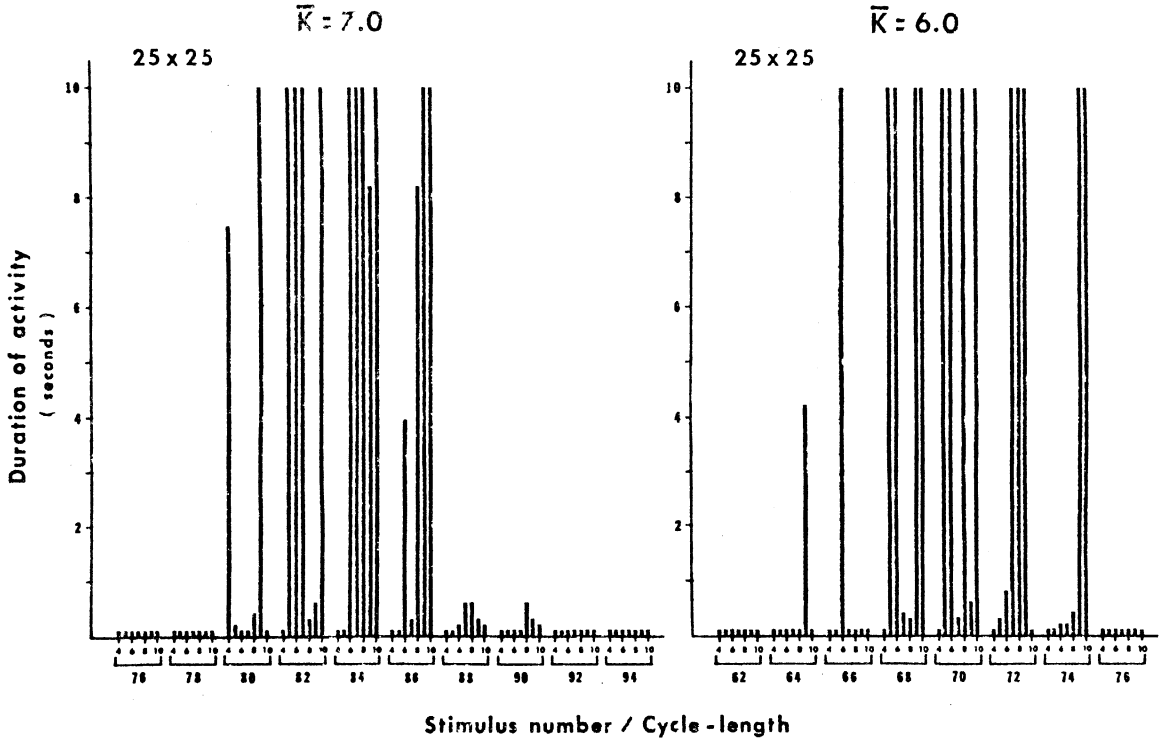

Figure 5.8. Persistence of Activity as a Function of Stimulus Number and Frequency. (See text.)

(a) $\bar{k} = 7.0$
(b) $\bar{k} = 6.0$

somewhat less spontaneous cessation of activity than with the network of figure 5.8(a). Thus lowering the average ARP duration allowed persistent reentrant activity to be established over a wider frequency range of stimuli, presumably because a network of a given size affords more reentry paths when the average ERP, and hence the minimum circuit length, is shorter.

The effect of raising the average value of k is shown in figure 5.9, in which the networks are identical to that of figure 5.8(a) except for scaling of the k values to a mean of 8, 9, 10, and 11 respectively. At higher average k values, the cycle length for effective stimulation must, of course, be increased. But persistent reentries became progressively harder to initiate (i.e. fewer of the stimulus patterns resulted in a persistent reentrant wave), until finally, when average k was 11.0, persistent reentry could not be established at all. Raising the mean k also reduced the range of stimulating frequencies over which reentry could be initiated.

The fact that lowering k (shortening the refractory period) enhanced the initiation of reentries in a quiescent network does not allow us to predict the effect of reducing the k of a network in which a reentrant wave has already been established. In particular, it would be interesting to know whether shortening the refractory period tends to cause fragmentation of a single reentrant wave into two or more wavelets.[7] Therefore, an additional experiment was performed in which a reentrant wave was established by applying a train of 20 stim-

[7] If this were true, it would support the suggestion that the mechanism by which acetylcholine converts flutter to fibrillation is primarily by shortening the refractory period.

uli at cycle length 84 to network N of table 3.2. This reentry pattern was known from other experiments to be very stable and persistent. At time 6199, the mean k value was reduced to 6.5 by scaling all cells' k values down proportionately;[8] similar reductions of 0.5 in the value of mean k were made approximately every 300 time-steps thereafter, while the reentry wave was observed on the CRT display. When the mean k had been reduced to 4.0, the simulation was allowed to run another 900 time-steps without further change in k.

The result can be simply stated: there was absolutely no tendency toward fragmentation. On the contrary, the wave seemed to become ever more regular and stable as k was reduced. The only significant statistical change was in average activation interval, which, as expected, grew shorter with the shorter ARP. This had the effect of permitting the wave to form a tighter spiral pattern in the network, so that even though the wavefront itself became quite regular, there was perhaps more variation in activity state from one part of the network to another due to the fact that there were essentially more waves in the network at any given time. It is conceivable that an analogous situation in heart muscle would cause the electrogram to exhibit a more rapid and irregular trace, i.e. that the "finer grained" fibrillation could be the result of a more tightly coiled spiral rather than

[8] Any such change in $\bar{k}$ caused the simulation program to re-compute the k_i values for the individual cells automatically and immediately; with respect to simulated time, the change was always "instantaneous". However, the corresponding ARP durations did not change instantaneously, for they were computed only when a cell fired. Thus, a change in $\bar{k}$ was not immediately reflected in altered variation of refractory period, but rather spread over the network along with the activity wave on its next cycle.

Figure 5.9. Persistence of Activity as a Function of Stimulus Number and Frequency.

Mean k values 8.0 to 11.0.

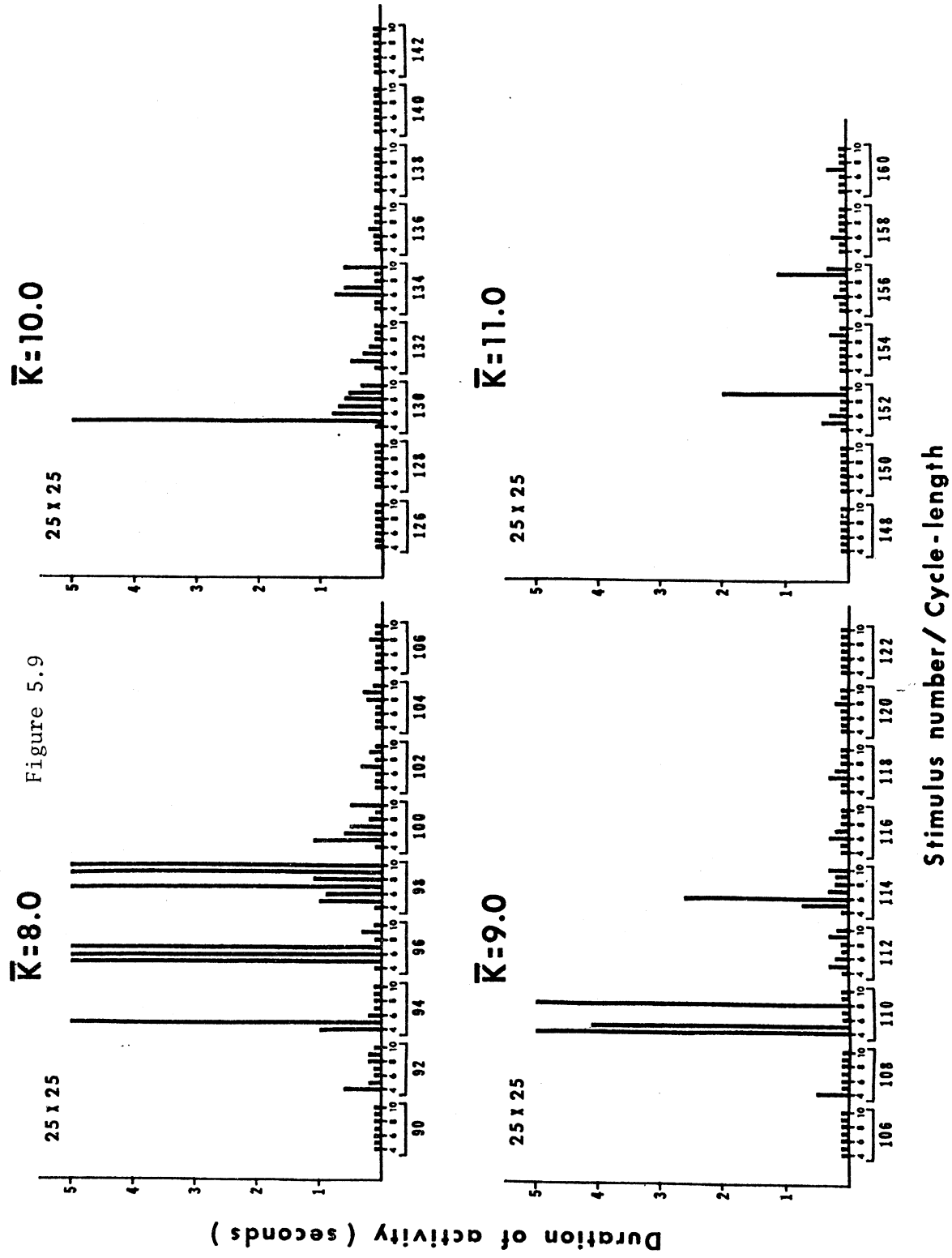
K=8.0
K=9.0
K=10.0
K=11.0
25 x 25
Duration of activity (seconds)
Stimulus number / Cycle-length

Figure 5.9

Figure 5.10. Persistence of Activity as a Function of Stimulus Number and Frequency. Variation in Network Size and Mean k.

(a) $\overline{k} = 7.0$
(b) $\overline{k} = 6.0$

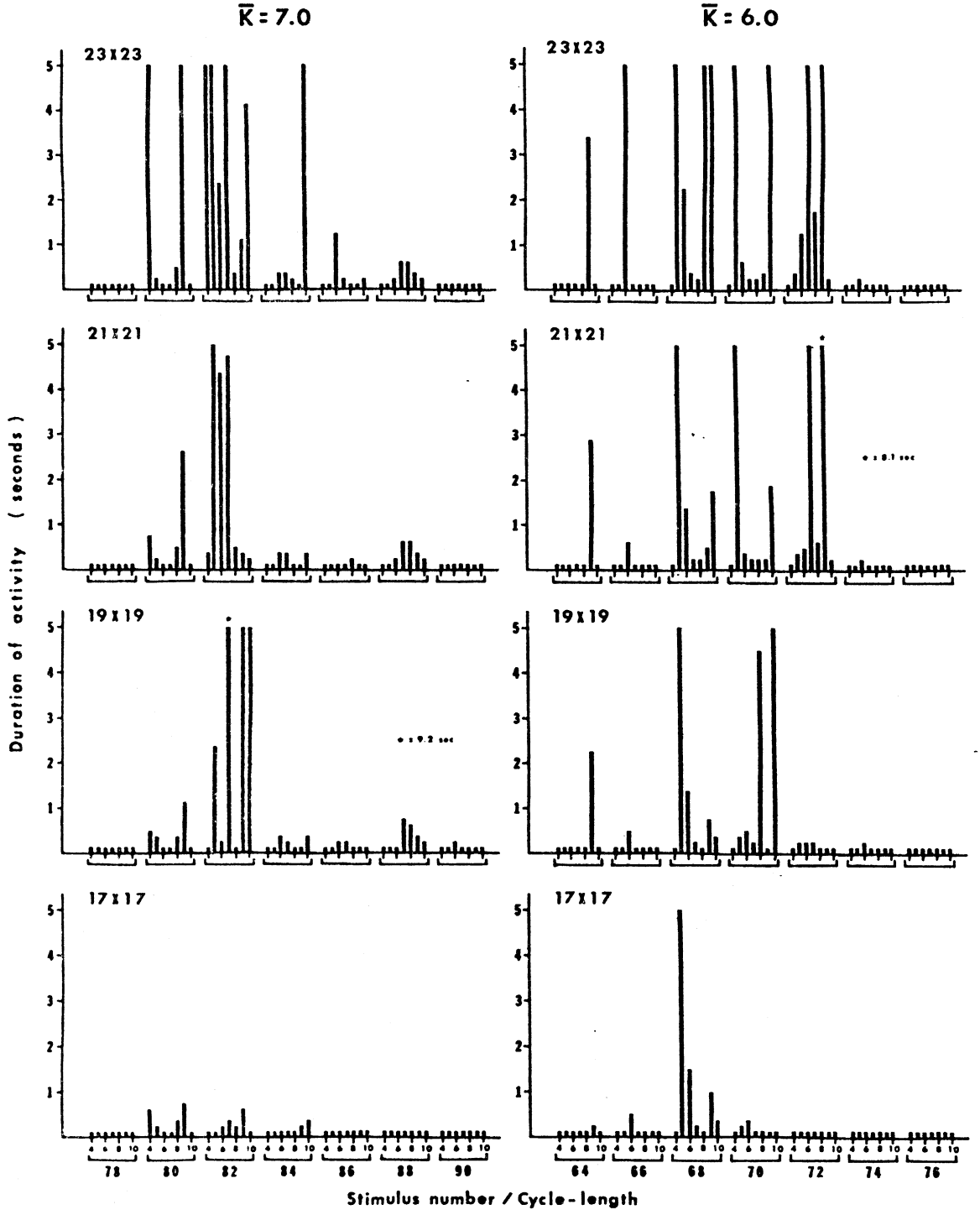
K̄ = 7.0
K̄ = 6.0
23x23
21x21
19x19
17x17
Duration of activity (seconds)
Stimulus number / Cycle-length
78 80 82 84 86 88 90
64 66 68 70 72 74 76
(a)
(b)

Figure 5.10

a true fragmentation of a single wave into multiple wavelets. This is, however, pure speculation, since the present model does not attempt to represent an electrogram in anything more than the crude form of total activity counts. It can be said, though, that simple, proportional shortening of the refractory period does not, of itself, lead to fragmentation of an existing reentrant wave.

B. Effect of Network Size

As described in Chapter III, the model network could be varied in size. Figure 5.10(a) shows the results of a succession of "scan" experiments performed on networks which are consecutively smaller in size but otherwise identical to that of figure 5.8(a); that is, each smaller network is a proper subset of the larger ones.

Trimming the network size caused a slight reduction in the range of stimulation frequencies over which reentries could be established, but the principal effect was on persistence. The decrease in size from 25 x 25 to 23 x 23 abolished reentry entirely at cycle length 90, and abolished persistent reentrant activity at cycle length 86. Further size reductions continued to decrease the persistence of activity, but reentries could still be produced across the same range of stimulation frequencies. Finally, when the network size was reduced to 17 x 17, persistent activity was completely abolished although a few reentries still occurred.

Inspection of the bar graph reveals some interesting phenomena:

i) Reentrant activity may sometimes be more persistent in a subset of a given network than in the network itself. For example, the 21 x 21 network in figure 5.10(a) does not sustain as many per-

sistent reentry waves as does its subset, the 19 x 19 network. This effect may arise either because the smaller net fails to sustain some reentry wave which otherwise would have collided with another reentry wave in mutual annihilation, or because a reentry wave in the smaller net encounters extra conduction delay (due to reduced summation near the edges) and so completes a reentry circuit which otherwise would have been insufficiently recovered.

ii) There is, in this case, no single pattern of external stimulation which is effective across the range of network sizes. The reasons for this are the same as for item (i). In other words, the fact that a certain stimulation pattern produced a persistent reentry in a given network does not imply that the same pattern would initiate a persistent reentry in a larger network.

Table 5.3 shows the effect of changing the network size after a persistent reentrant wave has already been established. Network size was reduced by "trimming off" the outer layers of cells, as described in Chapter III.

In 5.3(a) the size reduction occurred about time 1750 (see legend). Even trimming one layer caused a substantial reduction in persistence, but there was not much difference between trimming off one layer and trimming off two. Cutting layer three caused persistence to drop again, but there was no further reduction after layer four was cut. Table 5.3(b) shows exactly the same networks as 5.3(a), except that the cuts were made at a later time. The reentry pattern had evidently become more stable, since cutting off layers one and two made essentially no difference in persistence. Cutting

Table 5.3(a). Effect of Decreasing Network Size on Persistence of an Established Reentrant Wave. Case I.

Network Size	Termination Time
25 x 25	8161
23 x 23	2448
21 x 21	2450
19 x 19	2075
17 x 17	2075
15 x 15	1871

Initiation by 8 stimuli at cycle length 86, using network of table N. "Cuts" made at time 1750, except for 17 x 17 and 15 x 15 nets where cuts were made at time 1800 when wave was better centered in net (to avoid undue direct interference with the wave).

Table 5.3(b). Effect of Decreasing Network Size on Persistence of an Established Reentrant Wave. Case II.

Network Size	Termination Time
25 x 25	8161
23 x 23	8157
21 x 21	8059
19 x 19	3931
17 x 17	3621

Same as above, except network allowed to run until time 3200 before cuts were made. Reentrant wave had become more stable, less affected by the reduction in network size.

Table 5.3(c). Effect of Network Size on Persistence of an Established Reentrant Wave. Case III.

Network Size	Termination Time	Cycle
25 x 25	∞	96
23 x 23	∞	96
21 x 21	∞	96
19 x 19	∞	96
17 x 17	∞	96
15 x 15*	7500	-
15 x 15	7500	-

Initiation by 8 stimuli at cycle length 88, using network N of table 3.2. Cuts made at time 7184, except item indicated by star (*), where cut was made at time 7275 when wave was better centered in net. All nets which remained persistent after cut became cyclic.

Table 5.3(d). Effect of Network Size on Initiation of a Reentrant Wave.

Network Size	Termination Time
25 x 25	∞
23 x 23	3875
21 x 21	20700
19 x 19	no reentry
17 x 17	no reentry

Same as above, except cuts were made at time 0 (before any stimuli were applied.) The 25 x 25 network is, of course, the same as above. Note that the 21 x 21 network had not become cyclic by time 20700, and showed no signs of termination.

layer three caused a major drop, and cutting layer four produced an additional, lesser shortening of persistence.

Table 5.3(c) shows a similar experiment run using an identical basic network but a slightly different stimulation pattern to initiate the reentry. In this network, the reentrant wave was quite stable and eventually became cyclic, even with as many as four layers removed. Cutting the fifth layer, however, terminated the arrhythmia either immediately or after a few cycles, depending on the exact timing of the cut. Table 5.3(d) shows the same network and stimulation pattern as table 5.3(c), but with the cuts made before stimulation was begun. The effect is striking. Cyclic behavior is completely absent, and reentry does not occur at all if more than two layers are cut. Yet the 21 x 21 network persists indefinitely, while in the larger 23 x 23 network the arrhythmia terminates spontaneously after a moderate duration.

C. Interaction between Network Size and Mean k

Figure 5.10(b) shows the outcome of a series of "scan" experiments on the network whose mean value of k is 6.0; i.e. it is analogous to figure 5.10(a), but starts with the network of figure 5.8(b) rather than that of figure 5.8(a). Comparing the two series, it is apparent that persistent reentrant activity could be initiated over a wider range of stimulation frequencies in the network with the smaller k values than in the network whose average k was higher. Moreover, a lower value of k allowed persistent reentrant activity to be initiated in a smaller network: when the mean k was 7.0, persistent reentries did not appear in networks smaller than 19 x 19, but reducing

the average k to 6.0 allowed such reentries to be initiated in networks as small as 13 x 13.

Conversely, increasing the size of the network allowed persistent reentry to be established in spite of long refractory periods. For example, figure 5.9 indicates that fixed-rate stimulation cannot initiate persistent reentrant activity in a 25 x 25 network whose mean k is 11; yet such activity was easily established in a 51 x 51 network with the same average value of k.[9]

D. Randomness

The networks described in sections A, B, and C (above) were all produced using the same sequence from the random number generator; that is, the spatial distribution of k values was the same in all nets, the only difference being a scale factor to adjust the mean values as required. Since focal blocks, which are the proximate cause of reentry, derive from spatial inhomogeneity in refractoriness, the question arises: To what extent does the observed behavior depend on the particular spatial distribution of k values? Specifically, is the present distribution in some way atypical; does it, by chance, introduce too many or too few conduction aberrations?

Such doubts can be partially allayed from considerations of symmetry: one can imagine the network divided in half (or thirds, or even sixths), with each part receiving the same (fraction of) drive stimulus. If focal block and reentry are due to unlikely coincidence, then one would not expect to find them developing simultaneously

[9] Using 8 stimuli at a cycle length of 160, in Program C.

Figure 5.11. Persistence of Activity as a Function of Stimulus Number and Frequency.

Alternate k-distribution, variation in network size.

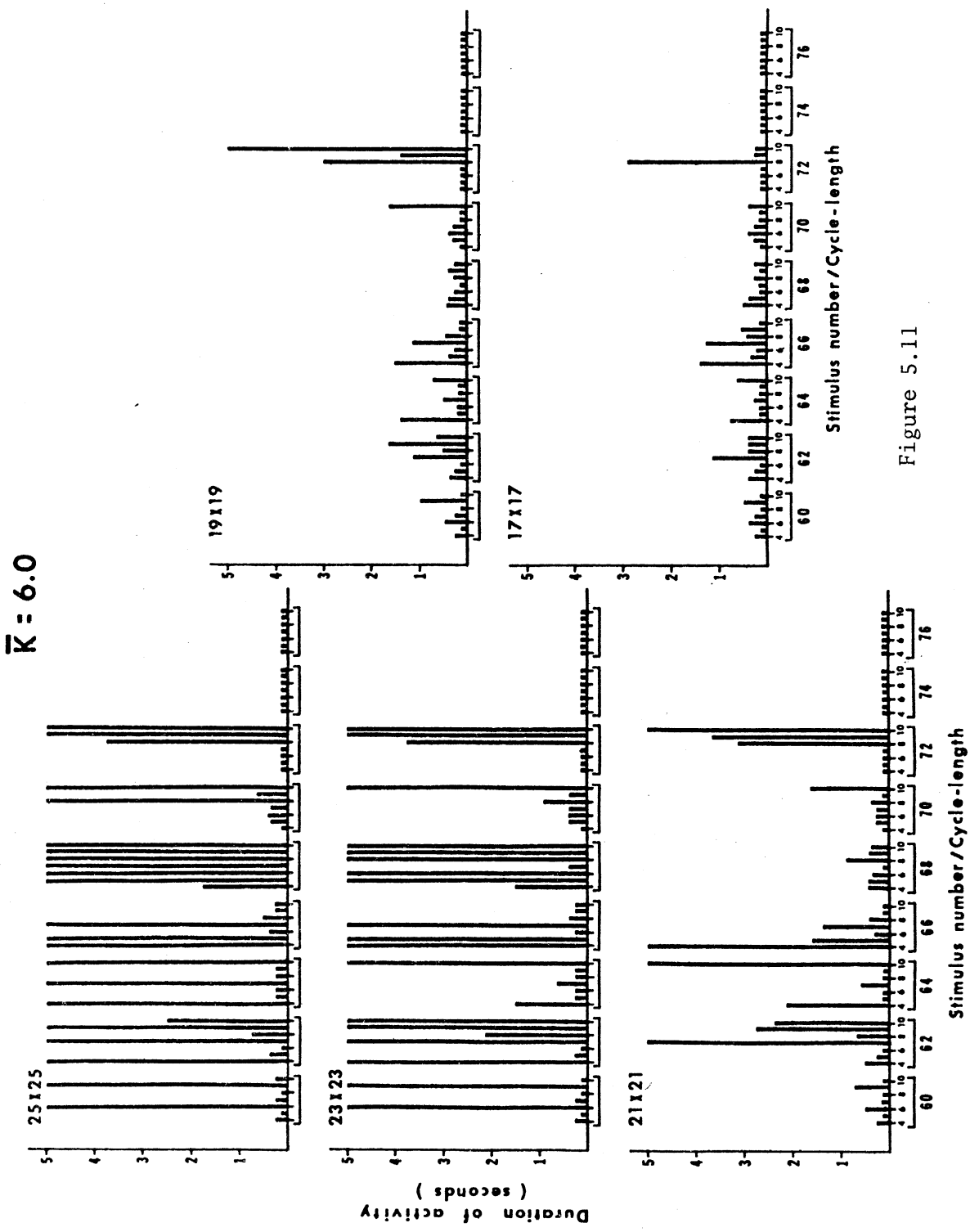
K = 6.0
25125
23123
21121
19119
17117
Duration of activity
(seconds)
Stimulus number/Cycle-length
Stimulus number/Cycle-length

Figure 5.11

in separated parts of the network. Yet that is exactly what is observed. Sometimes one such block grows faster than the others, becoming "the" focal block of the network. But often several reentries occur at the same time in different areas of the network, with little apparent interaction until after the reentrant waves are fully formed, at which time they usually collide.

As an additional check, a series of experiments similar to those of section B (above) was performed using a network in which the k values had been computed from a different random number sequence. This network had a completely different spatial distribution of k values, even though the mean and variance were approximately unchanged. It thus provides a control against the network used for other experiments: roughly similar behavior would indicate that the observed results were not merely accidental or atypical, whereas radically different behavior would suggest some strong dependence on the exact spatial distributions.

The outcome of a "scan" experiment on this network, with a mean k of 6.0 and with the size varied from 25 x 25 to 17 x 17, is shown in figure 5.11. Comparison with the corresponding network in figures 5.8(b) and 5.10(b) shows that, with the different distribution, reentrant activity was initiated over a wider range of cycle lengths at the larger net sizes; but the range of effective stimuli diminished faster as the net size was shrunk. The expansion in effective stimulation frequency range occurred at the higher end (lower cycle length).

Both the range expansion and the faster cutoff at smaller net size are reasonable in view of the actual nature of the altered k-value distribution (see figure 4.4 for a comparison of the k-values of the

two networks). The second network, i.e. that of figure 5.11, has lower k values near the external stimulator; this allows stimuli applied at a higher rate to be effective in producing propagated beats, but also means that a greater part of the conduction delay will occur further away from the stimulator, so that focal blocks will tend to develop further from the stimulator. Such blocks, being closer to the borders of the network, will be affected more quickly by reductions in network size.

The general behavior of this network (figure 5.11) seems sufficiently similar to that of the standard network (figures 5.8(b) and 5.10(b) to warrant the conclusion that the particular distribution of k values is not critical. However, in some experiments--most notably the strength-interval determination--the behavior of the whole network depends on the responses of just a few cells near the stimulator. Results of these experiments therefore differ considerably in detail when the distribution of k values is altered, although their general features, e.g., existence of no-response and multiple-response phenomena, remain similar (compare figures 4.2 and 4.3).

E. Effect of Network Homogeneity

The amount of inhomogeneity built into the model network is determined by the parameter k_σ, which specifies the maximum excursion of any k_i from the mean of the distribution, $\bar{k}$. (A uniform distribution was used in all experiments reported here.) Reducing k_σ thus forces the model cells to be more alike; when k_σ is made zero, they are all identical, each having a value of k equal to $\bar{k}$.

Figures 5.12 and 5.13 show the results of "scan" experiments on networks identical to that of figure 5.8(b), except that (i) the value

of k_σ was varied from 1.5 to 0.5, and (ii) the distance-biased stimulator was employed. In 5.13(a) and 5.13(b), the "scan" series was done on successively smaller networks, in order to gauge the interaction between size and homogeneity.

Comparing the 25 x 25 network (figure 5.12), it is evident that reducing k_σ did not reduce the range of stimulating frequencies over which persistent reentrant activity could be established, but did diminish the number of stimulus patterns that were effective. That is, reduced inhomogeneity made it "harder" to initiate persistent reentries, but not through any strong interaction with the frequency of stimulation; rather, the number of stimuli in the train had to be increased. (When k_σ was 0.5, the range of effective stimulus frequencies was shifted slightly, though not shortened.)

In the smaller networks, however, the effect of reducing inhomogeneity became much more pronounced. For example, a comparison of the two 21 x 21 or the two 19 x 19 networks (figure 5.13) shows that the initiation of reentrant activity was not much different in one net than in the other, but that there was quite a difference in persistence. The more homogeneous networks are, apparently, more likely to exhibit spontaneous termination of reentrant waves even though it is not more difficult to initiate such waves.

A few experiments were performed to see how changes in network homogeneity would affect a reentrant wave that had already been established. A priori, one might expect that uniformity and regularity in the wave pattern would be correlated with the homogeneity of the network, so that making the network completely uniform would regularize the wave while increasing the network inhomogeneity would produce a more irregular wave. The questions remain: Would such a regularized

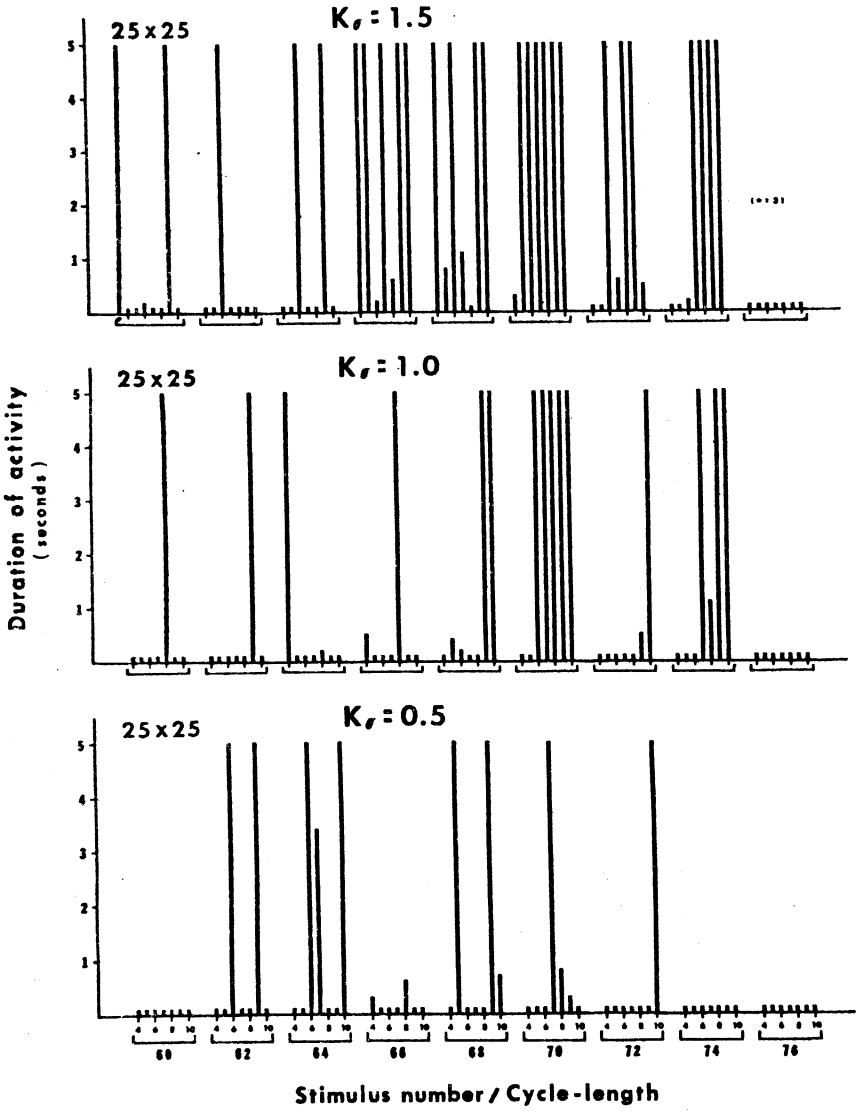

Figure 5.12. Persistence of Activity as a Function of Stimulus Number and Frequency.

Variation in Network Homogeneity. (Network N_4 of table 3.2.)

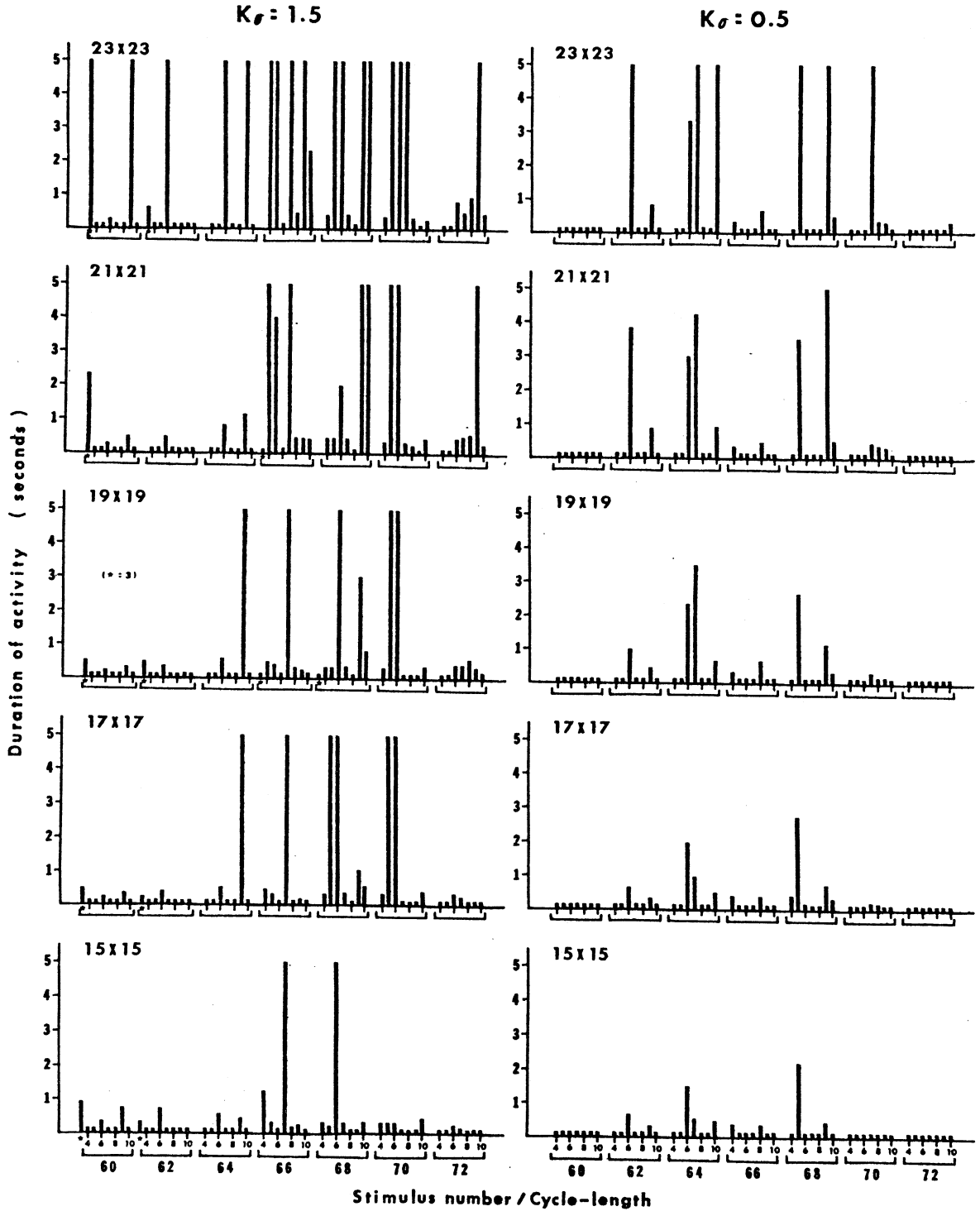

(a) (b)

Figure 5.13. Persistence of Activity as a Function of Stimulus Number and Frequency. Variation in network size, comparing the standard (network N_4 of table 3.2) with a more homogeneous network.

wave tend to become cyclic? Or does reentry somehow depend on variation in refractory period in such a way that a regularized wave would not persist? With respect to more inhomogeneous networks, should the single reentrant wave be expected to fragment into multiple wavelets,[10] perhaps repeatedly?

Network N_4 of figure 3.2 was subjected to a train of six stimuli at a cycle length of 72; the resulting wave pattern is known to persist indefinitely (figure 5.12). At time-step 1000, when the reentrant wave appeared to have become quite stable, the simulation was interrupted and the value of k_σ changed as described below.[11]

In the first experiment, k_σ was set to zero at time-step 1000, so that all k values became equal. (The dependence of ARP duration on firing rate was retained, however.) There was very little change in the appearance of the wave pattern: over several cycles, it became slightly more regular in outline, but still retained the same basic spiral shape. Reentry continued in exactly the same pattern as previously. The simulation was allowed to run until time-step 5000, at which time the reentrant wave was still quite stable, but not cyclic. There was a downward trend in the variance of activation intervals (recall that a wave becomes cyclic when that variance reaches zero, i.e. when all the cells are firing at the same frequency), but complete

[10] The ability to produce a continuous CRT display of the state of the model network, which was described in Chapter III as being of general utility during simulation runs, was particularly useful in experiments such as these where one is mainly asking qualitative questions about wave patterns, i.e. "what does it look like?"

[11] As with changes in $\bar{k}$, such alterations in k_σ were reflected in different refractory period durations following the next passage of the wave over the network.

synchrony was far from imminent. Curiously, at time-step 5000 in the control experiment, with k_σ equal to 1.5, the wave was much more nearly cyclic, in the sense that the variance of its activation intervals was smaller by a factor of 35. Other statistics showed only slight differences: conduction delay per cell was about the same, but with less variance in the homogeneous network; safety factor of conduction was somewhat higher in the inhomogeneous network, but its variance was about the same in both cases. Altogether, removing the network inhomogeneity seems to have made little difference in the behavior of an established wave.

In the second experiment, k_σ was raised to 2.0 at time-step 1000, and then to 2.5, 3.0, 3.5, and 4.0 at time-steps 1300, 1800, 2100, and 2500 respectively. After each change the reentry wave became more irregular in outline, but did not fragment into multiple wavelets. Reentry nearly failed after k_σ was raised to 3.5, due to a chance formation of a barrier by a group of cells with long refractory periods; subsequent reentries remained somewhat tenuous. Shortly after k_σ was set to 4.0, reentry did in fact fail; activity in the network ceased at time-step 2647. (Such large values of k_σ are undoubtedly rather unphysiological; see Alessi, et al. (1958).)

Not surprisingly, raising the variance in refractory periods also increased the variance of the measured statistics (activation interval, conduction delay, safety factor). Perhaps more significantly, the mean values of the activation interval and the safety factor also rose, suggesting that (as actually observed on the screen) the activity wave was slowed by refractory patches but raced through the well-recovered regions in between. However, it is difficult to say exactly why the

reentry ultimately failed; a conduction pathway simply did not develop adequately at one point when the activity wave happened to be in a precarious position.

F. Reentry after a Single Premature Stimulus

Since the "scan" experiments described above indicate that reducing $\bar{k}$ and/or increasing k_σ make the networks more vulnerable to reentry following fixed-rate stimulation, a brief experiment was done to see whether those two parameters would affect the occurrence of extra beats after a single premature stimulus. The result is shown in table 5.4. Ordinarily, a single premature stimulus (designated "P_1") does not cause reentry.[12] But if the absolute refractory period duration is shortened sufficiently, or if a lesser shortening of the ARP is coupled with an increase in network inhomogeneity, then a properly-timed P_1 may produce several or many extra beats.[13]

G. Effect of Distance-Biased Stimulator

The "scan" experiments described in sections A through D were all run using the radius-1 stimulator, i.e. only the seven central cells were subjected to external stimulation. However, in the course of these and other experiments, it became apparent that the radius-n stimulator[14] (also called the "distance-biased" stimulator, because of the inverse-

[12] Depending on the strength of the stimulus; see figures 4.2 and 4.3.

[13] Curiously, it is not the earliest-possible P_1's that lead to reentry, but rather those that are timed somewhat later.

[14] n=12 in 25 x 25 nets; n=25 in 51 x 51 networks.

Table 5.4. Effect of ARP Duration and Network Homogeneity on Reentry after a Single Premature Stimulus.

$\bar{k}$	k_σ	P_1 Timing	No. of Beats
7.0	1.5	< 99	0
		$\geq$ 99	1
7.0	2.5	< 94	0
		$\geq$ 94	1
6.0	1.5	< 85	0
		$\geq$ 85	1
6.0	2.5	< 79	0
		79 - 93	1
		94,95	> 10
		> 95	1
5.0	1.5	< 70	0
		70 - 73	1
		74	3
		75	> 10
		> 75	1

(25 x 25 network, drive stimulus cycle length 200, stimulation strength 200.)

square law relating stimulus intensity to distance from the stimulator) was more realistic. Particularly for the experiments involving variation in network homogeneity, it seemed desirable to change the "scan" protocol to use the radius-n stimulator even though a new control series had to be performed. As a by-product, we obtain a good comparison between the radius-1 and radius-n stimulators.

Figures 5.12 and 5.13(a) show the results of a series of "scan" experiments on network N_4 of table 3.2, in which the size of the network was varied from 25 x 25 to 15 x 15. Comparison of these figures with figures 5.8(b) and 5.10(b) shows the difference between the two stimulation modes: the distance-biased stimulator was uniformly more effective than the radius-1 stimulator, particularly at shorter cycle lengths. It consistently elicited more persistent reentries over a wider range of stimulation frequencies, at all sizes of network. Although not shown in these graphs, the distance-biased stimulator was also the more effective at higher values of $\overline{k}$.

III. Effect of Factors Related to Conduction Delay and to the Safety Factor of Conduction

As described in Chapter III, conduction delay in the model is primarily determined by a cell's degree of refractoriness at the time it receives an adequate stimulus. Refractoriness is measured by the ratio of the cell's present threshold to the minimum threshold, that is,

$$\text{refractoriness} = r = \frac{\theta}{\theta_{min}} \qquad 1 < r < \theta_{max}/\theta_{min}$$

The safety factor of conduction is defined as the ratio of stimulus to threshold,

$$\text{safety factor} = s = \frac{\Lambda}{\theta}$$

By definition, the cell fires if and only if the safety factor is at least 1. Expressing conduction delay in terms of refractoriness and safety factor, then, we have

$$\tau_S = F_1 r + F_2/s + F_3$$

Parameters which the experimenter can manipulate are: the F's, which directly affect conduction delay; λ_{max}, θ_{max}, and θ_{min}, which directly affect the safety factor[15]; and the duration of the relatively refractory period, τ_R, which affects both conduction delay and safety factor, indirectly.

Experiments concerning these parameters have been aimed mainly at investigating their effects on both the persistence and the conduction patterns of established circus waves. Tests of their effects on the initiation of reentries, using the "scan" protocol described in the previous section, have not been done. Consequently, the discussion of these results will be mainly qualitative. We are interested in the ranges of these parameters that are compatible with self-sustaining activity, and would like to know whether any of them are related to the fragmentation of a circus wave into the multiple wavelets that previous investigators have described or hypothesized as the basis of fibrillation.

[15] λ_{max} is the maximum value of the local response; see Chapter III.

The basic procedure followed in these experiments was to establish a persistent circus wave by using a stimulation sequence of known effectiveness, and then to vary the parameter of interest, observing the result both on the CRT display and in the network statistics.

Since the conduction delay is computed only when a cell fires, a change in the delay coefficients (F_1,F_2,F_3) does not affect all the cells immediately, but rather spreads over the network along with the next passage of an activity wave (the same being true of the ARP duration factors, $\bar{k}$ and k_σ). The other parameters of interest here--λ_{max}, θ_{max}, θ_{min}, and τ_R--are all involved in expressions that are computed every time-step; hence, any change in them has immediate effect throughout the network.

A. The Duration of the Relative Refractory Period, τ_R

1. Shortening the Relative Refractory Period

A stable reentry wave was established by applying six stimuli at a cycle length of 72 to the 25 x 25 network N_4 of table 3.2. The wave pattern that developed consisted of a relatively symmetric pair of spiral waves reentering at a common focal block.

At time-step 1000, τ_R was reduced from 40 to 35. The activity wave appeared to speed up slightly in response to the quickened recovery of excitatability, then stabilized again. Further reductions in τ_R, in steps of 5, produced the same result.

When τ_R reached the value 10, however, the wavefront became very ragged and the reentry pattern changed, leading to multiple reentries and considerable fragmentation into separate wavelets. At $\tau_R = 5$, there was even more fragmentation; activity waves could be observed

dividing, colliding, and coalescing in all parts of the network (figure 5.14). At $\tau_R = 1$, extreme fragmentation occurred; no distinct wavefronts were visible, the activity was completely chaotic. It appeared that this activity pattern would persist indefinitely, since no trend towards organization was discernible. Simultaneous stimulation of the entire network might have caused it to revert, but that capability was not built into the simulation programs; stimulation at any point would obviously have had little effect.

The statistics collected during this experiment (table 5.5(a)) did not show marked changes, but instead drifted slowly as τ_R was reduced. The mean and variance of the safety factor rose somewhat; the average delay per cell declined slightly, while its variance increased; and the mean activation interval fell substantially as the total refractory period shortened. The major exception was the variance of the activation interval, which fluctuated noticeably, then increased at the short values of τ_R.

2) Lengthening the Relative Refractory Period

A persistent circus rhythm was established by using the same procedure as in section (1). Starting at time-step 1000, τ_R was raised in increments of 5 every 300 time-steps.

The activity pattern changed only gradually. The wave's conduction velocity slowed somewhat, and the wavefront become more uniform. The active segment of the advancing wave (the layer of cells in the firing state) grew thinner, a consequence of the slowed conduction. The spiral pattern became larger (less tightly coiled), and its focus

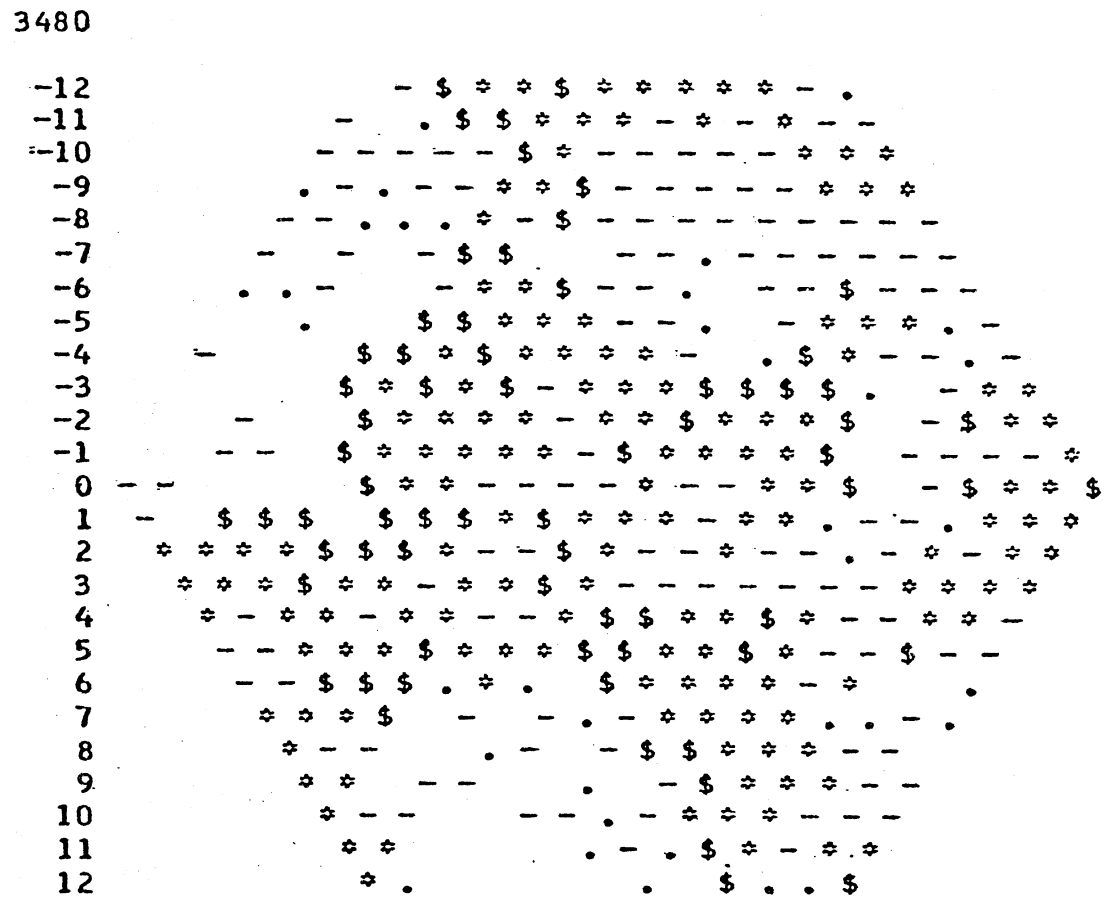

Figure 5.14. Typical Pattern of Reentrant Activity when the RRP is very short.

(Network N_4 of table 3.2; τ_R has been gradually reduced to 5.)

Legend: $ = stimulated
* = firing
- = absolutely refractory
· = relatively refractory
blank = quiescent

Table 5.5. Effect of Shortened RRP - Statistical Summary

(a) Changing τ_R			(b) Changing τ_R with τ_A compensation		
τ_R	Statistic	Mean (std. dev.)	$\tau_R(\Delta\tau_A)$	Statistic	Mean (std. dev.)
40	A.I.	80 (7.5)	40 (0)	A.I.	80 (7.5)
	δ	5.0 (1.6)		δ	5.0 (1.6)
	s	1.7 (0.8)		s	1.7 (0.8)
35	A.I.	77 (6)	35 (5)	A.I.	85 (4.5)
t=1000	δ	5.0 (1.6)	t=1000)	δ	5.0 (1.6)
	s	1.8 (0.8)		s	1.8 (0.8)
30	A.I.	70 (2.5)	30 (10)	A.I.	86 (6)
t=1300	δ	5.0 (1.7)	t=1300)	δ	5.3 (1.8)
	s	1.8 (0.8)		s	1.8 (0.8)
25	A.I.	65 (3)	25 (15)	A.I.	92 (6)
t=1600	δ	5.0 (1.9)	t=1600	δ	4.6 (1.9)
	s	1.9 (0.8)		s	2.2 (1.0)
20	A.I.	60 (3.5)	20 (20)	A.I.	95 (9)
t=2100	δ	5.0 (2.2)	t=2100	δ	4.9 (2.3)
	s	1.9 (0.9)		s	2.1 (1.0)
15	A.I.	57 (5)	15 (25)	A.I.	99 (20.5)
t=2400	δ	4.7 (2.3)	t=2700	δ	4.8 (2.4)
	s	2.1 (1.0)		s	2.2 (1.0)
10	A.I.	55 (9)	10 (30)	A.I.	105 (23)
t=2700	δ	4.5 (2.3)	t=3600	δ	4.5 (2.4)
	s	2.4 (1.2)		s	2.4 (1.1)
5	A.I.	48 (11)	5 (35)	A.I.	105 (24)
t=3300	δ	4.6 (2.4)	t=3900	δ	4.0 (2.0)
	s	2.3 (1.3)		s	2.6 (1.4)
1	A.I.	38 (13)			
t=3600	δ	4.5 (2.9)	(activity ceased spontaneously)		
	s	2.4 (1.1)	at time 4743		

A.I. = Activation Interval (inter-stimulus interval)
δ = delay per cell
s = safety factor of conduction

--the center around which the actual reentry seemed to be occurring--grew in diameter.

At time-step 2200, τ_R was increased from 60 to 70, and at time-step 2500, from 70 to 80. The conduction pattern continued its gradual shift; the wave remained slow and stable.

The network statistics were consistent with the changes observed grossly: the average activation interval increased, from about 85 to 109; the safety factor dropped slightly, from 1.8 to 1.5; and the delay per cell rose, from 5.0 to 5.9.

3) Initiation of Reentry when RRP is Short

In view of the disorganization of an established reentry wave wrought by the shortened relative refractory period in (1), a brief experiment was performed to see whether a reentry wave could be initiated under those same conditions. Network N_4 of table 3.2, with τ_R set equal to 1, was stimulated three times at cycle length of 34. (The shortened total refractory period made this high stimulation rate necessary. The short RRP left a very small "window" for premature beats: stimuli arriving slightly early met totally refractory cells; those slightly late, fully recovered ones.)

The first wave propagated normally. The second was irregular, but did not lead to reentry. The third was conducted very erratically, continually meeting refractory barriers left by the second wave. The wavefront disintegrated, becoming a collection of wavelets that spread irregularly over the network. The pattern became progressively more disorganized, soon resembling the chaotic activity described above in

section (1). In fact, the two cases were indistinguishable by either appearance or statistics.

At time-step 300, and about every 300 time-steps thereafter, τ_R was increased while the network's pattern of activity was monitored on the CRT display. The first increment $\tau_R = 5$, made little difference. At $\tau_R = 10$, the number of distinct wavelets decreased noticeably, through coalescence. When τ_R was raised to 15, reentry nearly failed completely; the activity collapsed into a single wave, which alternately broke into several waves and recombined again. Because of its variability, this case was allowed to run for 600 time-steps, during which time it seemed to stabilize with several distinct waves active simultaneously. As τ_R was increased further, in the range 20 to 40, the wavefront became smoother and the wave appeared to grow more stable, resembling ever more the "control" pattern established by external stimulation in (1) above.

The disorganization produced by drastically shortening the relative refractory period, then, was completely reversible. One could establish a persistent reentrant wave and convert it into chaotic activity, or initiate chaotic activity and convert it back into a stable reentrant pattern.

This reversal was reflected in the network statistics, which all returned to normal values (for reentrant waves), as though the time axis had simply been reversed. As τ_R was increased from 1 to its control value of 40, the average activation interval rose from 39 to 80. The safety factor declined slightly, from 2.4 to 1.7, and the delay per cell increased from 4.3 to 5.2, both moving somewhat erratically.

4) Shortening the RRP with "ARP Compensation"

In the previous experiments, shortening the relative refractory period also shortened the total refractory period, allowing the cells to fire at at a greater rate--which they did, as indicated by the shorter average activation intervals. It was thus not clear how much of the observed behavior to attribute to the lessened RRP, and how much to that combined with the shorter overall cycle length. Consequently, an experiment similar to that of section (1) was performed, except that each reduction in τ_R was matched by an equal increase in the duration of the absolute refractory period, τ_A. This permitted the relative refractory period duration to be decreased without shortening the overall length of an activity cycle.

A stable reentrant wave was established using the same procedure as in section (1). Starting at time-step 1000, τ_R was decreased (and τ_A increased) in steps of 5. With each increment, the wave became somewhat less stable, especially in comparison with its counterpart from section (1). The reentry path became rather tenuous, although a second reentry path appeared sporadically. The total conduction pathway of the circus wave grew longer. When τ_R had been reduced to 25, the wavefront began fragmenting into separate segments. This process continued as τ_R decreased, but there was little formation of truly separate wavelets: the wave fragments were seldom able to reenter on their own, because of the long ARP's. Hence the single main reentry wave continued to dominate the network, although its path varied considerably from cycle to cycle. The "RRP gap" between the absolutely refractory cells of one wave and the advancing front of the next wave thinned noticeably, as one would expect.

With τ_R reduced to 5, there was considerable fragmentation of the wavefront (though much less than the corresponding case from section (1), without the extended ARP), but still no persisting secondary reentries. Suddenly, the main circus wave failed to reenter, and activity in the network died out. No unusual event preceded this conduction failure; the reentry wave had been precarious all along, and seemed to fail at this time simply by chance.

The network statistics from this experiment (table 5.5(b)) were roughly the same as in the experiment of section (1), except that the average activation interval rose, instead of falling, as a result of the lengthened ARP's. Also, the variance of the activation interval fluctuated much more than in the earlier experiment.

A similar experiment was performed using the 51 x 51 network (N_7 of table 3.2) of Program C. (The reentrant wave was established by applying five stimuli at a cycle length of 84.) The network statistics from this run are shown in figure 5.15. As in the previous experiment, the only marked change is the substantial, erratic increase in the variance of the activation interval. The wave fragmentation patterns were similar to those of the 25 x 25 network.

B. The Threshold of Excitation, θ

As described in Chapter III, a cell's threshold during the relative refractory period falls linearly from a maximum value, θ_{max}, to minimum value, θ_{min}, where it remains for the duration of the quiescent state. The control values of these parameters, in arbitrary units, are 100 for θ_{max}, 25 for θ_{min}. Reducing θ_{max} after a reentrant wave

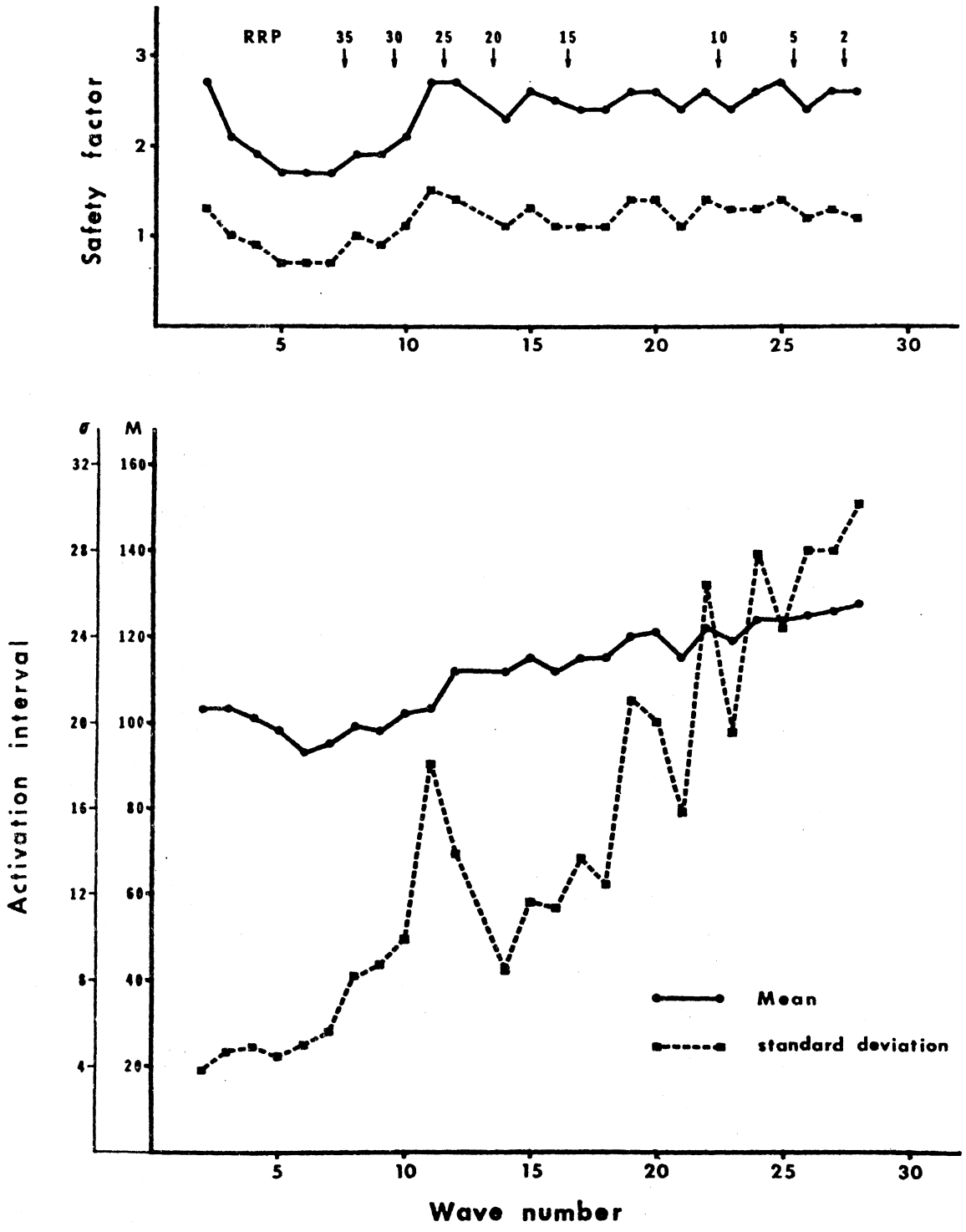

Figure 5.15. Effect of Shortened RRP on Network Statistics.

had been established produced effects similar to those resulting from a shortened relative refractory period, described above. But neither increasing θ_{max} nor changing θ_{min} seemed to have much effect on the reentrant wave.

1) Decreasing the Maximum Threshold, θ_{max}

Persistent reentrant activity was established using the procedure of section A(1). At time-step 1000, θ_{max} was reduced to 75. The activity wave's spiral pattern became tighter. (This was reflected in the network statistics as a shortening of the activation interval without a reduction in the delay per cell: hence, average path length must have shortened.)

At time-step 1300, θ_{max} was set to 50. The spiral pattern became still tighter, as the advancing wavefront penetrated noticeably further into the RRP region of the "preceding" wave (it is, of course, really all the same wave). The wavefront became ragged, and developed gaps where it approached too closely to areas still in the ARP. Conduction became tenuous at times, and it appeared that activity might cease spontaneously, so this case was allowed to run for 600 time-steps. Subsequently, further fragmentation occurred, forming a number of smaller wavelets, each with a relatively well-defined wavefront.

Decreasing θ_{max} to 37.5, at time-step 1900, led to very fragmented activity with indistinct wavefronts. The network resembled that described in section A(1) when the RRP duration was very short. At time-step 2200, θ_{max} was set to 25, the same value as θ_{min}. This effectively abolished the relative refractory period altogether, and had the expected effect on the network: activity became completely

chaotic. Distinct waves were not visible, activity consisting instead of small, irregular, ever-changing patches. Most of the cells were in the stimulated, firing, or absolutely refractory states nearly all the time. This disorganized state nevertheless appeared quite stable, and it was evident that external stimulation at any single point would have little effect.

From gross observation, then, reducing θ_{max} and reducing τ_R produced similar results. Network statistics from the two series were also rather similar (tables 5.5(a) and 5.6(a)), except that in the θ_{max} case the final chaotic state was associated with a marked jump in safety factor and fall in delay per cell, while in the τ_R case those statistics showed no change. Also, the variance of the delay was much higher in the τ_R series. It is clear that these statistics, derived from the individual cells, are not good measures of the activity state of the whole network.

It is also evident that the development of chaotic activity was not influenced by the slope of the threshold function, since decreasing θ_{max} reduced the slope to zero while decreasing τ_R increased it forty-fold.

2) Increasing the Maximum Threshold, θ_{max}

A persistent reentrant wave was established using the procedure described in (1). At time-step 1000, θ_{max} was increased to 125; one more reentry occurred, but on the second cycle conduction failed, and activity ceased at time-step 1122. From observation of the network display, it seemed likely that the conduction failure had been caused by increasing the threshold at a particularly unlucky time, when con-

Table 5.6. Effect of Threshold Variation--Statistical Summary

(a) θ_{max}	Activation Interval		Delay Per Cell		Safety Factor		Time-Step
	μ	(σ)	μ	(σ)	μ	(σ)	
250	98	(9.0)	5.0	(2.7)	2.2	(1.0)	2500
200	93	(6.8)	5.4	(2.5)	1.9	(0.9)	2200
175	92	(5.0)	5.2	(2.4)	2.0	(0.9)	1900
150	91	(5.4)	4.8	(1.9)	2.0	(0.9)	1600
125	86	(5.8)	5.2	(1.8)	1.8	(0.7)	1300
100*	83	(7.5)	5.0	(1.5)	1.8	(0.7)	--
75	71	(3.6)	5.3	(0.9)	1.6	(0.5)	1000
50	46	(10)	5.0	(0.6)	1.7	(0.6)	1300
37.5	37	(11)	4.0	(0.4)	2.3	(1.0)	1900
25	35	(10)	2.6	(0.4)	4.0	(2.0)	2200

(b) θ_{min}	Activation Interval		Delay Per Cell		Safety Factor		Time-Step
	μ	(σ)	μ	(σ)	μ	(σ)	
50	82	(4.2)	3.9	(0.5)	1.6	(0.4)	1300
37.5	82	(5.3)	4.3	(0.8)	1.6	(0.5)	1000
25*	83	(7.5)	5.0	(1.5)	1.8	(0.7)	--
18.75	84	(5.2)	5.6	(2.1)	2.1	(1.1)	1000
12.5	85	(5.6)	6.7	(3.2)	2.4	(1.5)	1300

"Time-step" indicates the time at which the parameter change was made; the statistics are as of the end of the interval, i.e. just prior to the next parameter change.

* = control value

conduction of the reentrant wave was dependent on the firing of only a few cells. Since conduction failure under those circumstances is, in a sense, an artifact of the procedure[16], the experiment was re-run with the change in θ_{max} being made at time-step 1300, when the activity was in a less precarious condition. This time, the reentrant wave showed no indications of failure. The only noticeable change was that the spiral pattern seemed to become more regular and perhaps larger; however, nothing in the statistics (shown in table 5.6(a)) supports this qualitative impression.

Subsequently, θ_{max} was increased in stages up to 250; but the effect of these changes, as either observed in the activity pattern or measured in the network statistics, was unremarkable. At 250, θ_{max} was 2.5 times its control values and the slope of the threshold curve was elevated by a factor of three. We conclude that the established reentrant wave simply was not very sensitive to the slope or maximum of the threshold function.

3) Changing the Minimum Threshold, θ_{min}

A brief experiment was performed to determine whether the maintenance of reentrant activity was particularly dependent on the value of the resting threshold, θ_{min}. A persistent reentrant wave was established using the procedure of section (1). From its control value

[16] This problem of chance sensitivities is potentially present in many computer experiments. Probably its best resolution is through many repetitions of the experiment using "different preparations." We have often done this. In other cases, for practical reasons, we have simply tried to avoid making parameter changes at critical moments.

of 25, θ_{min} was decreased to 18.75 at time-step 1000, and to 12.5 at time-step 1300. At time-step 1600, the simulation was stopped and the network restored to its state as of time-step 1000 (effectively "backing up" to that time). θ_{min} was increased to 37.5, and at time-step 1300, to 50. The network statistics from this experiment are shown in table 5.6(b).

Reducing θ_{min} caused both the safety factor and the delay per cell to increase; increasing θ_{min} caused them both to decrease. The inverse relationship between the safety factor and the threshold might have been anticipated, just from the definition of the safety factor; but it seems perverse that the delay should vary in the same direction as the safety factor. The explanation lies in the expression for the conduction delay, whose most important term includes the ratio θ/θ_{min} as a measure of refractoriness.

Despite the variation in delay and safety factor, changing θ_{min} made very little difference in the average activation interval; nor was there much change in the observed activity pattern, except perhaps a larger spiral at $\theta_{min} = 50$. Altogether, the reentrant wave seemed not very sensitive to the value of θ_{min}.

C. The Local Response, λ

A cell's effectiveness as a stimulus to its neighbors is represented by its local response, which, though expressed only during the firing state, decays linearly during both the stimulated and firing states from its initial value, λ_{max}, to zero. By varying λ_{max}, one can alter the safety factor of conduction without directly affecting excitability or refractory period durations.

A persistent reentrant wave was established by stimulating network N_2 of table 3.2 eight times at a cycle length of 88. Simulation was continued (as part of another experiment) until time-step 13000, when the network's state was saved in a file. By that time the activity had become cyclic, with a period of 96. The general procedure for this experiment was to restore the network's state from the save-file, set λ_{max} as desired, and let the simulation run until either it reached time-step 15,500 or the activity ceased spontaneously, whichever came first; the procedure was repeated for each value of λ_{max} tested.

The effect of λ_{max} on the average activation interval is shown in figure 5.16. The control case, $\lambda_{max} = 75$, was obviously perfectly stable, being cyclic. Increasing λ_{max} to 100 caused the mean activation interval to oscillate about a value of approximately 88. Further increases in λ_{max} led to progressively shorter activation intervals and increasingly tighter spiral wave patterns, reaching an apparent minimum activation interval of 70 at a λ_{max} of 225 (three times the control value). For all values of λ_{max} above 100, the network became quite stable (although not cyclic) at the faster average firing rate.

Reducing λ_{max}, even by a factor of two, had very little effect on the activation interval, raising it only a few percent. But when λ_{max} was dropped to 25, at which a single cell was no longer capable of stimulating its neighbor[17] (thus making summation essential to the maintenance of conduction), a dramatic change occurred in the activity

[17] Because τ_S is never zero, a cell's local response, λ, is never as large as λ_{max}. Thus with λ_{max} and θ_{min} both at 25, $\lambda < \theta_{min}$.

Figure 5.16. Effect of Variation in the Strength of the Local Response. Alteration in the average inter-stimulus interval (activation interval) of well-established, persistent, reentrant activity.

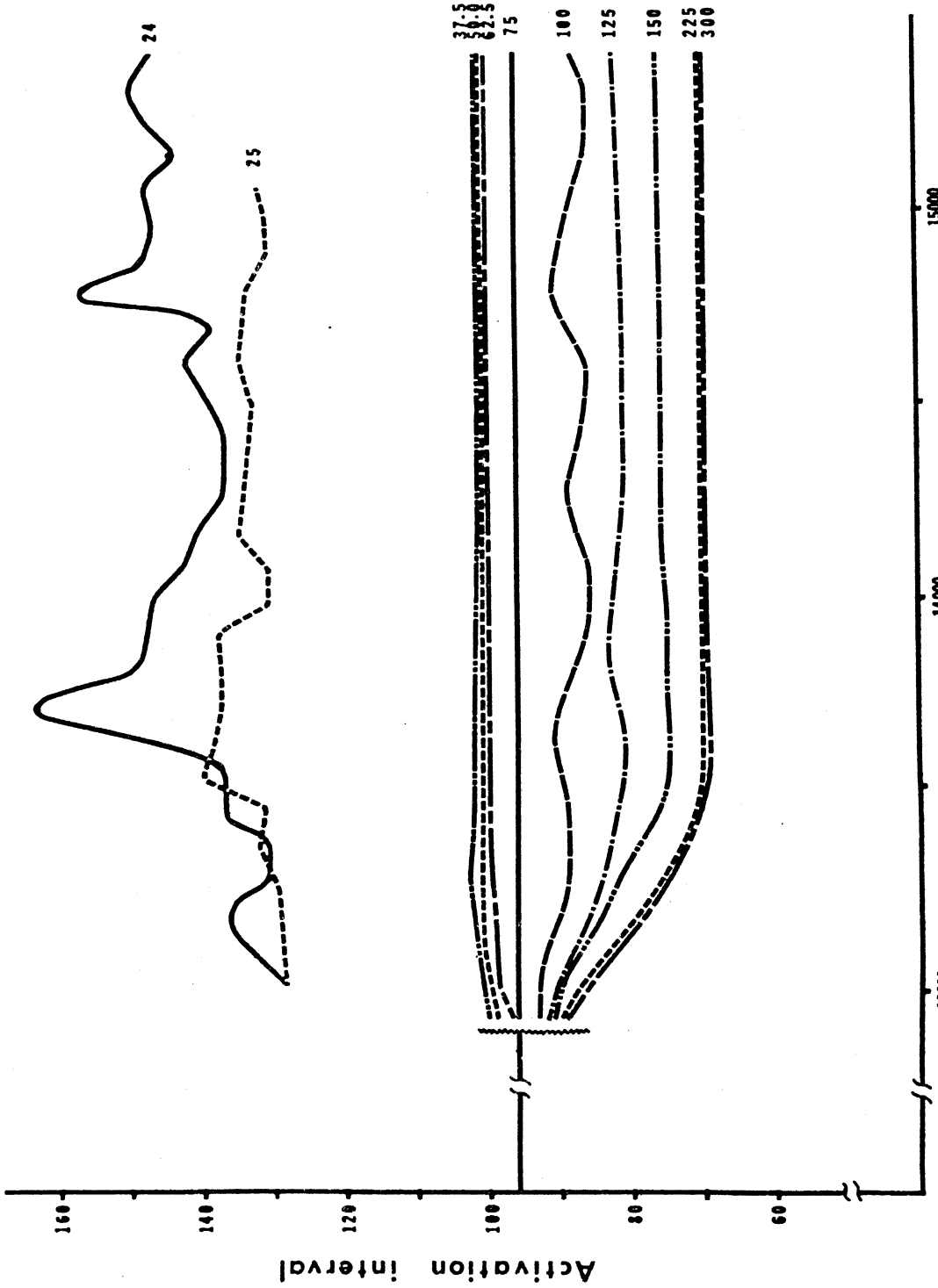
Activation interval
160
140
120
100
80
60
24
25
37·5
50·0
62·5
75
100
125
150
225
300
13000
14000
15000
Time-step

Figure 5.16

pattern. The average activation interval increased markedly and began fluctuating erratically, as the wave advanced slowly and symmetrically through fully recovered cells, never penetrating the relative refractory regions as it had formerly. After 2139 time-steps, activity suddenly ceased spontaneously.

At a λ_{max} of 24 the activity wave moved still more slowly, and showed wild fluctuations in the average activation interval; spontaneous activity persisted for the entire duration of the 2500 time-step test interval. Setting λ_{max} to 20 caused complete conduction failure, and activity stopped immediately.

The conduction of these two "low-strength" waves (λ_{max} = 24, 25), as displayed on the cathode-ray tube, reminded the author of the slow-moving waves that sometimes become visible in a dog's ventricle as the preparation degenerates during fibrillation. It is tempting to speculate about possible similarity of mechanism.

4) The Conduction Delay Coefficients, F_1, F_2, and F_3

These coefficients, which appear in the expression for the conduction delay, are purely creatures of the model; they do not correspond directly to any property of cardiac muscle. Consequently, the motivation for the following experiments was simply to determine, in a general way, the ranges of the coefficients compatible with reentrant activity, and to verify that conduction was not particularly sensitive to the F values.

Two experimental procedures were used. The first was identical to that described in section C, except that the F's were varied instead of λ_{max}; the results are shown in table 5.7(a). The second was as

described in section A(1), with the F's in place of τ_R; its results are shown in table 5.7(b). In both cases we were mainly concerned with the effect of the F values on short-term persistence.

The results can be summarized as follows:

i) F_1 in the range 0 to at least 5 is compatible with reentrant activity, although some spontaneous termination was seen at $F_1 = 0$ and $F_1 > 2.5$;

ii) F_2 in the range 0 to 3 appears to be compatible, although spontaneous termination was seen sometimes at $F_2 = 3$;

iii) Some minimum delay is necessary[18]--if both F_1 and F_2 are zero (when $F_3 = 0$), then spontaneous activity stops quickly. Also, the case of $F_1 = 0.5$ leads to termination if $F_2 = 0$.

iv) F_3 in the range 2 to at least 12 (when $F_1 = F_2 = 0$) is compatible with reentrant activity, though spontaneous termination sometimes occurs for $F_3 \geq 6$, depending capriciously on the timing of the change to F_3. The larger delays produced particularly stable-looking patterns.

Therefore, it seems reasonable to conclude that reentrant activity is not especially sensitive to the values of the F coefficients; that a constant delay per cell (i.e. independent of the cell's condition) is compatible with self-sustaining activity; that quite large delays per cell can be tolerated; and that very small delays lead to spontaneous termination of reentrant activity.

[18] In addition to the inherent delay of one time-step.

Table 5.7. Effect of Delay Coefficients on Short-Term Persistence of Reentrant Activity.

(a) Experimental procedure described in section C.

All cases start at time-step 13,000.

F_1	F_2	F_3	Mean Activation Interval	Persistence	
2	2	0	96	>2500	cyclic (control)
2	0	0	91	>2500	
2	0	1	90	>2500	
1.5	0	0	83	>2500	cyclic
1	0	0	73	>2500	
0.5	0	0	80- 68	470	
2.5	0	0	95	>2500	
3.0	0	0	98	>2500	
2	2	1	102	>2500	
2	2	2	106	1410	
2	1	0	93	>2500	
2	3	0	97	>2500	
0	0	2	74	>2500	
0	0	4	90	>2500	cyclic (18-cell path)
0	0	6	105	>2500	cyclic (15-cell path)
0	0	8	126	>2500	cyclic (14-cell path)
1.5	2	0	93	>2500	
1.0	2	0	84	>2500	
0.5	2	0	75	>2500	
0	2	0	69 - 87	436	
2.5	2	0	101	>2500	
3.0	2	0	99 - 121	2486	
0	0	0	-	57	

Table 5.7, cont'd. Effect of Delay Coefficients on Short-Term Persistence of Reentrant Activity.

(b) Experimental procedure described in section A(1). Cases were done in separate series. Each series started at time-step 1000, cases within series started at times shown.

Time-step	F_1	F_2	F_3	Persistence	
1000	2	2	0	>2000	(control)
1000	1.5	2	0	>2000	
3000	1.0	2	0	>2000	
5000	0.5	2	0	>2000	
7000	0.0	2	0	>2000	
1000	2.5	2	0	380	
1000	2	1.0	0	>2000	
3000	2	0.0	0	>2000	
1000	2	3.0	0	291	
1000	1.5	0	0	>2000	
3000	1.0	0	0	>2000	
5000	0.5	0	0	1427	
1000	2.5	0	0	>2000	
3000	3.0	0	0	>2000	
5000	3.5	0	0	>2000	
1000	2	2	1.0	299	
1000	0	0	2.0	>2000	cyclic, period 55
3000	0	0	4.0	>2000	cyclic, period 75
5000	0	0	6.0	1003	

IV. Miscellaneous Experiments

In the course of this study, several experiments were performed which are not properly categorized with any of those already described. For the most part, they constitute relatively brief explorations of various ideas, rather than more systematic studies of the effects of parameters. They are reported here because they demonstrate interesting properties of the model tissue or interesting kinds of simulation experiments.

A. Attempt to Abolish an Established Circus Wave by External Stimulation

A reentrant wave was established in the 25 x 25 network by means of the fixed-rate stimulation procedure. The activity pattern was known from previous experiments to be persistent; in fact, it eventually became cyclic. In this particular case, the spiral wave's focus happened to lie near the center of the network, which was also where the external stimulator was located.

While observing the network's activity pattern on the CRT display, the experimenter attempted to disrupt the reentrant wave by judicious application of external stimuli.[19] Several tactics were tried: to stimulate areas ahead of the reentering wave, so that the latter would find them refractory; to generate an additional activity wave that would interfere with the "real" reentry wave; to agument the reentrant wave, forcing it into poorly-recovered areas where conduction would fail. None of these worked; the circus wave persisted unperturbed.

The next attempt was continuous stimulation: an external stimulus

[19] Using the fixed-radius stimulator.

was applied on 150 consecutive time-steps, which easily spanned a full period of the rotating spiral wave. The reentry was essentially unaffected.

Apparently, the external stimulator's ineffectiveness was largely a result of its location near the focus of the reentrant wave: by the time the cells under the stimulator became excitable at all, the reentrant wave was nearly upon them. Consequently, external stimulation was not very different from stimulation by the reentry itself; hence, it had little effect. All it managed to do was to divert the reentrant wave slightly, making the focus more centered in the network. (As a result of this, the circus wave survived a more drastic trimming of the network's size than it had been able to withstand earlier, before the attempt to abolish it.)

In a similar experiment, the same reentrant wave was initiated, but was allowed to run until it had become cyclic; by that time, its focus had moved somewhat more toward one corner of the network. The external stimulator was then moved to the opposite corner of the network. While monitoring the activity on the display, the experimenter applied various patterns of external stimulation in an attempt to suppress the reentry focus.

The reentrant wave had a period of 96 time-steps. When external stimuli were applied at a faster rate (period 88), the external stimulator gradually took over a progressively larger portion of the network. That is, the point where activity from the reentry focus collided with activity initiated by the external stimulator, moved ever closer to the reentry focus. Eventually, the spiral pattern was completely disrupted; however, the phase differences between the cells at the

site of the former reentry focus were not abolished, for abortive reentries occurred there as each stimulated wave passed by. When the external stimulator was turned off, a successful reentry occurred, and soon the spiral pattern was fully re-established.

Then the experiment was re-run, except that at the point where the external stimulator had been turned off, its rate was simply slowed instead: the period was raised to 94 for a few stimuli, then to 98. The object was to see whether, having gained control of the network through high-rate stimulation, one could retain control while backing down to a more moderate rate. But as the stimulation rate dropped, the reentry waves grew larger, pacing a progressively greater fraction of the network. Eventually, the reentry focus completely dominated the external stimulator.

B. Repolarization-Phase Stimulation

It has been observed that a single premature stimulus is much more likely to initiate fibrillation in "sick" cardiac tissue than in healthy. In a discussion of mechanisms that might account for this, it was suggested that local inhomogeneities in recovery time might lead to electrotonic current flow between repolarized cells and those still depolarized, and that the net effect of these currents might be excitatory. Presumably, then, their degree of excitatoriness would depend on the amount of inhomogeneity in recovery time, which one might expect to be larger on premature beats in poorly-conducting tissue. Thus, such beats could trigger "dynamic ectopic foci" which would generate additional premature beats, more ectopic foci, and so on in a self-sustaining pattern.

As a preliminary test of the dynamics involved in this hypothetical mechanism, the simulation program was modified so that whenever a cell entered the relative refractory state, the difference in recovery times between it and each of its better-recovered neighbors was added together. That is, at the time the i'th cell entered the RRP, the following sum was computed:

$$\sum_{j \in N_i} q_j \cdot \min[(t_{R_i} - t_{R_j}), \tau_R]$$

where t_{R_i} is the time the i'th cell enters RRP,

τ_R is the duration of the RRP,

N_i is the index set of the neighbors of cell i,

and q_j is 1 if cell j is in states R or Q, 0 otherwise.

This sum provides a measure of the extent to which a cell's recovery state differs from its neighbors'; it was multiplied by a scale factor, r, and added to Λ_i, the total stimulation being received by cell i. Appropriate values for r were determined by trial. It is clear that by making r large enough, ectopic foci can be produced; it is less clear that they can be made to arise only after premature beats, and that they will then be self-sustaining.

Various combinations of stimulus timing and r values were tried in an effort to induce "fibrillation" through the above mechanism. The tests were certainly not exhaustive, but some general conclusions seem warranted:

(a) The shortened absolute refractory periods after a premature beat (the result of the effectively shortened cycle length) swamped out the effects of inhomogeneities resulting from differences in conduction.

That is, the absolute differences in recovery times following a single premature beat were less, not greater, than after a normal beat.

(b) If the program is altered to remove the dependence of ARP duration on cycle length (but still retain the random variation from cell to cell), then a premature stimulus can induce one or more ectopic foci and, consequently, an extra beat--but only one. The extra beat is conducted so slowly, at first, that the requisite inhomogeneity for a second extra beat doesn't develop.

(c) This mechanism did lead to a sort of bigeminy at slow stimulation rates, where the long refractory periods produced relatively large absolute differences in recovery times, even though there was little or no inhomogeneity in conduction. However, whenever an extra beat was generated by an ectopic focus, the next regular beat followed an effectively shorter cycle; hence the refractory periods were shorter, recovery times were more uniform, and ectopic foci did not arise. Thus, every alternate stimulated beat was followed by an "extrasystole."

If this experiment were continued, it would be interesting to see whether increased inhomogeneity of refractory period durations would enhance the formation of ectopic foci in the absence of the dependence of ARP duration on cycle length.

In another experiment, cells in a strip along the edge of the network were assigned various patterns of abnormally high k values in an attempt to establish, via the long refractory periods, a very slow-conducting reentry path, to see whether this would produce a bigeminy rhythm that would be abolished by an increase in the rate of external stimulation. As far as it was carried, the experiment was

unsuccessful, because the dependence of refractory period duration on cycle length made it difficult--if not impossible--to obtain the proper combinations of conduction block, conduction delay, and recovery of excitability. This experiment thus demonstrates a shortcoming of the present model: the uniformity of the cells in every respect except k value (ARP duration). It would have been desirable to be able to introduce differences in, say, conduction velocity that were not dependent on recovery state.

Chapter VI

DISCUSSION

The results of the simulation experiments described in the preceding sections can be classified broadly into three categories:

(i) Essential behavior--that which we felt the model must demonstrate in order to be adequate for the kinds of experiments we wished to perform;

(ii) Expected behavior--desirable properties, which ought to be present if indeed the model is a good one;

(iii) Unexpected behavior--seen with surprise in the model, but either analogous to known properties of the heart, or interesting phenomena suggestive of possible mechanisms in real cardiac tissue.

In this section, the principal simulation results are summarized according to these categories.

A. Essential Behavior

At the most basic level, it is necessary that those properties defined into the model cells be reasonably reflected in the behavior of the network as a whole. Particularly in the strength-interval experiments, it is evident that the network is capable of cell-to-cell conduction of activity; that following each beat there is an absolute refractory period, during which it is impossible to evoke a conducted response regardless of the strength of the stimulus; and that this is followed by a relative refractory period, during which a beat can

be evoked only by a greater-than-normal stimulus. The network's threshold of excitation declines continuously during the relative refractory period; also, beats evoked during this period are conducted more slowly and more erratically than normal beats. All of these characteristics are direct, anticipated consequences of the neighborhood relation and transition function, and so, may be considered to be "built in" properties of the network.

It is less predictable that sequences of premature stimuli should produce sufficient variation in conduction of the activity waves along different paths in the network that temporary conduction blocks would develop in some regions but not in others. But if such blocks could not arise, then it is difficult to see how self-sustaining activity could be initiated by patterns of stimulation analogous to those known to induce fibrillation in the heart. (Actually, self-sustaining activity might easily arise as a result of intrinsic automaticity of the tissue, or through continuous conduction around a fixed "anatomical" barrier. These mechanisms have been deliberately omitted from the model, not in the belief that they are never the cause of atrial fibrillation, but because their definition in the model would have to be rather arbitrary; the simulation experiments would be much less useful if they focused on a property that was built into the model, arbitrarily, beforehand.)

Conduction blocks are important because they lead to gaps in an active wavefront, through which reentry of excitation can occur. The reentrant wave itself has a gap, at approximately its point of origin, thereby making a subsequent reentry likely. Through this form of continuous conduction, activity may sustain itself in the network indefinitely.

That self-sustaining activity can arise in this network, in response to abnormal patterns of stimulation, without changes in the properties of the individual cells, and that this activity takes the form of a wave circulating around a purely dynamical obstacle (no anatomical pathway), is an early but important result of this study. We classify it as "essential behavior", however, because it forms the basis of most of the subsequent experiments.

B. Expected Behavior

In the model, the conduction of premature beats (those arising from a stimulus applied to cells that are relatively refractory) varies greatly, depending primarily on the degree of prematurity of the stimulus. Generally speaking, premature beats are conducted more slowly than normal beats, with the greatest propagation delays occurring near the site of external stimulation. One would expect the premature wave to gain speed as it moved away from the stimulator, because the trailing edge of the previous beat (a sort of "recovery wave") propagates at the same speed as that beat, so the premature wave should find increasingly better-recovered tissue in its path. Indeed, this is what was observed in simulation experiments, but the results were somewhat dependent on the degree of homogeneity in the network: in the completely homogeneous networks, the velocity of premature waves increased smoothly with their distance from the external stimulator; but in the normal, rather inhomogeneous case, the premature wave's velocity often remained depressed over a considerably larger portion of its path.

When a series of premature beats is evoked by a train of rapid stimuli, propagation delays accumulate from one wave to the next. That

is, each wave travels at reduced velocity for a greater distance than its predecessor did; eventually, however, a wave's velocity must increase to normal (in the model, the edge of the network is often reached before this occurs.) If a premature wave encounters a conduction block, its velocity may be very markedly reduced over a substantial portion of its path, or it may appear to have a negative conduction velocity, at certain points on the path of measurement, as a result of crossing the latter sideways instead of propagating radially as usual.

The slowed conduction experienced by a premature beat applies not only to its leading edge, or active wavefront, but also to its trailing edge, or recovery wave. Thus, if a normal beat follows a series of beats that were all quite premature, it is possible for activity from the normal wave to overtake the last of the premature waves and encounter delayed conduction at some distance from the site of original stimulation.

In addition to being more irregular, a premature wave is also thinner than a normal one--that is, the distance between its leading and trailing edges is reduced. (This is true in spite of the fact that both the leading and the trailing edges are slowed equally, which might at first seem to imply that the distance between them should remain the same.) Even if all phases of the cells' activity cycles were of normal duration, a premature wave would be thinner simply because the wavefront does not advance as far during a given interval of time as it would normally. But in addition, the durations of both the firing state and the absolute refractory period are reduced on premature beats--the former because slowed conduction implies a larger fraction of time spent in the stimulated (delay) state, the latter

because of its dependency on cycle length. The combination of these two factors can lead to a marked difference in thickness between normal and premature waves. (In a typical simulation experiment, a normal wave will reach the edges of the network while the center--where the stimulator is--is still early in the absolute refractory period; subsequently, the entire network will become absolutely refractory for a while, and then the recovery process will begin, irregularly, starting near the center and progressing outward. In a premature wave, on the other hand, the entire distance from the active wavefront to the trailing relative refractory period may span only a few cells, and the spatial pattern may be quite irregular.) Their thinness and variability makes premature waves susceptible to conduction failure and the development of gaps in the wavefront, which is a prelude to reentry.

Erratic and failing conduction (which is usually much more pronounced on second and third premature beats than on first) develops simultaneously at multiple sites in most cases, depending both on the distribution of k values and on the local history. Self-sustaining activity often begins with several independent reentrant foci, but it is unusual for more than one of them to persist, at least in the smaller (25 x 25) networks. Multiple, seemingly independent waves have occasionally been observed, however; they seem to be more likely in the larger networks.

Stimulation very early in the relative refractory period may result in the firing of a few cells (a "local response") without producing a propagated beat, since a poorly-recovered cell may, when stimulated, respond too weakly to stimulate a neighbor. Thus, the

effective refractory period of the network is, in general, larger than the absolute refractory periods of the cells under the stimulator. Also, conduction during the early relative refractory period often depends on spatial and temporal summation.

Varying the values of the model's parameters affected reentrant activity in reasonable ways. It is more easily produced in larger networks than in smaller ones, and it is favored by shorter refractory periods (lower $\overline{k}$) and by increased inhomogeneity (higher k_σ); these effects do not seem to depend very much on the specific distribution of k values among the cells. Inhomogeneity is necessary for the initiation of self-sustaining activity, but not for its maintenance. Once self-sustaining activity has been established, moderate changes in the other parameters (duration of relative refractory period, values of threshold and local response, and delay factors) have relatively little effect. Finally, the initiation of reentrant activity does not depend very critically on either the timing or the pattern of the external stimulation.

C. Unexpected Behavior

It is possible to construct a strength-interval diagram for the model, as for real tissue, by plotting its response to stimulation as a function of the stimulus' strength (on the ordinate) and timing (on the abscissa). When this is done, the model's curve has many characteristics in common with those obtained from cardiac tissue: the threshold rises steadily as the stimulus is advanced earlier into the relative refractory period, then increases abruptly in the very early RRP; there is a no-response phenomenon, whereby a strong

stimulus is sometimes ineffective while a weaker one, timed the same, produces a conducted response; there is a multiple-response phenomenon, in which a single super-threshold stimulus results in two or more conducted beats; and there is a vulnerable period, during which a single strong stimulus may initiate self-sustaining activity that persists indefinitely. One of the more noticeable differences, in this area, between the model and real tissue is that the model's threshold, after increasing abruptly, does not rise very far before cutting off completely, while the cardiac tissue's threshold can usually be measured at quite high values before becoming effectively infinite. However, this high-threshold property does appear in the model when the positions of the driving and testing "electrodes" are separated by a small distance. Also, in these experiments, the use of a distance-biased stimulator produced more realistic results.

In studying the conduction of premature beats in the model, the choice of measurement sites often affected the results. Very high (or even negative) conduction velocities were sometimes observed; these were found to be the result of conduction blocks that diverted activity waves from their normal directions of propagation, so that instead of sweeping along the paths on which conduction was being measured, they crossed them from the side or even moved in a retrograde manner. The high apparent velocity in such cases was really a phase velocity, a sort of measurement artifact.

The total time required for a premature wave to reach the edge of the network was often nearly constant, being surprisingly independent of the path along which it was conducted. The propagation delay a wave would encounter upon being forced to skirt a conduction block was

usually compensated by faster conduction beyond the blocked area, since the tissues there had received additional time for recovery. Thus, it was often impossible to detect, simply from conduction-time measurements, the presence of even fairly sizeable conduction blocks.

A similar sort of compensatory delay mechanism operates on every premature beat, regardless of the presence of conduction blocks: moving the stimulus earlier produces an offsetting increase in initial conduction delay, preventing the wave from reaching the edge of the network much, if any, earlier. (In the model, increased prematurity of stimulation was almost exactly cancelled by increased delay in conduction, so that a wave's arrival time at the edge of the network would remain about the same even though the stimulus timing was varied by as much as 30 msec.[1]) This mechanism serves to make the functional refractory period (minimum interval between responses) larger than the effective refractory period (minimum interval between effective stimuli).

The effective refractory periods (ERP) following successive premature beats were found to vary irregularly in the model, owing to an interaction between conduction delay and the dependence on cycle length of the individual cells' absolute refractory periods. Thus, the ERP duration following P_{n+1} bore no simple relation to the ERP following P_n. When the ERP duration of P_1 was plotted against P_1's inter-stimulus interval, the curve showed a surprising upturn (longer ERP) for the earliest P_1's (whereas the ARP duration of the individual cells is a monotonically decreasing function of inter-stimulus interval). This

[1] The amount of time by which a second premature stimulus (P_2) could be varied without change in the wave's final arrival time depended on the timing of P_1; P_2's range was greatest when P_1 was timed slightly later than the earliest possible.

phenomenon, which has also been observed in animals, was found to result primarily from two factors. First, moving a stimulus earlier may shorten its ERP without necessarily shortening its functional refractory period (FRP) (see above); that is, advancing the stimulus does not necessarily advance the activity cycles of cells all along the path of conduction. Hence, making P_1 earlier does not necessarily mean that P_2 can be applied earlier and still be conducted. And second, the effective radius of the external stimulator is diminished when the tissue is more refractory, making a conducted response to P_2 still more difficult to obtain.

Self-sustaining activity can be induced in the model by at least three different kinds of external stimulation patterns. For fixed-rate stimulation, there is a rather sharp frequency threshold or "critical fibrillation frequency", above which persistent activity ensues. For paired-premature stimulation, the critical combinations may be represented by a scatter diagram. And for vulnerable-period stimulation, a strength-interval diagram indicates the critical region. All three methods of initiation share a common mechanism: a localized, temporary conduction failure results in the formation of a gap in an active wavefront, through which activity reenters to re-excite areas previously excited by that same wave. Fixed-rate stimulation produces gaps that are relatively small and further from the stimulator, while vulnerable-period stimulation leads to large gaps very close to the stimulator; paired-premature stimulation produces an intermediate case.

The basic pattern of reentrant activity is that of a rotating spiral wave, although irregular conduction often causes considerable distortion in the spiral shape. A single, dominant wave was seen most

commonly, but multiple, independent waves were also observed, particularly in the larger networks. Fragmentation of the wavefronts increased markedly as certain parameters (threshold, RRP duration) were pushed toward extreme values.

Sometimes activity in the network became periodic with period equal to one rotation of the spiral wave (that is, all cells' firing cycles had the same duration.) Longer cycles may have occurred also, but were not specifically checked. Cyclic networks persist indefinitely, of course, but in other cases, persistence is difficult to characterize. Reentrant activity often seems quite stable, at other times capricious; spontaneous termination of activity has been observed even after thousands of time-steps.

An attempt was made to characterize the state of a "fibrillating" network in terms of various statistics, but without success. That the likelihood of reentry, its method of initiation, the persistence of activity, even its imminent termination could not be forecast reliably from global averages stands as an unexpected result of these experiments.

Many of the experiments involving variation of the model's parameters confirmed one's intuition, but some results were surprising. A priori, it seemed likely that reducing the average ARP duration (lowering $\bar{k}$) might lead to fragmentation of a reentrant wavefront through an increased number of potential conduction paths. However, the effect was just the reverse: the spiral pattern became more tightly coiled and, if anything, more uniform. Similarly, it was expected that increasing the network's inhomogeneity (raising k_σ) would produce some fragmentation of the wavefront; but although the wavefront did become more ragged, it remained a single entity. The reentry became more

tenuous, however, and finally failed. Curiously, the average safety factor of conduction increased along with the inhomogeneity. Lowering k_σ (increased homogeneity) had no effect on established reentrant waves, but did make the activity more sensitive to reductions in network size.

Several of the model's parameters led to interesting behavior when altered toward extreme values. Reducing τ_R (duration of the relative refractory period) to low values after persistent activity had been established led to fragmentation of the wavefront and then to its degeneration into totally chaotic activity. This same situation could be produced ab initio by applying three rapid stimuli to a network whose τ_R had been set to a low value, and a similar but somewhat less chaotic pattern developed when each reduction in τ_R was matched by an equal increase in τ_A (the ARP duration), so that the relative refractory period was shortened without much change in the length of the total refractory period. Raising τ_R toward normal values abolished the chaotic activity and restored the "normal" spiral reentry pattern. The same sort of chaotic activity resulted when θ_{max} (the maximum threshold value) was reduced nearly to θ_{min} (the resting threshold value).

A twofold reduction in the value of λ_{max} (the local response maximum) had little effect; but further reductions, to the point where summation of responses was necessary for the propagation of activity, produced a very slow and symmetric wave with large fluctuations in the cells' average firing frequency.

Since the course of reentry waves is plainly visible in the simulation, and since the stimulator can be freely moved around and switched on or off, it seemed likely that reentrant activity could be

abolished by external stimulation. Attempts to do this failed, however, even in cases where the external drive was able to take over the pacing of the network.

Some Generalizations from the Results of this Study

1. The timing of a premature stimulus is, in one sense, quite critical: small variations in the timing can make substantial differences in the response of the model tissue. But in another sense the timing is not critical at all: self-sustaining activity can usually be initiated by fixed-rate stimulation over a range of frequencies and train lengths, by two successive stimuli if both are quite early, or by a single stimulus that is early and strong. The only way to determine whether a particular stimulating pattern will be successful in initiating reentrant activity is by trial; but if a given pattern fails, it is usually not too hard to find another that will succeed.

2. There is a rather sharply defined threshold frequency for fixed-rate stimulation, such that stimulating at a higher rate leads to reentrant activity while stimulating at a lower rate does not. This threshold frequency is approximately that rate at which the model cells with the longest absolute refractory periods (largest k values) cannot respond to every stimulus. (The cells in this case fail to respond not because they are absolutely refractory when the stimulus arrives, but because their thresholds are too high (early in the relative refractory period) for them to respond to the propagated stimulus.)

3. To oversimplify somewhat, the effects of the factors related to the network size and to the duration of the absolute refractory period can be summarized as follows:

a) Variation in $\overline{k}$ primarily affects the range of stimulating frequencies that will be effective in initiating reentrant activity;

b) Variation in k_σ primarily affects the number of stimuli at a given frequency that will be required to initiate reentrant activity;

c) Variation in the size of the network mainly affects the persistence of reentrant activity rather than the ease of initiating it.

Relationships to other Models

1. Self-sustaining activity in the present model usually takes the form of one or a few rotating spiral waves. Self-sustaining spiral waves have been observed previously in simulations of densely-connected nerve nets (Farley, 1962) and the myocardium (Lukashevich, 1964), and have been predicted by theoretical models of fibrillation (Balakhovskii, 1965; Krinskii, 1966). In the present study, the spiral waves maintained a relatively stationary focus in some cases, while in other cases the focus moved about, sometimes in a gradual precession, sometimes erratically. However, the spiral depended on local variations in excitability and refractoriness only for its initiation; once established, it seemed to be independent of "anatomical" variations and, in fact, was unaffected by the imposition of complete homogeneity on the network (setting k_σ to zero). Such spiral waves are reminiscent of the older notion of a circulating "mother wave", hypothesized as a mechanism for fibrillation or flutter (Lewis, 1925); however, the spiral is a purely dynamic thing, corresponding to no anatomical pathway.

2. Since Mayer's demonstration (1908) of continuous conduction in the mantle of the jellyfish, a number of authors have proposed that a similar sort of circus rhythm might be the basis of atrial flutter

and/or fibrillation (Mines, 1913; Lewis, 1925; Wiener and Rosenblueth, 1946; and others). It has seemed fairly clear that circulating waves of activity could exist in atrial muscle, particularly where a nonconducting obstacle is present; but it has been much less clear how such a unidirectional wave might be initiated in the absence of rather marked asymmetry in the conducting properties of the myocardium. The present model demonstrates how a reentry can develop following a localized conduction failure in a region of depressed excitability, and how such reentries naturally lead to pairs of self-sustaining spiral waves; and how, frequently, one of the spiral waves in such a pair is crowded out by its twin or fails in some other way. Thus, a kind of unidirectional wave can be produced relatively easily, even in the absence of directional asymmetry in the conducting properties of the excitable medium. Objections have been raised to the circus rhythm theory of atrial flutter and fibrillation on the grounds that some extraordinary, and hence unlikely, initiating event was required. But the results of this study suggest that the initiation of self-sustaining activity in an inhomogeneous excitable medium is not particularly unlikely, given an appropriate pattern of stimulation.

3. Brooks, et al. (1955) have proposed a mechanism to account for the no-response and vulnerable period phenomena described in Chapter IV, in which a strong shock applied early in the relative refractory period may (i) fail to elicit a conducted response even though a weaker stimulus applied at the same point in the cardiac cycle evokes a distinct extrasystole, or (ii) may evoke multiple extrasystoles that often pass on into fibrillation. According to the Brooks hypothesis, the recovery process, like the excitatory wavefront,

expands outward from the stimulating electrode in a pattern that is roughly circular but highly irregular, owing to variations in conduction velocity and refractory period durations. When a premature stimulus is applied, its effective range depends on its strength. An adequate stimulus will excite the cells in the immediate vicinity of the stimulating electrode, producing a wave that is conducted slowly, at first, but relatively symmetrically. A very strong stimulus will depolarize a larger region of tissue, but the cells at the edge of that region, being poorly recovered from the previous wave, will exhibit such a slow rate of rise of membrane potential that they will be incapable of exciting their still-more-poorly-recovered neighbors, and hence the activity will not be conducted. However, if this conduction failure at the borders of the excitable region is incomplete (which would be favored by a slightly later timing of the stimulus), then small patches of activity would remain at the periphery as the excited region entered its refractory period. These patches of activity could, presumably, lead to reentry, multiple wavelets, and thus fibrillation.

The results of this study support the Brooks hypothesis, for we have observed during simulation that the no-response and multiple-response phenomena occur in the model by exactly the mechanisms described above. The model also indicates that the no-response and multiple-response regions of the strength-interval graph are not demarcated by clear thresholds, and that they are sensitive both to variations in the tissue's properties and to spatial separation of the drive and test electrodes.

4. Moe and his associates (Moe, 1962; Moe, et al., 1964) have suggested that atrial fibrillation is associated with the development

of multiple independent wavelets of activity in the myocardium. They did observe such wavelets in a computer simulation (1964), but found that the raw number of wavelets was not a good predictor of the persistence of self-sustaining activity. In contrast, activity wavefronts tend to be cohesive in the present model (probably owing to its inclusion of thresholds and spatial and temporal summation); multiple independent waves are relatively uncommon, at least in the smaller (469-cell) networks. The predominant pattern of activity is one or a few spiral waves. Independent wavelets may indeed be "thrown off" from a spiral, but they rarely become self-sustaining.

A dramatic increase in the number of independent wavelets was observed when certain parameters were pushed to extreme values, viz., when the duration of the relative refractory period (τ_R) was made very short, or when the maximum allowable threshold during RRP (θ_{max}) was reduced substantially. As either of these parameters was reduced, wavefronts first became more ragged in outline, then fragmented into separate wavelets, and finally (with τ_R or θ_{max} at minimum values) disappeared entirely as activity became completely chaotic with no discernible wavefronts at all. It is tempting to argue that the latter state represents "true" fibrillation, but the associated parameter values are just too unphysiological. However, reducing τ_R or θ_{max} does make the model more like the Moe model in one respect: conduction failure due to elevated threshold becomes less likely. (In the Moe model, every stimulus is effective unless the recipient cell is absolutely refractory; only the delay depends on the cell's recovery state.)

5. Some investigators believe that fibrillation is due to continuous, rapid discharge from an ectopic focus somewhere in the atrial myocardium, rather than to reentrant mechanisms (e.g., Scherf and Schott, 1953). According to this hypothesis, fibrillation is not a self-sustaining process, and can be terminated by supression of the initiating focus. The present study does not directly address this problem, since automaticity has been deliberately omitted from the model. However, it has been observed in simulation experiments that stimulation at a rate just below the "critical fibrillation frequency" produces a pattern of activity which is difficult to discriminate, either by statistical means or by direct observation, from the pattern generated by stimulation just above the critical frequency; yet the former is not self-sustaining whereas the latter may persist indefinitely. Since the model demonstrates two similar kinds of fibrillation-like activity, one dependent on continuous stimulation, the other not, perhaps it is less puzzling that some investigators have found fibrillation to be dependent on focal discharge (Scherf and Schott, 1953) while others have shown it to be self-sustaining (Garrey, 1914; Moe and Abildskov, 1959).

Moreover, a factor that is said to favor the formation of ectopic foci, namely, an increased local inhomogeneity of the myocardium, also favors the initiation of self-sustaining activity by reentrant mechanisms, if the analogy to simulation of this model is valid.

Relationships to the Heart

1. In studying intra-atrial conduction, Curtis (1971) found that very premature beats often propagated in a highly irregular fashion,

and that sometimes activity arrived at sites distant from the stimulating electrode before arriving at closer sites. Similar results have been observed in simulation experiments, in which the erratic conduction and "negative" velocities are seen to be the result of localized, temporary conduction blocks caused by random variation in refractory period durations. It is particularly striking, in the model, how much the results are affected by the choice of a path along which to measure the propagation of activity: a wave may be conducted quite adequately along one path while simultaneously suffering complete block on another. It is also evident that an average conduction velocity derived from a wave's total propagation time may be quite different from its instantaneous velocity at intermediate points.

2. A stimulus which is too premature to evoke a conducted response may nevertheless interfere with a subsequent, closely-spaced stimulus, causing it to fail also, so that a propagated beat results when the second stimulus is applied alone but not when both stimuli are applied (Lewis and Drury, 1926; Fukushima, unpublished observations). It has been suggested that this phenomenon is the result of a local, nonpropagated response to the first stimulus which interrupts the tissue's recovery process and leaves it insufficiently excitable for the second stimulus to evoke a conducted beat. The same phenomenon has been observed in simulation experiments, and the mechanism there is similar to that hypothesized for the heart: several cells are excited by the first stimulus, but they are so early in their relative refractory periods that their responses are weak and inadequate to excite the neighbors; thus there is no conducted response. Nevertheless, the cells responding to the first stimulus are sufficiently out of syn-

chrony (if not absolutely refractory) with the cells responding to the second stimulus that the temporal and spatial summation is reduced and conduction fails. The model thus supports the reasonableness of Lewis and Drury's interpretation of their results.

3. West and Landa (1962) have investigated the minimal mass of atrial tissue necessary to sustain an arrhythmia. Working with isolated segments of rabbit atrium, they found that, in the presence of acetylcholine, a short burst of rapid stimuli would usually induce an arrhythmia of varying duration, consisting of a rapid, regular series of ecoptic beats. After evoking an arrhythmia they divided the tissue segment in half, retaining one piece and discarding the other, repeating the procedure on the retained half. They continued the process until an arrhythmia could not be produced; the tissue segment remaining at that time was taken to represent the minimal arrhythmic mass.

The average minimal mass determined by this procedure was 32 mg.; assuming an average tissue thickness of one mm. and unit density, the average area of the minimal mass was 32 mm^2. For a circular shape, the corresponding diameter is 6.4 mm.

In order to compare these figures with the results of simulation experiments in which the size of the model network was varied, it is necessary to adjust the scale of the model to correct for the difference between the conduction velocity observed in West and Landa's preparation (0.2 to 0.33 mm./msec.) and that assumed in Chapter III of the present study (1.0 mm./msec.). Thus rescaled, the model cells represent tissue segments about 0.6 to 1.0 mm. in diameter each.

Only a few simulation experiments were done in which the network size was reduced to the point at which no reentry at all could be produced, but the largest non-arrhythmic network (analogous to West and Landa's "minimal arrhythmic mass") appears to be about 11 model cells in diameter (with $\bar{k}$ equal to 6.0). Using the scale factors just mentioned, this would represent a tissue segment 6.6 to 11.0 mm. in diameter, which is in reasonable agreement with West and Landa's value of 6.4 mm. (The latter may be somewhat understated, since successive samples differed in size by a factor of two.)

Although an attempt has been made to give the model realistic parameters and properties, it is not expected that such a simple representation of a complex system can be relied upon for quantitative results. It is therefore surprising that the simulation should be as close as it is, in this case, to actual experiment.

4. In a simulation experiment in which a self-sustaining spiral wave had been firmly established, the model cells' ability to stimulate each other was reduced (by reducing the value of λ_{max}, the maximum of the local response) to the point where single cell-to-cell conduction was impossible, summation of two or more cells' responses being required to stimulate even a quiescent cell. As a result, the activity wave slowed markedly and became quite erratic in its propagation; the effect was reminiscent of the later stages of an open-chest preparation in the dog, in which activity waves in a fibrillating ventricle sometimes move so slowly as to become visible to an observer. One might speculate that the latter effect, as in the model, is a consequence of greatly reduced safety factors of conduction resulting from impaired amplitude and rate of rise of the cells' action potentials.

5. Curtis (1971) found that restimulation was usually effective in terminating episodes of electrically-induced fibrillation in control preparations, but that it was frequently ineffective in preparations that had received an arrhythmia-enhancing drug (e.g., acetylcholine). Restimulation was tested only a few times in the model, but in no case did it succeed in terminating previously-established self-sustaining activity. Two modes of failure were observed: one, in which external stimulation was ineffective because the region "under" the stimulator was nearly always excited, or soon to be excited, anyway; and a second in which the external stimulation was effective and even capable of pacing the network (if applied at the right frequency), but unable to abolish the phase differences between cells at the site of the original reentry focus, so that the reentrant wave reestablished itself as soon as the external stimulation was removed.

Some Retrospective Comments

In the course of developing this model and conducting simulation experiments with it, many arbitrary decisions were necessary. Most of them seem to have been reasonably satisfactory, but there are several which, in retrospect, might better have been made differently. These are not important deficiencies (otherwise they would have been corrected earlier), but rather modifications that could be incorporated in any future experiments to improve the model's realism. Specifically:

(i) The model cells are sensitive to the summed stimulation of their neighbors only during the quiescent and relative refractory periods; during the stimulated, firing, and absolute refractory periods their behavior is autonomous. If several of a cell's neighbors are

firing at nearly the same time, but slightly out of synchrony, then the cell might be triggered, and have its own delay computed, on the basis of excitation from just one neighbor, even if several others fire a time-step or two later. In this case, the conduction delay is probably excessive and the propagated stimulus unduly weak. Additional excitation received during the stimulated (delay) state should serve to hasten the transition to the firing state.

(ii) The use of the square root law for computing absolute refractory period duration as a function of cycle length has disadvantages that have already been mentioned, the principal one being that the ARP duration can grow arbitrarily large at long cycle lengths. The exponential law proposed by Hoffman and Cranefield (1960) should be adopted instead.

(iii) Pulses from the external stimulator have a duration of only one time-step; because of the discrete nature of simulated time, this may introduce artifacts. A strength-duration study would probably be useful in determining whether a longer pulse duration from the external stimulator would be advisable.

(iv) In experiments with fixed-rate stimulation, there is a problem in choosing an appropriate intrinsic or basic driving rate, i.e. the state of the network before the fixed-rate stimulus is turned on. The most realistic approach would probably involve a moderate driving rate with a gradual transition up to the testing frequency; but this is expensive of computer time, and introduces several additional variables, namely, the choice of basic drive rate and the transition sequence. The procedure used here, in which the network was started in a quiescent condition but the initial refractory periods were calcu-

lated as though it were already being driven at the testing frequency, is admittedly a departure from realism; but it avoids the difficulties mentioned above and focuses on the development of irregular and failing conduction, which are the matters of primary interest. Nevertheless, experiments using other protocols might be worthwhile.

Future Research

As the present study has been exploratory rather than exhaustive, there is much room for further work using this or similar models. It would be particularly interesting, for example, to study the effects of additional parameters (especially those related to conduction delay, thresholds, and the relative refractory period) on the initiation of self-sustaining activity. Also, with the availability of greater computing capacity, it will become feasible to repeat the sort of experiments described here using "different" networks, that is, different random patterns of k assignment, in order to put the results on a firmer basis. Then, there is the interesting and potentially promising problem of the direct simulation of drug effects on the myocardium.

A number of interesting extensions of the model can be envisioned. For example, the geometry of the network might be modified to represent more realistically the actual shape and topology of the atria; in that case, one could also consider calculating the analog of an electrocardiogram. Finally, of course, there is the ventricle: a three-dimensional, anisotropic solid with important specialized conducting systems. Extension of the model to any of these cases represents an interesting and challenging research problem to which the solution is far from apparent.

It is the author's belief that the future of biological modelling, in general, will be enhanced greatly if the modellers are able to build structures upon which experiments can truly be performed, with verifiable or falsifiable outcomes. Until there is a definite closing of the loop, with the results of simulation becoming directly useful in the design of biological experiments, we will see little of that productive union of the two which is often discussed but so seldom achieved.

REFERENCES

Abakumov, A.S., Gulyayev, A.A. and Gulyayev, G.A.: Propagation of excitation in an active medium. Biofizika 15: 1074-1080, 1970, tr. in Biophysics 15: 1113-1120, 1970.

Alessi, R., Nusynowitz, M., Abildskov, J.A. and Moe, G.K.: Nonuniform distribution of vagal effects on the atrial refractory period. Amer. J. Physiol. 194: 406-410, 1958.

Arshavskii, Y.I., Berkinblit, M.B., Kovalev, S.A. and Chailakhyan, L.M.: Periodic transformation of rhythm in a nerve fibre with gradually changing properties. Biofizika 9: 365-371, 1964, tr. in Biophysics 9: 392-399, 1964.

Arshavskii, Y.I., Berkinblit, M.B. and Dunin-Barkovskii, V.L.: Propagation of pulses in a ring of excitable tissues. Biofizika 10: 1048-1054, 1965, tr. in Biophysics 10: 1160-1166, 1965.

Balakhovskii, I.S.: Several modes of excitation movement in ideal excitable tissue. Biofizika 10: 1063-1067, 1965, tr. in Biophysics 10: 1175-1179, 1965.

Bazett, H.C.: An analysis of the time-relations of electrocardiograms. Heart 7: 353, 1918-21.

Berkinblit, M.B., Kovalev, S.A., Smolyaninov, V.V. and Chailakhyan, L.M.: Input resistance of syncytial structures. Biofizika 10: 309-316, 1965, tr. in Biophysics 10: 341-350, 1965a.

_____. Features of the distribution of the potential in syncytial structures. Biofizika 10: 883-885, 1965, tr. in Biophysics 10: 977-980, 1965b.

Brender, R.F.: A programming system for the simulation of cellular spaces. Doctoral Dissertation, The University of Michigan, 1970.

Brooks, C.McC., Hoffman, B.F., Suckling, E.E. and Orias, O.: The Excitability of the Heart. Grune and Stratton, New York, 1955.

Brown, B.B. and Acheson, G.H.: Aconitine-induced auricular arrhythmias and their relation to circus-movement flutter. Circulation 6: 529-537, 1952.

Chebotarev, Y.P.: Modelling of the process of conduction of excitation in cardiac muscle. Biofizika 13: 483-491, 1968, tr. in Biophysics 13: 577-587, 1968.

Curtis, G.P.: Experimental atrial fibrillation. Doctoral Dissertation, The University of Michigan, 1971.

Dawes, G.S.: Experimental cardiac arrhythmias and quinidine-like drugs. Pharmacol. Rev. 4: 43-84, 1952.

Ericksen, J.E.: On the influence of the coronary circulation on the action of the heart. London Med. Gazette 2: 561, 1842.

Farley, B.G.: Some results of computer simulation of neuron-like nets. Federation Proc. 21: 92-96, 1962.

Flanigan, L.K.: A cellular model of electrical conduction in the mammalian atrioventricular node. Doctoral Dissertation, The University of Michigan, 1965.

Flanigan, L.K. and Swain, H.H.: Computer simulation of A-V nodal conduction. Univ. Michigan Med. Center J. 33: 234-241, 1967.

Frantz, D.R. and Brender, R.F.: The CESSL programming language. University of Michigan Technical Report LCG-123, 1971.

Garrey, W.E.: The nature of fibrillary contraction of the heart--its relation to tissue mass and form. Amer. J. Physiol. 33: 397-414, 1914.

_____. Auricular fibrillation. Physiol. Rev. 4: 215-250, 1924.

Gaskell, W.H.: Phil. Trans., p. 1017, 1882, cited in Mines, G.R.: On dynamic equilibrium in the heart. J. Physiol. 46: 349-383, 1913.

Gel'fand, I.M. and Cetlin, L.M.: Continuous models of control systems. Dokl. Akad. Nauk SSSR 131: 1242, 1960, tr. in Soviet Mathematics 1: 409-412, 1960.

Gel'fand, S.I. and Kazdan, D.A.: An integral equation connected with a pulse motion along a circle. Dokl. Akad. Nauk SSSR 141: 527, 1961, tr. in Soviet Mathematics 2: 1476-1479, 1961.

Hecht, H., Katz, L.N., Pick, A., Prinzmetal, M. and Rosenblueth, A.: The nature of auricular fibrillation and flutter--a symposium. Circulation 7: 591-613, 1953.

Hoffa, M. and Ludwig, C.: Einige neue Versuche ueber Herzbewegung. Ztschr. rat. Med. 9: 107, 1850.

Hoffman, B.F. and Cranefield, P.F.: Electrophysiology of the Heart. McGraw-Hill, New York, 1960.

Katz, L.N. and Pick, A.: Current status of theories of mechanisms of atrial tachycardias, flutter and fibrillation. Progr. Cardiovasc. Dis. 2: 650-662, 1960.

Kholopov, A.V.: Spread of excitation in a fibre, the refractoriness of which depends on the period of excitation. Biofizika 13: 670-678, 1968, tr. in Biophysics 13: 793-804, 1968a.

_____. Spread of excitation and the formation of closed pathways of conduction in a plane medium the refractoriness of which depends on the period of excitation. Biofizika 13: 1058-1069, 1968, tr. in Biophysics 13: 1231-1243, 1968b.

Kinosita, H.: Initiation of entrapped circuit wave in a scyphomedusa, Mastigias papua. Jap. J. Zool. 9: 209, 1941.

Krinskii, V.I.: Spread of excitation in an inhomogeneous medium (state similar to cardiac fibrillation). Biofizika 11: 676-683, 1966, tr. in Biophysics 11: 776-784, 1966.

_____. Fibrillation in excitable media. In Problemy Kibernetiki, ed. by A.A. Lyapunov, tr. in Systems Theory Research, Vol. 20, Plenum, New York, 1971.

_____. Non-steady velocity of propagation of excitation, latent periods and their connexion with fibrillation of the heart. Biofizika 16: 87-94, 1971, tr. in Biophysics 16: 88-96, 1971.

Krinskii, V.I., Fomin, S.V. and Kholopov, A.V.: Critical mass during fibrillation. Biofizika 12: 908-914, 1967, tr. in Biophysics 12: 1041-1048, 1967.

Krinskii, V.I. and Kholopov, A.V.: Echo in excitable tissue. Biofizika 12: 524-528, 1967, tr. in Biophysics 12: 600-606, 1967a.

Krinskii, V.I. and Kholopov, A.V.: Conduction of impulses in excitable tissue with continuously distributed refractoriness. Biofizika 12: 669-675, 1967, tr. In Biophysics 12: 772-780, 1967b.

Krinskii, V.I., Kukushkin, N.I. and Sakson, M.Y.: Reduction in latency as criterion of the effectiveness of anti-arrhythmic agents. Biofizika 16: 488-493, 1971, tr. in Biophysics 16: 506-513, 1971.

Lewis, T.: The Mechanism and Graphic Registration of the Heart Beat (3rd Ed.). Shaw & Sons, Ltd., London, 1925.

Lewis, T. and Drury, A.N.: Revised views on the refractory period, in relation to drugs reputed to prolong it, and in relation to circus movement. Heart 13: 95-100, 1926.

Lillie, R.S.: Resemblances between the electromotor variations of rhythmically reacting living and non-living systems. J. Gen. Physiol. 13: 1, 1929a.

_____. Circuit transmission and interference of activation waves in living tissues and in passive iron. Science 69: 309, 1929b.

Lukashevich, I.P.: Investigation with a computer of continuous models of control systems. Biofizika 8: 715-721, 1963, tr. in Biophysics 8: 776-783, 1963.

Lukashevich, I.P.: Rhythmic pattern of homogeneous tissue and modelling the behaviour of the heart muscle. Biofizika 9: 731-738, 1964, tr. in Biophysics 9: 797-805, 1964.

Mayer, A.G.: Rhythmical pulsation in Scyphomedusae. Papers from the Tortugas Laboratory, Carnegie Institute of Washington 1: 115, 1908.

_____. Nerve-conduction in Cassiopea xamachana. Papers from the Department of Marine Biology of the Carnegie Institution of Washington 11: 1, 1917.

McWilliam, J.A.: Fibrillar contraction of the heart. J. Physiol. 8: 296-310, 1887.

Mines, G.R.: On dynamic equilibrium in the heart. J. Physiol. 46: 349-383, 1913.

_____. On circulating excitations in heart muscles and their possible relation to tachycardia and fibrillation. Trans. Roy. Soc. Canada [Biol.] 8: 43-52, 1914.

Moe, G.K.: On the multiple wavelet hypothesis of atrial fibrillation. Arch. Int. Pharmacodyn. 140: 183-188, 1962.

Moe, G.K. and Abildskov, J.A.: Atrial fibrillation as a self-sustaining arrhythmia independent of focal discharge. Amer. Heart J. 58: 59-70, 1959.

Moe, G.K., Preston, J.B. and Burlington, H.: Physiologic evidence for a dual A-V transmission system. Circulation Res. 4: 357-375, 1956.

Moe, G.K., Rheinboldt, W.C. and Abildskov, J.A.: A computer model of atrial fibrillation. Amer. Heart J. 67: 200-220, 1964.

Prinzmetal, M., Corday, E., Brill, I.C., Oblath, R.W. and Kruger, H.E.: The Auricular Arrhythmias. Charles C. Thomas, Springfield, Ill., 1952.

Rytand, D.A.: The circus movement (entrapped circuit wave) hypothesis and atrial flutter. Ann. Int. Med. 65: 125-159, 1966.

Schamroth, L.: The Disorders of Cardiac Rhythm. Blackwell Scientific Publications, Oxford, 1971.

Scherf, D., Schaffer, A.I. and Blumenfeld, S.: Mechanism of flutter and fibrillation. Arch. Int. Med. 91: 333, 1953.

Scherf, D. and Schott, A.: Extrasystoles and Allied Arrhythmias. Grune and Stratton, New York, 1953.

Scherf, D. and Terranova, R.: Mechanism of auricular flutter and fibrillation. Amer. J. Physiol. 159: 137-142, 1949.

Selfridge, O.: Studies on flutter and fibrillation. V. Some notes on the theory of flutter. Arch. Inst. Cardiol. Mexico 18: 177, 1948.

Swain, H.H. and Valley, S.L.: Critical fibrillation frequency. Univ. Michigan Med. Center J. 36: 122-126, 1970.

Swain, H.H. and Yanagita, T.: A model circus. Univ. Michigan Med. Bull. 29: 338-347, 1963.

Tenney, S.M. and Wedd, A.M.: Disturbances in rhythm in the cold-blooded heart under aconitine. Circulation Res. 2: 28-34, 1954.

West, T.C. and Landa, J.F.: Minimal mass required for induction of sustained arrhythmia in isolated atrial segments. Amer. J. Physiol. 202: 232-236, 1962.

Wiener, N. and Rosenblueth, A.: The mathematical formulation of the problem of conduction of impulses in a network of connected excitable elements, specifically in cardiac muscle. Arch. Inst. Cardiol. Mexico 16: 205, 1946.